Papers Presented to the

CONFERENCE ON

HEAT & DETACHMENT IN CRUSTAL EXTENSION ON CONTINENTS AND PLANETS

SEDONA, ARIZONA
OCTOBER 10 - 12, 1985

Sponsored by

Lunar and Planetary Institute
U.S. Geological Survey, Flagstaff
American Geophysical Union
Geological Society of America
Rio Grande Rift Consortium

UNIVERSITIES SPACE RESEARCH ASSOCIATION
LUNAR AND PLANETARY INSTITUTE
3303 NASA ROAD 1
HOUSTON, TEXAS 77058

Papers Presented to the Conference on

HEAT AND DETACHMENT IN CRUSTAL EXTENSION ON CONTINENTS AND PLANETS

Sedona, Arizona

October 10-12, 1985

Sponsored by:

Lunar and Planetary Institute
U.S. Geological Survey, Flagstaff
American Geophysical Union
Geological Society of America
Rio Grande Rift Consortium

Compiled by:

Publications Office
Lunar and Planetary Institute
3303 NASA Road One
Houston, TX 77058-4399

LPI CONTRIBUTION NO. 575

Compiled in 1985 by the Lunar and Planetary Institute

PREFACE

This volume contains abstracts that have been accepted by the Program Committee for presentation at the Conference on Heat and Detachment in Crustal Extension on Continents and Planets, held in Sedona, Arizona, October 10-12, 1985. Program Committee members included the following:

Conveners: I. Lucchitta *(U.S. Geological Survey, Flagstaff)*
P. Morgan *(Purdue University)*
L. Soderblom *(U.S. Geological Survey, Flagstaff)*

Committee Members: E. Frost *(San Diego State University)*
G. R. Keller *(University of Texas, El Paso)*
A. S. McEwen *(Arizona State University, Tempe)*
J. Sass *(U.S. Geological Survey, Flagstaff)*

Logistics and administrative support for the conference was provided by the LPI Projects Office. The Lunar and Planetary Institute is operated by the Universities Space Research Association under contract no. NASW-3389 with the National Aeronautics and Space Administration.

* * * * * * * * * *

CONTENTS

EXTENT AND CHARACTER OF EARLY TERTIARY PENETRATIVE DEFORMATION, SONORA, NORTHWEST MEXICO;

T. H. Anderson, Department of Geology and Planetary Science, University of Pittsburgh, Pittsburgh, PA 15260

Reconnaissance field work has led to the recognition of extensive Early Tertiary gneiss and schist which are distinguished by weakly developed to highly conspicuous northeast to east-trending stretching lineation commonly accompanied by low-dipping foliation. This structural fabric has been imposed on Precambrian to Paleogene rocks. Regionally, minimum ages of deformation are based upon interpreted U-Pb isotopic ages from suites of cogenetic zircon from the Paleogene orthogneiss. Locally, the interpreted ages indicate that ductile deformation continued as late as Oligocene (Anderson and others, 1980; Silver and Anderson, 1984). The consistency of the deformational style is such that, although considerable variation in intensity exists, the fabric can be recognized and correlated in rocks away from the Paleogene orthogneiss.

Outcrops of Tertiary gneiss and schist (Tgn-s) generally coincide with a north-northwesterly-trending belt, recognized by L.T. Silver (Silver and Anderson, 1984), within which the rock and mineral isotopic systems record a pronounced mid-Tertiary thermal disturbance. The axis of the belt, which broadens northward, extends from Mazatan, east of Hermosillo, toward Nogales on the Sonora-Arizona border. Deformed rocks do not crop out continuously within this band but occur as domains segmented by sharp or transitional boundaries. In northern Sonora extensive outcrops of Tgn-s exist between the Mojave-Sonora megashear and a series of straight, northwesterly-trending lineaments which are interpreted as normal faults, orthogonal to the stretching direction, developed in brittle sequences. Within this extensive area Tgn-s have been formed from supracrustal rocks of Jurassic(?) age intruded by the "Laramide" and younger plutons. Outside this region the volcanic and volcaniclastic rocks of the Jurassic(?) sequence are characterized by tight folds which commonly trend northwesterly to westerly. These folds are generally obliterated in areas of intense Tertiary ductile deformation. Boundaries parallel to stretching are difficult to characterize because they commonly are obscured by superposed normal faults. In northwestern Sonora, Tgn-s are not known from the region south of the Mojave-Sonora megashear. We conclude that this discontinuity influenced the existing distribution of Tertiary ductile deformation. In central Sonora, south of the megashear, lineated rocks are not widely distributed and are best developed in rocks contiguous to Paleocene plutons. In this region boundaries between lineated and unlineated rocks are transitional.

The heterogeneous crustal sequence of Sonora did not lend itself to the development of regional detachments as have been documented in Arizona and California. However, ductile normal faults are common and listric normal faults as well as detachments between crystalline rocks and structurally higher sequences are locally developed.

RIFTING ON VENUS: IMPLICATIONS FOR LITHOSPHERIC STRUCTURE

W. B. Banerdt and M. P. Golombek, Jet Propulsion Laboratory, California Institute of Technology, Pasadena, CA 91109

Introduction

Several approaches have been used to estimate the elastic lithosphere thickness (L) on Venus. In particular, Solomon and Head [1] have used a number of compressional (elastic and viscous folding) and tensional (wedge subsidence, imbricate normal faulting, and plastic necking) models to predict L based on the hypothesis that the linear bands of greater and lesser backscatter observed in earth-based radar images of Ishtar Terra are of tectonic origin. All of these models predict very thin lithospheres, on the order of 0.3 to 8 km. These values are in agreement with those obtained from strength calculations based on laboratory measurements of crustal rocks ([1]; see below) which give negligible yield stresses at shallow depths due to the high surface temperature and a probable earth-like thermal gradient [2].

However, rift-like features which are at least superficially similar in size, morphology, and association with volcanism and doming to continental rifts on the earth [3] also exist on Venus. They typically have widths on the order of 75-100 km. Estimates of L derived from the widths of these features in Aphrodite Terra and Beta Regio using a wedge-subsidence model are on the order of 50-70 km [4], which is inconsistent with our knowledge of rock rheology at probable Venus temperatures. Plastic necking models also require a relatively thick, strong high viscosity zone (about 30 km thick [5]), again too thick for expected crustal temperatures.

How can these large rift structures which appear to require a thick, strong lithosphere be reconciled with the hot, apparently thin lithosphere implied by rock rheology at venusian conditions and the spacing of the banded terrain? In this abstract we briefly review lithospheric strength envelopes and explore their implications for large scale rifting on Venus. We then use these results to constrain possible crustal thicknesses and thermal gradients.

Lithospheric Strength Envelopes

The maximum stress levels found in the earth's crust are accurately predicted by Byerlee's law [6,7]. This relation is based on laboratory measurements of the frictional resistance to sliding on pre-existing fractures, which occurs at stresses less than those required to break intact rock. Byerlee's law is of the form $\sigma_1=\mu\sigma_3+b$, where σ_1 and σ_3 are, respectively, the maximum and minimum principle effective stresses (stress minus pore pressure), μ is the coefficient of friction, and b is a constant. Laboratory friction measurements show that μ and b are virtually independent of stress (except for a slight change at 135 MPa), rock type, displacement, surface conditions, and temperature. Because the vertical stress is generally quite

close to the lithostatic load, this relation predicts a linear increase in yield stress with depth.

With increasing temperature, rock deformation occurs predominantly by ductile flow. Flow laws for many rocks and minerals have been experimentally determined for stresses up to 1-2 GPa and strain rates down to 10^{-8}/sec. These results can be extrapolated to geological strain rates via creep equations, which generally are of the form $\dot{\varepsilon}=A(\sigma_1-\sigma_3)^n \exp(-Q/RT)$, where $\dot{\varepsilon}$ is the strain rate, R is the gas constant, T is absolute temperature, and A, Q (the activation energy), and n are experimentally determined constants. As a result, the ductile strength is negligible at depths where T is high and increases exponentially with decreasing depth. Flow laws are also highly dependent on rock composition, with a silicic crust much weaker than a mafic mantle.

The failure criterion for a given depth in the lithosphere is determined by the weaker of the frictional or ductile strength at that depth (Figure 1). The yield stress increases with depth according to Byerlee's law until it intersects the crustal flow law. It then decreases exponentially until it reaches the moho, where the mantle flow law causes an abrupt increase in yield stress followed by another exponential decrease. In actuality, semibrittle and low temperature ductile processes tend to round off the intersection points between the brittle and ductile curves in Figure 1 [8]. The lithosphere will behave elastically for stresses less than the yield stress.

This type of analysis has been used by many investigators to study lithospheric strength on the earth and the terrestrial planets (e.g. [9-12]). However determining the geometry and characteristics of faults at failure for this type of lithospheric model has not received much attention. Based on an analysis of two phases of extension in the Rio Grande rift, Morgan and Golombek [13] suggested that during the early phase a shallow brittle-ductile transition along with the absence of a zone of upper mantle strength (due to an elevated geotherm) allowed a shallow decollement to develop with significant strain between the brittle upper crust and the ductilely extending material below. Thus, large strains resulted in the strongly rotated blocks bounded by numerous listric (curved) or planar normal faults which are characteristic of this period (see also Smith and Bruhn [10]). During the late phase of extension that formed the present horst and graben physiography the geotherm had cooled enough to allow a significant zone of ductile strength in the upper mantle (although most of the strength was still in the crust) which prevented large scale intracrustal decoupling and steep rotation of upper crustal blocks.

Lithospheric Strength on Venus

Figure 1 illustrates a typical lithospheric strength curve for Venus with a crustal thickness (c) of 10 km. For these calculations we assume a crustal density (ρ_c) of 2.8 Mg/m^3, a mantle density (ρ_m) of 3.3 Mg/m^3, a surface temperature of

740°C, a thermal gradient of 12°/km [2], and $\dot{\epsilon}=10^{-15}$/sec (equivalent to about 3% extension per million years). Based on surface geochemical measurements which indicate a basaltic composition, we use a dry diabase flow law [14] for the crustal layer. A dry olivine flow law [15] is assumed for the mantle. In this abstract we are interested in horizontal tensional stresses, which correspond to the left-hand branch of the curves in Figure 1.

Implications for Rift Width and Crustal Thickness

One consequence of this model is that the mechanical structure of the lithosphere depends strongly on the crustal thickness. For crusts thicker than about 30 km, there is no appreciable strength in the mantle and the brittle extension of the upper crustal layer should be effectively decoupled from the mantle. This was the implicit assumption of Solomon and Head [1]. However if the crust is thin, the lithospheric strength will be dominated by the upper mantle, and it is possible that this layer will control the style of deformation. In this case the effective lithosphere which controls rift width would be much thicker than the few km expected from crustal rock rheology. Instead, the elastic lithosphere thickness would be on the order of 20-30 km, based on an olivine flow law.

Here we will consider the implications for one theory for rift formation, the wedge-subsidence hypothesis of Vening Meinesz [16,17]. This theory predicts that the graben width w will be given by $w=\pi\alpha/4$, where $\alpha=(EL^3/3g\rho(1-\nu^2))^{1/4}$, E is Young's modulus, g is gravitational acceleration, ρ is the difference in density between the layers above and below the faulted layer, and ν is Poisson's ratio. For rifting of a crustal layer, ρ is just ρ_m. However for a layer at depth with an effectively fluid layer above it, $\rho=\rho_m-\rho_c$. Assuming $E=1.25\times10^{11}$ Pa, $\nu=.25$, $\rho_m-\rho_c=0.5$ Mg/m^3, and L=20 km gives the width for a graben formed in the mantle brittle zone of 98 km, in good agreement with observed rift widths on Venus' surface.

This result requires that the crust be no thinner than ∿3 km (in order for there to be a viscous layer over the mantle strong zone) and no thicker than ∿20 km (in order for there to be a brittle zone in the mantle). In addition, the thermal gradient could not be significantly greater or less than 10-15°/km, since L should be ∿20 km. It should be noted that these values depend on flow laws which are somewhat uncertain due to their extrapolation from laboratory conditions.

This model is not inconsistent with the thin lithosphere implied by the banded terrain. One might expect smaller scale fault blocks whose widths are controlled by the thickness of the crustal strong layer to be superimposed upon the rift structure (see Figure 2). In Ishtar Terra, where no rifts are observed, the bands could have been formed by compressive stresses [1,18], or the crust in this region might be thicker than in rifted areas [2,18].

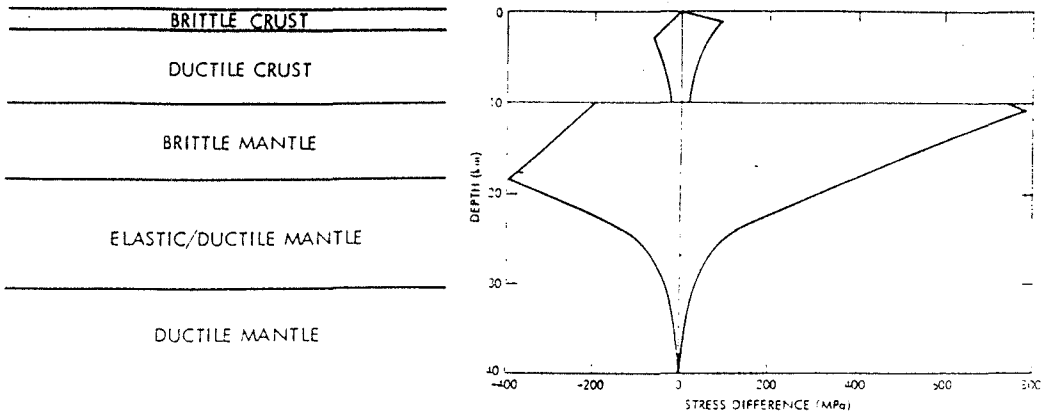

Figure 1. Lithospheric strength envelope for Venus. Stress difference is the vertical minus the maximum or minimum horizontal stress. Thus negative values denote tension and positive values correspond to compression. The horizontal line at 10 km shows the crust-mantle boundary assumed for this case. The flow laws used for the crust and mantle are dry diabase [14] and olivine [15], respectively; both assume a strain rate of 10^{-15}/sec, a surface temperature of 730^{0}C, and a thermal gradient of 12^{0}/km. The properties of the layers delineated by the tensional envelope are shown to the left. The elastic/ductile portion of the mantle deforms ductilely when its yield stress is exceeded, but behaves elastically at the stress levels required for ductile flow in the lower crust.

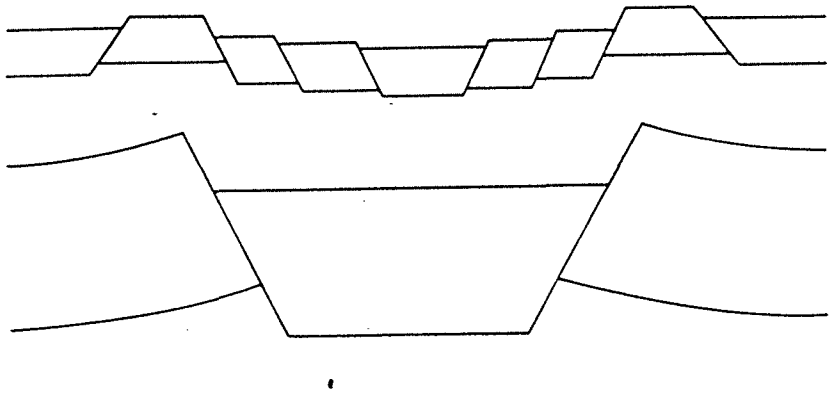

Figure 2. Schematic diagram of a modified Vening Meinesz model for rift formation on Venus, with the strong mantle layer controlling rift width and the brittle crustal layer controlling fault spacing.

References

[1] Solomon, S.C. and J.W. Head (1984) Venus banded terrain: Tectonic models for band formation and their relationship to lithospheric thermal structure, JGR, 89, 6885-6897.

[2] Morgan, P. and R.J. Phillips (1983) Hot spot heat transfer: Its application to Venus and implications to Venus and Earth, JGR, 88, 8305-8317.

[3] McGill, G.E., S.J. Steenstrup, C. Barton and P.G. Ford (1981) Continental rifting and the origin of Beta Regio, Venus, GRL, 8, 737-740.

[4] Schaber, G.C. (1981) Venus: Limited extension and volcanism along zones of lithospheric weakness, GRL, 9, 499-502.

[5] Zuber, M.T., E.M. Parmentier and J.W. Head (1985) Ductile lithosphere extension: Implications for rifting on the earth and Venus (abs.), Lunar Planet. Sci. XVI, 948-949.

[6] Byerlee, J. (1978) Friction of rocks, Pageoph, 116, 615-626.

[7] Brace, W.F. and D.L. Kohlstedt (1980) Limits on lithospheric stress imposed by laboratory experiments, JGR, 85, 6248-6352.

[8] Kirby, S.H. (1980) Tectonic stresses in the lithosphere: Constraints provided by the experimental deformation of rocks, JGR, 85, 6353-6363.

[9] Vink, G.E., W.J. Morgan and W.-L. Zhao (1984) Preferential rifting of continents: Asource of displaced terranes, JGR, 89, 10072-10076.

[10] Smith, R.B. and R.L. Bruhn (1984) Intraplate extensional tectonics of the eastern basin-range: Inferences on structural style from seismic reflection data, regional tectonics, and thermal-mechanical models of brittle-ductile deformation, JGR, 89, 5733-5762.

[11] Banerdt, W.B. and M.P. Golombek (1985) Lithospheric strengths of the terrestrial planets (abs.), Lunar Planet. Sci. XVI, 23-24.

[12] Solomon, S.C. (1985) The elastic lithosphere: Some relationships among flexure, depth of faulting, lithosphere thickness, and thermal gradient (abs.), Lunar Planet. Sci. XVI, 799-800.

[13] Morgan, P. and M.P. Golombek (1984) Factors controlling the phases and styles of extension in the northern Rio Grande rift, N.M. Geol. Soc. Guide. 35th Field Conf., 13-19.

[14] Shelton, G. and J. Tullis (1981) Experimental flow laws for crustal rocks (abs.), EOS Trans. AGU, 62, 396.

[15] Goetze, C. (1978) The mechanisms of creep in olivine, Phil. Trans. R. Soc. Lond., A288, 99-119.

[16] Vening Meinesz, F.A. (1950) Les graben africains, résultat de compression ou de tension dans la croûte terrestre?, Bull. Inst. R. Colon. Belge, 21, 539-552.

[17] Bott, M.H.P. (1976) Formation of sedimentary basins of graben type by extension of the continental crust, Tectonophys., 36, 77-86.

[18] Banerdt, W.B. (1985) Support of long wavelength loads on Venus and implications for internal structure, submitted to JGR.

THERMAL REGIMES IN THE DETACHMENT FAULT ENVIRONMENT AS DEDUCED FROM FLUID INCLUSIONS; Richard E. Beane, AMAX Exploration, Inc., Tucson, Arizona, Joe Wilkins, Jr., St. Joe American, Tucson, Arizona, Tom L. Heidrick, Gulf Oil Corp., Bakersfield, California

Extensional tectonism, which dominates middle- and late-Tertiary geology in western Arizona, southeastern California, and southern Nevada, is characterized by normal displacement of Precambrian through Tertiary rocks along regionally extensive, low-angle detachment faults. The decollement movement of upper plate rocks relative to lower plate assemblages created extensive zones of dilatency, including synthetic and antithetic listric normal faults, tear faults, tectonic crush breccias, shatter breccias, and gash veins in lithologic units above and below the detachment. The tectonically enhanced permeability above and below the detachment fault permitted mass migration of large volumes of hydrothermal solutions along the fault zone during and following upper plate movement. Major quantities of MgO, CaO, K_2O, FeO/Fe_2O_3, SiO_2 and CO_2 were added to rocks in and near the detachment and related structures. Also introduced were varying amounts of trace elements including Mn, Cu, S, Mo, Ba, Au, Pb, Zn, U and/or Ag. Deposition of sulfide/oxide minerals and gangue containing all or part of this elemental suite occurred in the following loci, which are keyed to Figure 1. Minerals containing fluid inclusions were

1. Along the detachment fault.
2. Replacing reactive units.
3. Listric fault breccias.
4. Gash veins.
5. Fold axes.
6. Chlorite breccia.
7. Tear fault zones (parallel to Figure 1 section).

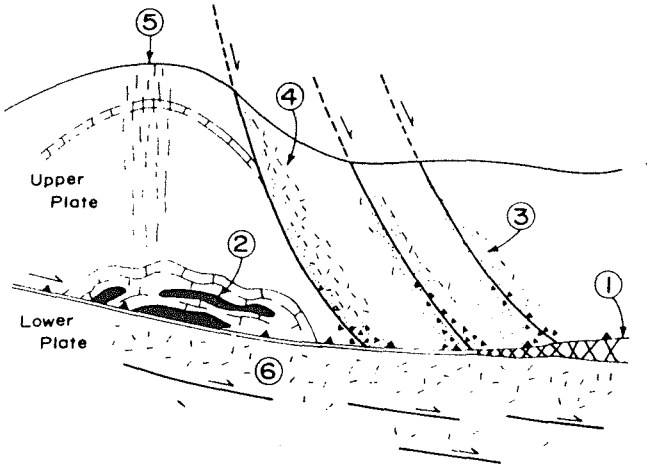

Figure 1. Structural-tectonic model of mineralization loci related to the detachment fault process (after Wilkins and Heidricks, 1980).

collected from all of these loci at locations in detachment faulted terranes in western Arizona and southeastern California.

Fluid inclusions are small cavities in minerals which form by entrapment of fluid in crystal irregularities during or after formation. In hydrothermal systems, these inclusions often provide a record of temperatures and salinities of the aqueous fluids from which minerals were precipitated. Fluid inclusions from minerals in detachment fault environments are consistently filled with a liquid accompanied by a relatively small vapor bubble (less than 30 volume percent), occasionally small daughter-product minerals are present. Freezing temperatures of liquids yield equivalent NaCl salinities of the included solutions. Temperature of homogenization of the liquid and gas phases when heated to a single high-density fluid phase provide minimum formation temperatures. By analogy, the temperature of formation of synkinematic mineralization provides a measure of the heat present during the detachment fault process.

Fluids flowing through structures temporally and spatially related to detachment phenomona precipitated quartz, specular hematite, chlorite, calcite, and lesser amounts of sulfide minerals. Inclusion fluids in the transparent phases from the above group are hypersaline, having salinities predominantly in the range 12 to 20 weight percent NaCl equivalent. Corresponding homogenization temperatures are in the range 200° to 325°C. There is no systematic relationship between homogenization temperature and salinity of these fluid inclusions. Younger and/or spatially higher fluids, were localized along listric or tear faults, produced a mineral assesmblage characterized by brown hematite, barite, fluorite, chrysocolla, and precious metals. Inclusions containing these fluids have generally lower homogenization temperatures (125° to 225°C) and somewhat lower salinities (5 to 20 weight percent NaCl equivalent) than the earlier/higher level fluids. Homogenization temperatures of both of these groups of fluid inclusions must be corrected upward at a rate of 75° to 100°C per kilobar of pressure obtaining at the time of fluid entrapment in order to define the actual formation temperatures of the minerals. The temperature-salinity relationship for all fluid inclusion determinations is shown on Figure 2.

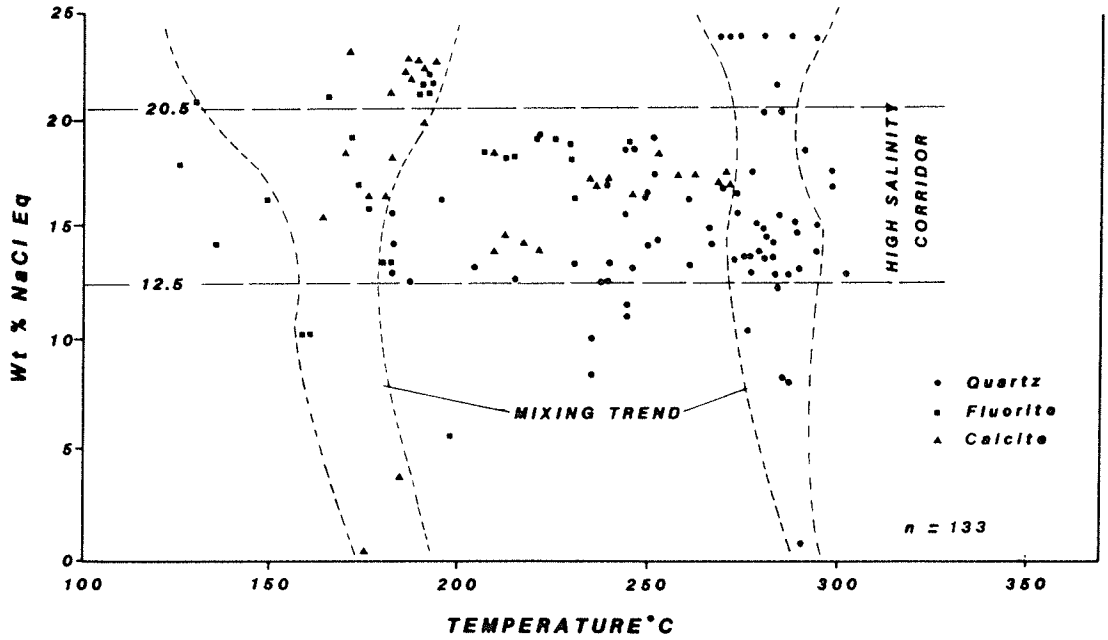

Figure 2. Homogenization temperature and salinity diagram for detachment fault-related mineralization.

The persistently high salinities (the high-salinity corridor on Figure 2) over a considerable range of apparent formation temperatures suggests that significant mixing with more dilute fluids is absent over an appreciable period of time at or near the detachment surface. However, mixing trends are recognized in the generally later and/or structurally higher-level fluids; two such trends are shown on Figure 2. Consistently high salinities of fluids associated with detachment fault mineralization could represent derivation from either 1) an igneous source, 2) basinal brines, or 3) semi-permeable filtration of originally less saline fluids. The presence of petroleum daughter-products or methane (CH_4) gas under pressure in the hypersaline and/or lower-salinity fluid types at several locations suggests that the solutions were derived from Tertiary orogenic basins. The temperatures obtained by the saline fluids flowing near the detachment structure were probably derived initially from deep basin burial in an elevated geothermal gradient and were augmented and maintained by heat supplied in or near the detachment fault.

(1) Wilkins, J. Jr., and Heidrick, T. L., 1982, Base and precious metal mineralization related to low-angle tectonic features in the Whipple Mountains, California and Buckskin Mountains, Arizona, in Frost, E. G., and Martin, D. L., eds., Mesozoic-Cenozoic tectonic evolution of the Colorado River region, California, Arizona, and Nevada: San Diego, Calif., Cordilleran Publishers, p. 182-204.

HEAT FLOW AND CONTINENTAL BREAKUP: THE GULF OF ELAT (AQABA)

Zvi Ben-Avraham, Dept. of Geophysics & Planetary Sciences, Tel Aviv University
Richard P. Von Herzen, Dept. of Geology and Geophysics, Woods Hole Oceanographic Institution, Woods Hole, MA 02543

Heat flow measurements were made in the major basins of the Gulf of Elat (Aqaba), northern Red Sea. The gulf is located at the southern portion of the Dead Sea rift which is a transform plate boundary. Gradient measurements at each site were made with a probe which allows multiple penetration of the bottom during a single deployment of the instrument. Thermal conductivity was determined by needle probe measurements on sedimentary cores.

The mean heat flux, about 80 mWm^{-2}, is significantly above the continental mean, and probably also above that from the adjacent Sinai and Arabian continental blocks. The heat flow appears to increase from north to south. Such an increase may be related to the more advanced rifting stage of the Red Sea immediately to the south, which presently includes creation of an oceanic crust. This trend also corresponds to the general trend of the deep crustal structure in the gulf. Evidence from various geophysical fields suggest a gradual thinning of the crust towards the direction of the Red Sea where a normal oceanic crust exists. The heat flow data, together with other geophysical data, indicate a propagation of mature rifting activity from the Red Sea into the Gulf of Elat. This process is acting simultaneously with the transform motion along the Dead Sea rift.

Figure 1: Geophysical profile along the axis of the Gulf of Elat. From top to bottom: heat flow, Bouguer gravity anomaly, free air gravity anomaly, magnetic anomaly, bathymetry and depth of Moho on the western margin.

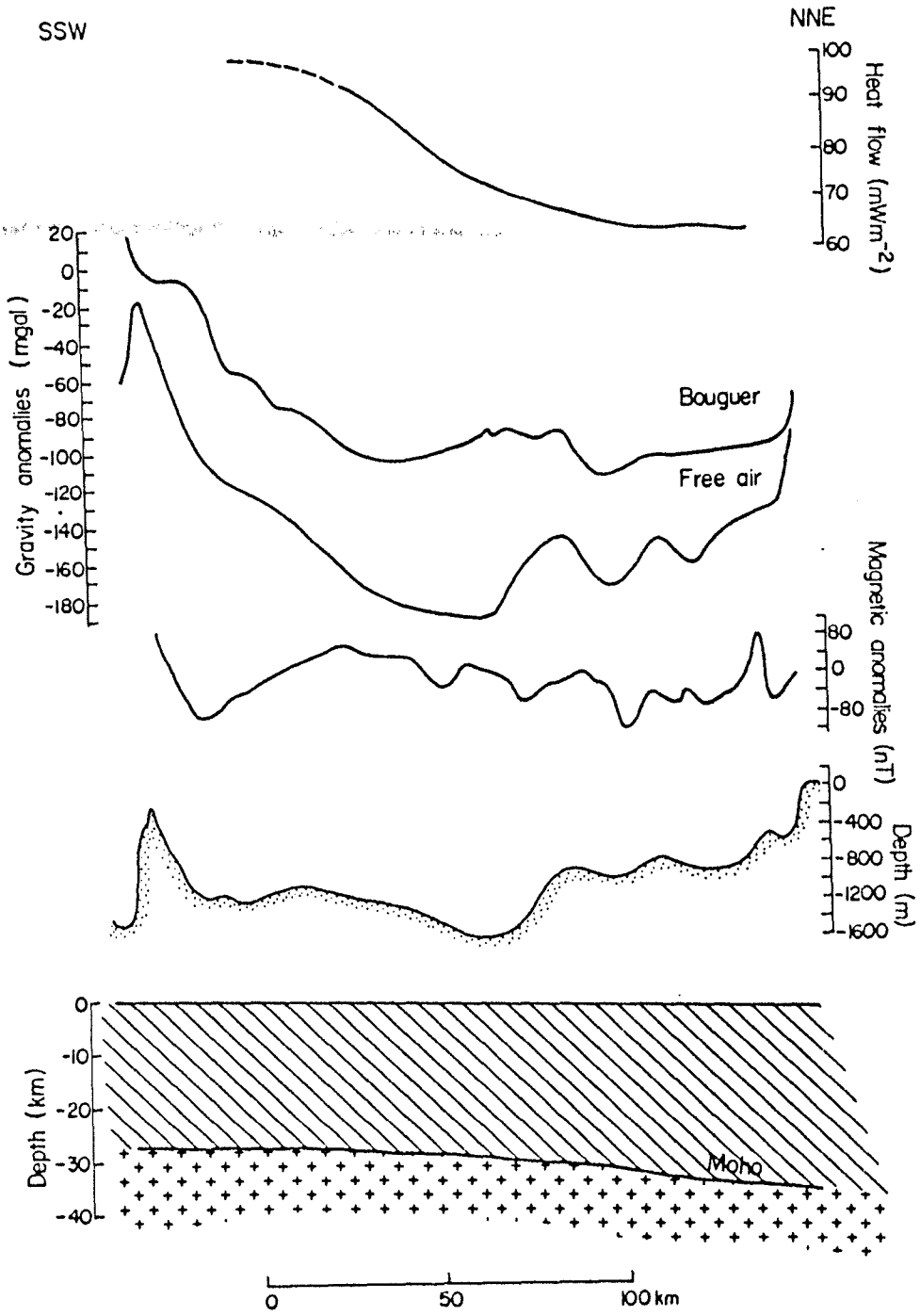
SSW
NNE
100
90
80
70
60
Heat flow (mWm⁻²)
20
0
-20
-40
-60
-80
-100
-120
-140
-160
-180
Gravity anomalies (mgal)
Bouguer
Free air
80
0
-80
Magnetic anomalies (nT)
0
-400
-800
-1200
-1600
Depth (m)
0
-10
-20
-30
-40
Depth (km)
Moho
0
50
100 km

EVOLUTION OF BASIN AND RANGE STRUCTURE IN THE RUBY MOUNTAINS AND VICINITY, NEVADA: D. D. Blackwell, N. M. Reese and S. A. Kelley, Department of Geological Sciences, Southern Methodist University, Dallas, TX 75275

The Ruby Mountains of central Nevada are one of the infrastructure regions exposed in the Basin and Range Province. Geologic studies of the Ruby Mountain have been carried out by Snoke and Howard (1984). We have used the results from various age dating techniques, seismic reflection profiling, hydrocarbon maturation studies, and structural analysis to evaluate the Cenozoic deformation in the Ruby Mountains and adjoining ranges (Pinyon Range and Cortez Range) in Elko and Eureka Counties, Nevada. Age dating techniques used include potassium-argon ages of biotites from granites published by Kistler et al. (1981) and fission track ages from apatite and zircon. Fission track ages from apatite reflect a closing temperature of 100±20°C, zircon fission track ages reflect a closing temperature of 175±25°C and potassium-argon ages from brotite reflect a closing temperature of 250±30°C. Thus these results allow a reasonably precise tracking of the evolution of the ranges during the Cenozoic. Seismic reflection data are available from Huntington Valley. The northeastern part of the valley is discussed in detail by Smith (1984). We have obtained access to seismic reflection data directly to the west of the Harrison Pass pluton in the central Ruby Mountains. In addition results are available from several deep exploration holes in Huntington Valley.

Age dating traverses across the Ruby Mountains at the latitude of the Harrison Pass pluton and to the north establish a progressive younging of ages from east to west across the range. This trend is reflected in both the apatite, zircon, and potassium-argon ages. Potassium-argon ages along the east flank of the range are about 35 MY. Along the west side of the range the potassium-argon ages are 20 to 25 MY. Apatite ages show a similar trend of

younging from east to west with values of 20 to 25 MY on the east and 10 to 15 MY on the west. Assuming the indicated closing isotherms and a background geothermal gradient 30°C/km (about the present Basin and Range value), the approximate rates of uplift are on the order of 0.5 km/MY.

The younging of ages from east to west across the central Ruby Mountains suggests that rates of uplift along the western side of the range have been faster than on the east side of the range. Our interpretation of the data is that the range block has been rotated to the east about 30° with the rotation beginning approximately 25 MYbp and continuing until at least 15 MYbp. During this period of rotation a set of early west dipping Basin and Range normal faults was truncated and rotated from high angle to low angle dips. As in many other areas the low angle faults have been mapped as thrust faults. However, the age data clearly document the rotation that has turned these high angle faults into low angle structures. Account has been taken in the interpretation of the effect of the emplacement of the Harrison Pass pluton at about 36 MY. The present range is blocked out by a subsequent set of high angle faults that is still active.

An interesting result of this deformation is that a Basin and Range geothermal system along the original high angle faults has been truncated and rotated up to present day exposure along the west-central part of the range. Silicification associated with this fossil geothermal system has been encountered in an exploration test in the Huntington Valley as well (Snoke, personal communication, 1984), documenting the basinward position of the rotated fault.

Interpretation of seismic reflection data extending from the west side of the Harrison Pass pluton for a distance of 22.4 km west across Huntington Valley support the uplift and structural interpretations from the age dating

evidence. In the seismic reflection profile adjacent to Harrison Pass, large scale faults are the dominant structural feature. These faults dip west into the basin cutting the contact between Paleozoic carbonate and Cenozoic clastical volcanic rocks, and terminating in subhorizontal reflectors at depth. In contrast the central and eastern parts of the reflection profile show very little evidence of normal faulting. Where normal faulting is recognized it is restricted to the Cenozoic rocks filling the basin. Eastward dipping reflectors in Cenozoic strata in the basin indicate that tilting may have been accommodated by movement along the normal faults. Associated with the tilting, a shift in sedimentation from the center of the basin eastward has resulted in an asymmetric basin with a thick wedge of sediment developed adjacent to the western front of the Ruby Mountains.

A combination of the relatively precise information on the timing and rate of uplift in the range associated with the structural information of the basin, allow an accurate reconstruction of the nature of Cenozoic deformation in the Ruby Mountains. This reconstruction, in conjunction with the regional setting, suggests that the Ruby Mountains are locally unique in that they reflect rapid erosion and uplift of deep crustal levels to shallow depths. The mechanism responsible for this behavior is postulated to be local ductile and brittle deformation of the crust in response to rapid unloading of a small portion of the crust by erosion or tectonic denudation.

Kistler, R.W., Ghent, E.D., and O'Neil, J.R. 1981. Petrogenesis of garnet two-mica granites in the Ruby Mountains, Nevada. J. Geophys. Res., 86, p.10591-10606.

Smith, K.A. 1984. Normal faulting in an extensional domain: Constraints from seismic reflection interpretation and modeling, M.S. Thesis, University of Utah, 165pp.

Snoke, A.W., and Howard, K. 1984. Geology of the Ruby Mountains-East Humboldt Range: A Cordilleran metamorphic core complex. Geol. Soc. Amer. Western Geol. Excursions, 4, p.260-303.

LATE CRETACEOUS EXTENSIONAL TECTONICS AND ASSOCIATED IGNEOUS ACTIVITY ON THE NORTHERN MARGIN OF THE GULF OF MEXICO BASIN

R. L. Bowen, D. A. Sundeen, Boxes 8152 & 8196, University of Southern Mississippi, Dept. of Geology, Hattiesburg, MS, 39406

Major, dominantly compressional, orogenic episodes (Taconic, Acadian, Alleghenian) affected eastern North America during the Paleozoic. During the Mesozoic, in contrast, this same region was principally affected by epeirogenic and extensional tectonism; one episode of comparatively more intense tectonic activity involving extensive faulting, uplift, sedimentation, intrusion and effusion produced the Newark Series of deposits and fault block phenomena. This event, termed the Palisades Disturbance, took place during the Late Triassic - Earliest Jurassic. In the present study, the authors document a comparable, although smaller in area affected, extensional tectonic-igneous event occurring during the Late Cretaceous (Early Gulfian; Cenomanian-Santonian) along the southern margin of the cratonic platform from Arkansas to Georgia (1).

Following extensive evaporite deposition (Louann Salt), in the later Jurassic and Early Cretaceous, petroliferous sands, mudstones and carbonates, with some evaporites, accumulated in the northern Gulf of Mexico area. Generally mature sedimentologically, these strata mostly thicken, while becoming finer grained, from the northern basin border southward towards the Gulf. As a package, they contrast markedly with the Late Cretaceous (Gulfian) units overlying them.

From the beginning of Gulfian time (ca 98 m.y.; early Cenomanian), warping, uplift, and igneous activity on an impressive scale affected the southern margin of the cratonic platform and the northern margin of the contemporaneous depositional basin. Deposits of the basal Upper Cretaceous Tuscaloosa Group, unconformably overlying a varied suite of rocks from Tennessee to the Carolinas around the southern Appalachians, rich in gravels (locally cobbly to bouldery) in the outcrop, record a major pulse of uplift of the southern Appalachians; some calculations suggest summits may have reached 3-4 km elevations at that time. These strata, non-marine and approximately 200 m thick in outcrop, thicken to >1 km southwesterly from the Appalachians while becoming a mixed sequence of continental and marine sands and mudstones. The sediments are largely immature and rich in volcaniclastics in the Mississippi Embayment region. Moreover, this interval of sedimentation coincides in time with the northward extension of the Mississippi Embayment into southern Illinois from a Lower Cretaceous border in southern Arkansas. This new depositional sag was a consequence of mild uplift in the Ouachita-Ozark region to the west and in the Appalachian Plateau region to the east.

Crustal extension, documented by warping and uplift along the eastern and western edges of the Mississippi Embayment and

the rapidly subsiding Gulf depocenter, also generated (or was generated by) fractures down into the mantle through which, synchronously, many irruptions rose (2). Kimberlite was injected into western Arkansas, while many alkalic dikes (lamprophyres) along with several carbonatite and nepheline syenite stocks invaded the Arkansas Ouachitas. South and east of these exposed hypabyssal rocks, petroleum exploration has disclosed numerous occurrences of igneous rocks within the sedimentary rocks of the Mississippi Embayment region overlapping parts of Arkansas, Louisiana, and Mississippi (3,4,5). Volcanic extrusive, hypabyssal, and volcaniclastic sediments occur in most wells which penetrate Cretaceous and older strata in this region. Twelve K-Ar isotope ages (72 to 91 m.y.) have been determined from selected cores and cuttings of igneous rocks from wells drilled in five counties in central-western Mississippi (4,5,6,7). Volcanic complexes, of at least 25 km diameter, such as the Jackson Dome, Sharkey Uplift, Midnight Volcano, and the Monroe Platform, have been defined in the process of oil and gas exploration; moreover, large gravity and magnetic anomalies suggest that comparable complexes occur beneath northwestern Mississippi and southeastern Arkansas in the vicinity of the Desha Basin (8).

The major effects of the extensional and thermal disturbance we here define are limited to the Lower Upper Cretaceous (Cenomanian - Turonian; 97 - 88 m.y.), although volcanism persisted at least to the end of the Campanian (73 m.y.) as reefoid deposits developed around the Jackson Volcano and others which rose through the Selma - Austin chalk seas.

REFERENCES

(1) Bowen, R. L. (1975) Post-Pennsylvanian geologic history of the southeastern United States: economic geology. Transactions - Gulf Coast Association of Geological Societies, v. 25, p. 100-103.

(2) Kidwell, A. L. (1949) Mesozoic igneous activity in the northern Gulf Coastal Plain. PhD dissertation, University of Chicago, 317 pages.

(3) Cook, P. L. (1975) Petrography of an Upper Cretaceous volcanic sequence in Humphreys County, Mississippi. MSc thesis, University of Southern Mississippi, 66 pages.

(4) Sundeen, D. A. (1979) Petrology and geochemistry of subsurface igneous rocks in Humphreys and Sharkey counties, Mississippi. Final Report on Project MMRI #787, Mississippi Mineral Resources Institute, University, MS, 38677, 122 pages, appendix, plates.

(5) Sundeen, D. A. (1980) Petrology and geochemistry of igneous rocks in Washington and Issaquena counties, west-central Mississippi. Final Report on Project #80-7S, Mississippi Mineral Resources Institute, University, MS, 38677, 731 pages, plates.

(6) Braunstein, J. and McMichael, C. E. (1976) Door Point: a buried volcano in southeast Louisiana. Transactions - Gulf Coast Association of Geological Societies, v. 26, p. 79 - 80.8

(7) Sundeen, D. A. and Cook, P. L. (1977) K-Ar dates from Upper Cretaceous volcanic rocks in the subsurface of west-central Mississippi. Geological Society of America Bulletin, v. 88, p. 1144-1146.

(8) Mallette, K. A. and Sundeen, D. A. (1977) Gravity-magnetic anomalies and Upper Cretaceous structure in west-central Mississippi. Geological Society of America Abstracts with Programs, v. 9, no. 2, p. 162-163.

A REGIONAL 17-18 MA THERMAL EVENT IN SOUTHWESTERN ARIZONA

William E. Brooks, U.S. Geological Survey, Denver, CO

A regional thermal event in southwestern Arizona 17-18 Ma ago is suggested by discordances between fission track (FT) and K-Ar dates in Tertiary volcanic and sedimentary rocks, by the abundance of primary hydrothermal orthoclase in quenched volcanic rocks, and by the concentration of Mn, Ba, Cu, Ag, and Au deposits near detachment faults. A high conodont alteration index (CAI) of 3 to 7, is found in Paleozoic rocks of southwestern Arizona (1). The high CAI may have been caused by this mid-Tertiary thermal event.

Resetting of temperature-sensitive FT dates (2) to 17-18 Ma with respect to K-Ar dates of 24 and 20 Ma has occurred in upper plate volcanic rocks at the Harcuvar and Picacho Peak detachments (3). Discordances between FT and K-Ar dates are most pronounced at detachment faults. However, on a regional scale FT dates from volcanic and sedimentary rocks approach 17-18 Ma, even in areas away from known detachment faults (fig. 1). Effects of detachment faulting on the K-Ar system suggest that dates of correlative rocks will be younger as the detachment fault is approached (4).

Anomalously high K_2O is common in volcanic and sedimentary rocks in the southwestern United States (5,6). In Arizona, anomalously high K_2O is present at the Harcuvar Mountains, 12 weight percent K_2O (7) and Picacho Peak detachments, 13 weight percent K_2O (8), and in listric faulted terrane in the Vulture Mountains area, 12 weight percent K_2O (9).

Introduction of hydrothermal potassium has resulted in anomalous orthoclase (2 to 10 microns) in upper plate volcanic rocks at the Picacho Peak, Harcuvar, and Trigo detachments. K-Ar dates on metasomatized rocks are suspect because the date becomes a function of potassium available upon eruption and potassium introduced during the detachment/metasomatic event 17-18 Ma.

Mineralization and potassium metasomatism caused by hydrothermal fluids is common near the detachments. Mn and Ba as well as Ag, Au, Cu, Pb, and Zn deposits are localized near most detachments (10,11,12,13). The presence of metasomatized and mineralized rock at the detachment faults indicates that the faults were likely pathways for the mineralizing fluids. Zirconium, considered to be an immobile element, occurs in concentrations as great as 350 ppm at the Picacho Peak detachment and decreases to a normal concentration of about 180 ppm (14,15) 7 km from the surface trace of the fault. Li, As, Zn, Ce, and Cd are also spatially distributed.

Paleozoic rocks with a high conodont alteration index (CAI of 3 to 7) indicate that a minimum regional temperature of 250°C was reached in southwestern Arizona. Correlative rocks in northeastern Arizona have a much lower CAI of 2 or less (1) where regional metamorphism should have affected the rocks equally. Also, several of the high CAI sites in southwestern Arizona are not near any mapped intrusions. Therefore, alteration of the conodonts by the 17-18 Ma thermal event seems likely.

A regional thermal event is postulated for southwestern Arizona 17-18 Ma. The event caused reheating, as indicated by discordances between FT and K-Ar dates; potassium metasomatism as indicated by primary hydrothermal orthoclase in volcanic rocks; and concentration of Mn, Ba, and Zr as well as Cu, Ag, and Au at detachment faults in southwestern Arizona.

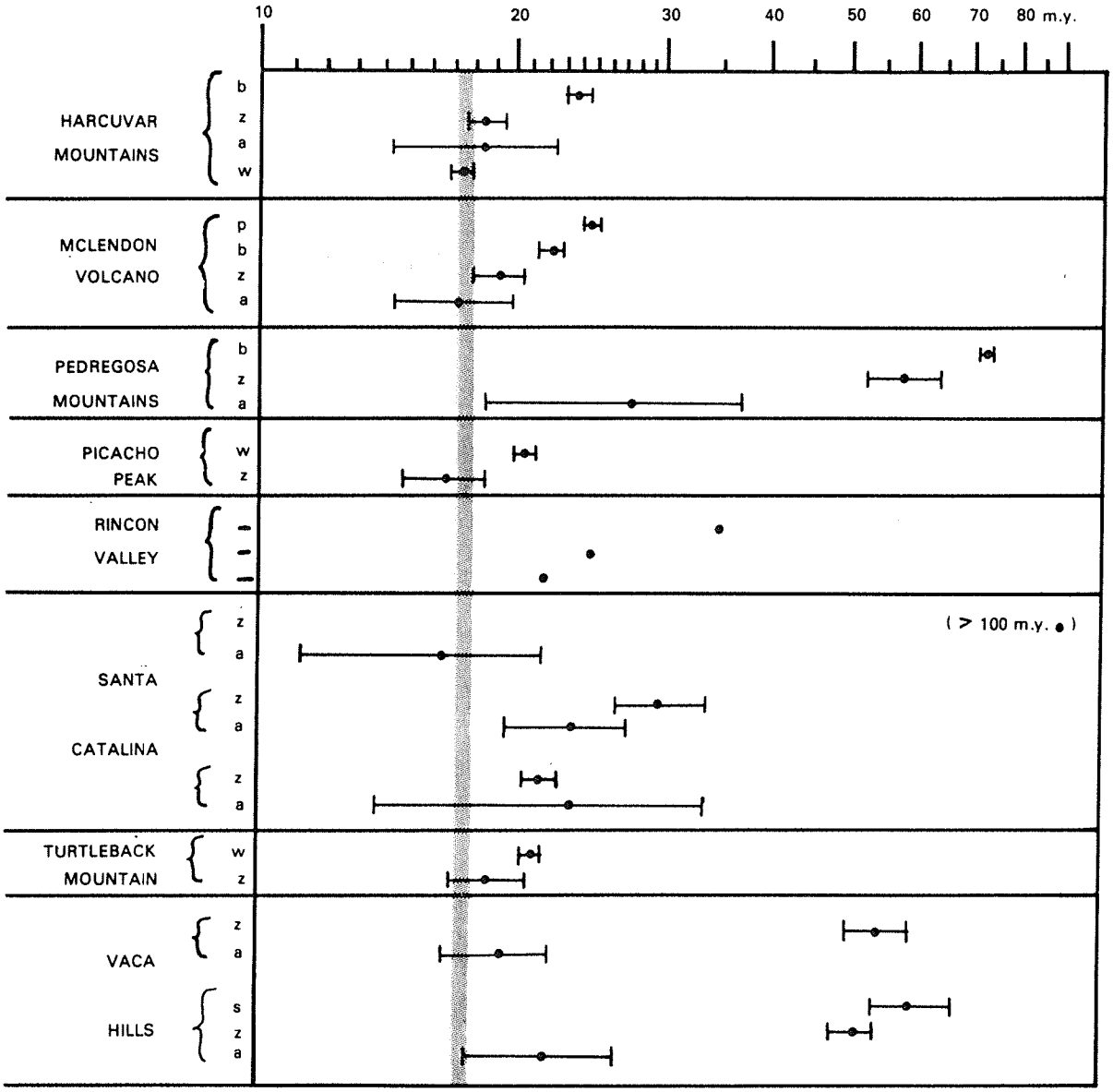

Figure 1.--Discordant FT and K-Ar dates from southwestern Arizona. Stippled pattern emphasizes 17-18 Ma. Brace indicates dates from a single sample; FT, a-apatite, z-zircon, s-sphene; K-Ar, b-biotite, p-plagioclase, w-whole rock. Harcuvar Mountains detachment, volcanic, b-(16), w-(17); McLendon volcano, volcanic, p-(18)., b-(16); Pedregosa Mountains, volcanic, b-(16); Picacho Peak detachment, volcanic, w-(8); Rincon Valley, volcanic, - no mineral or standard deviation given, (19); Santa Catalina detachment, sedimentary (20); Turtleback Mountain, volcanic, w-(21); Vaca Hills, volcanic, (22); all other dates by author.

REFERENCES CITED

(1) Wardlaw, B. R., and Harris, A. G., 1984, Conodont-based thermal maturation of Paleozoic rocks in Arizona: Am. Assoc. Petrol. Geologists Bulletin, v. 68, p. 1101-1106.
(2) Naeser, C. W., 1976, Fission-track dating: U.S. Geological Survey Open-File Report 76-190, 31 p.
(3) Brooks, W. E., and Marvin, R. F., 1985, Discordant isotopic ages and potassium metasomatism in volcanic rocks from Yavapai County, Arizona (abs.): Geol. Soc. America Abs. with Programs, v. 17.
(4) Martin, D. L., Krummenacher, D, and Frost, E. G., 1981, Regional resetting of the K-Ar isotopic system by mid-Tertiary detachment faulting in the Colorado River region, California, Arizona, and Nevada (abs.): Geol. Soc. America Abs. with Programs, v. 13, n. 7, p. 504.
(4) Chapin, C. E., and Glazner, A. F., 1983, Widespread K_2O metasomatism of Cenozoic volcanic and sedimentary rocks in the southwestern United States (abs.): Geol. Soc. America Abs. with Programs, v. 15, p. 282.
(6) Lindley, J. I., D'Andrea Dinkleman, J. F., Glazner, A. F., and Osburn, G. R., 1983, Chemical and mineralogic variations associated with potassium metasomatism of Tertiary volcanic rocks from the Rio Grande Rift and Mojave Desert (abs.): Geol. Soc. America Abs. with Programs, v. 15, p. 282.
(7) Brooks, W. E. 1984, Volcanic stratigraphy of part of McLendon volcano, Anderson Mine area, Yavapai County Arizona: U.S. Geological Survey Open-File Report 84-350, 42 p.
(8) Shafiqullah, M., Lynch, D. J., Damon, P. E., and Pierce, H. W., 1976, Geology, geochronology, and geochemistry of the Picacho Peak area, Pinal County, Arizona: Arizona Geological Society Digest, v. 10, p. 305-324.
(9) Rehrig, W. A., Shafiqullah, M., and Damon, P. E., 1980, Geochronology, geology, and listric normal faulting of the Vulture Mountains, Maricopa County, Arizona: Arizona Geological Society Digest, v. 12, p. 89-110.
(10) Garner, W. E., Frost, E. G., Tanges, S. E., and Germinario, M. P., 1982, Mid-Tertiary detachment faulting and mineralization in the Trigo Mountains, Yuma, Arizona: in Frost, E. G., and Martin, D. L., eds., Mesozoic-Cenozoic tectonic evolution of the Colorado River Region, California, Arizona, and Nevada (Anderson-Hamilton volume): Cordilleran publishers, San Diego, p. 159-171.
(11) Keith, S. B., Schnabel, L., DeWitt, E., Gest, D. E., and Wilt, J., 1983, Map, description, and bibliography of the mineralized areas of the Basin and Range province in Arizona: U.S. Geological Survey Open-File Report 84-0086, 129 p.
(12) Meyers, I. A., Smith, E. I., and Wyman, R. V., 1984, Relationship of mineralization to detachment faulting at the Cyclopic mine, Mohave County, northwestern Arizona (abs.): Geol. Soc. America Abs. with Programs, v. 16, p. 324.
(13) Naruk, S. J., 1984, A model for detachment fault gold mineralization (abs.): Geol. Soc. America Abs. with Programs, v. 16, p. 607.
(14) Turekian, K. K., and Wedepohl, K. H., 1961, Distribution of elements in some major units of the earth's crust: Geol. Soc. America Bull., v. 72, p. 175-192.

(15) Taylor, S. R., 1969, Trace element chemistry of andesites and associated calc-alkaline rocks: in Proceedings of the Andesite Conference, Oregon State Dept. of Geology and Mineral Industries Bull., v. 65, p. 43-64.
(16) Marvin, R. F., 1982, written communication.
(17) Scarborough, R. B., and Wilt, J. C., 1979, A study of the uranium favorability of Cenozoic sedimentary rocks, Basin and Range Province, Arizona: U.S. Geological Survey Open-File Report 79-1429, 101 p.
(18) Suneson, Neil, 1978, written communication.
(19) Thorman, C. H., and Drewes, Harald, 1981, Mineral resources of the Rincon Wilderness Study area, Pima County, Arizona: U.S. Geological Survey Bulletin 1500, 62 p.
(20) Naeser, C. W., 1984, written communication.
(21) Shafiqullah, M., Damon, P. E., Lynch, D. J., Reynolds, S. J., Rehrig, W. A., and Raymond, R. H., 1980, K-Ar geochronology and geologic history of southwestern Arizona and adjacent areas: Arizona Geological Society Digest, v. 12, p. 201-260.
(22) Banks, N. G., Dockter, R. D., Silberman, M. L., and Naeser, C. W., 1978, Radiometric ages of some Cretaceous and Tertiary volcanic and intrusive rocks in south-central Arizona: U.S. Geological Survey Journal of Research, v. 6, p. 439-445.

GEOMETRIC AND CHRONOLOGIC EVOLUTION OF THE VERDE AND PAYSON BASINS OF CENTRAL ARIZONA AND POSSIBLE RELATIONSHIPS TO DETACHMENT FAULTING; D. S. Brumbaugh, Dept. of Geology, Box 6030, NAU, Flagstaff, AZ 86011

The Transition Zone of Arizona and the structural basins therein have been poorly understood features from a structural standpoint. This is true both of their overall geometry as well as their formation. Yet these basins have developed within the last 13 million years and thus represent perhaps the most recent phase of development related to the extensional tectonics of the Basin and Range province.

Recent work (Smith, 1984; Vance, 1983) as well as some older studies (Anderson and Creasy, 1958; Pedersen and Royce, 1970) provide data on the geometry of the Verde and Payson basins which can be used to constrain some hypotheses related to the development of these basins.

The work of Cloos (1968), Anderson et. al. (1983), Wernicke and Burchfiel (1982) and Davis et. al. (1980) suggest a spatial and chronologic relation exists between planar high angle normal faults and low angle detachment faults. Perhaps one of the clearest examples from the Basin and Range area appears to be from seismic reflection profiles of the Sevier Desert Basin area of Utah (Fig. 1). These profiles suggest the existence of a detachment surface which acts as a zone of structural accommodation for fault-controlled extensional basin development above it. Faults that appear either listric or planar intersect it from above. Note that the basins are asymmetric with the basin deepening in the direction of dip of the detachment surface.

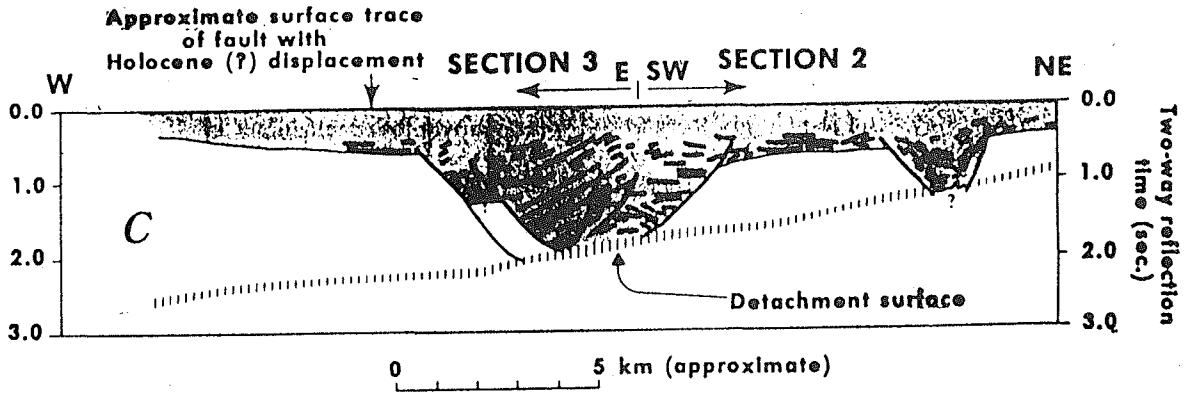

Figure 1. Seismic line across Sevier Desert Basin (Anderson et. al. Figure 7).

The question of interest then is whether or not the Verde and Payson basins might be related to a detachment fault at depth. This question can be discussed by taking the known geometry of the basins and comparing them to such a detachment fault model.

The Verde Valley is a structural basin which appears to be very similar to structures produced in Cloos' (1968) classic clay model experiments. One side of his basin was dominated by a master normal fault with displacement on the other side being accommodated by a number of smaller faults. The Verde Normal fault with over 2,000' of stratigraphic offset dominates the west boundary of the Verde Valley. It is a high angle planar normal fault. This is suggested by map trace, lack of rotation of the beds, and mining information.

The Payson basin, although less well known, appears quite similar with the west side of the basin bounded by a large fault. The Payson basin appears less mature with less offset on the master fault, and a thinner sequence of basin fill than the Verde Valley.

Radiometric (McKee and Anderson, 1971) and faunal (Nations et. al., 1982) data suggest that both basins began to develop at about the same time about 13 my ago. Chronologically this agrees well with the documented age of movement on the Rawhide detachment fault of SW Arizona 16-9 mya (Shackelford, 1980). If these basins are related to movement on the detachment fault there must be a spatial, as well as chronologic relation. The spatial question may be addressed by using as a starting point the Sevier Desert Basin model, and assuming that the planar high faults forming the Verde and Payson basins probably terminate against a projection of the Rawhide fault to the NE under these basins and further under the Colorado Plateau. This projection of the Rawhide Fault has been suggested (Shackelford, 1980) and would answer questions raised about the continuation of the Rawhide detachment fault.

The method used to analyze the question of possible spatial relation between the basin and detachment faults is one of projection based on the Sevier Desert Basin detachment fault. The planar high angle faults of the Verde basin are projected downward to locate an intersect point (Fig. 2). This is done for a number of profiles across the Verde Valley from Smith (1984). These intersect points represent the lowest possible points that would lie along the projected Rawhide detachment fault surface based on the Sevier Desert Basin model. The Rawhide detachment fault may be projected under the Verde basin by taking several reasonable average dips from the outcrop area and projecting to the northwest.

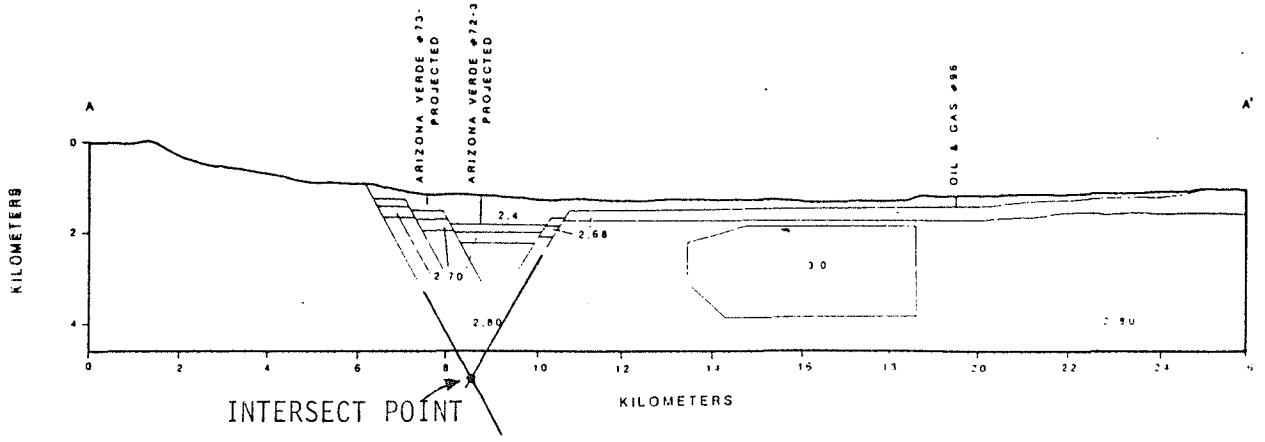

Figure 2. Verde Valley cross section A-A' (Smith, 1984, after Figure 5b)

The results of geometric projection suggest that the Rawhide fault does not appear to be a suitable candidate for a detachment fault for the Verde and Payson basins based on the Sevier Desert Basin model. This raises some interesting questions about the formation of these basins and detachment faults in general. Should other detachment fault-basin models be developed which would fit the Verde and Payson basins better? Do other detachment faults exist which have not been adequately recognized which would fit the spatial situation better? Or perhaps are the Verde and Payson Basins not related to detachment fault tectonics at all in their development?

REFERENCES CITED

Anderson, C.A., and Creasy, S.C. (1958). Geology and ore deposits of the Jerome area, Yavapai County, Arizona. U.S. Geological Survey Professional Paper 308, 185 pp.

Anderson, R.E., Zoback, M.L. and Thompson, G.A. (1983). Implications of selected subsurface data on the structural form and evolution of some basins in the northern Basin and Range province, Nevada and Utah. Geol. Soc. Am. Bull., 94, p. 1055-1072.

Cloos, E. (1968). Experimental Analysis of Gulf coast fracture patterns. Amer. Assoc. Pet. Geol. Bull., 52, p. 420-444.

Davis, G.A., Anderson, J.L., Frost, E.G., and Shcakelford, T.J. (1980). Mylonitization and detachment faulting in the Whipple-Buckskin-Rawhide mountains terraine, southeastern California and western Arizona, in Cordilleran Metamorphic Core Complexes, Geol. Soc. Am. Mem. 153, ed. by Crittenden, M.D., Coney, P.J., and Davis, G.H., p. 79-130.

McKee, E.D., and Anderson, C.A. (1971). Age and chemistry of Tertiary volcanic rocks in north-central Arizona and relation of the rocks to the Colorado Plateaus. Geol. Soc. Am. Bull., 82, p. 2767-2782.

Nations, J.D., Landye, J.J., and Hevly, R.H. (1982). Location and chronology of Tertiary sedimentary deposits in Arizona: a review, in Cenozoic Nonmarine Deposits of California and Arizona Pacific section SEPM, e.d. Ingersoll, R.V. and Woodburne, M.O., p. 107-122.

Pedersen, E.P., and Royse, C.F. (1970). Late Cenozoic geology of the Payson basin, Gila County, Arizona. Jour. Arizona Acad. Sci., 6, p. 168-178.

Shackelford, T.J. (1980). Tertiary tectonic denudation of a Mesozoic-early Tertiary (?) gneiss complex, Rawhide mountains, western Arizona. Geology, 8, p. 190-194.

Smith, M.A. (1984). Analysis of gravity data from the Verde Valley, Yavapai County, Arizona. M.S. Thesis, Northern Arizona Univ., 59 pp.

Vance, R. (1983). Geology of the Hardt Creek-Tonto Creek area, Gila County, Arizona. M.S. Thesis, Northern Arizona Univ., 99 pp.

Wernicke, B., and Burchfiel, B.C. (1982). Modes of extensional tectonics J. Struc. Geol., 4, p. 105-115.

POTASSIUM METASOMATISM OF VOLCANIC AND SEDIMENTARY ROCKS IN RIFT BASINS, CALDERAS, AND DETACHMENT TERRANES. Chapin, C. E., New Mexico Bureau of Mines and Mineral Resources, Socorro, NM 87801 and Lindley, J. I., Department of Geology, University of North Carolina, Chapel Hill, NC 27514

Potassium metasomatism of volcanic and sedimentary rocks is a common type of alteration in areas of regional extension. The alteration is chemically and mineralogically distinctive but is visually subtle and easily overlooked in outcrop and thin section. In highly metasomatized volcanic rocks, K_2O is as high as 13.5 wt. % and Na_2O, CaO, and MgO are each commonly less than 1 wt. %. Metasomatism tends to homogenize volcanic rocks of diverse composition to a mixture of K-feldspar (adularia) + hematite ± quartz ± illite-montmorillonite, yet rock textures are faithfully preserved. Potassium-bearing phenocrysts, such as sanidine and biotite, are little affected and give the illusion that the rocks are fresh.

In this paper, we describe the chemical, mineralogical, and oxygen-isotopic changes accompanying K-metasomatism and point out the similarities with diagenetic reactions in both deep marine and alkaline, saline-lake environments. The common occurrence of K-metasomatism in upper-plate rocks of detachment terranes indicates that the early stage of severe regional extension causes crustal downwarping and, in arid to semi-arid regions, development of closed hydrographic basins.

Our data come mainly from detailed studies of K-metasomatism in the Socorro area of the Rio Grande rift, especially studies by Lindley (1; 2) and D'Andrea (3). The Socorro area affords an unusual opportunity to study K-metasomatism because five regional ash-flow tuff sheets extend across the potassium anomaly and well beyond it. Thus, sample traverses can be made from fresh rock into progressively more altered rock within the same stratigraphic unit. The interbedding of basaltic andesite lavas between the ash-flow sheets allows examination of alteration effects on both mafic and silicic rocks. Alteration of overlying early rift fanglomerates permits analysis of clasts of different rock types within the same small volume of rock. Stratigraphic relationships and correlations have been established during more than 30 thesis and mapping projects over the past 15 years; the results are summarized in Osburn and Chapin (4).

The most important feature of the Socorro potassium anomaly is its large size. An L-shaped area 40 to 50 km on a side and at least 20 km in width has been outlined by analysis of more than 200 samples of ash-flow tuffs. Unaltered tuffs outside the anomaly average 5.1% K_2O; the same stratigraphic units within the anomaly average 8.0% K_2O, with K_2O ranging as high as 10.4%. The tuffs average 500 m in cumulative stratigraphic thickness; their volume within the potassium anomaly is approximately 900 km^3. Limited data indicate that interbedded basaltic andesite lavas are much less affected and show an erratic distribution of alteration. Clasts of both tuffs and mafic lavas in early-rift fanglomerates are highly altered with K_2O contents as high as 11.6%. Using only the volume of altered tuffs (900 km^3) and an average enrichment of 2.9% K_2O, a minimum of 6.4×10^{10} tons of potassium (K) have been added! The magnitude

of this figure and the size of the area affected impose important constraints on the origin of the alteration.

One arm of the L-shaped potassium anomaly at Socorro trends northward along the axis of the early rift Popotosa basin. Late-rift (<10 Ma) block faulting has exposed pervasively metasomatized ash-flow tuffs overlain by early-rift clastic sedimentary rocks and by as much as 300 m of fine-grained playa deposits. Crustal extension along the basin axis has been estimated by Chamberlin (5) to be 200 ± 50%. The other arm of the Socorro potassium anomaly extends about 50 km southwest from Socorro across an overlapping series of late Oligocene calderas that were downwarped beneath the Popotosa basin as they underwent extension of 30 to 200%. K-metasomatism is restricted to the stratigraphic interval between the first major ash-flow sheet (the 32.0 Ma Hells Mesa Tuff) and an as yet undefined level within sedimentary deposits of the Miocene Popotosa basin. Lateral boundaries vary from relatively sharp (<2 km), cross-cutting both structural grain and stratigraphic boundaries, to relatively diffuse with marked stratigraphic control. Permeability and composition of stratigraphic units were major vertical controls of K-metasomatism; lateral controls were permeability, salinity, and possibly temperature of altering fluids.

Chemically, the alteration is distinctive. As K_2O increases, Na_2O and CaO decrease. Total alkali content increases by 1 to 2% in welded tuffs and by as much as 5% in mafic lavas (6). Clasts of mafic lavas in early rift fanglomerates show the most extreme metasomatism, perhaps because of their reactive composition and location in permeable, silica-rich basin sediments. K_2O/Na_2O ratios for unaltered ash-flow tuffs outside the anomaly average 1.2; the same stratigraphic units within the anomaly have K_2O/Na_2O ratios as high as 42.1. Unaltered basaltic andesite lavas outside the anomaly have an average K_2O/Na_2O ratio of 0.7; similar lavas within the anomaly have K_2O/Na_2O ratios as high as 35.0. Thus, the K_2O/Na_2O ratio provides a sensitive index useful in scanning lists of chemical analyses for signs of K-metasomatism.

Other chemical changes accompanying K-metasomatism in the Socorro area are increases in Rb and Ba and decreases in Sr, Mn, and MgO (3; 6). The Fe^{+3}/total Fe ratio increases markedly in mafic to intermediate rocks but remains relatively unchanged in rhyolitic tuffs, probably because of the higher initial oxidation state of the tuffs. TiO_2, total Fe, Zr, Y, Th, and U remain unchanged (3; 6). Agron and Bentor (7) describe very similar chemical and mineralogical changes in K-metasomatized Precambrian rhyolites bordering the Dead Sea rift. Glazner (8) reports similar changes in K-metasomatized volcanic and sedimentary rocks of the Cady Mountains, Mojave Desert, California. Both studies determined that rare earth elements were essentially immobile during metasomatism.

Mineralogically, K-metasomatism is characterized by pervasive replacement of diverse rock types by K-feldspar (adularia) + hematite ± quartz ± illite-montmorillonite (2). In ash-flow tuffs, groundmass tridymite and cristobalite recrystallize to low quartz (2). Phenocrystic plagioclase is replaced by a fine-grained, intimate mixture of approximately equal amounts of adularia and quartz (2). Groundmass plagioclase undergoes patchy replacement by adularia. Phenocrystic quartz, sanidine, and biotite typically remain unaffected.

With extreme alteration, groundmass quartz and phenocrystic sodic sanidine are also replaced by adularia (2). In basaltic andesite lavas, groundmass plagioclase is replaced by adularia and both phenocrystic and groundmass pyroxene are converted to hematite (2). Groundmass magnetite is also hematized. The first visible sign of alteration in hand samples of either rock type is a chalky appearance of plagioclase; the first sign in thin section is patchy replacement of plagioclase by adularia.

The secondary K-feldspar is very pure (Or 96 to 100), contains 15.8 to 16.3 wt. % K_2O, is monoclinic, and has a slightly ordered structural state approaching that of orthoclase (2). This secondary feldspar is fine grained (20 microns) and has the rhombohedral habit characteristic of diagenetic/hydrothermal adularia (2). In altered phenocrystic plagioclase, where adularia is intimately associated with fine-grained quartz, the two minerals are coprecipitated in a chaotic manner, beginning along cleavages. This results in creation of void spaces which imparts a secondary porosity and decreases rock density (9).

Isotopically, $\delta^{18}O$ increases in rhyolitic tuffs from values of +8 to +10 permil, typical of unaltered rock, to +11 to +13 permil, typical of altered rock (2). Secondary K-feldspar has a minimum $\delta^{18}O$ of +12.7 permil and secondary quartz has an estimated minimum $\delta^{18}O$ of +15.4 permil (2). Phenocrystic quartz and sanidine retain their magmatic values of approximately +8 and +7 permil, respectively. In contrast to the rhyolitic units, basaltic andesite lavas become isotopically lighter with metasomatism. Unaltered mafic lavas, have ^{18}O values of approximately +9 permil compared to +6 permil in altered lavas (2). The strong tendency of iron oxides to concentrate light oxygen (10) and the alteration of abundant pyroxene to hematite in the altered lavas may be responsible.

Previous interpretations of K-metasomatism have been in terms of fossil geothermal systems (11; 6; 7; 8). Chapin and Glazner (12) listed 14 areas in the southwestern United States where K-metasomatism is known and pointed out that in all these areas the upper crust has been severely disrupted by regional extension, caldera collapse, or both. The association seems to be with areas of high heat flow and severely fractured crust. The Biq'at Hayareah area in the Sinai-Negev Desert, studied by Agron and Bentor (7), also displays this association. There the volcanic rocks dip 25° to 90° and are situated on the margin of the Dead Sea rift.

In a recent study of discordant K-Ar and fission-track ages of upper-plate volcanic rocks associated with the Harcuvar Mountains detachment terrane in western Arizona, Brooks and Marvin (13) suggest that K-metasomatism occurred at temperatures greater than the $\sim$200°C annealing temperature of fission tracks in zircon. Kerrich and others (14) report that K-metasomatized upper-plate rocks in the nearby Picacho detachment terrane are oxidized and $\delta^{18}O$ enriched, as are the rocks at Socorro, and postulate that alteration occurred during expulsion of metamorphic fluids from the lower plates at temperatures less than 300°C. The $\delta^{18}O$ values of K-metasomatized rocks at Socorro can be interpreted as indicating either equilibration with waters enriched in heavy oxygen (+5 to +10 permil) at temperatures of 250° to 350°C or reaction with meteoric waters at temperatures of 30° to 80°C (2). An independent measure of paleotemperature is needed

at Socorro. However, geologic evidence and data from the literature on diagenetic reactions in both deep-marine and alkaline, saline-lake environments strongly favor a relatively low-temperature regime.

Diagenetic changes in sea-floor sediments and volcanic rocks have been well documented by studies arising from the Deep Sea Drilling Project. Mellis (15) and Mathews (16; 17) discovered early on that calcic cores of plagioclase phenocrysts in deep-sea basalts were replaced by water-clear K-feldspar similar to orthoclase. Since then, numerous studies of sea-floor diagenesis have documented that basalts typically gain K, Rb, Ba, Cs, $\delta^{18}O$, and Fe^{+3}/total Fe and lose Ca, Mg, Na, Sr, and Mn to the pore waters (see for example 17; 18; 19; 20; 21). Most of the ions removed are taken up in secondary minerals such as Ca in calcite and Mg in smectites. The mobility of some ions is strongly temperature-dependent, but most alteration of sea-floor basalts occurs at temperatures less than 100°C and the results are rather uniform over large areas of the ocean floor (20). Bloch and Bischoff (22) have shown that when saline fluids react with basaltic rocks at low temperatures potassium is fixed, while at temperatures above 150°C sodium is fixed. Munha' et al. (23) report that sea-floor rhyolites show strong enrichment in potassium, development of an adularia-quartz-hematite assemblage, depletion in Na, Ca, Mg, Mn, and Zn, and enrichment in heavy oxygen. These changes are strikingly similar to potassium metasomatism at Socorro.

Even more relevant, however, are studies by Hay (24, 25), Sheppard and Gude (26; 27; 28; 29) and Surdam and Sheppard (30) which have shown that silicic vitric tuffs interbedded in sediments of alkaline, saline lakes can be progressively altered basinward through a sequence of zeolites to K-feldspar. The diagenetic reactions occur rapidly in a low-temperature, near-surface environment. Increased alkalinity and salinity drives the reactions toward the anhydrous phase. An alkaline, saline environment at Socorro is indicated by abundant zeolites (clinoptilolite, mordenite, analcite) and gypsum in the playa deposits of the Popotosa basin, as well as traces of halite and anomalous lithium content of ash beds (31). Popotosa fanglomerates and sandstones are reddish brown and extremely well indurated within the potassium anomaly, but are buff colored and only moderately indurated outside the anomaly. Reddish coloration and unusually strong induration are typical of coarse clastic rocks in other areas of K-metasomatism, including upper plates of detachment terranes.

The oldest sedimentary deposits of the Popotosa basin have been dated at about 26 Ma (32); the basin persisted as a broad (60-km-wide), shallow, closed hydrographic entity until about 7 Ma when Basin and Range faulting broke the basin into a series of three narrow basins with intervening ranges. Thus, as much as 19 m.y. was available for downward percolation of alkaline, saline waters into permeable volcanic and sedimentary units beneath the basin floor. Closely spaced, domino-style normal faults and strong rotation of beds accompanying severe extension of the basin floor may have aided the downward migration of saline waters. The great areal extent of the K-metasomatism (1800 km^2), its subtle nature, simple mineral assemblage, enrichment in heavy oxygen, and location in a rift basin argue strongly for a diagenetic rather than hydrothermal origin.

Increased temperature also drives zeolitic reactions towards the anhydrous feldspar end members (33). Maximum depth of burial

of K-metasomatized rocks at Socorro was approximately 1.8 km. Reasonable temperature estimates at this depth vary from 74°C (heat flow 80 mw/m^2) to 92°C (heat flow 107 mw/m^2) depending on whether an intermediate or high heat flow is assumed (average Basin and Range heat flow is 89 mw/m^2). Thus, temperature was probably not the dominant factor causing K-metasomatism at Socorro. Elevated temperatures may have played a more important role in K-metasomatism in calderas such as the Bachelor Mountain caldera, San Juan volcanic field, Colorado, where Ratte' and Steven (34) discovered a 10 x 16-km potassium anomaly. However, the adjacent and slightly younger Creede caldera (26.5 Ma) hosted an alkaline, saline-lake system in which lacustrine sediments underwent diagenetic reactions to clays, zeolites, and moderately abundant K-feldspar (35) without evidence of significant temperature control. The subtle nature of K-metasomatism and lack of conspicuously altered zones, such as occur where convecting geothermal waters are channelized along permeable pathways, indicates that the thermal gradient during K-metasomatism was less than that required for hydrothermal convection (36).

The initial response of continental lithosphere to thinning by regional extension is downwarping to form broad, shallow depressions. Isostacy requires this response and numerous studies of continental rifts have documented it in spite of the widely held misconception of early doming (37). The detachment terranes of the southwestern United States are located in an area which has had an arid to semi-arid climate throughout much of Cenozoic time. Subsidence in such a setting should lead to formation of closed hydrographic basins and development of alkaline, saline lakes. The widespread occurrence of K-metasomatized volcanic rocks in the upper plates of detachment terranes, together with the nearly ubiquitous presence of reddish-brown, highly indurated clastic sedimentary rocks interbedded with upper-plate volcanic units, indicates that early stages of detachment faulting produce subsidence. At Socorro, the subsidence stage lasted for nearly 20 m.y. (26-7 Ma) and was followed by uplift and block faulting in typical Basin and Range style. The preservation of upper-plate rocks and detachment surfaces in many ranges of the Basin and Range province also indicates that uplift was a late-stage event. We suggest that the term "metamorphic core complex", with its implications of domal uplift, is a misnomer. Such complexes are merely exposures of planar or gently curved, low-angle detachment surfaces that spent most of their existence beneath broad downwarps which, in arid climates, contained closed hydrographic basins.

REFERENCES

(1) Lindley, J. I. (1979) Chemical changes associated with the propylitic alteration of two ash-flow tuffs, Datil-Mogollon volcanic field, New Mexico. M.S. Thesis, Univ. North Carolina, Chapel Hill, 197 pp.

(2) Lindley, J. I. (1985a) Potassium metasomatism of Cenozoic volcanic rocks near Socorro, New Mexico. Ph.D. Thesis, Univ. North Carolina, Chapel Hill, 563 pp.

(3) D'Andrea, J. F. (1981) Chemical changes associated with potassium metasomatism of ash-flow tuffs near Socorro, New Mexico. M.S. Thesis, Florida State Univ., Tallahassee, 243 pp.

(4) Osburn, G. R. and Chapin, C. E. (1983) Nomenclature for Cenozoic

rocks of northeast Mogollon-Datil volcanic field, New Mexico. N.M. Bur. Mines and Min. Res. Strat. Chart 1.
(5) Chamberlin, R. M. (1983) Cenozoic domino-style crustal extension in the Lemitar Mountains, New Mexico: A summary. N.M. Geol. Soc. Guidebook 34, p. 111-118.
(6) D'Andrea-Dinkelman, J. F., Lindley, J. I., Chapin, C. E., and Osburn, G. R. (1983) The Socorro K_2O anomaly: A fossil geothermal system in the Rio Grande rift. N.M. Geol. Soc. Guidebook 34, p. 76-77.
(7) Agron, N., and Bentor, Y. K. (1981) The volcanic massif of Biq'at Hayareah (Sinai-Negev): A case of potassium metasomatism. J. Geol. 89, p. 479-495.
(8) Glazner, A. F. (1979) Geochemistry of ultrapotassic metasomatism in the Sleeping Beauty volcanic area, central Mojave Desert, California (abstract). Geol. Soc. Amer. Program 11, p. 79.
(9) Lindley, J. I. (1985b) Diagenetic changes accompanying fluid-rock interaction in permeable volcanic rock (abstract). Am. Assoc. Petroleum Geol. Bull. 69, p. 279.
(10) Taylor, H. P. (1967) Oxygen isotope studies of hydrothermal mineral deposits. In Geochemistry of Hydrothermal Ore Deposits, Holt, Rinehart and Winston, N.Y., p. 109-142.
(11) Chapin, C. E., Chamberlin, R. M., Osburn, G. R., White, D. W., and Sanford, A. R. (1978) Exploration framework of the Socorro geothermal area, New Mexico. N.M. Geol. Soc. Spec. Publ. 7, p. 115-129.
(12) Chapin, C. E. and Glazner, A. F. (1983) Widespread K_2O metasomatism of Cenozoic volcanic and sedimentary rocks of the southwestern United States (abstract). Geol. Soc. Amer. Program 15, p. 282.
(13) Brooks, W. E. and Marvin, R. F. (1985) Discordant isotopic ages and potassium metasomatism in volcanic rocks from Yavapai County, Arizona (abstract). Geol. Soc. Am. Program 17, p. 344.
(14) Kerrich, R., Rehrig, W. S., and Willmore, L. M. (1984) Deformation and hydrothermal regimes in the Picacho metamorphic core complex detachment-Arizona: Oxygen isotope evidence (abstract). EOS (Trans. Amer. Geophys. Union) 65, p. 1124.
(15) Mellis, O. (1952) Replacement of plagioclase by orthoclase in deep-sea deposits. Nature 169, p. 624.
(16) Mathews, D. H. (1962) Altered lavas from the floor of the eastern North Atlantic. Nature 194, p. 368-369.
(17) Mathews, D. H. (1971) Altered basalts from Swallow Bank, an abyssal hill in the NE Atlantic, and from a nearby seamount. Phil. Trans. Roy. Soc. London A268, p. 551-571.
(18) Honnorez, J. (1981) The aging of the oceanic crust at low temperature. In The Sea 7, p. 525-587.
(19) Humphris, S. E. and Thompson, G. (1978) Trace element mobility during hydrothermal alteration of oceanic basalts. Geochim. Cosmochim. Acta 42, p. 127-136.
(20) Sayles, F. L. (1981) The composition and diagenesis of interstitial solutions-II. Fluxes and diagenesis at the water-sediment interface in the high latitude North and South Atlantic. Geochim. Cosmochim. Acta 45, p. 1061-1086.
(21) Staudigel, H. and Hart, S. R. (1983) Alteration of basaltic

glass: Mechanisms and significance for the oceanic crust-seawater budget. Geochim. Cosmochim. Acta 47, p. 337-350.
(22) Bloch, S. and Bischoff, J. L. (1979) The effect of low-temperature alteration of basalt on the oceanic budget of potassium. Geology 7, p. 193-196.
(23) Munha', J., Fyfe, W. S., and Kerrich, R. (1980) Adularia, the characteristic mineral of felsic spilites. Contrib. Mineral. Petrol. 75, p. 15-19.
(24) Hay, R. L. (1966) Zeolites and zeolitic reactions in sedimentary rocks. Geol. Soc. Amer. Spec. Paper 85, 130 pp.
(25) Hay, R. L. (1978) Geologic occurrence of zeolites. In Natural Zeolites, Occurrence, Properties, Use, Pergamon N.Y., p. 135-143.
(26) Sheppard, R. A. and Gude, A. J. 3rd (1968) Distribution and genesis of authigenic silicate minerals in tuffs of Pleistocene Lake Tecopa, Inyo County, California. U.S. Geol. Survey Prof. Paper 597, 38 pp.
(27) Sheppard, R. A. and Gude, A. J. 3rd (1969) Diagenesis of tuffs in the Barstow Formation, Mud Hills, San Bernardino County, California. U.S. Geol. Survey Prof. Paper 634, 34 pp.
(28) Sheppard, R. A. and Gude, A. J. 3rd (1973) Zeolites and associated authigenic silicate minerals in tuffaceous rocks of the Big Sandy Formation, Mohave County, Arizona. U.S. Geol. Survey Prof. Paper 830, 36 pp.
(29) Sheppard, R. A. and Gude, A. J. 3rd (1973) Boron-bearing potassium feldspar of authigenic origin in closed-basin deposits. J. Res. U.S. Geol. Survey 1, p. 377-382.
(30) Surdam, R. C. and Sheppard, R. A. (1978) Zeolites in saline, alkaline-lake deposits. In Natural Zeolites, Occurrence, Properties, Use, Pergamon, N.Y., p. 145-174.
(31) Brenner-Tourtelot, E. F. and Machette, M. N. (1979) The mineralogy and geochemistry of lithium in the Popotosa Formation, Socorro County, New Mexico. U.S. Geol. Survey Open-File Report 79-839, 23 pp.
(32) Machette, M. N. (1978) Geologic map of the San Acacia quadrangle, Socorro County, New Mexico. U.S. Geol. Survey Geol. Quad. Map GQ-1415, scale 1:24,000.
(33) Iijima, Azuma (1978) Geological occurrences of zeolite in marine environments. In Natural Zeolites, Occurrence, Properties, Use, Pergamon, N.Y., p. 175-198.
(34) Ratte', J. C. and Steven, T. A. (1967) Ash flows and related volcanic rocks associated with the Creede caldera, San Juan Mountains, Colorado. U.S. Geol. Survey Prof. Paper 524-H, 58 pp.
(35) McCrink, M. T. (1982) Diagenesis in the Creede Formation, San Juan Mountains, Creede, Colorado. M.S. Thesis, New Mexico Inst. Mining and Tech., Socorro, 161 pp.
(36) Turcotte, D. L. and Schubert, G. (1982) Geodynamics: Application of Continuum Physics to Geological Problems, Section 9-9, Thermal convection in a porous layer. Wiley and Sons, N.Y., p. 402-406.
(37) Mohr, Paul (1982) Musings on continental rifts. In Continental and Oceanic Rifts, Amer. Geophys. Union and Geol. Soc. Amer. Geodynamics Series, 8, p. 293-309.

EXTENSIONAL TECTONICS AND COLLAPSE STRUCTURES IN THE SUEZ RIFT (EGYPT)

Chenet, P.Y.[1]; Colletta, B.[1]; Desforges, G.[2]; Ousset, E.[2] and Zaghloul, E.A.[2]
1 - Institut Français du Pétrole, BP 311, 92506 Rueil Malmaison CEDEX
2 - Total Proche-Orient, Gameat Dowal Arabia, 65 Mohandeseen - Cairo

The Suez Rift is a 300 km long and 50 to 80 km wide basin which cuts a granitic and metamorphic shield of Precambrian age, covered by sediments of Paleozoic to Paleogene age. The rift structure is dominated by tilted blocks bounded by NW-SE normal faults. The reconstruction of the paleostresses indicates a N 050 extension during the whole stage of rifting.

Rifting began 24 My ago with dikes intrusions; main faulting and subsidence occurred during Early Miocene producing a 80 km wide basin (Clysmic Gulf). During Pliocene and Quaternary times, faulting is still active but subsidence is restricted to a narrower area (Present Gulf).

On the Eastern margin of the Gulf two sets of fault trends are predominant - 1) N 140-150 E faults parallel to the gulf trend with pure dip-slip displacement - 2) cross faults, oriented N00 to N 30 E that have a strike-slip component consistent with the N 050 E distensive stress regime. The mean dip of cross fault is steeper (70-80°) than the dip of the faults parallel to the Gulf (30 to 70°). These two sets of fault define diamond shaped tilted block.

The difference of mechanical behaviour between the basement rocks and the overlying sedimentary cover caused structural disharmony and distinct fault geometries.

In the basement faults display a planar geometry while in the sedimentary cover (Cretaceous to Eocene sands, shales and limestones) faults are spoon shaped. Spoon faults are generally superimposed over concave wedges of the basement blocks but are decoupled from basement fault sets (Fig. 1). The decoupling is accommodated by plastic deformation in the Cretaceous marls. Along major normal faults, gravity sliding produced collapse structures with recumbent folds and thrusts (Fig. 2). Collapse structures are sealed by Early Miocene marine depostis and occurred during the first stage of rifting.

This kind of collapse structures may be found in various parts of the rift. They are related with normal faulting and should not be interpreted as the result of compressive events during the rifting.

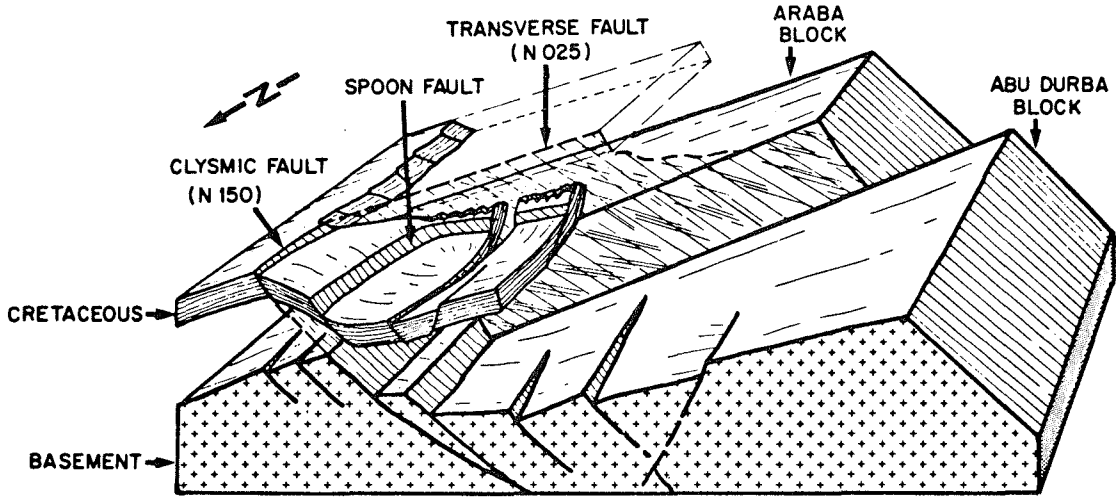

Fig. 1: Schematic block diagram of the Wadi Araba area (Western Sinaï).

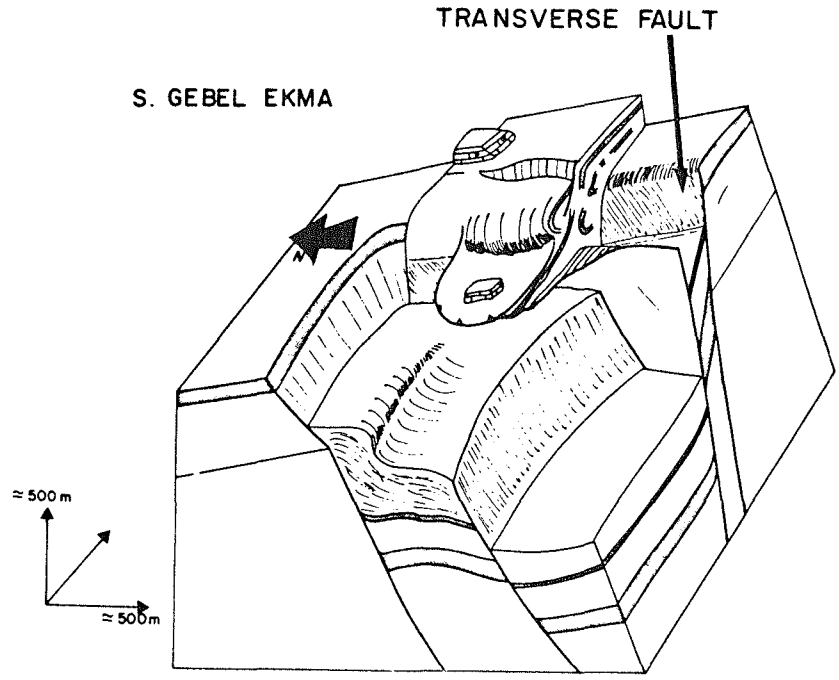

Fig. 2: Schematic block diagram of the collapse structure associated with major normal faults in the Gebel Ekma (Western Sinaï)

TECTONIC DETERMINATIONS OF LITHOSPHERIC THICKNESSES ON GANYMEDE AND CALLISTO. Steven K. Croft, Lunar and Planetary Laboratory, University of Arizona, Tucson, Arizona 85721

Introduction. Thermal lithospheric thicknesses provide fundamental constraints on planetary thermal histories that complement the constraints provided by dateable surface deposits of endogenic origin. Lithospheric constraints are of particular value on the icy satellites where our understanding of both rheology and surface ages is considerably poorer than it is for the terrestrial planets. Certain extensional tectonic features can and have been used to estimate lithospheric thicknesses on Ganymede and Callisto (1,2). These estimates, however, refer to the depth of the elastic lithosphere defined by the zone of brittle failure. The relation between the elastic lithosphere and the thermal lithosphere (generally defined by the zone of conductive heat transport, 3) is not straightforward, because the depth of brittle failure depends not only on the thermal profile, but also on rheology and strain rate (or the characteristic time over which stresses build towards failure). Characteristic time considerations are not trivial in this context because stresses generating brittle failure on the icy satellites may be produced by impacts, with characteristic times of seconds to days, or by "geologic" processes (e.g., convection, differentiation) with time scales of millions to hundreds of millions of years. In this abstract, the concept of the Maxwell time, tm, of a viscoelastic material (4,5) is used in conjunction with calculated thermal profiles to evaluate the significance of tectonic estimates of lithospheric thickness.

Maxwell Time Profiles. The definition adopted here for the Maxwell time is $tm = 2\mu/E$ (5), where μ is the local viscosity and E is Young's modulus. The viscosity is both temperature and depth dependent:

$$\mu = \mu o \exp(A((Tm - k\rho gZ)/T - 1))$$

where μo is the viscosity at the melting temperature, Tm, at zero pressure. A is an empirical constant related to the activation energy, ρ is density, g is the local gravity, Z is depth, k is a constant set to yield Tm = 252 °K at a pressure of 2.08 kb (the pressure at melting where ice I changes to ice III), and T is the local temperature. The temperature dependence of Young's modulus, a minor effect, is also included: E=144.7-0.177 T kb (derived from 6). The nominal temperature profiles used in this calculation are shown in figure 1. They are calculated assuming the mass and density of Ganymede, chondritic radioactive abundances, whole-planet, heated-from-within convection, and viscosity parameters $\mu o = 10^{15}$ and A=25. A Maxwell time is calculated at each depth Z using the appropriate temperature along each temperature profile.

The resulting Maxwell time profiles are shown in figure 2. Stresses building towards failure over times short compared to the Maxwell time cause the material to fail in a brittle manner, while stresses building over times long compared to the Maxwell time cause the material to deform viscously. Thus, each profile divides the brittle field above the curve from the ductile field below the curve. Following the thermal profiles (temperature is by far the dominant variable), each curve exhibits a similar Maxwell time dependence: little change in the depth of the brittle field over a large range of "geologic" characteristic times grading into a sharp increase in brittle depth at time scales of less than a year or so. The general increase in the depth of the brittle field with age represents the thickening of the lithosphere as the radioactive heat flux declines. These curves result from a particular thermal calculation. Thermal models assuming different input parameters will yield slightly different Maxwell profiles. Choosing a "stiffer" viscosity relation, for instance, forces temperatures at depth to rise in order to deliver the same heat flux at a given

age (forcing the steep portion of the Maxwell profile to shorter times), but simultaneously thickens the brittle layer at "geologic" time scale. Thus, the relative insensitivity of the brittle depth for geologic time scales means that if a set of structures can be established as having "geologic" origins and an approximate age derived, then the inferred lithospheric depth constrains the rheology.

Tectonic Features on Ganymede and Callisto. The structures of interest on Callisto are the graben-like depressions forming a concentric network around the Valhalla basin, a large impact structure. The widths and spacing between the graben where best developed are, respectively, 15-20 km and about 70 km (1,7). The structures on Ganymede are the graben-like furrows with raised edges that permeate several of the large blocks of dark terrain. First recognized in Voyager 2 imagery (8), the furrows generally occur in enormous sub-parallel systems in which furrow width and spacing are remarkably regular. The best developed furrow systems are located in Galileo Regio and neighboring Marius Regio. The planform of each system is broadly arcuate, and both are crudely consistent with a single concentric pattern (9). This, plus some similarities to the graben system around Valhalla have led to the common suggestion that they are both parts of a single tectonic system, possibly of impact origin (1,7,8,9). However, the width and spacing of the furrows in Galileo Regio are about 10 km and 50 km, respectively, whereas they are only about half that, about 6 km and 22 km (9) respectively, in Marius Regio. These characteristics are consistent within each Regio, yet the regiones are separated by a strip of grooved terrain only about 300 km wide. Less well developed furrow systems are found in other blocks of dark terrain on Ganymede, as indicated in table 1, each with characteristic widths and separations either roughly equal to or equal to about half the dimensions of the furrows in Galileo Regio. Again, the blocks of differing furrow dimensions are separated by relatively narrow strips of bright terrain.

Interpretation. For the furrow systems on Ganymede, the rheology is presumably everywhere uniform to first order. Also the crater counts on the dark terrain are similar, particularly between Galileo and Marius Regiones, hence the furrow systems all date to the same geologic era - at most several hundred million years long. For a given rheology, the factor of 2 in lithospheric thickness inferred from the variations in furrow widths implies a comparable variation in heat flux. Variations by factors of 2 in heat flux due to planetary cooling are difficult to achieve over a period as short as several hundred million years for an object as large as Ganymede. However, variations of 2 to 3 in heat flux are commonly obtained in convective heat transport calculations between areas over upwelling warm material and areas over down flowing cold material (10). In a new scenario of differentiation on Ganymede (11), light terrain emplacement occurs in regions over warm rising mantle material. Thus, the geometric pattern of light and dark terrain, which bears a resemblance to theoretical geometrical patterns of rising and sinking material convecting in a spherical shell (12), is interpreted as reflecting a convection pattern with the cool sinking plumes under the large regiones: Galileo, Perrine, and Nicholson (13). By inference, the theoretical thermal lithosphere is 2-3 times thicker within the large regiones than elsewhere, a variation consistent with the observed variations in elastic lithospheric thicknesses inferred from furrow widths. Thus, the overall light-dark geometry, the emplacement mechanism of bright terrain, and the regional variation in furrow dimensions are all consistent with their interpretation as geologic elements reflecting the global convective heat flow pattern on Ganymede between 3 and 4 billion years ago.

Even given this interpretation of furrow origin, it is not suggested that the furrows are the direct result of convective stress. If such were the case, furrow systems unassociated with impacts would be found on Callisto (where convective stresses are only slightly less), but they are not. Thus the furrows may be due to a slight expansion caused by marginal differentiation (13). This interpretation of the variation of furrow dimensions does not, as yet, eliminate an impact origin for the furrows because: 1) the Maxwell profiles resulting from more realistic thermal calculations may drop farther into the short impact time scales (they may also go higher), and 2) the type of impact induced, sub-lithospheric restorative flow envisioned by (14) as the cause of the Valhalla graben system may persist from months to years, yielding shallower brittle layers. The slightly thicker inferred lithosphere around Valhalla compared to that on Ganymede may be due simply to a months-years time scale restorative flow around the Valhalla basin compared to a much longer building endogenic stress source for furrows on Ganymede (see figure 2), rather than differences in global heat flux or rheology. Since the local thickness of the brittle layer depends on the local heat flux, a single impact-induced restorative flow passing through areas of differing heat flux may produce extensional surface features of differing dimensions. Such a flow could have produced the Galileo-Marius system; asymmetries in the Valhalla system (15) may also be due to local variations in heat flux.

The characteristics of the Maxwell time profiles and their sensitivity to rheology and calculated thermal profiles implies that detailed analysis of furrow dimensions (in progress) on Ganymede and ring structures on Callisto can provide significant constraints on model thermal histories (in progress) and estimates on two-dimensional heat flow patterns on planets other than the Earth. They may also ultimately provide the decisive clues to whether the enigmatic furrow systems on Ganymede are of impact or endogenic origin.

References

1. McKinnon W.B. and H.J. Melosh, Icarus 44, 454-471 (1980).
2. Golombek M.P., 13th LPSC, J. Geophys. Res. Suppl., 87, A77-A83 (1982).
3. Houseman G. and D.P. McKenzie, Geophys. J. R. Astr. Soc. 68, 133-164 (1982).
4. Peltier W. R., Rev. Geophys. Space Phys. 12, 649-669 (1974).
5. Turcotte D.L. and G. Schubert, Geodynamics, 450 pp., J. Wiley & Sons (1982).
6. Fletcher N.H., The Chemical Physics Of Ice, p. 169-173, Cambridge (1970).
7. Passey Q. R. and E. M. Shoemaker, in Satellites of Jupiter, p. 379-434, University of Arizona (1982).
8. Smith B. A. and 21 others, Science 206, 927-950 (1979).
9. Zuber M. T. and E. M. Parmentier, Icarus 60, 200-210 (1984).
10. Jarvis G. T. and W. R. Peltier, Geophys. J. R. Astr. Soc. 68, 389-427 (1982).
11. Croft S.K. in Lunar & Planetary Science XVI, p. 152-153, Lunar & Planetary Institute (1985).
12. Busse F. H. and N. Riahi, J. Fluid Mech. 123, 283-301 (1982).
13. Croft S.K., Proc. 16th LPSC, J. Geophys. Res., in review.
14. Melosh H. J., J. Geophys. Res. 87, 1880-1890 (1982).
15. Hale W. S., J. W. Head, and E. M. Parmentier, LPI Contrib. 414, 30-32 (1980).

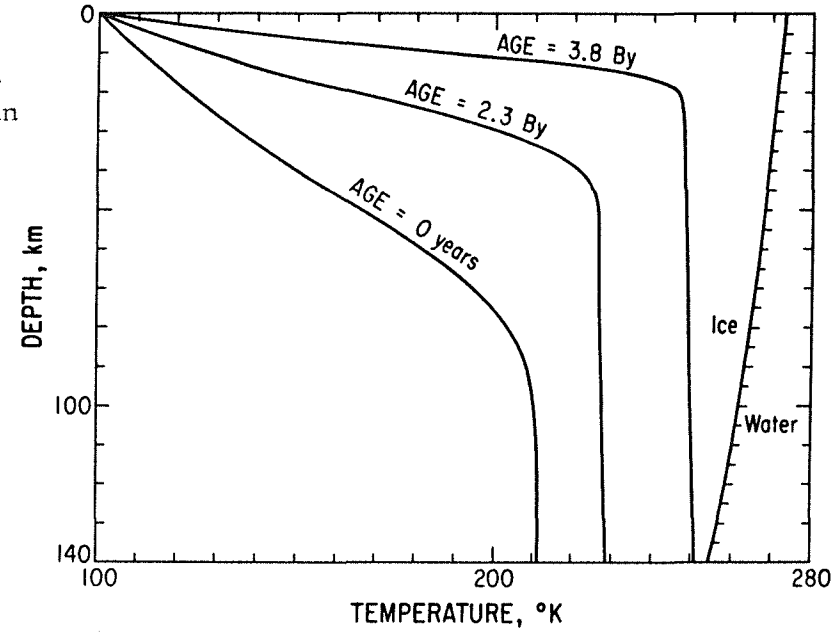

Figure 1. Ganymede Thermal Profiles. Ages are in billions of years before the present; e.g., age=0 is present time.

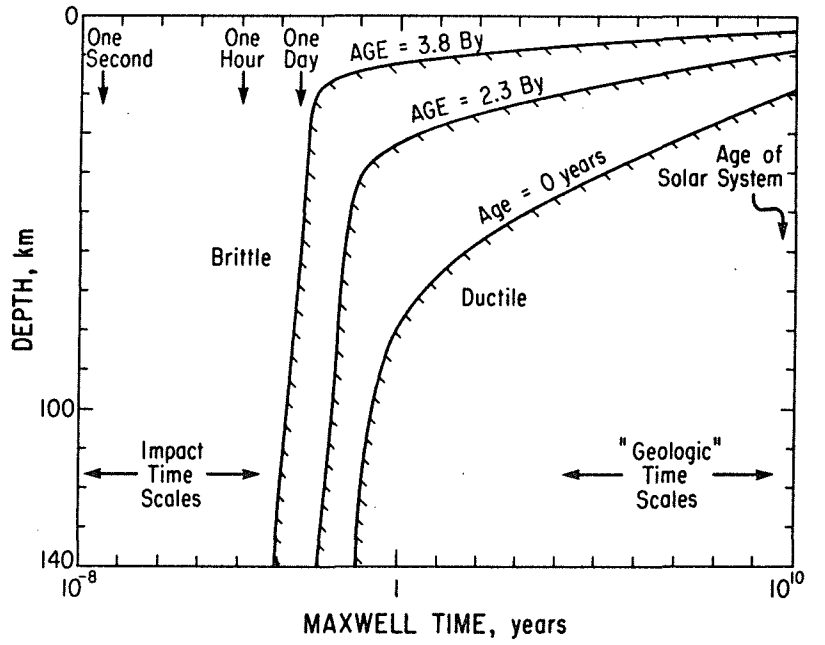

Figure 2. Maxwell Time Profiles. Each profile corresponds to thermal profile in figure 1 of the same age.

Table 1. Furrow Widths and Spacing

Area	Image FDS#	Width (km)	Spacing (km)	Comments
Galileo Regio	-	8-10	30-50	Refs. 1,7,8
Marius Regio	-	~6	~22	Ref. 9
NE Perrine Regio	16405.46	7-8	~33	Low resolution
NW Perrine Regio	16402.02	7-9	~38	Low resolution
E Central Barnard Regio	16405.18	5-6	20-25	
Central Nicholson Regio	16405.02	10-13	40-50	Few furrows

METAMORPHIC CORE COMPLEXES -- EXPRESSION OF CRUSTAL EXTENSION BY DUCTILE-BRITTLE SHEARING OF THE GEOLOGIC COLUMN; G.H. Davis, Dept. of Geos., University of Arizona, Tucson, Arizona 85721

Metamorphic core complexes and detachment fault terranes in the American Southwest are products of stretching of continental crust in the Tertiary. The physical and geometric properties of the structures, fault rocks, and contact relationships that developed as a consequence of the extension are especially well displayed in southeastern Arizona. The structures and fault rocks, as a system, reflect a ductile-through-brittle continuum of deformation, with individual structures and fault rocks showing remarkably coordinated strain and displacement patterns. Careful mapping and analysis of the structural system has led to the realization that strain and displacement were partitioned across a host of structures, through a spectrum of scales, in rocks of progressively changing rheology. By integrating observations made in different parts of the extensional system, especially at different inferred depth levels, it has been possible to construct a descriptive/kinematic model of the progressive deformation that achieved continental crustal extension in general, and the development of metamorphic core complexes in particular.

The physical and geometric nature of structures, fault rocks, and contact relationships in metamorphic core complexes of southeastern Arizona can be understood in the context of shear-zone deformation. When so viewed, metamorphic core complexes emerge as mountain-size geologic exposures of low-dipping regional ductile-brittle shear zones. The zones vary in thickness from approximately .3 km to 3 km, and appear to taper upward. Normal-slip simple shear within individual shear zones resulted in kilometers of translation of hanging-wall crust. The tectonic denudation which accompanied progressive simple-shear raised early formed, deep level mylonites through higher and higher structural levels. The mylonites thus experienced a progressive deformation carried out under conditions of steadily decreasing temperature and confining pressure. The record of fault rocks and fabrics displays this history strikingly: mylonite gneiss comprising the interior of the shear zones is transformed upward into microbrecciated mylonite gneiss, which in turn is converted to cataclasite and ultracataclasite derived from microbrecciated mylonite gneiss. In outcrop the cataclasites typically form a resistant tabular ledge, the upper surface of which is a gently dipping detachment fault, or decollement. This surface of profound structural discontinuity sharply separates mylonitic and cataclastic fault rocks below from nonmylonitic, noncataclastic hanging-wall rocks.

When the brittle-ductile shear zones formed initially, as a response to continental crustal extension, they probably dipped at angles of 45 degrees or more, and not at their presently observed inclinations of 30 degrees or less. At the time of formation of the brittle-ductile shear zones, only the uppermost brittle surficial expression(s) of the zones would have been exposed to view. However, the brittle-ductile shear zones now lie on their sides, having been passively rotated to gentle inclinations through crustal extension that continued beyond their inception. While actively accommodating simple-shear deformation and displacement, the shear zones were geometrically required to rotate to shallower inclinations as the crust was distorted into a stretched, thinned counterpart of its original shape and size. Following this early-to mid-Tertiary deformation, the rotated shallow-dipping brittle-ductile shear zones were cut and differentially displaced along younger high-angle normal faults, which are fundamentally responsible for

blocking-out the basins and ranges of southeastern Arizona today. Because of the combination of these structural circumstances, broad expanses of sub-regional brittle-ductile shear zones can be examined in single and/or adjacent mountain ranges. By traversing range to range, parallel to the direction of shear, the once-shallow and once-deep parts of a common shear zone may be examined right at the surface of the earth.

THERMAL HISTORY OF A METAMORPHIC CORE COMPLEX.

Roy K. Dokka and Michael J. Mahaffie, Department of Geology, Louisiana State University, Baton Rouge, LA 70803; Arthur W. Snoke, Department of Geology and Geophysics, University of Wyoming, Laramie, WY 82071

Fission track (FT) thermochronology studies of lower plate rocks of the Ruby Mountains-East Humbolt Range metamorphic core complex provide important constraints on the timing and nature of major middle Tertiary extension of northeast Nevada. Rocks analyzed include several varieties of mylonitic orthogneiss as well as amphibolitic orthogneisses from the non-mylonitic infrastructural core. Oligocene-age porphyritic biotite granodiorite of the Harrison Pass pluton was also studied. The minerals dated include apatite, zircon, and sphene and were obtained from the same rocks that have been previously studied using the ^{40}Ar-^{39}Ar method (1).

FT ages are concordant and range in age from 26.4 Ma to 23.8 Ma, with all showing overlap at 1 sigma between 25.4-23.4 Ma (Figure 1). Concordancy of all FT ages from all structural levels indicates that the lower plate cooled rapidly from temperatures above ~285°C (assumed sphene closure temperature; (2)) to below ~150°C (assumed apatite closure temperature; (2)) near the beginning of the Miocene. This suggests that the lower plate cooled at a rate of at least ~36°C/Ma during this event. The general concordance of FT with ^{40}Ar-^{39}Ar biotite and hornblende plateau ages (1) suggests an even more pronounced cooling during this event (above ~500°C to below 150°C) during latest Oligocene-earliest Miocene time.

Rapid cooling of the region is considered to reflect large-scale tectonic denudation (intracrustal thinning), the vertical complement to intense crustal extension. Rocks originating in the middle crust (10-15 km) were quickly brought near the surface along detachment faults (brittle-ductile shear zones) and juxtaposed against brittlely extended rocks deformed under upper crustal conditions. FT data firmly establish the upper limit on the timing of mylonitization during detachment faulting and also coincide with the age of extensive landscape disruption.

References

1. Snoke, A. W., Dallmeyer, R. D., and Fullagar, P. D. (1984) Superimposed Tertiary mylonitization on a Mesozoic metamorphic terrane, Ruby Mountains-East Humbolt Range, Nevada, Geol. Soc. Am. Abs. with Progs. 16, 662.
2. Zeitler, P. K., Johnson, N. M., Naeser, C. W., and Tahirkheli, R. A. K. (1982) Fission-track evidence for Quaternary uplift of the Nanga Parbat region, Pakistan, Nature, 298, 255-257.

3. Dokka, R. K., and Mahaffie, M. J., in review, Significance of concordant fission track ages from continental basement terranes, 45p.

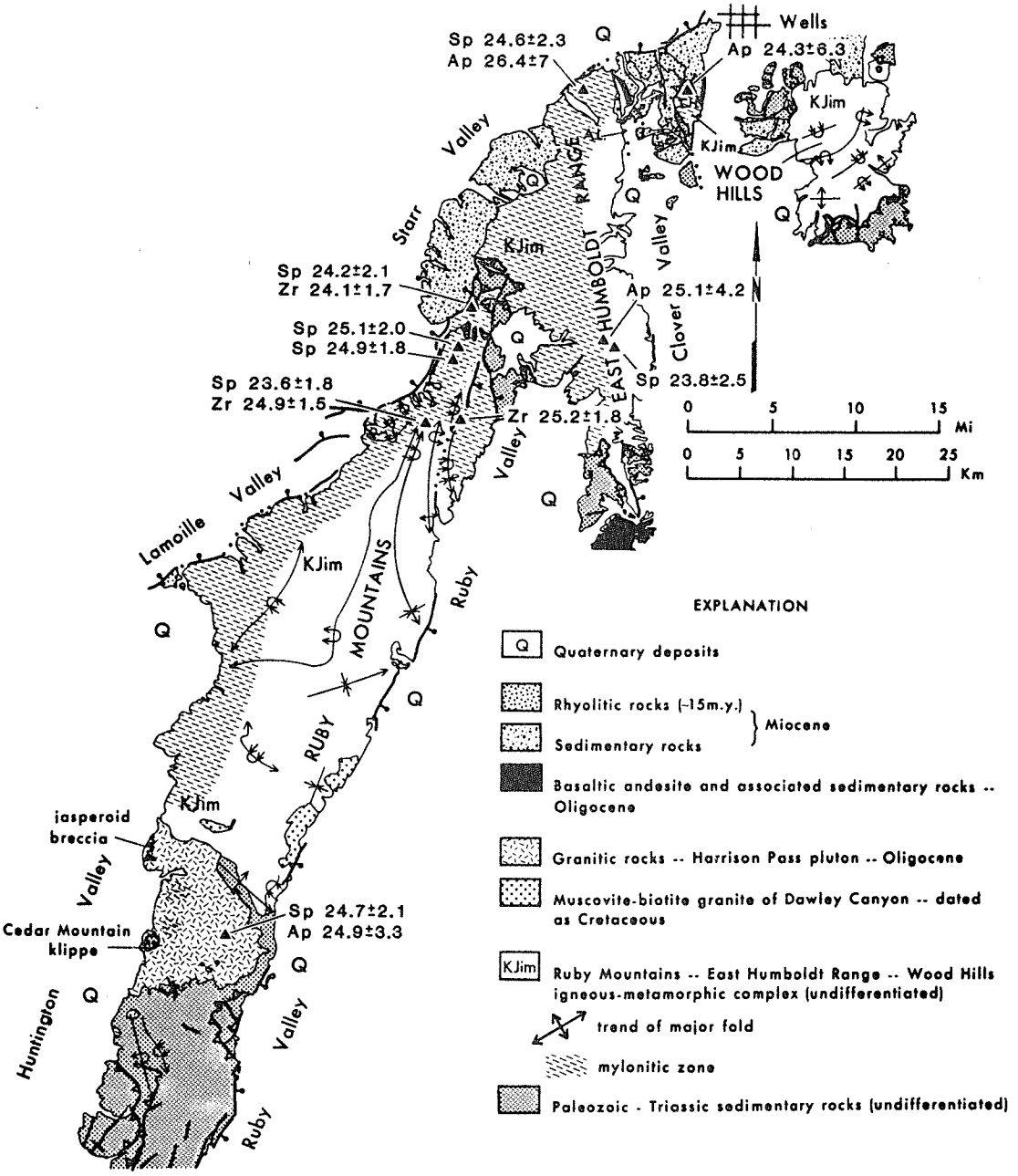

Figure 1. Generalized geological map of the Ruby Mountains-East Humbolt Range, Nevada (3). Triangles show location of FT samples; age (±error) and mineral dated (Sp=sphene; Zr=zircon; Ap=apatite) is shown at each locality.

THERMAL-MECHANICAL RESPONSE TO SIMPLE SHEAR EXTENSION; K.P. Furlong, Department of Geosciences, Pennsylvania State University, University Park, PA 16802

The mechanism of extension in the continental crust is apparently much more complex than that acting in the oceanic lithosphere. Recently, Wernicke (1,2) has proposed that a significant fraction of extension in the continental lithosphere may occur by a simple shear mechanism along discrete fault/shear zones which cut the crust, and perhaps extend into the uppermost mantle. Clearly much of the surface evidence for extension supports this concept, but the depth extent of simple shear extension in the continental crust is unclear. In this study I have determined, using numerical simulations, the thermal and associated mechanical behavior of the continental lithosphere in response to lithosphere extension along a low-angle simple shear zone which cuts through the lithospheric plate (Figure 1), in order to evaluate the resolving ability of thermal (heat flow and metamorphic P-T-time paths) and elevation observations in constraining the mode of continental extension. The general gometry of the region is shown in Figure 1 at a time after extention has ceased (points x and x' were initially adjacent). The initial crustal thickness across the region was assumed to be constant. The surface heat flow and elevation response to this extension for the region between A and C is given in Figures 2a and 2b. Extension was assumed to have occurred over a 15 Ma period with a net vertical motion of 20 km. During the period of active extension, the heat flow response is dominated by the effects of (vertically) advected heat causing a strong anomaly in the vicinity of the thinnest upper plate. After the cessation of extension (time > 15 Ma) the heat flow anomaly decrease and the location of the maximum migrates to the regions of thicker upper plate as a function of the conductive time lag. In the regions of thinnest crust, the heat flow decays to values below those assumed initially as a consequence of removal of (assumed) radiogenically enriched upper and middle crust. The width of the heat flow anomaly varies in time, but for an assumed dip for the shear zone of 20°, the anomaly is approximately 75-100 km wide. By 25 Ma (time = 40 Ma) after the cessation of extension, however, the heat flow anomaly has decayed to a point where it is likely to be difficult to resolve. The elevation response to this extension is dominated by the effects of crustal thinning (and hence the specifics of the geometry of the shear zone) with only a small transient effect from the thermal perturbations. For the rates of extension used here, the maximum average temperature increase in the lithospheric plate (during extension) is <200°C restricting the effects of thermal/density effects in elevation to <600 meters. Clearly the dominant effect (approximately 3 km of subsidence) is related to crustal thinning, and thus also dependent on the initial crustal structure.

The thermal and associated mechanical (elevation) response of the continental lithosphere to simple shear extension is greatest during the period of active extension. The 'relaxation' of the thermal field occurs over a time scale of 10's of millions of years, while the elevation response is virtually complete by the end of the extension. The ability to constrain this extension mechanism requires either detailed control on the subsidence/uplift history of the region and some control over the patterns of the perturbations in the thermal field. The utilization of metamorphic pressure-temperature-time trajectories (3) may provide a means to constrain

the thermal history and consequently constrain the extension mechanism. Without such constraints, it is unlikely that present day thermal and elevation measurements will provide adequate information to discern the mechanism of extension in continental regions.

(1) Wernicke, B., (1981) Low-angle normal faults in the Basin and Range province--Nappe tectonics in an extending orogen. Nature, 291, p. 645-648.

(2) Wernicke, B., (1985) Uniform-sense normal simple shear of the continental lithosphere. Can. J. Earth Sci., 22, p. 108-125.

(3) Spear, F.S., Selverstone, J., Hickmott, D., Crowley, P. and Hodges, K.V., (1984) P-T paths from garnet zoning: A new technique for deciphering tectonic processes in crystalline terrances. Geology, 12, p. 87-90.

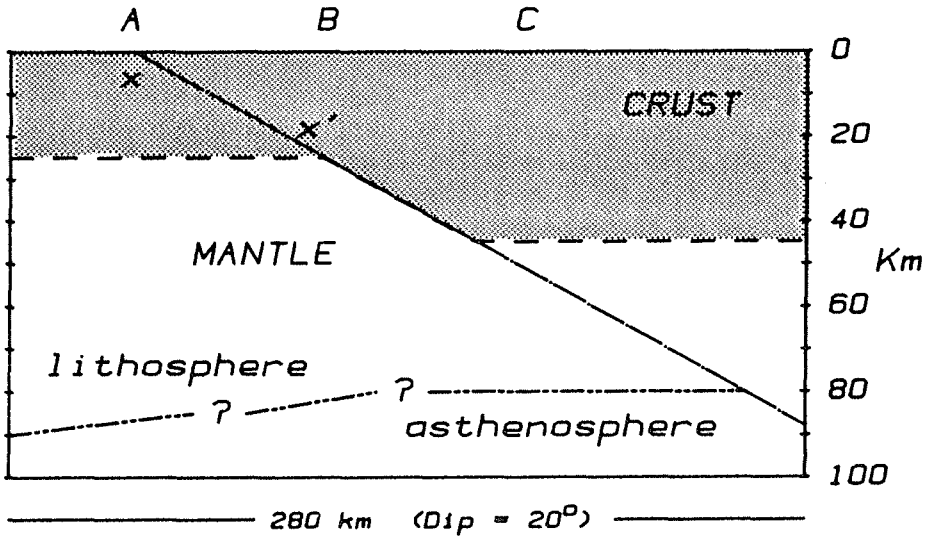

Figure 1. Schematic of model domain and geometry for simple shear model. Shaded region represents crust. A, B, and C mark locations referred to by Wernicke (2) as extensional allocthons (or "core complexes"), limit of significant upper crustal extension, and Moho "hinge" respectively. Positions labeled x and x' were adjacent prior to extension. For a shear zone dipping at 20, the region between A and C is approximately 140 km wide.

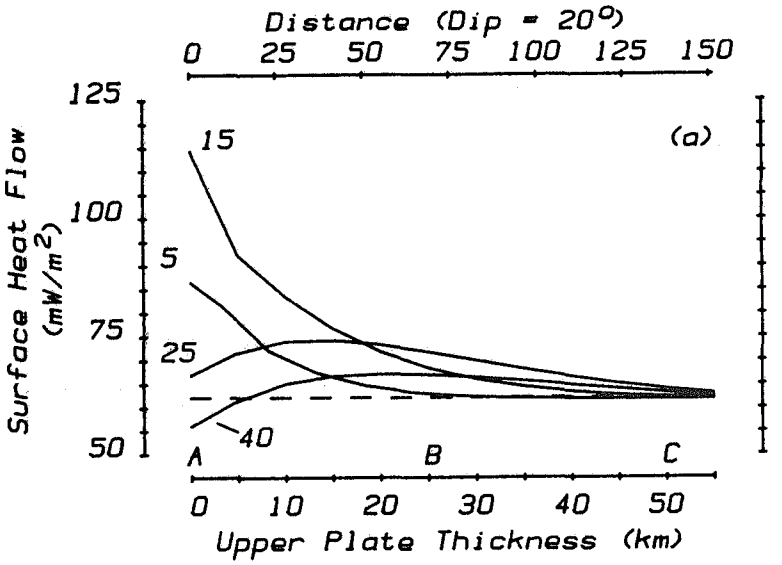

Figure 2a. Predicted surface heat flow response during (0-15 Ma) and after (> 15 Ma) simple shear extension along finite width shear zone. Dashed line is assumed intial heat flow regime.

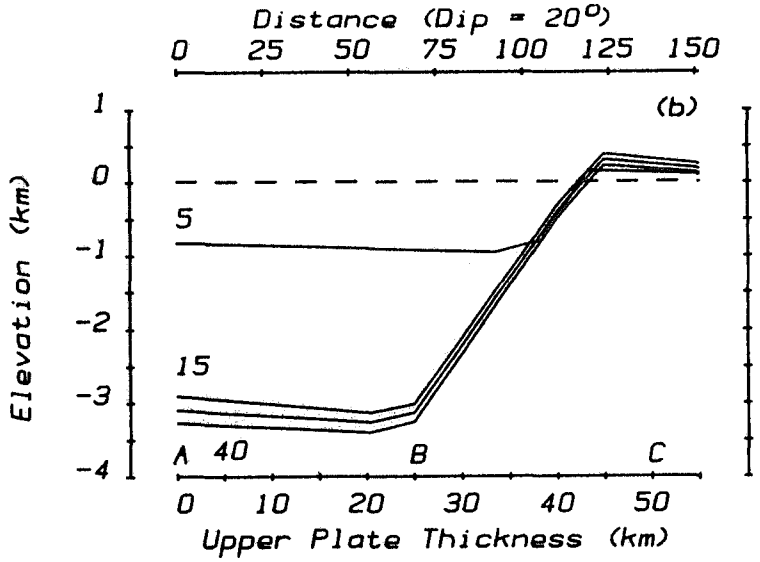

Figure 2b. Predicted elevation response during and after simple shear extension. Dashed line is initial datum surface.

LITHOSPHERIC STRENGTH OF GANYMEDE: CLUES TO EARLY THERMAL PROFILES FROM EXTENSIONAL TECTONIC FEATURES; M.P. Golombek and W.B. Banerdt, Jet Propulsion Laboratory, California Institute of Technology, Pasadena, CA 91109

Introduction

While it is generally agreed that the strength of a planet's lithosphere is controlled by a combination of brittle sliding and ductile flow laws, predicting the geometry and initial characteristics of faults due to failure from stresses imposed on the lithospheric strength envelope has not been thoroughly explored. In this abstract we will use lithospheric strength envelopes to analyze the extensional features found on Ganymede. This application provides a quantitative means of estimating early thermal profiles on Ganymede, thereby constraining its early thermal evolution.

Extensional Tectonics on Ganymede

Ganymede is the third and largest of the four Galilean satellites. Although it is larger than the planet Mercury, its low density indicates it is roughly one-half silicates and one-half water with a gravitational acceleration similar to the moon. About one-half of its surface is covered by low-albedo heavily cratered terrain and the other half by higher albedo, less cratered grooved terrain (1). Grooved terrain consists of numerous parallel sets of narrow linear to curvilinear troughs or depressions that separate various sized polygons of cratered terrain. Most photogeologic evidence suggests that the grooves formed by some extensional tectonic and resurfacing process involving shallow flooding of wide grabens with high-albedo water ice and subsequent refracturing of the ice to form grooves (1,2,3,4). Given that the grooved terrain probably formed from extensional faulting of one-half of the surface, grooves may be a result of planetary expansion. Attempts to estimate the amount of expansion suggest that a maximum of one percent is needed to form all the grooved terrain (5,6,7).

The largest remnant of cratered terrain on Ganymede is Galileo Regio, upon which a well preserved system of arcuate troughs called rimmed furrows can be found. These furrows which mark the first tectonic event preserved on Ganymede (well before the beginning of the formation of grooved terrain) have been interpreted as grabens (5,8), perhaps resulting from a large impact (8).

A number of attempts have been made to estimate the thickness of the lithosphere from the width or spacing of these extensional tectonic features. To first order, two independent lines of evidence suggest a thin lithosphere early in Ganymede's history. The theory of ringed basin formation (8) and the early high heat flow inferred from crater relaxation studies (9) both imply thin lithospheres (less than a few tens of km). The simplest model for determining lithosphere thickness from furrows and grooves suggests that both structures are simple grabens with flat floors and two exactly equal bounding faults that converge downward (5,8). These simple grabens probably form when normal faults initiate at the base of a brittle layer and propagate up yielding grabens with similar widths, similar displacements, and similar distances between members of a set. Assuming the bounding faults have the most probable 60^{o} dips suggests lithospheric thickness of about 10 km for the furrows on Galileo Regio (5,8) and about 4 km average for the grooves. A more complicated model for extensional instabilty of a brittle plastic surface layer overlying a ductile interior (10) yields ~10 km brittle layer for the ~50 km spaced furrows and ~2 km for the ~8 km (11) spaced grooves. Given the various uncertainties (and the narrower furrows on Marius Regio) the brittle lithosphere thickness was probably 5-10 km at the time of furrow formation and

2-7 km at the time of groove formation. With these geologic constraints on the thickness of the brittle surface layer in mind we now explore possible lithospheric strength envelopes to quantitatively evaluate temperature profiles for these times of deformation in Ganymede's history.

Lithospheric Strength of Ganymede

To calculate the lithospheric strength on Ganymede we use a combination of Byerlee's law and the ductile flow law for ice (see Banerdt and Golombek, this volume, for more thorough discussion of lithospheric strength envelopes). At low pressures we use the sliding friction as determined by Byerlee, which has been found to hold for a wide variety of geologic materials. At higher confining pressures we have used the friction data for ice (12). At higher temperatures deformation in the outer few tens of km of Ganymede is controlled by creep of ice I_h. We have used the flow law of Durham et al. (13) with modifications (Durham, written communication) for pure ice extrapolated to geologic strain rates of 10^{-15}/sec (~3%/m.y.). Because the mantle of Ganymede is probably also water-ice, the lithosphere has only one strength peak. A surface temperature of 100°K and a thermal gradient of 1.5°/km yield the strength envelope shown in Fig. 1. It has been shown at high temperatures that the inclusion of a small amount of silicates into the ice will greatly increase the creep strength of ice I_h (14). However, quantitatively determining the amount of hardening for our application is not possible because the creep processes that control the deformation of ice are not well known for the temperatures and strain rates of interest on Ganymede. For lack of a better constraint we will assume that the hardening resulting from the addition of less than a few percent of silicates in Ganymede's lithosphere can be bracketed by an order of magnitude increase in creep strength.

Predicting the type of failure from the lithospheric strength envelopes is straightforward. With increasing stress, elastic strain will be built up in the elastic part of the lithosphere until its strength is exceeded (roughly the yield stress of the brittle-ductile transition). At that time major throughgoing faults will initiate near the depth of the transition between the brittle and ductile deformation regimes (the brittle-ductile transition) (e.g., 15). Thus the brittle lithosphere defined by the simple graben and extensional instability models is dependent on the depth to the brittle-ductile transition. This depth is most dependent on the temperature gradient. Fig. 2a shows the relationship between brittle-ductile transition depth and thermal gradient for clean and simulated dirty ice. As a result we can quantitatively determine the thermal gradient at the times of furrow and groove formation on Ganymede.

It is important to note that the "brittle" lithosphere defined by the strength envelope is delineating areas of brittle versus ductile behavior at stresses exceeding the yield strength. As such it is inherently different from a "thermal" lithosphere derived from convection models, an "elastic" lithosphere derived from dynamic bending or membrane stress models, or a "seismic" lithosphere defined from discontinuities in seismic properties. Care must be used in selecting the properly defined lithosphere for interpreting specific structural features observed on a planet's surface.

The 10 km thick brittle lithosphere on Galileo Regio at the time of furrow formation indicates a thermal gradient of 1.5°/km for clean ice and a little above 2°/km for dirty ice. On Marius Regio the 5 km thick brittle-ductile transition requires respective thermal gradients of 4 and 6°/km. An average 4 km brittle lithosphere at the time of groove formation yields

thermal gradients of 6.5 and 8.5°/km for clean and dirty ice. The given variations in groove width and spacing (implying brittle lithospheres of 2-7 km) yield thermal gradients of 2.5 - 15°/km and 3.5 - 20°/km for clean and dirty ice, respectively.

Variations in thermal gradient, through their effects on the depth to the brittle-ductile transition, also significantly affect the total strength of the lithosphere (defined as the integral of the yield stress versus depth curve (16,17)). Figure 2b shows the relationship between lithospheric strength and brittle lithosphere thickness for Ganymede. For example, the lithospheric strength under extension for a thickness of 10km (corresponding to a gradient of 1.5°/km) applicable to Galileo Regio is about 0.15 in units of 10^6 MPa-m. Marius Regio had lower strengths of 0.05. Lithospheric strengths for grooves varied locally from 0.02 to 0.07 with an average of about 0.03. Note that these strength estimates are insensitive to assumptions regarding the ductile flow law; they are determined almost solely from the inferred thickness of the brittle lithosphere.

Brittle extensional tectonic features on Ganymede indicate a significant lateral variability in thermal gradient and lithospheric strength at the times of their formation. Galileo Regio's long life as a relatively undisturbed remnant of cratered terrain is likely a result of its low temperature gradient and thus increased lithospheric strength. By comparison Marius Regio was fractured and fragmented to its current small size due to its weakness (lithospheric strength 2.5 times lower than for Galileo Regio at the time of furrow formation) imposed by its higher thermal gradient. The thermal gradient during groove formation could have varied from place to place by as much as a factor of 6 and was an average 4 times greater than earlier gradients during furrow formation. This increase in thermal profile is at least partly a result of local heating due to the water ice volcanism that accompanied groove formation and may not indicate a whole-satellite heating event. Nevertheless the variations in temperature gradient shown by the variations in furrow and groove thickness indicate that the cooling of Ganymede was highly inhomogeneous with significant lateral thermal anomalies.

Conclusions

Brittle lithospheric thicknesses estimated from tectonic features formed during the two periods of extensional tectonism during Ganymede's history allow the quantitative determination of thermal gradients because the thickness to the brittle-ductile transition is a function of the temperature gradient. Lithospheric thicknesses inferred from for furrow spacing, 10 and 5 km, indicate temperature gradients of 1.5 - 2°/km and 4-6°/km respectively. An average lithosphere thickness for the grooves of 4 km suggests thermal gradients of 6.5 - 8.5°/km; local variability in the thickness of 2-7 km implies wide variations in temperature profile, 2.5 - 20°/km. This increase in thermal gradient may be a result of local heating during water-ice volcanism accompanying groove formation and may not indicate whole satellite heating. The stability of large remnants of cratered terrain (e.g., Galileo Regio) can be understood in terms of a lower temperature gradient which resulted in an increased lithospheric strength.

LITHOSPHERIC STRENGTH OF GANYMEDE
Golombek, M. P. and W. B. Banerdt

REFERENCES

1) Smith, B.A., and Voyager Imaging Team (1979) The Jupiter system through the eyes of Voyager I, Science, 204, 951-972.
2) Golombek, M.P., and Allison, M.L. (1981) Sequential development of grooved terrain and polygons on Ganymede, Geophys. Res. Lett., 8, 1129-1142.
3) Lucchitta, B.K. (1980) Grooved terrain on Ganymede, Icarus, 44, 481-501.
4) Parmentier, E.M., Squyres, S.W., Head, J.W., and Allison, M.L. (1982) The tectonics of Ganymede, Nature, 295, 290-293.
5) Golombek, M.P. (1982) Constraints on the expansion of Ganymede and the thickess of the lithosphere, Proc. 13th Lun. Plan. Sci. Conf., J. Geophys. Res., 87, A77-A83.
6) McKinnon, W.B. (1981) Tectonic deformation of Galileo Regio and limits to the planetary expansion of Ganymede, Proc. Lunar Planet. Sci. 12B, 1585-1597.
7) Squyres, S.W. (1980) Volume changes in Ganymede and Calisto and the origin of grooved terrain, Geophys. Res. Lett., 7, 593-596.
8) McKinnon, W.B., and Melosh, H.J. (1980) Evolution of planetary lithospheres: Evidence from multiringed structures on Ganymede and Callisto, Icarus, 44, 454-471.
9) Passey, Q.R., and Shoemaker, E.M. (1982) Early thermal histories of Ganymede and Callisto (abs.), Lunar and Planetary Science XIII, 619-620.
10) Fink, J.H. and Fletcher, R.C. (1981) Variations in thickness of Ganymede's lithosphere determined by spacings of lineations (abs.), Lunar and Planetary Science XII, 277-278.
11) Grimm, R.E., and Squyres, S.W. (1985) Spectral analysis of groove spacing on Ganymede, J. Geophys. Res., 90, 2013-2021.
12) Beeman, M.L., Durham, W.B., and Kirby, S.H. (1984) Frictional sliding of ice (abs.), EOS Trans. AGU, 65, 1077.
13) Durham, W.B., Heard, H.C. and Kirby, S.H. (1983) Experimental deformation of polycrystalline H_2O ice at high pressure and low temperature: Preliminary results, Proc. 14th Lunar Planet. Sci. Conf., J. Geophys. Res., 88, B377-B392.
14) Baker, R.W., and Gerberich, W.W. (1979) The effect of crystal size and dispersed-solid inclusions on the activation energy for creep of ice, J. Glaciol., 24, 179-194.
15) Jackson, J., and McKenzie, D. (1983) The geometrical evolution of normal fault systems, J. Struct. Geology, 5, 471-482.
16) Vink, G.E., Morgan, W.J., and Zhao, W.-L. (1984) Preferential rifting of continents: A source of displaced terranes, J. Geophys. Res., 89, 10072-10076.
17) Banerdt, W.B., and Golombek, M.P. (1984) Lithospheric strengths of the terrestrial planets (abs.), Lunar Plan. Sci. XVI, 23-24.

LITHOSPHERIC STRENGTH OF GANYMEDE
Golombek, M. P. and W. B. Banerdt

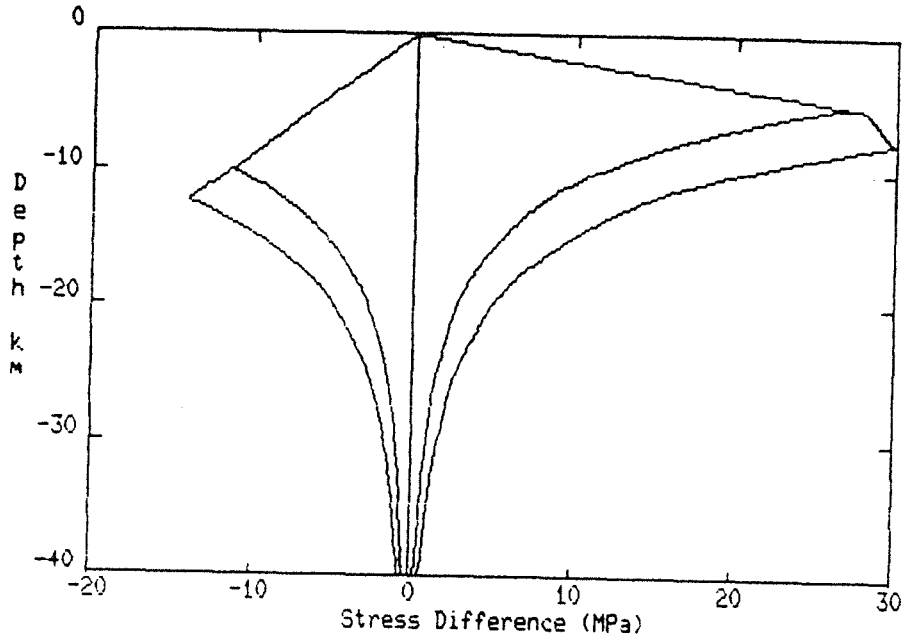

Figure 1. Lithospheric strength envelope as a plot of yield stress versus depth for compression (to the right) and extension (to the left). Linear part of curve is for brittle deformation at shallow levels. Ductile flow of ice I_h for a thermal gradient of 1.5^{o}/km and a surface temperature of 100^{o}K occurs at deeper levels. The upper flow curve is for clean ice deformed at 10^{-15}/sec. The lower curve is an order of magnitude stronger to simulate strengthing due to inclusion of silicates. The intersection between the brittle and ductile fields is the brittle-ductile transition.

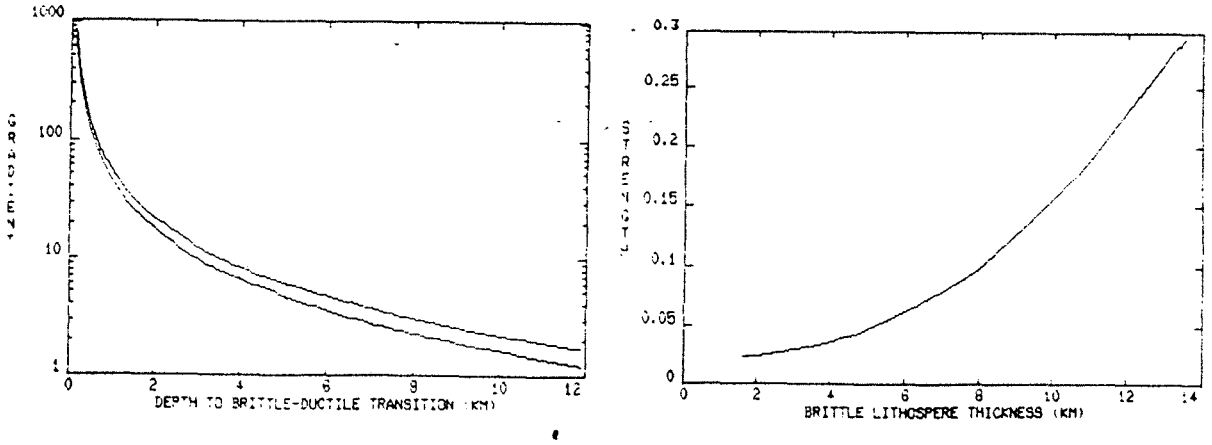

Figure 2. a) Plot of thermal gradient in degrees per km (surface temperature = 100^{o}K) versus depth to the brittle-ductile transition for clean (lower curve) and dirty ice (upper curve). b) Plot of lithospheric strength (integral of yield stress versus depth) in units of 10^{6} MPa-m versus brittle lithosphere thickness under tension. Strength under compression is roughly 50% greater.

IO: MOUNTAINS AND CRUSTAL EXTENSION.

M. J. Heath, Department of Extra-Mural Studies, University of London, 26 Russell Square, London WC1B 5DQ, England.

Schaber (1) has presented a preliminary map of Io detailing surface morphology of an area located between 60°W and 240°W, across the 0° meridian, and below 40°N, covering some 26.5% of the globe. Mountainous terrain, represented by separate massifs as opposed to continuous chains, occupies some 1.9% of the mapped area. Massifs may achieve altitudes exceeding 9 ± 1km above their surroundings and it is considered (2,3,4,5) that topography of this amplitude must be supported by material of largely silicate composition. Mountains are often associated with a unit which Schaber (1) terms 'layered plains', which is characterised by 'an extensive, smooth, flat surface, boundary scarps ranging in height from 150 to 1700m, and abundant grabens'. Scarps are probably controlled by normal faults (1), and extensively eroded in places due to the escape of sub-surface SO_2 at free faces (6).

The role of extensional tectonics in controlling the edges of plateaus is well illustrated in the case of the plateau at 48°S, 320°W. This has an almost straight northeast edge, trending NW - SE. The southeast projection of this lineament passes through the volcanic centre named Aten Patera, and continues along a fissure-like feature from which dark material has effused on either side.

Studies of Earth's mountains benefit from field surveys, geophysical investigations, levelling data and data provided by engineering projects. Our knowledge of Io's mountains is more rudimentary, being based on images of resolution no better than 0.5km per line pair. Nevertheless, available images indicate that these mountains on the Solar System's most active body will provide a challenging subject for future work.

Schaber (1) speculated that massifs might be volcanic constructs or vent deposits fringing giant volcano-tectonic depressions, and identified possible volcanic vents on mountain flanks. Notwithstanding, the evident role of tectonism in

controlling massif morphology may point to an origin by tectonic processes. Mountain and plateau uplift on Io may be polygenetic, however, and it is not possible to reject mechanisms for uplift which involve injection of large thicknesses of magma into the lower part of the crust, as recently discussed for terrestrial examples by McKenzie (7). Such processes might accompany crustal extension.

The mountain at 35°S, 335°W rises as a relatively simple plateau from the low relief 'intervent plains'. Many of the mountains, however, are modified by extensional features, with the implication that extensional processes were involved in mountain formation. Several massifs occur on the shoulders of graben or graben-like features. Haemus Mons (70°S, 50°W) exhibits pervasive lineations of similar trend to those of nearby terrains where extension is in evidence. This might imply a tilted 'pack of cards' structure produced by a style of extensional tectonics similar to that envisaged for certain terrestrial regions by Angelier and Colletta (8). Another possibility is that extension in some areas is accommodated by compression in others, with lateral movements and local uplift along fault planes. Schaber (1) noted a possible lateral displacement near 10°S, 280°W.

There is good reason to conclude that mountains on Io, like those on Earth, are subject to growth and decay. The decay of mountains will be assisted by the ability of SO_2 to rot silicate rock (J. Guest, personal communication) and explosive escape of sub-surface SO_2 from 'aquifers' (Haemus Mons is seen to be covered by bright material, presumably fallout from a SO_2 rich plume which had been active on the mountain flanks). On the west side of the massif at 10°S, 270°W a rugged surface consists of long ridges running perpendicular to the downslope direction, suggesting tectonic denudation with crustal blocks sliding down the mountain flank. Tectonic denudation may be assisted, as in the case of the Bearpaw Mountains, Montana (9) by overloading mountain flanks with volcanic products. The surfaces of some massifs exhibit a well developed, enigmatic 'corrugated terrain',

consisting of complex ridge systems. Ridges may bifurcate, anastomose to form closed depressions and form concentric loops. One possible mechanism for their formation is the deformation of a sheet which is detached from and free to glide over underlying layers in response to gravity. Movements down mountain flanks will be encouraged if there are layers rich in sulphur, SO_2, or other sulphur compounds, providing suitable surfaces of décollement.

None of the disrupted surfaces on or around mountains bear recognisable impact craters down to the limits of resolution, with the implication that these surfaces, like the rest of Io's terrain (see ref. 10) are younger than 1 Myr, and that denudation has been rapid. The mountains on Io are ephemeral.

If this inference is correct, it follows that the presence of mountains on Io requires that mountain formation, continuous or episodic, has been active close to the present day. There is morphological evidence for uplift of massifs. For example, lobes of material debouch onto the layered plains from the massif at 47°S, 340W (northeast of Creidne Patera) in response to tilting. Corrugated terrain on mountain flanks appears to be cut or controlled by lineaments running into mountains from adjacent layered plains. On the massif at 10°S, 270°W the inner edge of a peripheral bench of layered plains seems to embay the south side of the mountain surface with no evidence of normal, thrust, or strike-slip faulting. The outer edge of the bench, however, appears to be controlled by a normal fault. Hence this scarp may represent an increment of uplift common to bench and massif.

Taken together, observations of morphology, heat flux, surface deposits and styles of volcanism may point to the existence of lithosphere domains with distinct compositions and tectonic regimes. Mountains and layered plains are concentrated around the eastern, southern and southwest peripheries of the mapped area, whilst the central part is free of mountains. Shield crater flows occur mainly on the northwest periphery of the area. From Earth based IR observations, Johnson et al. (11) found that

Io's heat flux peaked in the vicinity of Loki (within Schaber's mapped area, near 315°W), the main volcanic centre at the time of the Voyager encounters, suggesting a deep seated, persistent source of volcanism to these workers. McEwen and Soderblom (12) distinguished short lived, energetic plumes, depositing dark material (Surt, Aten and Pele) from long lived, less energetic, SO_2 rich plumes, and noted Loki as a hybrid. Aten, Pele and Loki lie within the mapped area, and Surt not far beyond it to the northwest. Nelson et al. (13) found that SO_2 frost was most abundant from 72°W to 137°W, and least abundant (in the area mapped by Schaber) between 250°W to 323°W. Images and thermal data from the forthcoming Galileo mission should provide a much improved global overview of tectonic and other crustal processes on Io.

REFERENCES

(1) Schaber, G. G. (1980). The Surface of Io: Geologic Units, Morphology, and Tectonics. Icarus 43, 302-333.

(2) Carr, M. H., Masursky, H., Strom, G. H., and Terrile, R. S. (1979). Volcanic features of Io. Nature 280, 729-733.

(3) Masursky, H., Schaber, G. G., Soderblom, L. A., and Strom, R. G. (1979). Preliminary geological mapping of Io. Nature 280, 725-729.

(4) Sagan, C. (1979). Sulfur flows on Io. Nature 280, 750-753.

(5) Clow, G. D., and Carr, M. H. (1980). Stability of sulfur slopes on Io. Icarus 44, 268-279.

(6) McCauley, J. F., Smith, B. A., and Soderblom, L. A. (1979). Erosional scarps on Io. Nature 280, 736-738.

(7) McKenzie, D. (1984). A possible mechanism for epeirogenic uplift. Nature 307, 616-618.

(8) Angelier, J., and Colletta, B. (1983). Tension fractures and extensional tectonics. Nature 301, 49-51.

(9) Reeves, F. (1946). Origins and mechanics of thrust faults adjacent to the Bearpaw Mountains, Montana, Geol. Soc. Am. Bull. 57, 1033-1047.

(10) Johnson, T. V., Cook II, A. F., Sagan, C., and Soderblom, L. A. (1979). Volcanic resurfacing rates and implications for volatiles on Io. Nature 280, 746-750.

(11) Johnson, T. V., Morrison, D., Matson, D. L., Veeder, G. J., Brown, R. H., and Nelson, R. M. (1984). Volcanic Hotspots on Io: Stability and Longitudinal Distribution. Science 226, 134-137.

(12) McEwen, A. S., and Soderblom, L. A. (1983). Two classes of Volcanic Plumes on Io. Icarus 55, 191-217.

(13) Nelson, R. M., Lane, A. L., Matson, D. L., Fanale, F. P., Nash, D. B., and Johnson, T. V. (1980). Io: Longitudinal Distribution of Sulfur Dioxide Frost. Science 210, 784-786.

PN VELOCITY BENEATH WESTERN NEW MEXICO AND EASTERN ARIZONA; Lawrence H. Jaksha, U.S. Geological Survey and New Mexico Institute of Mining and Technology, Socorro, New Mexico

Crustal thinning has usually been associated with a wide-spread heat source in the upper mantle. The low compressional wave (Pn) velocities (≃7.6 km/s) reported beneath extended terrains contrast strongly with normal (≃8.0 km/s) Pn velocities found beneath cratons.

The U.S. Geological Survey began a study of the association between thinned crust and low Pn velocity in 1984. The study area is in the transition zone between the Colorado Plateau and the Basin and Range provinces and lies along the New Mexico-Arizona border at approximately 34.5^{o}N latitude. The study area contains a segment of the Jemez lineament (1), an extensive, late Cenozoic alignment of basaltic volcanism that extends from east-central Arizona to northeastern New Mexico (Figure 1).

Our experiment involves observing Pn arrivals on an areal array of 7 seismic stations located in the transition zone and along the Jemez lineament. We are using explosions from coal and copper mines in New Mexico and Arizona as well as military detonations at White Sands Missile Range, New Mexico, Yuma, Arizona, and the Nevada Test Site as energy sources. Mining explosions at Morenci, Arizona and Gallup, New Mexico will be used later in the study to deduce the velocity structure of the crust above the Pn refractor.

Very preliminary results suggest a Pn velocity of 7.94 km/s (with a fairly large uncertainty) beneath the study area. The Pn delay times, which can be converted to estimates of crustal thickness given knowledge of the velocity structure of the crust increase both to the north and east of Springerville, Arizona. As a constraint on the velocity of Pn we analyzed the reversed refraction line GNOME-HARDHAT which passes through Springerville oriented NW-SE. This analysis resulted in a Pn velocity of 7.9-8.0 km/s for

the transition zone.

These preliminary results along with those reported earlier (2,3) suggest that a normal Pn velocity might persist even though the crust thins (from north to south) by 15 km along the length of the Arizona-New Mexico border. If the upper mantle is currently hot anywhere in western New Mexico or eastern Arizona then the dimensions of the heat source (or sources) might be small compared to the intra-station distances of the seismic arrays used to estimate the velocity of Pn.

References Cited

1. Mayo, E.B. (1958) Lineament tectonics and some ore districts of the southwest. American Institute of Mining Engineers Transactions, 10, p. 1169-1175.

2. Jaksha, L. H. (1982) Reconnaissance seismic refraction-reflection surveys in southwestern New Mexico. Geological Society of America Bulletin, 93, p. 1030-1037.

3. Jaksha, L. H. and Evans, D. H. (1984) Reconnaissance seismic refraction - reflection surveys in northwestern New Mexico Bulletin of the Seismological Society of America, 94, p. 1263-1274.

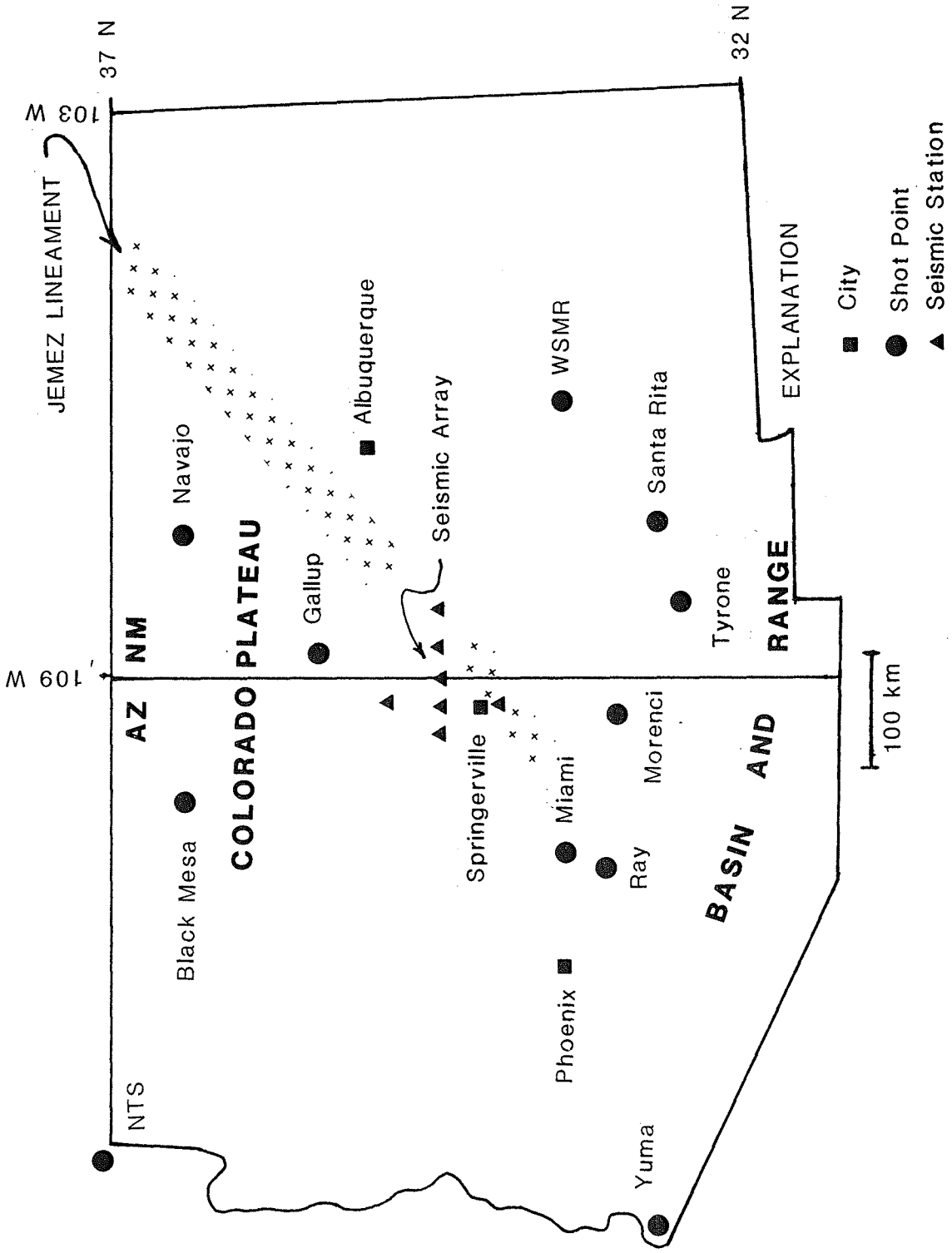
37 N
32 N
103 W
109 W
JEMEZ LINEAMENT
NM
AZ
COLORADO PLATEAU
BASIN AND RANGE
EXPLANATION
City
Shot Point
Seismic Station
Navajo
Albuquerque
Gallup
Seismic Array
WSMR
Santa Rita
Tyrone
Black Mesa
Springerville
Miami
Morenci
Ray
Phoenix
NTS
Yuma
100 km

Figure 1

BRITTLE EXTENSION OF THE CONTINENTAL CRUST ALONG A ROOTED SYSTEM OF LOW-ANGLE NORMAL FAULTS: COLORADO RIVER EXTENSIONAL CORRIDOR; Barbara E. John and Keith A. Howard, U.S. Geological Survey, Menlo Park, California 94025

A transect across the 100 km wide Colorado River extensional corridor of mid-Tertiary age shows that the upper 10 to 15 km of crystalline crust extended along an imbricate system of brittle low-angle normal faults. The faults cut gently down section in the NE-direction of tectonic transport from a headwall breakaway in the Old Woman Mountains, California. Successively higher allochthons above a basal detachment fault are further displaced from the headwall, some as much as tens of kilometers. Vertical excision across the faults may be as much as 15 km. The basal fault(s) cut initially to paleodepths of at least 10 to 15 km, the measured paleothickness of an upended allochthonous slab of basement rocks above the Chemehuevi-Whipple Mountains detachment fault(s). Allochthonous blocks are tilted toward the headwall as evidenced by the dip of the capping Tertiary strata and originally horizontal Proterozoic diabase sheets. Block tilt and degree of extension increase northeastward across much of the corridor. On the down-dip side of the corridor in Arizona, the faults root under the unbroken Hualapai Mountains and the Colorado Plateau. Slip on faults at all exposed levels of the crust was unidirectional. Brittle thinning above these faults affected the entire upper crust, and wholly removed it locally along the central corridor or core complex region. Isostatic uplift exposed metamorphic core complexes in the domed footwall. These data support a model that the crust in California moved out from under Arizona along an asymmetric, rooted normal-slip shear system. Ductile deformation must have accompanied mid-Tertiary crustal extension at deeper structural levels in Arizona.

THERMOMECHANICAL MODELING OF THE COLORADO PLATEAU-BASIN AND RANGE TRANSITION ZONE; Michael D. Londe, Department of Geology and Geophysics, University of Wyoming, Laramie, WY 82071

The Colorado Plateau (CP) - Basin and Range (B & R) boundary is marked by a transition zone on the order of 75 to 150 km in width. As one moves westward across this transition from the CP interior to the B & R there is a variation in the surface topography, surface heat flow, Bouguer gravity, seismicity, and crustal structure. This transition extends eastward into the western CP from the Wasatch-Hurricane fault line and is largely coincident with the high plateaus of Utah and the Wasatch Mountains. Figure 2 shows the variation in surface heat flow, topography, and Bouguer gravity for the three profiles shown in Figure 1. It has been suggested that this transition zone marks a thermal and tectonic encroachment of the CP by the B & R [1, 3, 4].

A simple two dimensional numerical model of the thermal regime for the transition zone has been constructed to test the hypothesis that the observed geophysical signatures across the transition are due to lateral heat conduction from steady state uniform extension within the B & R lithosphere. Surface heat flow, uplift due to flexure from thermal buoyant loading, and regional Bouguer gravity are computed for various extension rates, crustal structures, and compensation depths. Figure 3 shows the dimensions of the models tested in this study. Model compensation depths of 65 and 120 km were chosen to correspond to the depth of the B & R lithosphere, as determined from surface wave studies, and the upper limit of thickness of the CP lithosphere. Two crustal structures are used in this study to examine the effect of the crustal structure on the flexural uplift and the Bouguer anomaly. For one case a thin crust is present to the mechanical boundary and in the second case a thickened block of crust extends 40 km to the west of the mechanical boundary.

Lachenbruch and Sass (1978)(2), have shown that uniform lithospheric extension can adequately explain the surface heat flow in the B & R interior. However theirs is a one dimensional model and cannot be used to examine thermal and mechanical effects near the boundary of the extending region. The use of two dimensional models allows the investigation of the effects of lateral heat conduction into a fixed block (the CP interior) bounding the extending region. Use of a state state model is justified by the fact that the thermal structure of the lithosphere should have reached a dynamic steady state if extension has been occurring for the last 20 to 40 my (2). In effect this model yields a "snapshot" of present conditions.

These models predict heat flow differences of 35 to 45 mW/m^2 across the transition zone. This is consistent with the step in heat flow shown in Figure 2 although the exact nature of the step is not clearly defined due to a lack of detailed observations.

Figures 4 and 5 show the results of uplift and regional Bouguer gravity calculations for a model with a compensation depth of 120 km, 1%/ma strain rate, and the two crustal structures discussed earlier. In Figure 4 a thin crust extends to the mechanical boundary. This structure yields relative uplifts (superposed on an average uplift of 1750 m) of 200-400 m,

depending on flexural rigidity, which are confined to the thick crust fixed block and a relative subsidence of 200 to 300 m within the extending region. The Bouguer anomaly, at a datum of 1750 m elevation, shows a step of approximately 50 to 60 mgals across the transition zone with a small broad low of -15 mgal corresponding to the uplifted zone.

In Figure 5 a thickened crust extends 40 km west of the mechanical boundary. An uplift of 400 to 800 m is generated largely within this zone of thickened crust with a relative subsidence of 200 to 300 m within the extending region. The gravity shows a step of 50 to 70 mgals across this transition with a relative low of -30 mgal corresponding to the zone of uplift.

The results of this simple modeling demonstrate excellent agree with the observed signatures shown in Figure 2. This suggests that a model of uniform lithospheric extension within the B & R with lateral heat conduction into the Colorado Plateau can explain the observed geophysical signatures of the transition zone. This work suggests that the uplift and gravity across the transition zone can be explained by a simple model of elastic plate flexure. The results of the flexural model suggests that the crustal thickness within the transition zone must be at least intermediate in thickness between the observed CP and B & R thicknesses, 30-45 km.

This model is being further refined by calculation of the transfer function of the topography and Bouguer gravity to further constrain the compensation mechanism and material properties.

References

(1) Keller, G.R., L.W. Braille, and P. Morgan, 1979, Crustal Structure, Geophysical Models, and Contemporary Tectonism of the Colorado Plateau, Tectonophysics, 61, 131-147.

(2) Lachenbruch, A.H., and J.H. Sass, 1978, Models of an Extending Lithosphere and Heat Flow in the Basin and Range Provence, in Cenozoil Tectonics and Regional Geophysics of the Western Cordillera, G.S.A. Memoir 152, edited by R.B. Smith and G.P. Eaton.

(3) Thompson, G.A., and M.L. Zoback, 1979, Regional Geophysics of the Colorado Plateau, Tectonophysics, 61, 149-181.

(4) Smith, R.B., 1978, Seismicity, Crustal Structure, and Intraplate Tectonics of the Interior of the Western Cordillera, in Cenozoic Tectonics and Regional Geophysics of the Western Cordillera, G.S.A. Memoir 152, edited by R.B. Smith and G.P. Eaton.

Figure Captions

Figure 1: Base map showing location of profiles 1, 2, and 3 across the CP - B & R Boundary. Heavy dashed line shows location of seismic refraction lines. Light dashed line shows the approximate boundary of the transition zone - central Utah.

Figure 2: Variation surface heat flow, Bouguer anomaly, and elevation across the transition zone. All profiles normalized so that the Wasatch

fault line is at 200 km.

Figure 3: Dimensions, crustal structures, and reference density columns used in the thermal and mechanical models.

Figure 4: Relative uplift and Bouguer gravity anomaly (1750 m datum) for model with a compensation depth of 1120 km, and a thin crust to the mechanical boundary. 1%/ma strain rate.

Figure 5: Same as Figure 4 except how a thickened block of crust extends 40 km west of the mechanical boundary.

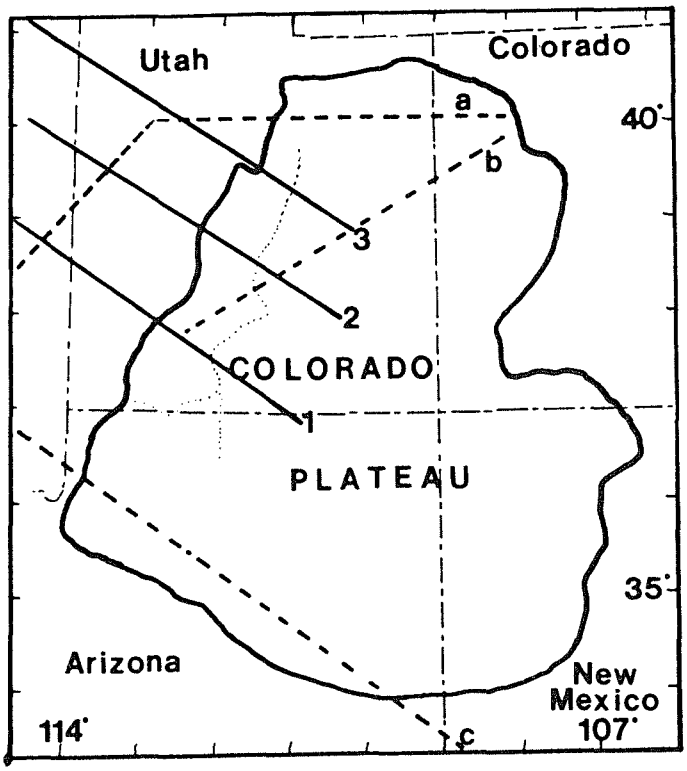

Figure 1

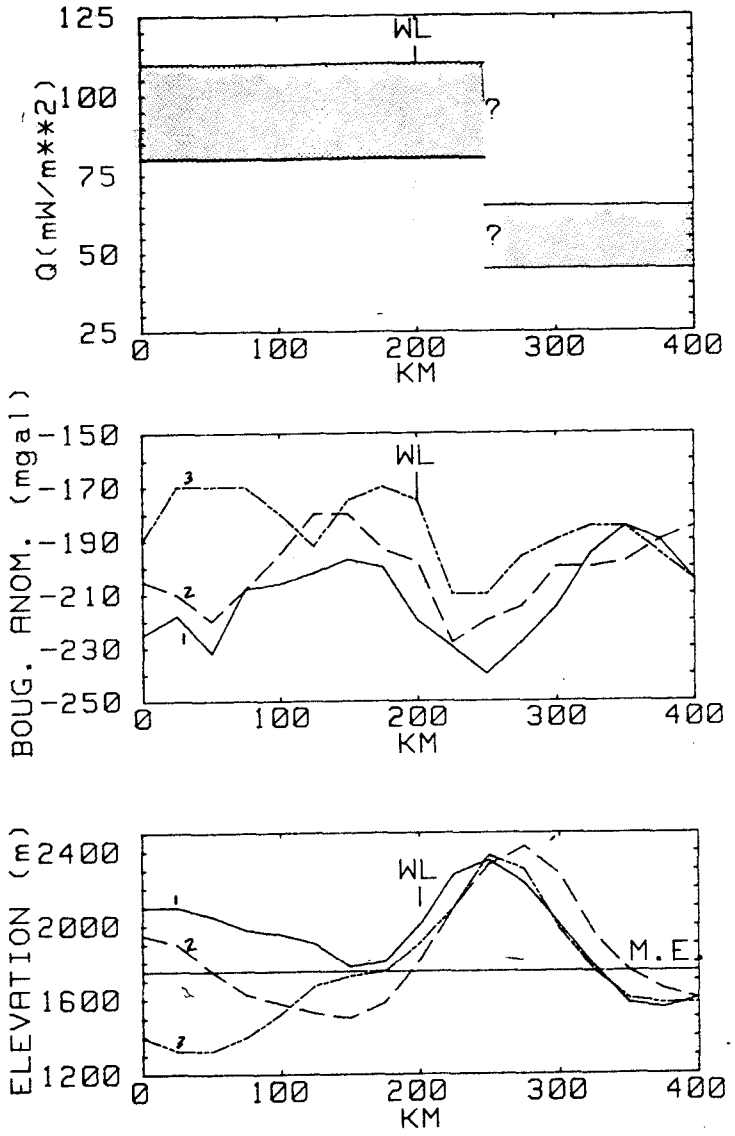

Figure 2

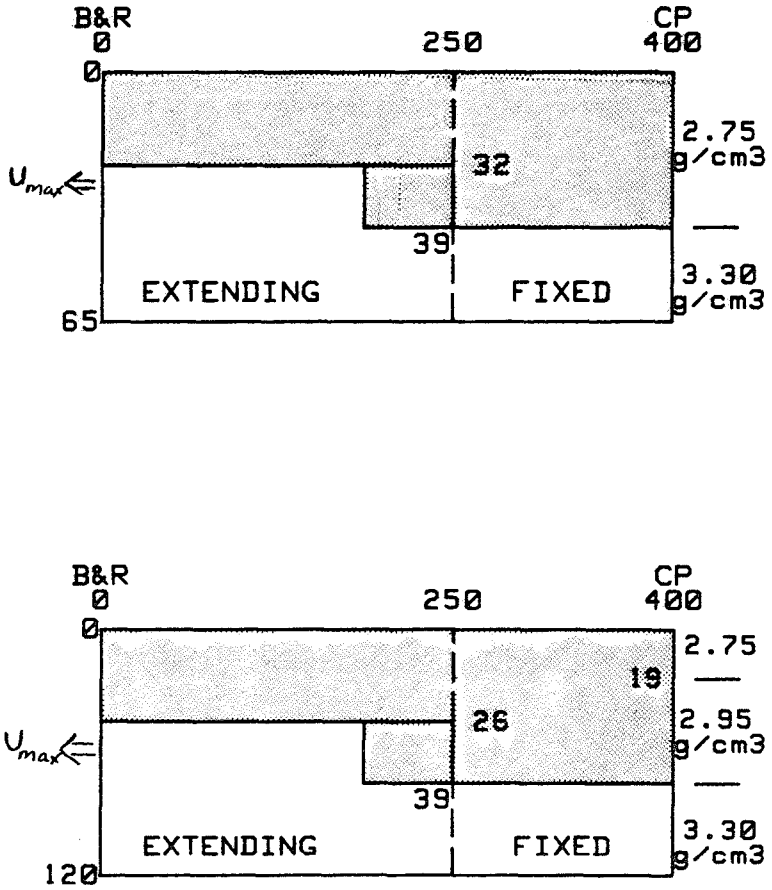

Figure 3

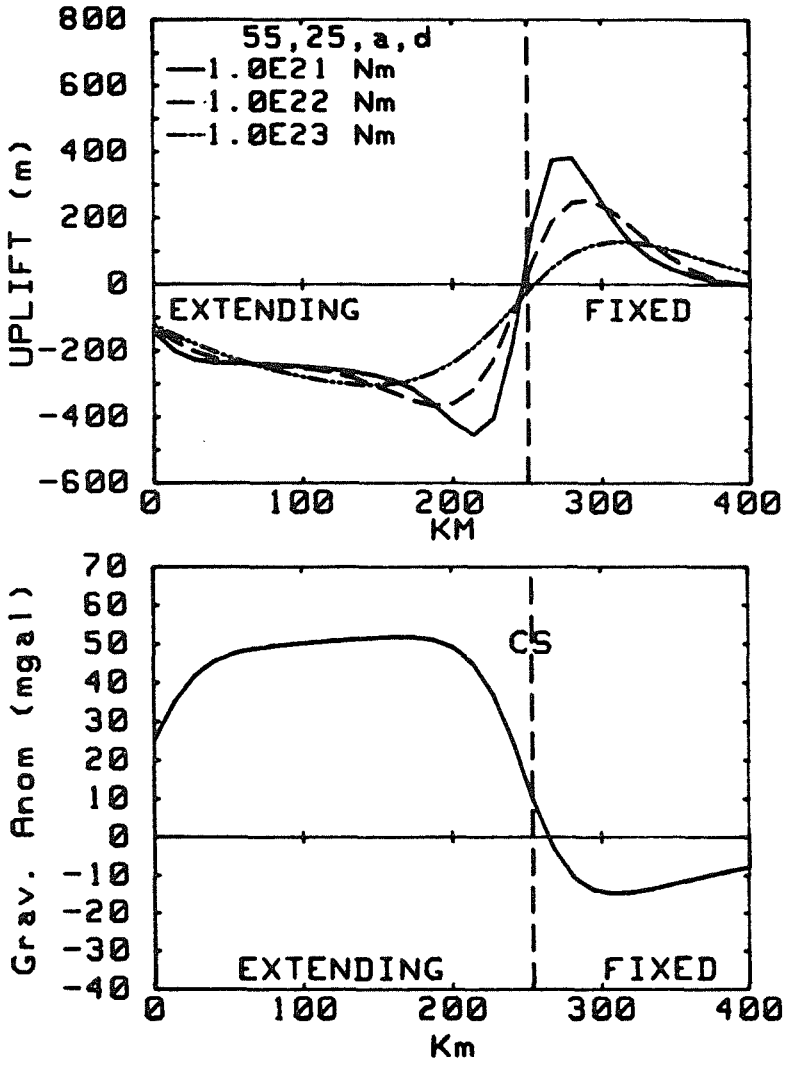

Figure 4

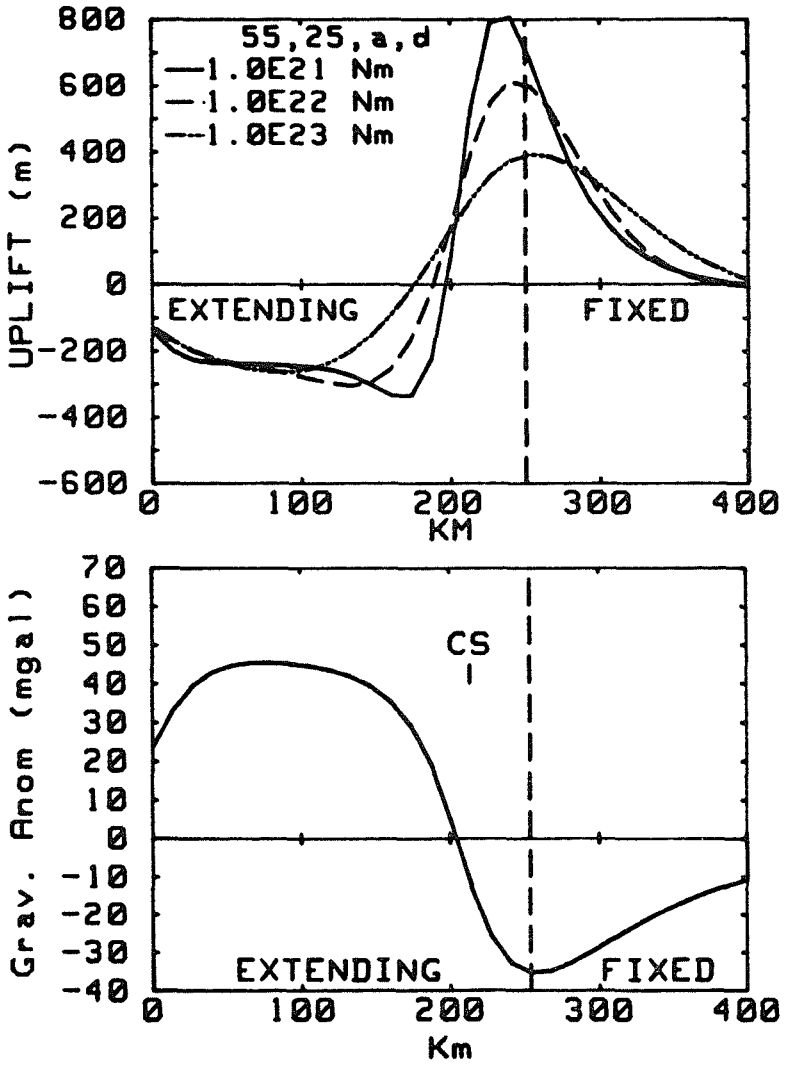

Figure 5

HEAT AND DETACHMENT IN CORE-COMPLEX EXTENSION; Ivo Lucchitta, U.S. Geological Survey, 2255 N. Gemini Drive, Flagstaff, Arizona 86001

The Basin and Range extensional province of western North America is characterized by normal faulting ranging in age from Miocene to Holocene. Two phases are generally present. The earlier Phase I is characterized by closely spaced faults that have strongly rotated intervening blocks through either curvature of the fault plane (listric faults) or progressive tilting of both faults and blocks like a row of dominos. Nearly horizontal faults are a common feature. Together, these characteristics define the "thin-skin" tectonic style of Anderson (1971). The later Phase II is characterized instead by high-angle normal faults that typically have different trends and wider spacing than those of Phase I. Rotation of intervening blocks is modest to absent. These are the faults that have produced the basins and ranges visible today. Similar faults, entirely devoid of rotation, extend onto the uplifted but little-deformed Colorado Plateau adjoining the extensional province. In the northern Basin and Range Province, faulting of Phase II is still going on today. In the Sonoran and Mojave desert regions of Arizona and southeastern California, by contrast, faulting has ceased entirely (Phase III). Bimodal volcanism, most abundant during Phase I and least abundant during Phase III, is the ubiquitous accompaniment to the extension. Each tectonic phase is accompanied and characterized by a distinctive sequence of co-eval deposits (respectively, Sequence I, II, and III). The contemporaneity and coupling of volcanism and tectonism suggest a genetic link between the two; a similar argument can be advanced for the close succession and partial contemporaneity of the three tectonic phases. In this paper I present the view that the volcanism and the three tectonic phases are the result of a single process acting and evolving through time.

Metamorphic core complexes are currently one of the most hotly debated features of the Basin and Range Province, where they are exposed in a belt parallel to and somewhat west of the western margin of the craton. Many core complexes have three chief components: 1. an upper plate composed of unmetamorphosed to weakly metamorphosed rocks that have failed in brittle fashion and Phase I style. 2. a lower plate composed typically of penetratively lineated cataclastic gneiss that has yielded in ductile fashion and is cut by no Phase I faults and only a few Phase II faults. Lineation becomes weaker upward, and chlorite microbreccia and a silicified zone appear as one approaches 3. the basal detachment fault, a gently undulating and nearly horizontal feature that separates the lower and upper plates and marks a sharp discontinuity in the style of deformation. The fault also marks a sharp and major break in metamorphic grade, except for those complexes whose lower plate exposes sedimentary rocks rather than mylonitic gneiss. Characteristic of many core complexes are small to large gravity-glide sheets embedded in sedimentary and volcanic rocks of the upper plate.

Current knowledge of core complexes leads to conflicting interpretations, the crux of which has to do with age of mylonitization, and the relation between mylonitization, detachment faulting, and brittle extension of the upper plate. One school holds that all these phenomena are contemporaneous, and typically of mid-Tertiary age. According to some, the detachment marks the transition from ductile to brittle behavior, the former occuring variously at middle- or upper-crustal levels. Others feel instead that the detachment has a gentle but constant dip, and now juxtaposes rocks originally formed at

different crustal levels. The second main school holds instead that the mylonites and the detachment with associated extension are entirely different in age (latest Cretaceous to early Tertiary versus Miocene), and thus not related genetically.

I propose that the volcanism, the three tectonic phases, and at least part of the lower-plate mylonitization are the result of a single mid-Tertiary thermotectonic process acting and evolving through time. I further propose that these phenomena may be superposed on earlier (Cretaceous) thermotectonic features, and localized by residual heat from the earlier event. These suggestions are based on detailed field work in west-central Arizona, where exposures are good, all three tectonic phases are well-represented, and all three elements of core complexes well-displayed. This area further benefits from the close proximity of the craton (Colorado Plateau) to a core complex, a boundary condition that helps refine and restrict possible interpretations.

A few years ago, it was widely held that the upper plate consisted of a sort of large gravity-glide sheet (for example, Shackelford, 1976). In the Bill Williams area of west-central Arizona, however, it is possible to start in the upper plate directly above the detachment fault, and travel northeastward toward the Colorado Plateau on essentially continuous bedrock exposure. This led Neil Suneson and me to conclude that the upper plate is continuous with basement rocks of the Colorado Plateau, and thus cannot be a gravity-glide sheet (Lucchitta and Suneson, 1981a; Lucchitta and Suneson, 1981b). Penetrative lineation in the lower plate indicates movement either to the northeast or the southwest. The argument given above suggests that the lower plate, a relatively small tectonic element, has moved relatively southwestward from under the craton, and is the active element. Brittle deformation of the upper plate is a passive response to lower-plate movement, as probably is the case with thin-skin tectonics in general. These concepts have been echoed by Wernicke and incorporated in his well-known hypothesis (Wernicke, 1981).

Movement along the detachment fault occurred throughout deposition of the Miocene syntectonic sedimentary and volcanic Sequence I, as shown by dips within the sequence that change gradually from nearly vertical in the lower beds to gently tilted in the upper ones. These dips were produced by rotation of blocks along faults that merge with or are truncated by the detachment, but do not continue beneath it. The sequence of K/Ar radiometric dates helps to document the history of the detachment (Suneson and Lucchitta, 1979; Suneson and Lucchitta, 1983). Basalt near the base of the sequence and 17-18 m.y. old dips steeply, and thus predates most of the movement. Conglomerate interbedded with 12-14 m.y. rhyolites dips only gently, and thus post-dates most faulting. This conglomerate nevertheless is cut by the detachment and listric faults, indicating that the late movements of Phase I were still going on. Concurrently with the faulting, the central area of the core complex was domed up, as indicated by ponding, reversal of drainage, and the emplacement within the Sequence I package of breccias and gravity-glide sheets derived from the uplifted area. Characteristic of this phase are mineralized veins emplaced along the listric faults, and deposits of carbonate, hematite, and copper sulfates, locally with respectable silver and gold concentrations, along the detachment fault. These features suggest hydrothermal activity, which also would explain the breccias (hydrofracturing) and gravity-glide sheets (pore overpressure).

Phase I gradually gave way to the classic basin-range faulting of Phase II, which was accompanied by minor tilting and emplacement of basalts typically 9 to 12 m.y. old. Rhyolites are absent. Both the faults and the basalts occur over much wider areas than the corresponding features of Phase I. Phase II graded into the tectonic quiescence of Phase III, whose early part was marked by the emplacement of small volumes of basalts 5.5-8.5 m.y. old, whereas no volcanic activity occurred later on.

The basalts and rhyolite of Phase I are the volcanic rocks most significant volumetrically, even though they are restricted to a relatively small area. This is especially true of the rhyolites which, however, were emplaced in small centers. Basalts of Phase II are widely distributed, but much smaller in volume than earlier volcanic rocks. Basalts of Phase III are negligible volumetrically.

The picture that emerges is this: (1) intense tectonism, doming, and volcanic activity in a relatively restricted area beginning about 17 m.y. ago, and peaking 12-14 m.y. ago, with emplacement of much rhyolite and accompanied by hydrothermal activity. (2) cessation of rhyolite activity, decrease in volcanism and change in tectonic style, but involvement of a much larger area between about 12 and 9 m.y. ago. Finally, (3) rapid decrease of volcanism and tectonism 8.5-5.1 m.y. ago, and complete quiescence after that.

The coexistence of tectonism and volcanism, and their systematic change with time, suggest that both are the result of thermotectonic processes whose evolution produced the various volcanic and tectonic styles that one sees. This idea is further reinforced by the probable hydrothermal activity, and especially by the fact that the various rhyolite masses, which are small individually and of lower-crust derivation (Suneson and Lucchitta, 1983), could not reach the surface without congealing unless the entire crust was hot. These and other observations are woven into the following model, which is derived from west-central Arizona but probably can be applied to other areas of core-complex or thin-skin tectonics as well.

In mid-Miocene time, probably starting about 17 m.y. ago, parts of west-central Arizona were affected by a thermal pulse associated with northeast-southwest extension. The pulse, which presumably reflects injection of basalts and perhaps of plutonic masses in the lower and middle crust as well, resulted in a steep thermal front migrating upward. Heating was not uniform, so that the surface defined by any isotherm within the front was mildly irregular and showed blister-like domes or welts in the hotter spots. Within the front was a critical surface marking the transition from ductile behavior below to brittle behavior above. This surface was defined primarily by temperature, but also by factors such as pressure and the presence of water. The surface coincided with the detachment fault, given the prevailing extensional regime. When the rhyolites were emplaced 12-14 m.y. ago, at the height of heating, the critical surface was at most a few km beneath the topographic surface in the hottest areas, which were marked by intense deformation along closely spaced Phase I listric faults that had a small radius of curvature and merged with the detachment. The position of the thermal front at this time may well have been controlled and stabilized by interaction with groundwater producing a convective hydrothermal system carrying heat to the topographic surface as fast as it was supplied from below, in the manner of Yellowstone. This mechanism permits elevated

temperatures and very steep thermal gradients to exist in a constant position at very shallow depths beneath the surface. The detachment fault, coincident with the critical surface, was the base of the zone of circulation because ductile flow sealed the rocks beneath it. Consequently, materials such as silica and calcite precipitated above or at the detachment, but at no significant depth beneath it.

With waning of the thermal pulse, rhyolite effusion was shut off, the isotherms sank, and the configuration of the critical surface became smoother through equilibration between areas previously relatively hot and those relatively cold. Even though the critical surface was now deeper than it had been previously in the hot spots, it was still shallow enough to be "seen" by faults at the topographic surface, and this over a wide area. The result was the widely distributed, widely spaced basin-range faults, with large radius of curvature (Phase II). In its descent, the critical surface would have generated and left behind many planes of detachment, none, however, as prominent as the upper one owing to much shorter residence times. This is what one sees in the field and in seismic profiles.

Finally, further cooling caused the critical surface to sink to a level unreachable by faults at the topographic surface, so that tectonism ceased and volcanism shut off as well. This is the quiescence of Phase III.

The model as presented accounts quite well for many of the structural and volcanic features of west-central Arizona as they changed through time. It does not account directly for two things: (1) the Cretaceous dates that have been obtained in places, and the relatively high-pressure phases that have been observed locally in rocks of the lower plate; and (2) the presence in other core complexes of major detachments at stratigraphic breaks within sedimentary sequence rather than at the interface between metamorphic and sedimentary rocks. I propose that these questions can be resolved in part by the characteristics of the K/Ar clock, in part by reactivation of older structural and tectonic features.

Several independent criteria suggest that the temperature in lower-plate rocks, below but near the detachment fault was in the range of 320-360° C. According to E.H. McKee (personal communication, 1983), this is the temperature at which the K/Ar clock begins to be reset at geologically significant rates through argon loss. One would therefore expect that varying amounts of "old" argon would be preserved, depending on the Tertiary thermal history of the particular rocks sampled. Considering that Precambrian igneous and metamorphic rocks probably were the protolith for much of the lower-plate mylonite gneiss, one would expect a wide range of K/Ar dates, as a result of contamination by "old" argon. According to this argument, only the youngest K/Ar ages would be significant with regard to the mylonitization event.

Mixing of older (late Cretaceous-early Tertiary) and mid-Tertiary ages can also result from mid-Tertiary resoftening of areas previously affected by late Cretaceous-early Tertiary thermal softening and deformation. Residual heat from the early event would cause such areas to fail preferentially during the Miocene thermal event, resulting in widespread juxtaposition of older and younger ages and deformation features.

Finally, given strong extension, mechanical inhomogeneities such as old near-horizontal faults and contacts between rocks of widely different strengths are likely to produce detachment and discontinuities in structural style above or even far away from a critical surface of the kind discussed above. Even in this case, however, a detachment related to the critical surface should be present at some depth. In fact, the logic of the critical surface dictates that such a detachment should be present everywhere, the only variable being depth and thus the kind and amount of effects visible at the topographic surface. The ultimate and perhaps outrageous consequence is that such a detachment should be present beneath an entire extensional terrane like the Basin and Range Province.

In summary, it is proposed here that the Miocene to Recent structural and volcanic features of the Basin and Range Province can be explained by a single thermotectonic process acting through time. This process consists of a thermal pulse resulting in a high-temperature regime that includes a steep thermal front moving first up toward the topographic surface, then down owing to cooling induced by a combination of convection and conduction. Within the front is a PT condition defining a critical surface that separates brittle from ductile behavior, and is marked by a nearly horizontal detachment fault. The most prominent and structurally highest position of the detachment results from interaction between the critical surface and a hydrothermal system near the topographic surface. These various features can be superposed on older ones through thermal remobilization or structural reactivation.

References

Anderson, R.E., 1971, Thin-skin distension in Tertiary rocks of southeastern Nevada: Geological Society of America Bulletin, v. 87, p. 43-58.

Lucchitta, I., and Suneson, N., 1981a, Comment on "Tertiary tectonic denudation of a Mesozoic-early Tertiary (?) gneiss complex, Rawhide Mountains, western Arizona": by T.J. Shackelford: Geology, v. 9, no. 2, p. 50-51.

Lucchitta, I., and Suneson, N., 1981b, Observations and speculations regarding the relations and origin of mylonitic gneiss and associated detachment faults near the Colorado Plateau boundary in western Arizona in Tectonic framework of the Mojave and Sonoran deserts, California and Arizona, K.A. Howerd, M.D. Carr, and D.M. Miller, eds.: U.S. Geological Survey Open-file Report 81-503, p. 53-55.

Shackelford, T.J. 1976, Structural geology of the Rawhide Mountains, Mojave County, Arizona [Ph.D. Dissertation]: Los Angeles, University of Southern California, 175 p.

Shackelford, T.J., 1980, Tertiary tectonic denudation of a Mesozoic-early Tertiary (?) gneiss complex, Rawhide Mountains, western Arizona; Geology, v. 8, p. 190-194.

Suneson, N., and Lucchitta, I., 1979, K/Ar ages of Cenozoic volcanic rocks, west-central Arizona: Isochron/west, no. 24, p. 25-29.

Sunson, N., and Lucchitta, I., 1983, origin of bimodal volcanism, southern Basin and Range Province, west-central Arizona: Geological Society of America Bulletin, v. 94, p. 1005-1019.

HEAT FLOW INCREASE FOLLOWING THE RISE OF MANTLE ISOTHERMS AND CRUSTAL THINNING; Jean-Claude Mareschal and George Bergantz, School of Geophysical Sciences, Georgia Institute of Technology, Atlanta, Georgia 30332

Heat flow measurements in the western United States define a zone of high heat flow which coincides with the Basin and Range Province where extension has taken place recently. In this region, the average reduced heat flow is $\sim$30 mW/m^2 higher than in stable continental provinces; locally (e.g., Battle Mountain High), the heat flow anomaly can be more than 100 mW/m^2 above average [1]. Estimates of the amount of extension range between 30% and 100% for the past 30 Ma [2]. In the Colorado Plateau, which has been uplifted without major tectonic deformation, the heat flow is only slightly above average [3].

Several hypotheses have been proposed that would account for the anomalous thermal flux and relate it to the mechanism of extension. Essentially, the models fall into three categories: thinning of the lithosphere by various processes [e.g., 4, 5], distributed injection of basic magmas [6], and increase in heat flow and/or temperature at the lithosphere-asthenosphere boundary.

One of the simplest models accounting for the higher heat flow requires a stepwise increase in heat flux or temperature at the base of a thermal boundary layer. Analytical calculations show that an abrupt change in heat flow at the base of the lithosphere 30 Ma ago would not affect the surface significantly. Uplift would proceed at a slow rate [e.g., 7]. A thermal perturbation at the base of a 40 km thick crust, however, would reach the surface faster and, after 30 Ma, the increase in surface heat flow would be about 75% of the amplitude of the heat flow anomaly. The calculations show that a 500°C increase in temperature at -30 Ma could account for at most 15 mW/m^2 increase in surface heat flow.

The amount of volcanic rocks in the Basin and Range suggests that magma intrusions may provide an effective heat transfer mechanism [6]. It can be shown [8] that if the source of the intrusions is at the base of the lithosphere, the response time will be much longer than 30 Ma, and most of the heat transferred from the asthenosphere will be absorbed in the lithosphere. Also, the amount of magma required to increase in steady state the heat flow by 30 mW/m^2 is equivalent to 100% of the volume of the lithosphere in 30 Ma; an extension of 100% is required to accommodate such an intrusion rate. Local increases in heat flow of the order of 100 mW/m^2 could never be accounted for by such models.

Crustal thinning could also increase the surface heat flow by steepening the geothermal gradient. The calculations show that, for long wavelength perturbations, the fractional increase in heat flow is equal to the ratio of crustal thickness after to thickness before thinning. If the mantle component of the heat flow was 30 mW/m^2 at -30 Ma, the crustal thickness must have been reduced to half its original value, i.e., the original crustal thickness would have been 60 km and the average elevation required by isostatic consideration would have been 3 to 4 km above the present. Geological data seem to rule out such an initial state for the western United States.

In view of these results, it seems that no mechanism is totally adequate to explain the increased surface heat flow and that a combination of effects is needed. The suggested evolution is the following:

The rapid rise of isotherms in the lithospheric mantle with an increase in temperature of the order of 500°C at the base of the crust. The only mechanism for a rapid increase is the mechanical replacement of the lower lithosphere by hotter asthenosphere. This could be the result of diapiric uprise or delamination. Numerical models investigated show that the replacement could occur in a short time (1 to 10 Ma) provided that the effective viscosity of the lithospheric mantle is low enough (10^{20}-10^{21} Pas). The numerical models also show that the rising diapirs spread out at the base of the crust and that the temperature could rise more or less uniformly by 500°C in a short time. Isostatic uplift and lithospheric extension will follow. As the lower crust is heated from below, it becomes more ductile and crustal extension proceeds by flow in the lower crust and fracturing of the upper brittle part of the crust.

The combined effect of the increased temperature at the base of the crust and crustal thinning by extension account for the average increased heat flow. The local high anomalies are not accounted for; they are probably transient effects that follow the intrusion of very large volumes of magma near the surface.

References

[1] Sass, J. H., Lachenbruch, A. H., Munroe, R. J., Greene, G. W., and Moses, T. H., Jr. (1971) Heat flow in the western United States. J. Geophys. Res., 76, p. 6376-6413.

[2] Stewart, J. H. (1978) Basin and Range structure in western North America: A review. GSA Memoir 152, p. 1-31.

[3] Bodell, J. M., and Chapman, D. S. (1982) Heat flow in the north-central Colorado Plateau. J. Geophys. Res., 87, p. 2869-2884.

[4] Bird, P. (1979) Continental delamination and the Colorado Plateau. J. Geophys. Res., 84, p. 7561-7571.

[5] Morgan, P. (1983) Constraints on rift thermal processes from heat flow and uplift, Tectonophys., 94, p. 277-298.

[6] Lachenbruch, A. H., and Sass, J. H. (1978) Models of an extending lithosphere and heat flow in the Basin and Range Province. GSA Memoir 152, p. 209-250.

[7] Mareschal, J. C. (1981) Uplift by thermal expansion of the lithosphere. Geophys. J. Roy. Astr. Soc., 6B, p. 535-552.

[8] Mareschal, J. C. (1983) Uplift and heat flow following the injection of magmas into the lithosphere. Geophys. J. Roy. Astr. Soc., 73, p. 109-127.

RELATIONS BETWEEN EXTENSIONAL TECTONICS AND MAGMATISM WITHIN THE SOUTHERN OKLAHOMA AULACOGEN

D.A. McConnell, Center for Tectonophysics and Department of Geology, and M.C. Gilbert, Department of Geology, Texas A&M University, College Station, Texas 77843.

Variations in the geometry, distribution and thickness of Cambrian igneous and sedimentary units within southwest Oklahoma are related to a late Proterozoic - early Paleozoic rifting event which formed the Southern Oklahoma aulacogen. These rock units are exposed in the Wichita Mountains, southwest Oklahoma, located on the northern margin of a Proterozoic basin, identified in the subsurface by COCORP reflection data [1]. Overprinting of the Cambrian extensional event by Pennsylvanian tectonism obscured the influence of pre-existing basement structures and contrasting basement lithologies upon the initial development of the aulacogen.

Gilbert [2] identified the beginning of the rifting stage as the rise of a basaltic liquid which formed the intrusive Glen Mountain layered complex (GMLC), with an extrusive equivalent, the Navajoe Mountain basalt-spilite group (NMBS) (Fig. 1b). This was probably accompanied by brittle faulting which accomodated extension in the upper crust (not shown in Fig. 1). The greater than 4 km thick GMLC [3] was intruded at shallow depths and must have resulted in extensive updoming of the overlying basement rocks of the Proterozoic basin margin. Thermal expansion must have added to the doming component, perhaps exposing the gabbros to erosion. The GMLC consists dominantly of heteradcumulate/adcumulate anorthositic layers. Abundant strongly laminated plagioclase layers indicate a high degree of compaction which may reflect seismicity (faulting) contemporaneous with consolidation. The associated NMBS formed uniformly thick (300 m) flows across the area [4].

Faulting of the area (now in the general vicinity of the Pennsylvanian Frontal Fault Zone) on arcuate, concave-upward, normal faults, resulted in rotation of the gabbro layering to a north dip as rifting initiated within the aulacogen (Fig. 1c). Dips estimated from mineralogical layering within compositional zones in the GMLC, and from the attitude of the zones themselves, are presently about 10 degrees to the north. Cambrian tilting would have been at higher angles but would have been rotated back during Pennsylvanian compression. Igneous activity was confined to the aulacogen and resulted in a relatively higher heat flow than on the surrounding craton. This suggests that extension occurred along low-angle normal faults analogous to those described for Cenozoic crustal thinning in the Basin and Range province [5]. Post-extensional isostatic re-equilibration resulted in further erosion of the gabbro body and overlying country rock (Fig. 1d). The latter may have provided the source for the Meers metaquartzite which was then deposited locally in fault block sub-basins.

A layering discordance is observed between the GMLC and later Roosevelt gabbros [2] which show a less well defined mineralogic layering, also dipping to the northeast. Therefore, block faulting must have rotated the host GMLC before intrusion of the Roosevelt Gabbros. A Cambrian age is inferred for faulting which truncated the Proterozoic basin layering to the south [1]. In addition, faulting is also documented to have taken place along strike, to the southeast, at this time [4]. Faulting continued during the unroofing erosional event of the two gabbro units because both show layering discordance with overlying granite/rhyolite.

Rhyolite was extruded onto the eroded gabbro unconformity during middle Cambrian. At the southeast end of the aulacogen the rhyolite is 1500 m thick to the northeast and absent to the southwest, indicating that it was laid down in a half graben [4]. North of the Wichita Mountains the Carlton rhyolite is known to be more than 1300 m thick, ranging up to 4000 m in places, but it is unknown to the south of the area. Consequently, a similar half graben structure is postulated for the Wichitas, rather than a later tilting and erosional event such as that suggested earlier [4].

Eruption of the rhyolite may also have been strongly fault controlled. Mapping of ash-flow eruptions elsewhere has shown them to be circular caldera structures overlying pendant-shaped silicic plutons. No caldera structures have been identified in the exposed Wichita Mountains. The lack of distinct gravity lows in the otherwise prominent positive Bouguer gravity confirm that subcaldera structures are missing. Therefore, the rhyolites must have been erupted along linear fissures, perhaps the normal faults themselves.

Within the Wichita Mountains, rhyolite is present overlying GMLC but it has not been shown to be as thick as to the northeast. This may be a consequence of erosion associated with Pennsylvanian uplift, however, the conglomerates derived solely from this erosion have a granitic source [6]. Alternatively, the intrusion of the Roosevelt gabbros may have stabilized the central Wichita 'block' sufficiently to lessen its subsequent rotation and subsidence. The largest volume of rhyolites was, therefore, laid down in rapidly subsiding fault basins north of the central block (Fig. 1e). COCORP evidence suggests that the rhyolites spread beyond the bounding faults of the aulacogen onto the cratonic platform [1, p. 111]. In the Arbuckle Mountains, to the southeast, no major basic intrusives are observed and the rhyolites are contained within the boundaries of the faulted region.

The rhyolite-gabbro contact on the stable central block was favored for the intrusion of the Wichita Granite Group as relatively thin (500 m), but laterally extensive, sills. The granites crystallized from a dry, high temperature (900°-1000°C+) magma which rose near its liquidus. Bulk compositions plot on or near the 4 kb dry boundary curve in the system Qtz-Ab-Or suggesting derivation from a source about 10-15 km deep. This implies rather large mafic plutons at intermediate depths in the crustal column as well as feldspathic-rich "continental" layers available for partial melting. The thermal pulse related to the granite/rhyolite formation would have been strong enough to have potentially generated geothermal gradients of 60-80°C/km within the aulacogen proper. The Meers metaquartzite shows variable metamorphism from low-grade involving chlorite/green-white micas through rare andalusite-bearing rocks to prevalent sillimanite-cordieritespinel grade. These had previously been thought due to contact metamorphism but may additionally reflect a more regional event of the higher postulated heat flows.

Because the granite/rhyolite source is thought to have been at about 10-15 km, and because the rhyolites may have erupted from the faults, it is possible that the listric basal zone for the extensional faults was the zone of partial melting itself. This zone would have directly overlain the gabbroic mass responsible for the melting and which later acted as a source for diabase dikes.

The last igneous activity was a set of late diabase dikes which show

trace element patterns of two interrelated types: 1) a monotonic pattern characteristic of primary continental tholeiites and 2) a modified monotonic pattern with small positive Eu anomalies. The latter set must have tapped crystallizing basaltic magma chambers in the crust. Presumably these are the ones providing the heat necessary to produce the silicic melts at 10-15 km depths.

Igneous activity ceased before the onset of deposition in the late Cambrian, as diabase dikes do not cut the Reagan sandstone at the base of the sedimentary section. This is consistent with a high level crustal heating which could then decay relatively rapidly. Normal gradients must have been obtained, and thus relative cooling, so that basin subsidence could begin.

The aulacogen trend influenced deposition in southern Oklahoma and northern Texas during the lower Paleozoic as the isopach map of the Arbuckle group (Upper Cambrian-Lower Ordovician) shows thinning from the aulacogen, to the southwest (Denison, 1984, personal communication). This thinning can not be explained by erosion along Pennsylvanian structures aligned east-west (Matador Arch, Red River Arch). It is suggested that the thinning occurs across a peripheral bulge which formed a positive feature adjacent to the aulacogen during the Lower Paleozoic. This is consistent with thermal models of basin evolution [7]. Within southern Oklahoma the axis of maximum deposition migrated northward, parallel to the aulacogen trend, during the Paleozoic [8, 9].

Pennsylvanian tectonism uplifted the igneous rocks to the surface along 30-40 degree reverse faults [1]. Prior to uplift these rocks would have been in the brittle field of deformation. As these rock types would have high ultimate strengths in compression it is suggested that they failed preferentially along suitably oriented pre-existing lines of weakness. Consequently, the faults delineated by COCORP [1] may represent reactivated Cambrian normal faults. Rotation along these faults would have been in the opposite sense during the Pennsylvanian, than in the Cambrian, causing shallowing of the original dips and rotating the granite sill until it dipped gently to the southwest in some places.

REFERENCES

[1] Brewer, J.A., Good, R., Oliver, J.E., Brown, L.D. and Kaufman, S., 1983, COCORP profiling across the Southern Oklahoma aulacogen: overthursting of the Wichita Mountains and compression within the Anadarko Basin; Geology, v. 11, p. 109-114.

[2] Gilbert, M.C., 1983, Timing and chemistry of the igneous events associated with the Southern Oklahoma aulacogen; Tectonophysics, v. 94, p. 439-455.

[3] Powell, B.N. and Phelps, D.W., 1977, Igneous cumulates of the Wichita province and their tectonic implications; Geology, v. 5, p. 52-56.

[4] Ham, W.E., Denison, R.E. and Merritt, C.A., 1964, Basement rocks and structural evolution of southern Oklahoma; Okla. Geol. Surv. Bull. 95, 302 pp.

[5] Spencer, J.E., 1984, Role of tectonic denudation of warping and uplift of low-angle normal faults; Geology, v. 12, p. 95-98.

[6] Edwards, A.R., 1959, Facies changes in Pennsylvanian rocks along the flank of Wichita Mountains; in, Petroleum geology of southern Oklahoma - a symposium, v. 2, AAPG, (Eds.) Mayes, J.W., Westheimer, J., Tomlinson, C.W. and Putman, D.M., p. 142-156.

[7] Oxburgh, E.R., 1982, Heterogeneous lithospheric stretching in early history of orogenic belts; in, Mountain building processes, (Ed.) Hsu, K.J., p. 85-93.

[8] Amsden, T.W., 1975, Hunton Group (Late Ordovician, Silurian and Early Devonian) in the Anadarko Basin of Oklahoma; Okla. Geol. Surv. Bull. 121, 214 pp.

[9] Hill, G.W., 1984, The Anadarko Basin: a model for regional petroleum accumulations; p. 1-23 in, Tech. Proc. 1981 AAPG Mid-Continent regional meeting, Oklahoma City Geological Society (Ed.) Borger, J.G., 221 pp.

FIGURE CAPTION

Figure 1. Development of the Southern Oklahoma aulacogen.

a. Postulated pre-aulacogen basement configuration;

b. initial extension accompanying intrusion of GMLC and extrusion of NMBS is masked by physical and thermal doming;

c. continued extension results in faulting and rotation of igneous units;

d. isostatic re-equilibration, intrusion and rotation of Roosevelt gabbros;

e. continued extension results in extrusive rhyolites accumulation northeast of central, stabilized Wichita block; granite sill intrudes along rhyolite/gabbro contact.

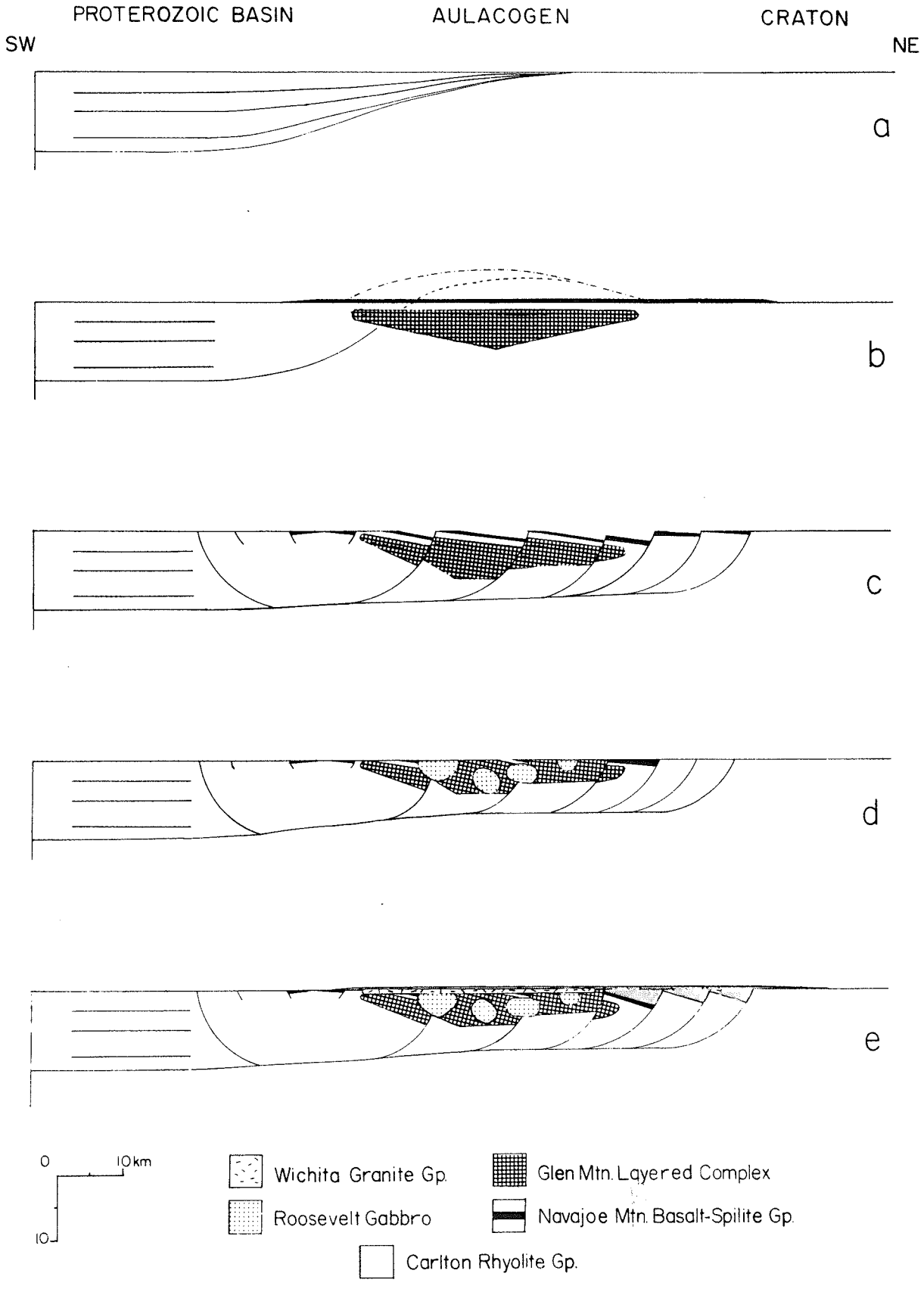
PROTEROZOIC BASIN
AULACOGEN
CRATON
SW
NE
a
b
c
d
e
0
10km
10
Wichita Granite Gp.
Glen Mtn. Layered Complex
Roosevelt Gabbro
Navajoe Mtn. Basalt-Spilite Gp.
Carlton Rhyolite Gp.

HOT-SPOT TECTONICS ON IO. Alfred S. McEwen, Department of Geology, Arizona State University, Tempe AZ 85287; U.S. Geological Survey, Flagstaff AZ 86001.

Introduction. The thesis of this paper is that extensional tectonics and low-angle detachment faults probably occur on Io in association with the hot spots. These processes may occur on a much shorter timescale on Io than on Earth, so that Io could be a natural laboratory for the study of thermotectonics. Furthermore, studies of heat and detachment in crustal extension on Earth and the other terrestrial planets (especially Venus and Mars) may provide analogs to processes on Io.

The geology of Io is dominated by volcanism and hot spots, most likely the result of tidal heating [1,2]. Hot spots cover 1-2% of Io's surface, radiating at temperatures typically from 200 to 400 K, and occasionally up to 700 K [3-7]. Heat loss from the largest hot spots on Io, such as Loki Patera [6], is about 300 times greater than the heat loss from the Hawaiian Swell [8] and 2000 times the heat loss from Yellowstone [9], so a tremendous quantity of energy is available for volcanic and tectonic work.

Active volcanism on Io results in a resurfacing rate as high as 10 cm per year [10], yet many structural features are apparent on the surface. Therefore, the tectonics must be highly active. Structural features on Io include calderas over 100 km wide and up to 2 km deep, grabens and scarps hundreds of kilometers long and up to 2 km high, and tectonically disrupted mountains up to 10 km high [11]. All of these structures appear to be local rather than global features, although tidal stresses may influence lineament directions [11]. Many of the structures may be related to broad isostatic uplift and rifting over thermal anomalies, due primarily to density changes in the lithosphere, as modeled by [12].

The surface of Io is covered by SO_2 and other sulfur-rich materials [2], but the tectonic features and topographic relief indicate that the lithosphere of Io, on the scale of kilometers, consists of some material with considerable strength, such as silicates [13]. Also, the bulk density of Io (3.55 g cm^{-3}) is consistent with a dominantly silicate composition. However, sulfur and SO_2 may be significant volatiles within the crust, and may influence fault movements. Sulfur and SO_2 should be liquids within the shallow subsurface (within a few kilometers depth, depending on the local thermal gradient). Several lines of evidence suggest that liquid sulfur is present at the surface or in the shallow subsurface near the hot spots [14]. Although SO_2 will vaporize near the hot spots, it may be present as a liquid in the shallow subsurface at some distance from the thermal anomalies, and many bright white, high UV-reflectivity deposits (consistent with SO_2 frost) are present along faults and lineaments on Io, so subsurface SO_2 may be common [15]. Liquid sulfur or SO_2 may provide high pore pressures to facilitate low-angle fault movements as does water on Earth [16].

HOT-SPOT TECTONICS ON IO

McEwen, A. S.

The total heat loss from Io is 6-10 x 10^{13} W [7,14], about twice that of Earth (4.2 x 10^{13} W [17]). However, Io is much smaller than Earth, so the mean global heat flow is 1.8 ± 0.5 W m^{-2} on Io compared to 0.08 W m^{-2} on Earth. If all of Io's heat flow was uniformly conducted to the surface, then the solid silicate lithosphere would be only about 5 km thick, overlying a molten interior [1,18]. However, most of the heat loss occurs through the hot spots [4], and the presence of mountains 5-10 km high suggests that the crust is (locally) at least 30 km thick [18,19]. These mountains, as well as ~90% of the hot-spot heat flow [14], and all of the very large volcanic plumes [20] are concentrated in one region of Io centered on 30° S, 310° W, covering about half of the surface; the opposite region of Io may have a much thinner crust [21].

Hot-Spot Tectonics. A number of thermotectonic models have been proposed to explain the late Cenozoic crustal extension of the Basin and Range [e.g. 22-26]. These models have a number of common elements, including high heat flow, associated magmatism, topographic uplift, and thin-skinned tectonics involving listric normal faults and low-angle detachment faults. The driving mechanisms are thermal, so similar tectonic styles might be found in association with the hot spots on Io.

According to the thermotectonic model of Lucchitta and Suneson [26], a detachment fault forms along a critical isotherm marking the brittle/ductile transition in hot spots with steep thermal gradients. This is an attractive model for Io because of the predominance of the hot spots and because the low equilibrium surface temperature of Io (~100 K) will contribute to steep thermal gradients. For movement to occur along a surface, the shear stress, τ, divided by the normal stress, σ, must exceed the internal friction of the material [27]. The ratio τ/σ along a surface (from x_1 to x_2) is given by:

$$\tau/\sigma = \int_{x_1}^{x_2} \frac{(\sigma_1-\sigma_3)2\sin\alpha\cos\alpha}{(\sigma_1+\sigma_3)+(\sigma_1-\sigma_3)(\cos^2\alpha-\sin^2\alpha)}\,dx$$

where σ_1 is the maximum principal stress, σ_3 is the minimum principal stress, and α is the slope of the fault. If a heat source at depth is modeled as a point and the surface is considered planar or parabolic, then the isotherms due to conduction will be parabolas (or paraboloids in 3-dimensions) [28]. Thus, if detachment occurs along a parabolic isotherm, $\sin\alpha$ and $\cos\alpha$ are:

$$\sin\alpha = 2x/a\ (1+4x^2/a^2)^{-1/2}$$

$$\cos\alpha = (1+4x^2/a^2)^{-1/2}$$

where a/4 is the distance from the isotherm to the heat source (Figure 1).

HOT-SPOT TECTONICS ON IO
McEwen, A. S.

A first-order model for the principal stresses considers the force of gravity:

$$\sigma_1 = \rho g d$$

$$\sigma_3 = \rho g (d - U)$$

where ρ = density, g = acceleration of gravity, d = depth to the isotherm, and U = topographic relief over the thermal anomaly. For reasonable values of internal friction for most silicate rocks (~0.5) and assuming a shallow depth to the heat source (a few kilometers), movement due to gravity may occur for a topographic relief greater than ~1 km (on both Earth and Io), provided that cohesive strength is overcome. Movement may occur from much smaller stresses if enhanced pore pressures are present. The first fracture in the upper plate will most likely occur over the apex of the parabola, due to the tensile stress created by the shearing stresses along the isotherm on each side of the apex (Figure 1). This may contribute to the occurance of rifting at the apex of domal uplifts.

Thermotectonic features on Io. The surface expression of hot-spot tectonics expected on Io, in the absence of significant erosion, includes elevated topography, normal faults, rotated blocks, detachment faults, and either an elevated heat flow or evidence for a formerly elevated heat flow (e.g. volcanic vents). Several features on Io show some or all of these characteristics. The best example is a rifted plateau just south of the vent to Pele (18° S, 256° W, where a plume eruption was active during the Voyager 1 encounter). The plateau is broken into four main segments which apparently have rotated and slid radially outwards. These segments fit together in a jigsaw-puzzle fashion, but have separated by ~30 km. The plains surrounding the plateau appear to be intact, suggesting that the segments moved along low-angle detachment faults. The vent region of Pele was detected as a hot spot by the Voyager 1 infrared spectrometer [6]. There are several other examples on Io of uplift and normal faulting associated with hot spots or volcanic vents (e.g. Ulgen Patera, 38° S, 286° W; Aten Patera, 48° S, 311° W; and a feature at 50° S, 35° W).

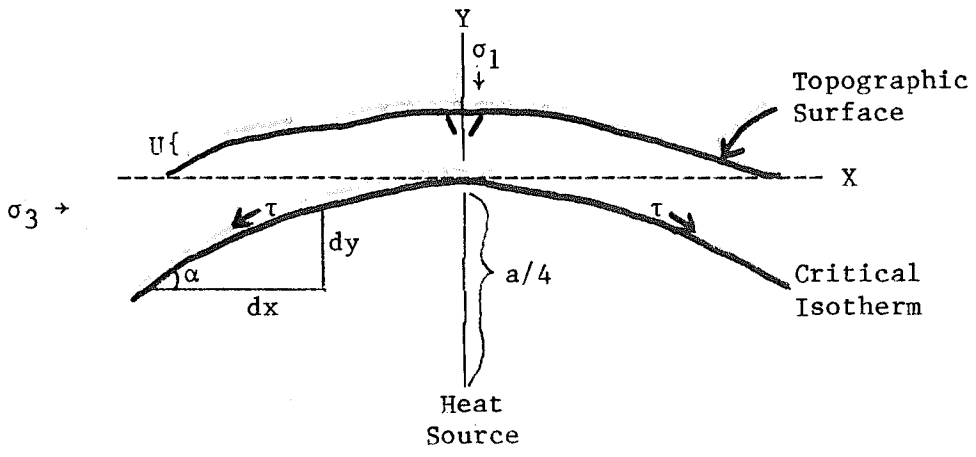

Figure 1. Stresses along a parabolic isotherm

References

[1] Peale, S.J., Cassen, P., and Reynolds, R.T., 1979, Melting of Io by tidal dissipation. Science 203, 892-894.
[2] Smith, B.A., and 26 others, 1979, The Jupiter system through the eyes of Voyager 1. Science 204, 951-972.
[3] Morrison, D., and Telesco, C.M., 1980, Io: Observational constraints on internal energy and thermophysics of the surface. Icarus 44, 226-233.
[4] Matson, D.L., Ransford, G.A., and Johnson, T.V., 1981, Heat flow from Io (J1). J. Geophys. Res. 86, 1662-1672.
[5] Sinton, W.M., 1981, The thermal emission spectrum of Io and a determination of the heat flux from its hot spots. J. Geophys. Res. 86, 3122-3128.
[6] Pearl, J.C., and Sinton, W.M., 1982, Hot spots of Io. In Satellites of Jupiter, 724-755.
[7] Johnson, T.V., D. Morrison, D.L. Matson, G.J. Veeder, R.H. Brown, and R.M. Nelson, Io volcanic hot spots, Stability and longitudinal distribution, Science, 226, 134-137, 1984.
[8] Detrick, R.S., von Herzen, R.P., Crough, S.T., Epp, D., and Fehn, U., 1981, Heat flow on the Hawaiian Swell and lithospheric reheating. Nature 292, 142-143.
[9] Fournier, R.O., White, D.E., and Truesdell, A.H., 1976, Convective heat flow in Yellowstone National Park, in Proceedings of the Second U.N. Symposium on Development and Use of Geothermal Resources, v.1, 731-740.
[10] Johnson, T.V., and Soderblom, L.A., 1982, Volcanic eruptions on Io: Implications for surface evolution and mass loss. In Satellites of Jupiter, 634-646.
[11] Schaber, G.G., 1980, The surface of Io: Geologic units, morphology and tectonics. Icarus 43, 302-333.
[12] Morgan, P., 1983, Constraints on rift thermal processes from heat flow and uplift. Tectonophysics 94, 277-298.
[13] Clow, G.D., and Carr, M.H., 1980, Stability of sulfur slopes on Io. Icarus 44, 729-733.
[14] McEwen, A.S., Matson, D.L., Johnson, T.V., and Soderblom, L.A., 1985, Volcanic hot spots on Io: Correlation with low-albedo calderas. J. Geophys. Res., in press.
[15] McCauley, J.F., Smith, B.A., and Soderblom, L.A., 1979, Erosional scarps on Io. Nature 280, 736-738.
[16] Hubbert, M.K., and Rubey, W.W., 1959, Role of fluid pressure in the mechanics of overthrust faulting. I. Mechanics of fluid-filled porous solids and its application to overthrust faulting. Geol. Soc. Am. Bull. 70, 115-166.
[17] Sclater, J.G., Jaupart, C., and Galson, D., 1980, The heat flow through oceanic and continental crust and the heat loss of the Earth. Reviews Geophys. Space Phys. 18, 269-311.
[18] O'Reilly, T.C., and Davies, G.F., 1981, Magma transport of heat on Io: A mechanism allowing a thick lithosphere. Geophys. Res. Lett. 8, 313-316.
[19] Carr, M.H., 1985, Silicate volcanism on Io. J. Geophys. Res., in press.

[20] McEwen, A.S., and Soderblom, L.A., 1983, Two classes of volcanic plumes on Io, Icarus 55, 191-217.
[21] Soderblom, L.A., McEwen, A.S., Johnson, T.V., and Mosher, J., 1985, The global dichotomy of Io, J. Geophys. Res., in press.
[22] Lachenbruch, A.H., and Sass, J.H., 1978, Models of an extending lithosphere and heat flow in the Basin and Range province. Geol. Soc. Am. Memoir 152, 209-250.
[23] Gastil, R.G., 1979, A conceptual hypothesis for the relation of differing tectonic terranes to plutonic emplacement. Geology 7, 542-544.
[24] Eaton, G.P., 1980, Geophysical and geological characteristics of the crust of the Basin and Range province. In Continental Tectonics, National Academy of Sciences, 96-114.
[25] Crittenden, M.D., Coney, P.J., and Davis, G.H., eds., 1980, Cordilleran Metamorphic Core Complexes, Geol. Soc. Am. Memoir 153, 490 pp.
[26] Lucchitta, I., and Suneson, N., 1983, Mid-and Late-Cenozoic extensional tectonism near the Colorado Plateau boundary in west-central Arizona. Geol. Soc. Am. Abstracts with Programs 14, 182.
[27] Hubbert, M.K., 1951, Mechanical basis for certain familiar geologic structures. Geol. Soc. Am. Bull. 62, 355-372.
[28] McEwen, A.S., and Roller, J., 1984, Experimental and theoretical modeling of hot-spot thermotectonics. Lunar and Planetary Science XV, 527-528.

THE HEART MOUNTAIN FAULT: IMPLICATIONS FOR THE DYNAMICS OF DECOLLEMENT; H.J. Melosh, Lunar and Planetary Laboratory, University of Arizona, Tucson, AZ 85721.

The Heart Mountain decollement in Northwestern Wyoming, U.S.A. originally comprised a plate of rock up to 750m thick and 1300km^2 in area. This plate moved rapidly down a slope no steeper than 2^o during Early Eocene time, transporting some blocks at least 50km from their original positions. Sliding occurred just before a volcanic erruption and was probably accompanied by seismic events. The initial movement was along a bedding plane fault in the Bighorn Dolomite, 2 to 3 meters above its contact with the Grove Creek member of the Snowy Range formation (see Fig. 1 for a stratigraphic section). The major pecularity of this fault is that it lies in the strong, cliff-forming Bighorn Dolomite, rather than in the weaker underlying shales (Pierce, 1973).

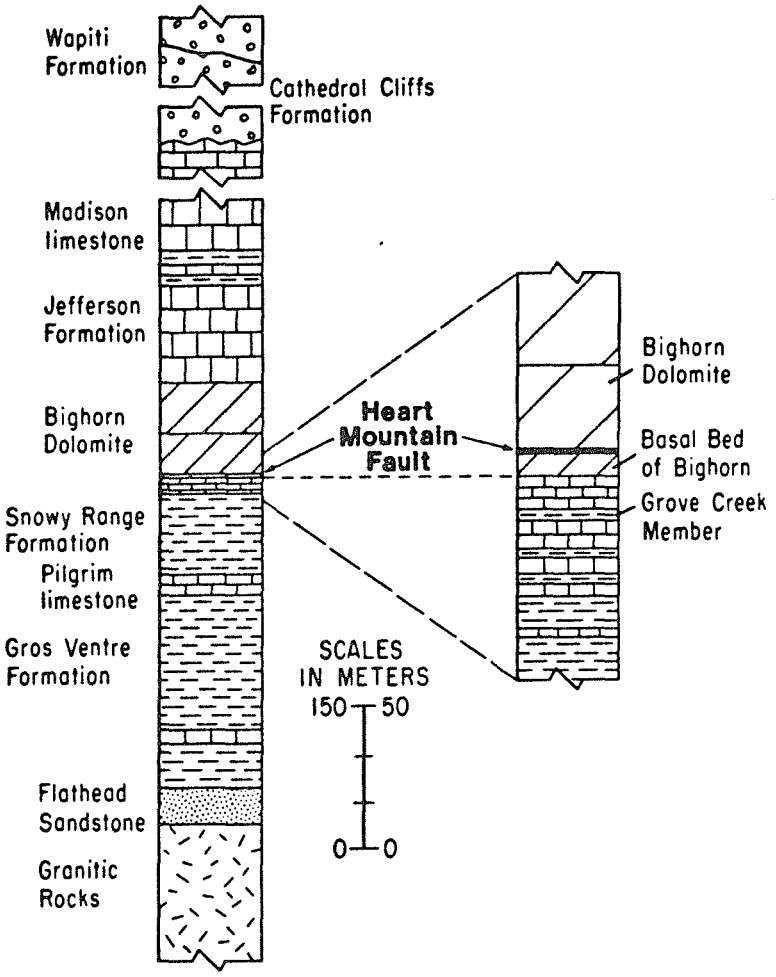

Figure 1. Simplified stratigraphic section showing the formations associated with the Heart Mountain fault. Inset shows a detailed section near the plane of the bedding fault. After Pierce (1973).

The Heart Mountain fault shares this pecularity with other, deeper seated, decollement such as the Keystone and Mormon Mountain systems in Southern Nevada, U.S.A. (Burchfiel et al., 1982). In these latter decollements the detachment horizon lies in strong platformal dolostones several hundred meters above a contact with weak underlying shales, siltstones and limestones. All of these decollements developed at shallow crustal levels (less than 5km depth). None of them show any evidence of having been lubricated by high pressure pore fluids (Guth et al., 1982).

The paradoxical localization of faulting in the strong geologic units in the Heart Mountain and the other decollements provides a strong constraint on the dynamics of the process that produces detachment. It is also clear that this process lubricates the fault plane to an extraordinary degree -- the Heart Mountain decollement slid freely down a slope of less than 2^{o}, and the classic discussions of the mechanics of overthrust faulting (Smoluchowski, 1909; Hubbert and Rubey, 1959) imply a similar degree of lubrication for the Keystone and Mormon Mountain systems. Although many mechanisms have been suggested to account for this reduction of friction, none so far explains the offset of the fault plane into the strongest of the adjacent rock units.

In previous work (Melosh, 1979; 1983) I attributed the fluidization of rock debris in impact crater collapse and large catastrophic landslides to the presence of a strong random acoustic field. A small fraction of the available potential energy is converted into sound waves that are sufficiently strong to briefly relieve the overburden pressure in a portion of the rock mass, there allowing sliding to occur under low net differential stress and, incidentally, also regenerating the sound energy.

A version of this theory also applies to the Heart Mountain fault (Melosh, 1985). The structure of a high-sound-velocity layer (e.g., dolomite) lying next to a low-velocity layer (e.g., shale), Figure 2, approximates an acoustic resonator, capable of partially trapping sound waves. Although fully trapped (Stoneley) waves cannot form under plausible conditions in sedimentary rock sequences, leaky wave modes are possible. Figure 3 shows one such mode and indicates that the maximum wave amplitudes occur in the high-velocity unit (e.g., the dolomite), almost exactly one-quarter wavelength above the lithologic boundary.

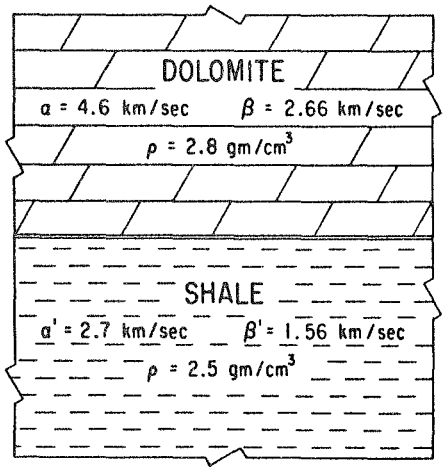

Figure 2. Idealized mathematical model of the rock units near the bedding fault shown in Figure 1. The mechanical properties used to compute the stresses shown in Figure 3 are shown here. The Grove Creek member of the Snowy Range Formation is mechanically grouped with the Bighorn Dolomite in this model.

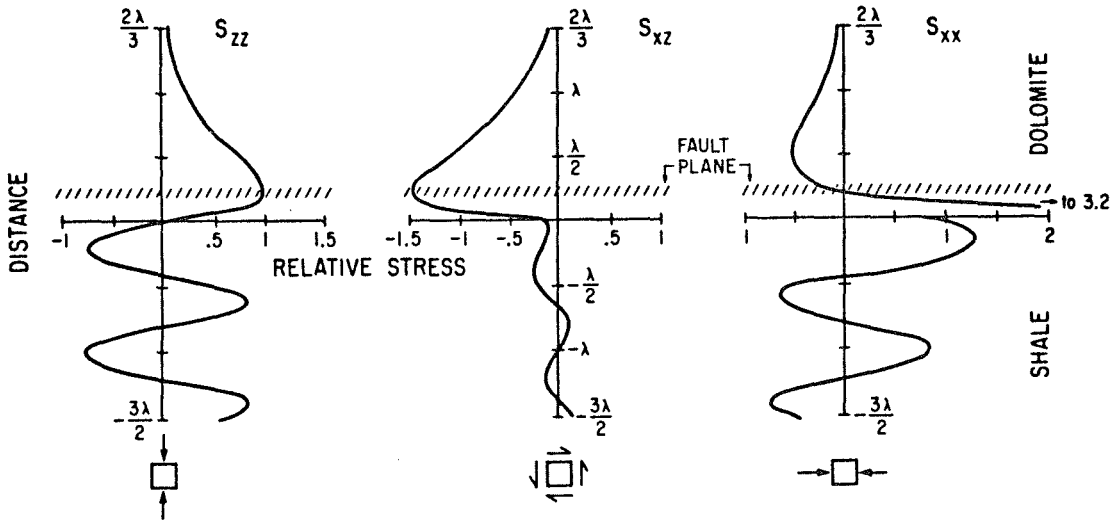

Figure 3. The relative magnitudes of three stress components are shown here as a function of distance away from the lithologic contact at one instant of time. Note that the maxima of both the vertical stress S_{zz} and the shear stress S_{xz} occur about 1/4 wavelength above the contact. This is the horizon where faulting is expected to occur.

The above analysis focusses attention on the partially trapped wave in the global sense, spanning many failure events. An equivalent, failure-by-failure, description can also be given from the viewpoint of renormalization theory (Allegre et al., 1982; Smalley et al., 1985) in which the elastic energy radiated from the failure of one element of the rock mass greatly enhances the probability of subsequent failure at a horizon one-quarter wavelength above the lithologic contact of the strong and weak units. The result is the same: sliding can take place under extremely small average stresses and is localized in the highest sound-velocity unit near a lithologic contact with a low sound-velocity unit.

The major difference between landslides or rapid decollement such as Heart Mountain and deeper-seated decollement such as the Keystone or Mormon Mountain systems is the source of the driving energy. In the first case it is gravitational potential energy, in the latter it is tectonically renewed elastic energy. The lubrication mechanism may be the same in both cases, one that dynamically relieves the overburden stresses by short-wavelength elastic waves radiated during sliding or episodic earthquakes on the fault plane.

This mechanism explains why motion (whether compressional or extensional) occurs preferentially along sub-horizontal fault planes that follow lithologic contacts rather than the steeply-dipping planes of the classic Anderson fault model. It also explains the otherwise emigmatic offset of the fault plane into the stronger (more exactly, higher velocity) of two adjacent geologic units.

Further elaboration of this model should proceed both theoretically, taking into account as much realistic detail as possible for well-studied decollement systems, and observationally, using either natural or artificial high-frequency sound sources to investigate the acoustic trapping properties of natural rock systems.

REFERENCES

C.J. Allegre et al., (1982) Nature 297, 47-49.
B.C. Burchiel et al., (1982) Nature 300, 513-514.
P.L. Guth et al., (1982) Geol. Soc. Amer. Bull. 93, 606-612.
M.K. Hubbert and W.W. Rubey, (1959) Geol. Soc. Amer. Bull. 70, 115-166.
H.J. Melosh, (1979) J. Geophys. Res. 84, 7513-7520.
H.J. Melosh, (1983) Am. Scientist 71, 158-165.
H.J. Melosh, (1985) submitted for publication.
W.G. Pierce, (1973) in Gravity and Tectonics, DeJong and Scholten (Eds.), pp.457-471
R.F. Smalley et al., J. Geophys. Res. 90, 1894-1900.
M.S. Smoluchowski, (1909) Geol. Mag. 6, 204-205.

OCEANIC STRUCTURES OF THE EARTH AND THE NORTH DEPRESSION OF MARS: A COMPARISON OF THE FORMATION MECHANISMS.

E.E.Milanovsky and A.M.Nikishin; Geological Faculty, Moscow State University,II9899,Moscow,USSR.

The system of contemporary oceans of the Earth and the North Depression of the Mars are quasi-simmetrical in reference to the center of one of the hemisphere (fig.I). Both systems had been formed over the common megacycle of evolution of planets and their origin is likely to have similar features.

The formation of the Earth's oceanic system within the South Hemisphere seems to have proceeded in three stages: I) the formation of a network of passive rifts at the center of the Gondwana (fig.2a); 2) the formation of the system of active rifts at the zones of forthcoming spreading (fig.2b); 3) the spreading of the oceanic crust (fig.Ia). The fig.3 displays a hypothetic interpretation of the stages. The first stage is a warm-up of isometric area at the center of the Gondwana Hemisphere,followed by an areal tension and passive rifting which are caused by decrease of the upper mantle density owing to the plunging down of the phase boundaries in the peridotite. During the second stage a redistribution of the heat flow within the upper mantle of the South Hemisphere and its focusing along linear zones,simmetrical to the center of the hemisphere,took place; an active rifting took place within the belts over the mantle zones of increased heat flow. At the third stage a convection in the zones of increased warm-up of the upper mantle reached a steady state,the movement of plates and the spreading of magmatic crust had begun.

The formation of the Mar's North Depression seems to have proceeded in two stages; I) a formation of a dense network of grabens and faults at the center of the North Hemisphere over the upper mantle zone characterized by an anomalous warm-up and a density decrease; 2) a collapse of the ancient crust and it's overflowing by basalts. The first stage of the ocean formation at the Earth (fig.2a) and the Mars is similar. But there seem to have been a thinner lithosphere at the Mars and asthenosphere had been characterised by less density,therefore the dense areal rifting was immediately followed by a total collapse. At the Earth,when the Gondwana had started breaking,the mantle heat flow seem to have been areal first and then it concentrated along the linear warmed-up zones. The zones had caused an origination of asthenospheric diapirs and an active rifting first and then initiated a steady-state convection under the zones of the lithospheric tension and the spreading of the lithospheric plates. It was that process of the heat flow concentration in the mantle which the Mars lacked.

The Tharsis upland on the Mars,as well as the North Depression,occupies the most part of one of the hemisphere and had been developing during the common megacycle of the planetary evolution after the epoch of the North Depression' formation (4). The period of the formation of rift and graben belts wit-

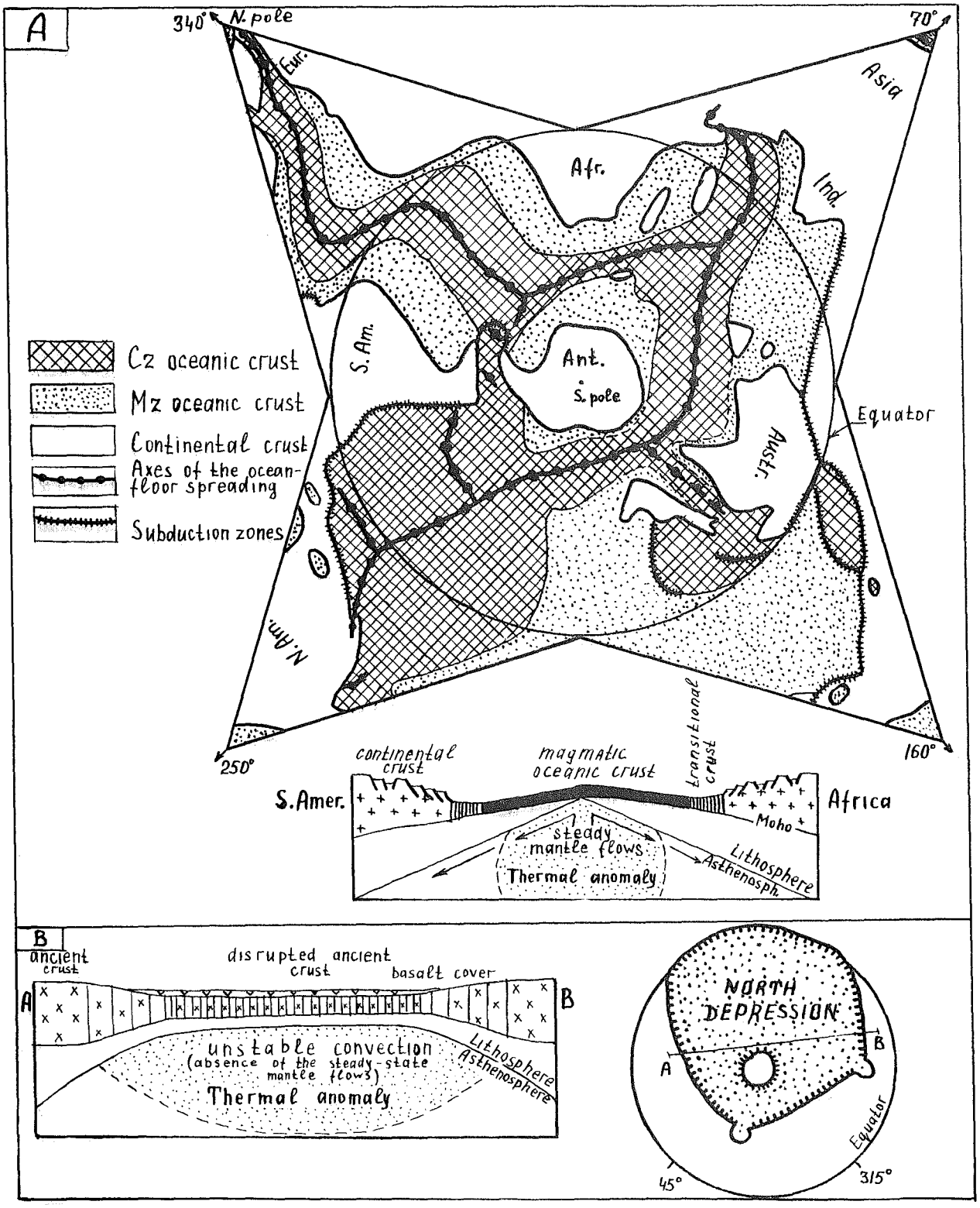

Fig.I. A - the system of the contemporary oceanic structures of the Earth; B - North Depression of Mars for the time of it's formation (adapted from (4)).

Fig.2. Gondwanaland for the Karoo time (A) and just before the splitting and the begining of sea-floor spreading (B). Paleogeographical reconstruction for "A" according to Zonenshine and Gorodnitsky (2) The paleogeographical reconstruction may be rather different. Rift pattern according to the data of (I, 3).

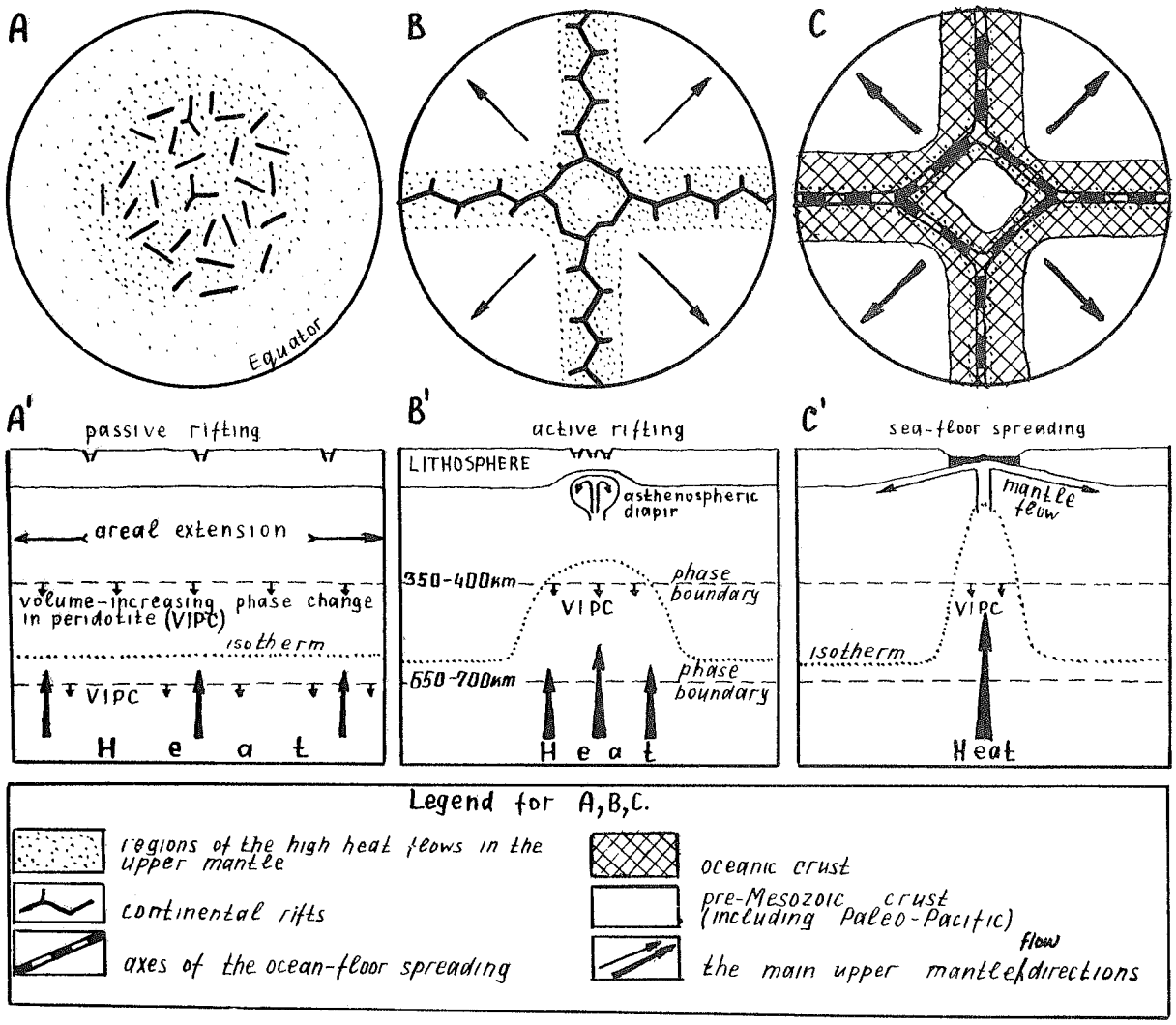

Fig.3. Idealized model of the ocean formation stages since the Late Paleozoic in the South hemisphere of the Earth.

hin the Tharsis upland is similar to the stage "2" of the Gondwana break (fig.2b). However the belts of lithospheric splitting and the zones of spreading of the magmatic crust had not been formed,becouse the Mar's lithosphere at the time of the formation of the Tharsis upland might have been thicker, then that of the Gondwana,and the convection under the Tharsis - weaker. The steady lateral flows within the upper mantle and the plate tectonics are characteristic features of the Earth,which are not observed at any other planets,where the "hot spots" tectonics seem prevail.

References: (I) Burce K.(I978).In: Tectonics and geophysics of continental rifts.Dordrecht:D.Riedel Publ.Co.,p.I-9. (2) Geophysics of oceans.V.2.Geodynamics (ed.by Sorokhtin O.G.) (I979).Moscow:Nauka. (3) Milanovsky E.E.(I983).Riftogenesis in the Earth's history.Moscow:Nedra.(4) Milanovsky E.E.,Nikishin A.M.(I982).Vestnik MGU,ser.geol.,N5,p.I4-26 (in Russian).

THE EVOLUTION OF RIFTING PROCESS IN THE TECTONIC HISTORY OF THE EARTH.

E.E.Milanovsky and A.M.Nikishin, Geological Faculty,Moscow State University,II9899,Moscow,USSR.

The continental rifting is the response of the lithosphere to the oriented tension (I,4). The distribution of viscosity in the lithosphere plays an essential role during all stages of the rifting. The viscosity is a function of the temperature,the lithostatic pressure,the rock composition,the deformation rate and other factors;the temperature being the most important one. The vertical section of continental lithosphere of the rift zone may be devided into the following layers: the upper crust,in which brittle deformation prevails;the medial crust,in which the role of plastic deformation increases;the lower crust,in which plastic deformation prevails;and the uppermost plastic part of the mantle overlapping asthenosphere. The depth of the boundaries in the crust layers are mainly controlled by the temperature.

Since the Early Archean to present days an average thickness of the continental lithosphere had increased from about 50 km,to approximately I50 km,and the temperature at the medial level of the crust and in the asthenosphere had decreased by 200-400^{0}C (2,5). Consequently,the younger the Earth had been, it's lithosphere was thinner,the thickness of the brittle crust reduced,the heat flow and the temperature of the asthenosphere were higher. A thin heated continental lithosphere overlapping a gently sloping surface of the asthenosphere is able to sustain considerable plastic tension without its disruption (e.g., contemporary Basins and Ridges province). On the contrary,a thick lithosphere,with asthenospheric diapir wedged-in,is capable of quick splitting under horisontal tension,since the stress focusses within a narrow heated zone of relatively low viscosity (e.g.,the Red Sea rift). The figure I displays models of the rifting at the different stages of the Earth's development, which illustrates the evolution of this process through the geological history. The splitting of the continental lithosphere and a notable spreading of the new build oceanic crust may occur under the two conditions only: the lithosphere subjected to tension and to wedging-in of the asthenospheric diapir should be thick; steady flows should exist in the upper mantle under rifts with the splitted crust.

All contemporary mid-oceanic rifts are linked into a global system of belts with ascending mantle flows. There was no such global belts 3,5-I,5 b.y.ago. The global systems of large mobile belts appered first in the Earth's history in the Late Precambrian (the Urals-Mongolian belt,the North-Atlantic belt, ets.). Only at that period the lithosphere aquired the fragility similar to that of the present lithosphere. The continental rifting is likely to have transformed into oceanic type rifting first at the end of the Precambrian and the magmatic oceanic crust had formed then for the first time.

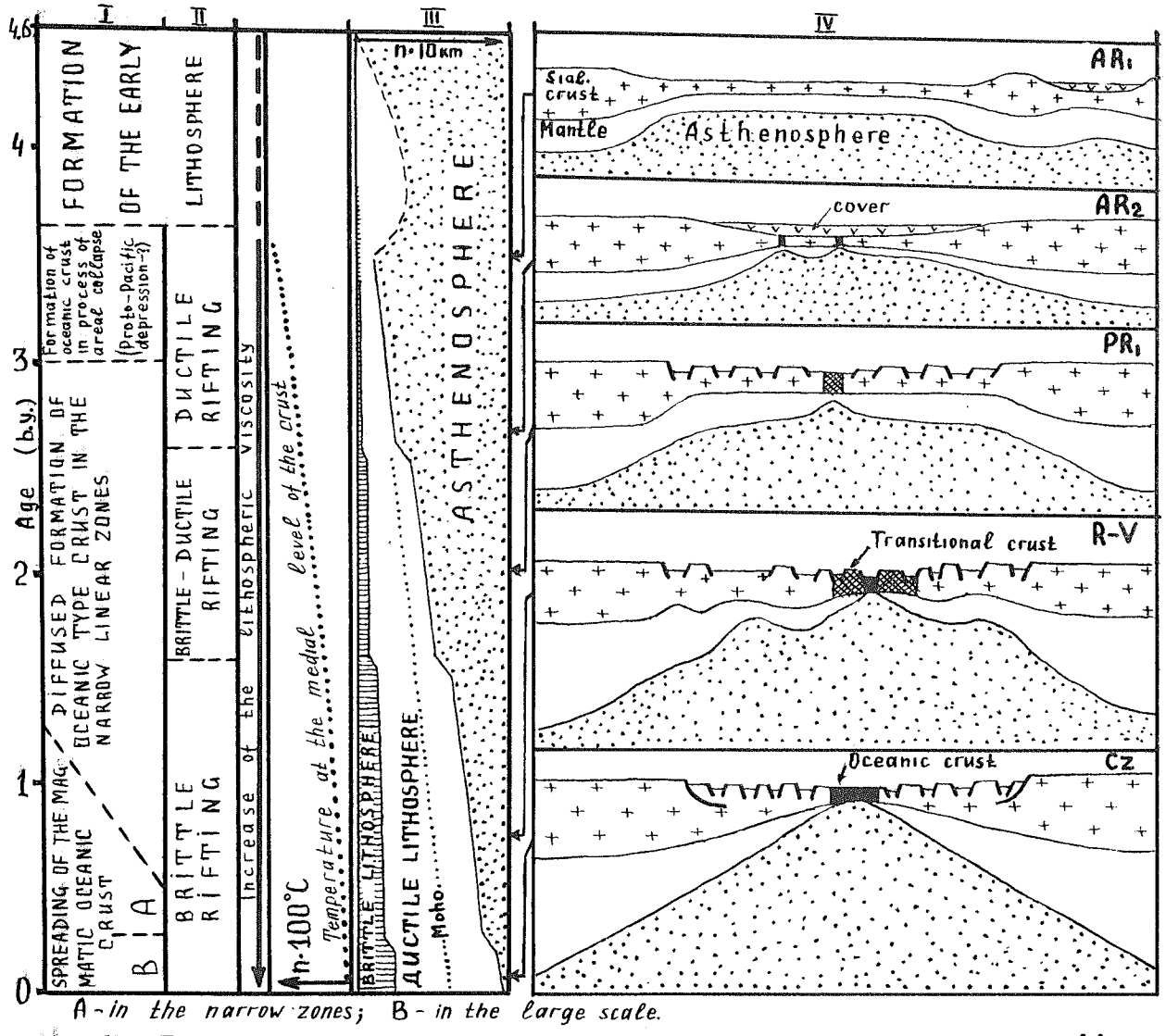

Fig.I. The model of the rifting evolution during the Earth's history. I - oceanogenesis, II - continental rifting, III - generalized section of the continental lithosphere, IY - the model of the rifting pattern. The values of the horizontal crust tension are believed to be nearly equal and less those for the model of the Late Archean "greenstone" basins. For the Early Archean the contemporary granulite (highly metamorphic) and the greenstone belts are shown; for the Late Archean - the zones of contiguous greenstone belts of the Eastern-Goldfield type; for the Cenozoic - the structure of the Red Sea type. A cover is shown for the Archean "greenstone" basins only. The models are based on the data of (2,3,4,5).

References: I. Artyushkov E.V.(I98I).Tectonophysics,v.73, p.9-I4. 2. Condie K.C.(I98I).Archean greenstone belts.Elsevier, Amsterdam. 3. Kroner A.(ed.)(I98I).Precambrian plate tectonic. Elsevier,Amsterdam. 4. Milanovsky E.E.(I983).Riftogenesis in the Earth's history.Nedra,Moscow (in Russian). 5. Wynne-Edwards H.R.(I976).Am.J.Sci.,v.276,p.927-953.

EXTENSIONAL TECTONICS OF THE SATURNIAN SATELLITES: Jeffrey M. Moore, Department of Geology, Arizona State University, Tempe, Arizona, 85287

The saturnian satellites were imaged by the Voyager spacecraft at sufficient resolutions to reveal landforms that indicate histories of extensional tectonics for several of these bodies. The relationships among landforms on various satellites imply that extensional tectonism is a consequence of several different energy sources. Case histories of several satellites will be discussed to illustrate the interaction of various phenomena associated with extensional tectonism.

Mimas

Long, linear, sub-parallel troughs on Mimas (satellite diameter 390 km) are interpreted to be graben formed by global-scale fracturing induced by the impact that formed the 130 km diameter crater Herschel(1). This suggestion is similar to one proposed for the formation of troughs or grooves on the martian satellite Phobos by its crater Stickney(2). It should be noted, however, that the troughs on Mimas do not obviously radiate from Herschel the way grooves do on Phobos from Stickney.

Tethys

A somewhat more complex relationship between impact and extension can be observed on Tethys (1060 km diameter). Ithaca Chasma, an enormous trough system extending at least 270^{o} around Tethys, is narrowly confined to a zone which lies roughly along a great circle that is concentric to the 400-km-diameter Odysseus impact basin(3,4). It was originally suggested that if Tethys was once a sphere of liquid H_2O covered with a thin solid crust, freezing the interior would have produced expansion of the surface comparable to the area of the chasm(3). This hypothesis failed to explain why the chasm occurs only within a narrow zone. Expansion of the satellite's interior should have caused fracturing to occur over the entire surface in order to effectively relieve stresses in a rigid crust(4). The Odysseus impact may have caused Tethys to become temporarily oblate if the satellite was composed of a brittle shell overlying a plastic interior. Forcing Tethys into an oblate spheroid could have induced near-surface tensional fractures along the intersection of the satellite's surface with a plane that is normal to a planetary radius from the center of impact(4). Alternatively, it has been recently proposed that the grabens composing the Ithaca Chasma were formed some time after the impact in response to stresses induced by viscous flow associated with the restoration of Odysseus' floor to match Tethys' geoid(1).

Dione and Rhea

Linear troughs and coalescing-pit chains observed on Dione (1120 km diameter) and Rhea (1530 km diameter) have been interpreted as evidence for episodes of extensional tectonics in these satellites' past(3,5,6,7,8). The globally widespread distribution of these features implies that they were formed by surface-layer tensional stresses created by the volumetric expansion of the satellites' interiors. Theoretical models suggest an early but relatively long-lived period of increasing volume resulting from thermal expansion and/or phase-density changes of H_2O (and hydrates) driven by the rise and fall of output from radionuclide energy sources (9,10).

The location and orientation of some extensional features on Dione may have been controlled by deep-seated fractures established by large impacts and later exploited by endogenic stresses(5,7). Additionally a loss of oblateness due to tidal despinning or orbital recession may have influenced global, extension-related lineament orientation(7). The orientation of extensional features on Rhea are not random. However, they do not form a pattern that can be explained by existing models for lineament trends(8).

Enceladus

The youngest and most tectonically modified surface observed in the saturnian system is that of Enceladus(3). Bands of parallel, alternating troughs and ridges (similar to "grooved" terrain of Ganymede), fissures, and coalescing-pit chains compose a suite of landforms on Enceladus thought to be due to extensional tectonics. Small fissures and troughs probably form initially as tension fractures or graben. Trough-ridge sets may be akin to horst and graben terrains. The morphology of these landforms has probably been significantly modified by the effects of viscous creep and mass wasting thus complicating the identification of the details of their formation. Like similar landforms on Ganymede, the mechanisms by which extensional features are formed on Enceladus is poorly understood(1).

The geological vigor of Enceladus is remarkable in that its diameter is 500 km, only a little larger that Mimas and less than half the diameters of Tethys, Dione, and Rhea. Like the Galilean satellite Io, it is probably heated by the tidal-torque flexing of its interior(11,12). Tidal heating joins large basin-forming impacts and radionuclide decay to form the three identified energy sources for extensional tectonics on the saturnian satellites.

REFERENCES

(1) McKinnon, W.B. (1985) Geology of icy satellites, submitted to Proc. NATO Conf. Ices in the Solar System, D. Reidel Pub.
(2) Thomas P. and Ververka, J. (1979) Icarus, 40, 394-405.
(3) Smith, B.A. et al. (1982) Science, 215, 504-537.
(4) Moore, J.M. and Ahern, J.L. (1983) Proc. Lunar Planet. Sci. Conf. 13th, in J. Geophys. Res., 88, A577-A584.
(5) Smith, B.A. et al. (1981) Science, 212, 163-191.
(6) Plescia, J.B. (1983) Icarus, 56, 255-277.
(7) Moore, J.M (1984) Icarus, 59, 205-220.
(8) Moore, J.M. et al. (1985), Proc. Lunar Planet. Sci. Conf. 15th, in J. Geophys. Res., 90, C785-C795.
(9) Ellsworth, K. and Schubert, G. (1983) Icarus, 54, 490-510.
(10) Pollack, J.B. and Consolmagno, G. (1984) in Saturn, T. Gehrels and M.S. Matthews, ed., pp. 811-866.
(11) Squyres, S.W. et al. (1983) Icarus, 53, 319-331.
(12) Lissauer, J.J. et al. (1984) Icarus, 58, 159-168.

Lithospheric and Crustal Thinning; Moretti, I. - Institut Français du Pétrole, B.P. 311, 92506 RUEIL MALMAISON CEDEX, France

In rift zones, both the crust and the lithosphere get thinner. The amplitude and the mechanism of these two thinning are different. The lithospheric thinning is a thermal phenomenon produced by an asthenospherical uprising under the rift zone. In some regions its amplitude can exceed 200 %. This is observed under the Baikal rift where the crust is directly underlain by the list mantellic asthenosphere (Zorin and Osokina, 1984). The presence of hot material under rift zones induces a large negative gravity anomaly (Ramberg and Morgan, 1984). A low seismic velocity zone linked to this thermal anomaly is also observed (Puzyrev et al., 1978). During the rifting, the magmatic chambers get progressively closer from the ground surface (Wendland and Morgan, 1982). Simultaneously, the Moho reflector is found at shallow depth under rift zones. This crustal thinning does not exceed 50 % (30 % in Suez, Makris et al., 1985; 25 % in East African Rift, Long, 1976; 30 % in Baikal rift, Puzyrev et al., 1978). Tectonic stresses and vertical movements result from the two competing effects of the lithospheric and crustal thinning. On the one hand, the deep thermal anomaly induces a large doming and is associated with extensive deviatoric stresses. On the other hand, the crustal thinning involves the formation of a central valley. This subsidence is increased by the sediment loading. The purpose of the paper is to quantify these two phenomena in order to explain the various morphologycal and thermal evolution of rift zones.

Geological records indicate that the rifting process can be fairly rapid, say 10 Ma. The time-scale has ruled out simple conductive mechanism based upon the effect of an asthenospheric thermal anomaly to explain the lithospheric thinning. Nevertheless, the propagation of a thermal perturbation across the whole lithosphere requires at least 50 Ma. Two mechanisms are thus postulated to respect the observed time scale: the first one considers a possible upward advection of hot material (Neugebauer, 1982; Turcotte and Emerman, 1983), the second one (Fleitout and Yuen, 1984) results from the ability of the thermal lithospheric structure to be destabilized on a short time scale by secondary convection. The model is based on a temperature- and pressure- dependent rheology; this yields a viscosity minimum at the base of the lithosphere and therefore favours a rapid convective thinning. The present paper adopts a similar approach; figure 1 depicts the general physical aspects of our model. The numerical code used to solve the thermo-mechanical equations (Anderson and Bridell, 1980) and the viscosity law are the same as those used by Fleitout et al. (1984). An initial thermal perturbation induces a convective flow; the resulting mass displacements and stresses affect the lithosphere and the gravity field. The stresses at the bottom of the crust are then used to quantify the vertical movements and the infered extensiv tectonic style.

The crustal behaviour in these extensional stress-field is very problematical. Seismic data point out a noconservation of the crustal mass during rifting (Chénet et al., 1982). The main phenomenon for crustal thinning may be different from the classical plastic flow commended by Mc Kenzie (1978). Mantellic dykes intrusions can also be envisaged at the base of the crust. These intrusions increases the mean density of the lower crust and changes this seismic velocity. We have tested these two extreme hypothesis.

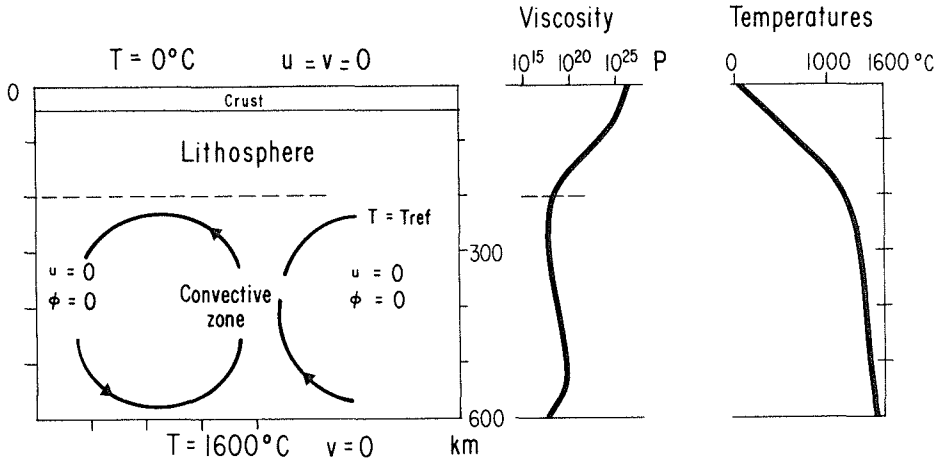

Fig. 1 : General hypothesis

Temperature boudary conditions are constant values at the surface and at the bottom of the box and lateral flow (φ) nul at the two side. u is the horizontal velocity and v the vertical velocity. The viscosity is gived by $\eta(T,z) = A \exp(Q/RT - Q/RT_r) \exp(z/B - Z^2/C)$

where z is the depth, Q the activation energy, R the gas constant and Tr is a reference temperature, A, B, C, are coefficents (Fleitout and Yuen, 1984).

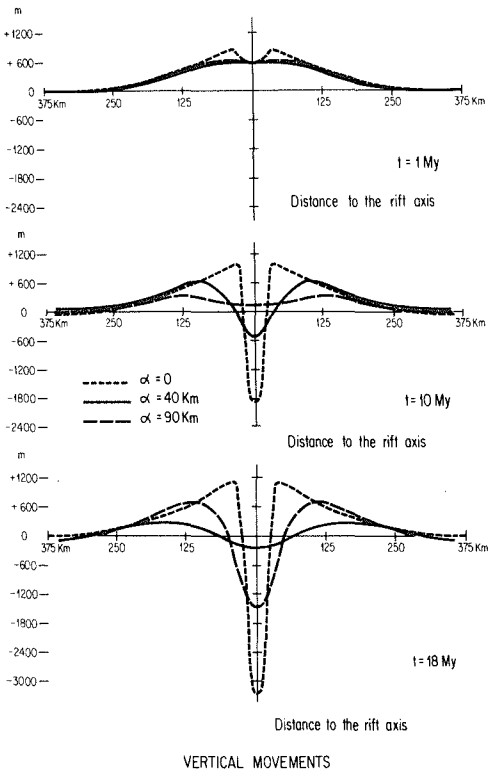

Fig. 2: vertical movements in meters function of the time. See other hypothesis in text. α is the flexural parameter.

As an example the figure 2 shows the topographic evolution for a crustal thinning of about 1 km/y with a velocity of the sedimentary loading of 0,125 mm/y in the 50 km.wide central valley without regional extension. Three crustal responses are assumed: a local and two regional distinct compensations (elastic behaviour with 40 and 90 km as flexural parameter). The possibility of a regional extensive stress is also envisaged. This induces an acceleration of both crustal and lithospheric thinnings. The displacement at the bottom of the crust and the heat flow variations at the surface are plotted on fig. 3; the horizontal velocity is constant (3 mm/y), the mass preservation is respected due to a mantle uprising.

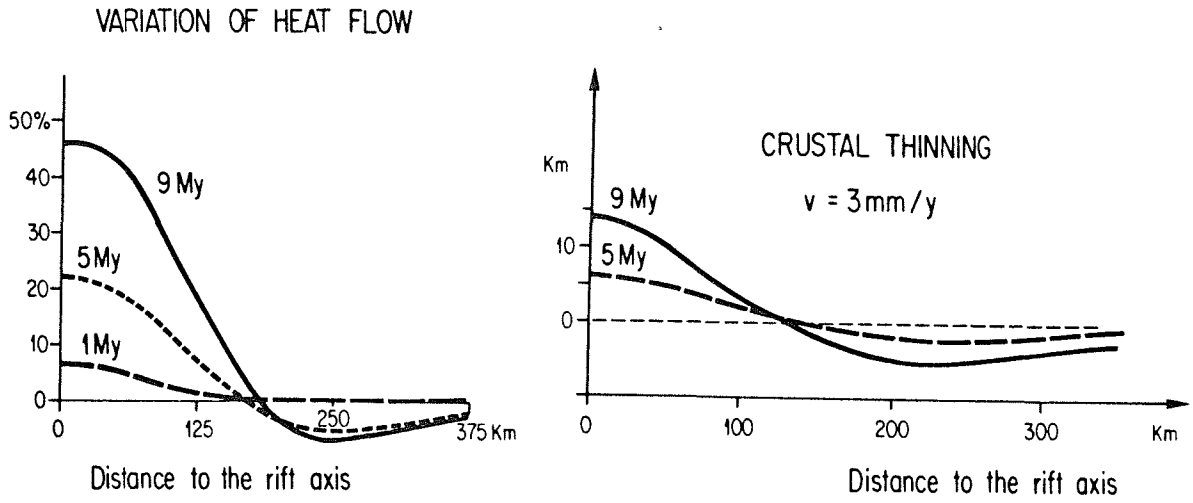

Fig. 3 : Heat flow variations and crustal thinning function of time. The horizontal fixed velocity is 3 mm/y. The mantle uprising induce a initial thermal anomaly of about 5 % in the central part.

In conclusion we show that many rift features and evolution patterns are best explained by these two scale processes. The mantle uprising first causes regional uplift. Too small crustal thinnings induce thermal doming whereas larger ones induce subsidence of the rift valley and uplift only on rift shoulders. When the crustal thinning stops, later, the whole region becomes uplifted; the potential subsidence of the already formed grabens in then only due to sediments loading.

Bibliography

Anderson, C., and Bridwell, R., 1980 - A finit element method for studying the transient non-linear thermal creep of geological structures. Intern. Journ. of numerical and analytical methods in geomechanics, 4, 255-276.

Chénet, P., Montadert, L., Gairaud, H., Roberts, D., 1982 - In Studies in continental margin geology, AAPG Mem. n°34, 703-715.

Fleitout, L., and Yuen, D., 1984 - Steady-state, secondary convection beneath lithospheric plates with temperature and pressure dependent viscosity, J.G.R., 89, 9227-9244.

Fleitout, L., Yuen, D., and Froidevaux, C., 1984 - Thermomechanical models of lithospheric deformation: application to the tectonics of western Europe. Thèse d'Etat, Université Paris Sud-Orsay.

Mc Kenzie, D., 1978 - Some remarks on the development of sedimentary basins, Earth Planet Sciences Letters, 40, 25-32.

Long, R., 1976 - The deep structure of the East African rift and its relation to Afar, in Afar between continental and oceanic rifting,

Schweizebart.

Mareschal, J.C., 1983 - Mechanism of uplift preceding rifting, Tectonophysics, 94, 51-66.

Makris, J., Stofen, B., Vees, R., Allam, A., Maamoon, M., Shebata, W., 1985 - Deep seismic soundings in Egypt: Part II: crust and upper mantle of the Red Sea Coast. In press.

Neugebauer, H., 1983 - Mechanical aspects of continental rifting, Tectonophysics, 94, 91-108.

Puzyrev, N.N., Mandelbaum, M.M., Krylov, S.V., Mishenkin, B.P., Petrik, G.V. and Krupskaya, G.V., 1978 - Deep structure of the Baikal and other continental rift zones from seismic data, Tectonophysics, 45, 15-22.

Ramberg, I., and Morgan, P., 1984 - Physical characteristics and evolutionary trends of continental rifts. In press.

Tiercelin, J.J. and Favre, H., 1978 - Rates of sedimentation and vertical subsidence in neorifts and paleorifts, Tectonics and geophysics of continental rifts.

Turcotte, D., and Emerman, S., 1983 - Mechanisms of active and passive rifting, Tectonophysics, 94, 39-50.

Wendlandt, R., and Morgan, P., 1982 - Lithospheric thinning associated with rifting in East Africa, Nature, 298, n° 5876, 734-736.

Zorin, Y., and Osokina, S., 1984 - Model of the transient temperature field of the Baikal rift lithosphere, Tectonophysics, 103, 193-204.

THERMAL CONTROL OF THE STYLE OF EXTENSIONAL TECTONICS; Paul Morgan, Department of Geosciences, Purdue University, West Lafayette, IN 47907, USA.

Crustal extension is accommodated by a wide range of structural styles ranging from high-angle normal faults to low-angle detachments. In some areas different structural styles are superposed by multiple extension events, and in other areas different structural styles are juxtaposed along strike in the same extension event. As shown below with examples from the Rio Grande rift and the Red Sea-Gulf of Aden rift system, high strains and low-angle faulting are commonly spatially and temporally associated with hot and probably thin lithosphere as indicated by major coeval magmatic activity. Theoretical studies of strength profiles in the lithosphere suggest that there may effectively be a critical range for the geotherm above which low-angle faulting and crustal decollement may be favored over high-angle faulting.

At least two phases of Cenozoic extension have been identified in the Rio Grande rift (1). Early phase extension began in mid-Oligocene (about 30 Ma) and may have continued to the Early Miocene (about 18 Ma). This phase of extension is characterized by local high-strain extension events (locally 50-100%, regionally 30-50%), low-angle faulting and the development of broad, relatively shallow basins. Extension events were not synchronous during early phase extension and were often temporally and spatially associated with major magmatism. Late phase extension occurred primarily in the Late Miocene (10 to 5 Ma) with minor extension continuing to the present. It is characterized by apparently synchronous, high-angle faulting giving large vertical strains with relatively minor lateral strain (5-20%) which produced the modern Rio Grande rift morphology. Late phase graben or half- graben basins cut, and often obscure early phase broad basins. A similar two-phase extension history has been reported for other areas of the Basin and Range province (2).

Evidence has recently been presented for the Red Sea-Gulf of Aden rift system to suggest that rotation of the Arabian peninsula away from north-east Africa has been accommodated synchronously by mechanisms ranging from sea-floor spreading in the central portion of the Red Sea to diffuse extension in the Afar triangle (3). Courtillot (3) has described this mechanism as the propagation of two rifts from the the Red Sea and the Gulf of Aden into the Afar region, the eventual interconnection of which will effect the complete separation of southern Arabia from the African continent. Of interest to the present study is the change in extensional style along strike in the Red Sea-Gulf of Aden rift system from continental separation to diffuse extension for the same total extensional strain. The diffuse extension is spatially associated with extensive volcanism (4).

Experimental rock mechanics data can be used to estimate lithospheric strength profiles for lithosphere of different compositional and thermal structures (5). These profiles show an approximately linear increase in brittle strength with depth in the lithosphere which is truncated by an approximately exponential decrease in ductile strength at the brittle- ductile transition. The depth of this transition depends primarily upon composition, temperature and strain rate, and compositional layering can result in "layers" of strength within the lithosphere, the most prevalent of which are a layer of upper crustal strength and a layer of uppermost mantle strength. The most fundamental result of studies of lithospheric strength profiles is that the lithosphere is significantly weaker in regions where the geotherm is elevated, resulting in shallow brittle-ductile transition(s), and to a lesser extent where the crust is thick, resulting in the replacement of ductilely strong mantle layers with relatively ductilely weak crustal layers at equivalent

depths and temperatures. This results suggests that the geotherm and/or crustal thickness may be important factors in the localization of extensional strain. The second important result of these studies is the prediction that the relative importance of the crustal and mantle strength layers may change as the geotherm changes: for low heat flow (stable areas) most of the strength in the lithosphere is in the uppermost mantle; at intermediate heat flow values the uppermost mantle and crustal strengths become similar; for high heat flow, negligible mantle strength is predicted, with all the strength residing in the uppermost crust.

Uncertainties in the extrapolation of laboratory rock mechanics data to lithospheric conditions limit the quantitative use of the lithospheric strength profiles calculated from these data. However, qualitative mechanisms can be proposed which are consistent with the calculated strength profiles and the tectonic observations in the Rio Grande rift and Red Sea-Gulf of Aden rift system. Major magmatic activity leading up to early phase extension in the Rio Grande rift indicates very high heat flow from which a strength profile with only strength in the uppermost crust is predicted. During this extension event the lithosphere was dominated by its ductile properties with shallow decollement at a shallow brittle-ductile transition resulting in low-angle faulting in a thin upper crustal brittle layer. A reduction in magmatism prior to late phase extension suggests lower heat flow, from which a strength profile with some uppermost mantle strength is predicted. Increased lithospheric strength may be one factor in producing smaller lateral strain during this event, but it is also possible that the layer of mantle strength prevented shallow crustal decollement resulting in high-angle planar or large-radius listric normal faults (1).

For the Red Sea-Gulf of Aden system variation in the volumes of volcanics along the strike of the rift system suggest variations in heat flow and the geotherm along strike. Abundant volcanics consistent with high heat flow in the Afar region suggests mechanical conditions similar to early phase extension in the Rio Grande rift, with a relatively ductile lithosphere resulting in diffuse extension. Distributed dike intrusion has made an important contribution to this diffuse extension (9). In the central portion of the Red Sea and the Gulf of Aden smaller volumes of volcanics consistent with lower heat flow suggest mechanical conditions similar to late phase Rio Grande rift extension, favoring high-angle faulting. As vertical strain is constrained by buoyancy considerations, however, continued extension on high-angle faults is limited, and can only be accommodated by dike intrusion, probably initially localized by the high-angle faults. To accommodate a high total strain in the lower heat flow areas an early transition from crustal extension to organized sea-floor spreading is predicted.

References: (1) Morgan, P. and Golombek, M. (1984) Factors controlling the phases and styles of extension in the northern Rio Grande rift. Field Conf. Guidebook, N. M. Geol. Soc., 35, p. 13-20. (2) Eaton, G. P. (1982) The Basin and Range province: Origin and tectonic significance. Ann. Rev. Earth Planet. Sci., 10, p. 409-440. (3) Courtillot, V. E. (1980) Opening of the Gulf of Aden by progressive tearing. Phys. Earth Planet. Int., 21, p. 343-350. (4) Barberi, F., Santacroce, R. and Varet, J. (1982) Chemical aspects of rift magmatism. Continental and Oceanic Rifts, Geodynamics Ser. 8, Am. Geopys. Un., p. 223-258. (5) Lynch, H. D. (1983) Numerical models of the formation of continental rifts by processes of lithospheric necking. Ph.D. dissertation, N. M. State U., Las Cruces, NM, 290 pp.

EXTENSIONAL TECTONICS ON CONTINENTS AND THE TRANSPORT OF HEAT AND MATTER; Horst J. Neugebauer, Institut für Geophysik, Technische Universität Clausthal, Federal Republik of Germany

Intracontinental zones of extensional tectonic style are commonly of finite width and length. Associated sedimentary troughs are fault-controlled. The evolution of those structures is accompanied by volcanic activity of variable intensity. The characteristic surface structures are usually underlayn by a lower crust of the transitional type while deeper subcrustal areas show delayed travel times of seismic waves especially at young tectonic provinces.

A correspondence between deep seated processes and zones of continental extension appears obvious, a genetic sequential order of mechanisms and their importance is discussed in the light of both modern data compilations as well as quantitative kinematic and dynamic approaches. For this purpose we refere to the Cenozoic extensional tectonics related with the Rhine River.

Kinematic modelling of fault controlled extensional troughs of sedimentation predicts crustal stretching of 10 % associated with a rather deep crustal detachment level at 20 km depth. Those surface structures obviously find mirror image like correspondence in the lower crust beneath the detachment level as demonstrated by Zucca[1]. Thereafter the broad and gentle domal upwelling of the lower crustal boundary which has approximately ten times the width of the surface tectonic structures is not neccessarily the consequence of mechanical stretching. It is more likely of an interlayered mafic and ultramafic lithology in accord with similar exposed structures and with transitional seismic velocities, Deichmann & Ansorge[2].

The small amount of crustal stretching on one side and the oversized lower crustal transition in addition with a period of 100 ma of volcanic activity indicate a rather puzzling situation. Geobarometric evidence, age and spatial distribution of volcanic rock samples reveal magmatic activity with lower lithosphere origin during a time span of 50 ma before the onset of fault-controlled sedimentation at the surface. Major volumes of magma, however, were extruded 30-40 ma after the extensional surface event.

An accretion of ultramafic mantle material in lower crustal position as well as the evidence of magmatic activity by volcanic erruptions over such a long period support the view of a controlling mechanism of crustal extension involving both the transport of matter and heat. Numerical models on the uprise of small volumes of material within a thermally self-consistent enviroment and the control of variable rheology offer a suitable concept for the understanding of (1) moderate to low heating of the lower crust, (2) the accretion of lense-shaped material, (3) the uprise of crustal detachment level with time, (4) a slow upwelling of upper mantle isotherms above the magma source and thus (6) the preparation of a thermal channel for late voluminous volcanic events and finally, (7) the gentle, continous crustal extension.

References

Zucca, J.J. The crustal structure of the southern Rhinegraben from re-interpretation of seismic refraction data, J. Geophys. 55, 13-23.

Deichmann, N. and Ansorge, J. (1983). Evidence for lamination in the lower continental crust beneath the Black Forest (southwest Germany). J. Geophys. 52, 109-118.

ON THE DIFFERENCES IN CONTINENTAL RIFTING AT THE EARTH,MARS AND VENUS.

A.M.Nikishin and E.E.Milanovsky; Geological Faculty, Moscow State University,II9899,USSR.

During the process of continental rifting at the Earth the lower ductile crust stretches forming a neck,while the upper brittle crust is broken in blocks by faults,and the blocks sink down the thinned lower crust (I,2); if the stretching continued, the neck may break and a newly originated oceanic crust is formed at this place. The figure displays some types of rifting. The rift system structure depends on the depth of the boundary surface between the brittle crust and the ductile crust,the litospheric thickness and a form of asthenospheric diapir,the tension value,ets..

The depth of the boundary surface between the brittle crust and the ductile crust is determined by PT-conditions,the stress value,the rock composition,ets.. It ranges from 5 to I5 km for the Earth's rift zones. At the Mars' Valles Marineris rift system the depth of the boundary surface between the brittle and the ductile crust during rifting was situated 2-4 times deeper then at the Earth (4),since the lithosphere was thicker and the heat flow was lower in comparison to that at the Earth (4,5), and since the lithostatic adverse pressure gradient was smaller owing to smaller gravitation. Therefore,when a belt-like area of the Valles Marineris rift system had expanded by several percents,only the deepest layers of the lithosphere experienced the plastic stretching. The thick brittle part of the lithosphere over the zones of plastic stretching of the lower part of the lithosphere underwent breaking and it's blocks sank down for I-I0 km. The form and the relative position of the troughs was governed by stress field and by the distribution of heterogeneities in the lithosphere.

At the Venus the rift-like structures are discovered in Aphrodite Terra,Beta Regio and in other areas (3). They are wider and shallower than the Earth's continental rifts. The temperature at the Venus' surface is about 475°C. At the Earth such temperature exists near the boundary surface between the brittle crust and the ductile crust. Therefore the Venus' lithosphere is considerably more plastic than that of the Earth. Hence,the ductile type of rifting must be characteristic of the Venus. With the plastic Venus' type of rifting the tension does not cause the breaking of its lithosphere,in consequence of this,the structures like the Earth's contemporary oceans are not characteristic of the Venus.

Therefore,the rigid brittle rifting when narrow "necks" in the lower crust form,is characteristic of the contemporary Earth; at the Mars the brittle rifting with large subsidence was characteristic of the Tharsis upland formation epoch; the ductile rifting is typical of the Venus. The difference of the rheologic features of the lithospheres of different planets causes the variation in types of rifting.

RIFTING AT THE PLANETS

Nikishin A.M. and Milanovsky E.E.

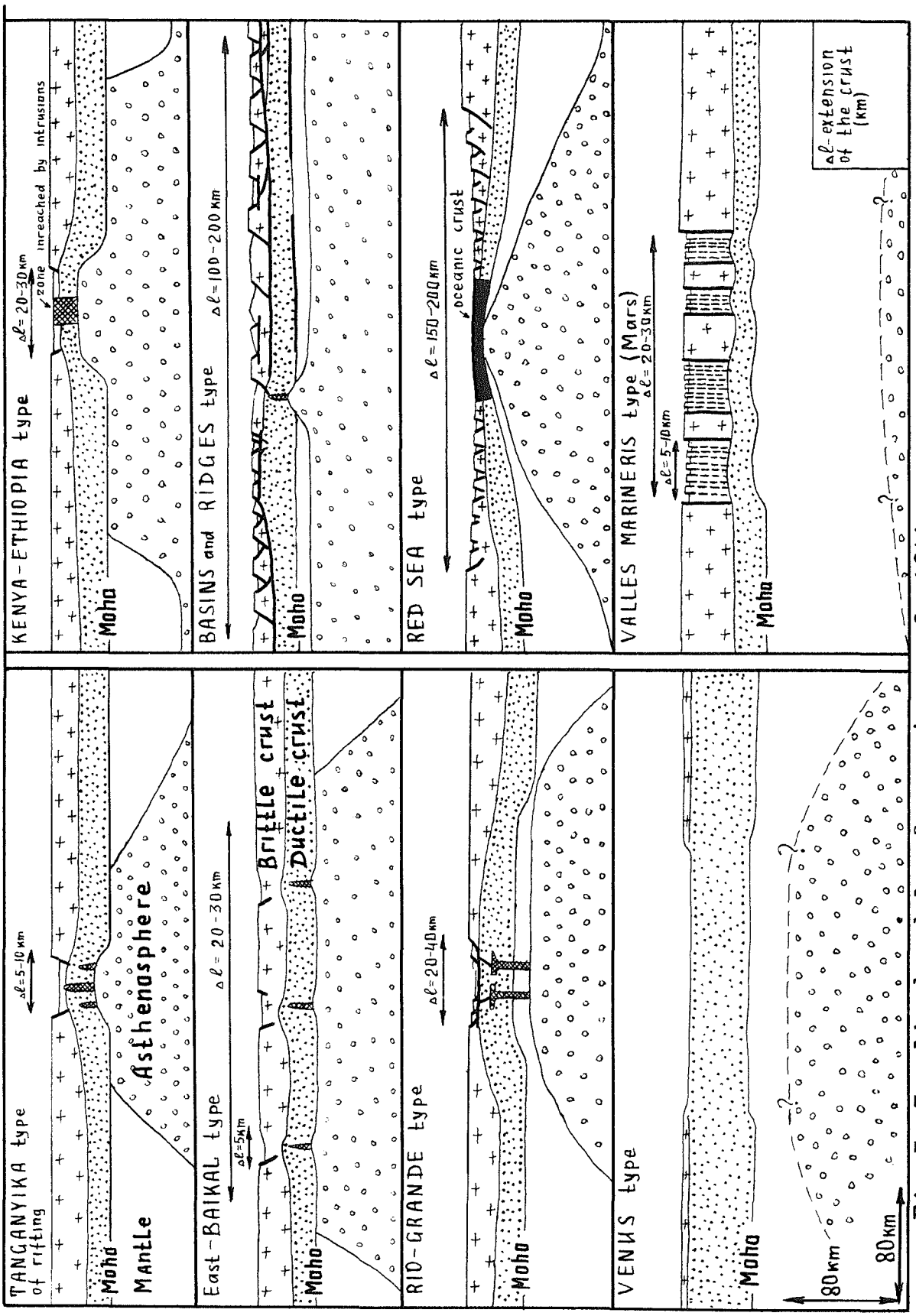

Fig. I. Idealized models of some types of rifting.

References:

(I).Artyushov E.V.(I98I).Mechanisms of continental riftogenesis.Tectonophysics,v.73,p.9-I4. (2).Bott M.H.P.(I98I). Crustal doming and the mechanism of continental rifting.Tectonophysics,v.73,p.I-8. (3).Masursky H.et.al.(I980).Pioneer Venus radar results: geology from images and altimetry.J.Geophys. Res.,v.85,p.8232-8260. (4).Milanovsky E.E.,Nikishin A.M.(I984). Differences in the formation mechanism of rifts of the Earth and rifts in the Valles Marineris system of Mars.Proc.Lunar Planet Sci.Conf.I5 th.,p.548-549. (5).Toksoz M.N.and Hsui A.T. (I978).Thermal history and evolution of Mars.Icarus,v.34, p.537-547.

HEAT AND EXTENSION AT MID- AND LOWER CRUSTAL LEVELS OF THE RIO GRANDE RIFT; Kenneth H. Olsen and W. Scott Baldridge, Los Alamos National Laboratory; Jonathan F. Callender, New Mexico Museum of Natural History.

The process by which large amounts (50-200 percent) of crustal extension are produced was concisely described by W. Hamilton (1,2) in 1982 and 1983. More recently, England (3), Sawyer (4), P. Morgan and coworkers (5,6), and others have moved toward quantifying models of lithospheric thinning by incorporating laboratory and theoretical data on rock rheology as a function of composition, temperature, and strain rate. Hamilton's description identifies three main crustal layers, each with a distinctive mechanical behavior: brittle fracturing and rotation in the upper crust, discontinuous ductile flow in the middle crust and laminar ductile flow in the lower crust. The temperature and composition dependent brittle-ductile transition essentially defines the diffuse "boundary" between upper and middle crust.

Perhaps the most distinctive feature of this extensional model is the lenticular, transposed nature of the middle crust—with lenses of more competent rocks ("megaboudins") interspersed with less competent material along ductile shear zones. These are closely akin to the metamorphic core complexes exposed by erosion in western North America. We have recently reviewed geophysical and petrologic data (7,8) on the Rio Grande rift and have attempted to formulate a broad interdisciplinary "picture" of the nature of the crust, tectonic development, and volcanism in the rift. One of our principal conclusions is that, within the rift, the structure of the middle crust is very probably lensoidal and horizontally stratified and the contact between the middle and upper crust is probably characterized by a low-angle detachment surface—all in accordance with Hamilton's generalized model. This type of crustal environment would very likely yield magma "pillows" and stratiform, sill-like intrusions in the middle crust, such as the Socorro magma body.

Perhaps somewhat surprisingly, our analysis also leads us to conclude that the heat responsible for the highly ductile nature of the lower crust and the lensoidal and magma body structures at mid-crustal depths in the rift was infused into the crust by relatively modest (< 10 percent by mass) magmatic upwelling (feeder dikes?) from Moho levels. Seismic velocity-versus-depth data, supported by gravity modeling and the fact that volumes of rift related volcanics are relatively modest (< 6000 km^3) for the Rio Grande system, all imply velocities and densities too small to be consistent with a massive, composite, mafic intrusion in the lower crust.

(1) Hamilton, W. (1982) Structural evolution of the Big Maria Mountains, northeastern California. In E. G. Frost and D. L. Martin (eds.) Mesozoic-Cenozoic Tectonic Evolution of the Colorado River Region, California, Arizona and Nevada, Cordillerian Publishers, San Diego, CA, p. 1-27.

(2) Hamilton, W. (1983) Mode of extension of continental crust. New Mex. Geol. Soc. Guidebook, 34, p. 9.

(3) England, P. (1983) Constraints on extension of continental lithosphere. J. Geophys. Res., 88, p. 1145-1152.

(4) Sawyer, D. S. (1985) Brittle failure in the upper mantle during extension of continental lithosphere. J. Geophys. Res., 90, p. 3021-3025.

(5) Morgan, P., and Golombeck, M. (1984) Factors controlling the phases and styles of extension in the northern Rio Grande rift. New Mex. Geol. Soc. Guidebook, 35, p. 13-20.

(6) Morgan, P., Seager, W. R., and Golombeck, M. P. (1985) Cenozoic thermal, mechanical and tectonic evolution of the Rio Grande rift. J. Geophys. Res. (submitted).

(7) Baldridge, W. S., Olsen, K. H., and Callender, J. F. (1984) Rio Grande rift: problems and perspectives. New Mex. Geol. Soc. Guidebook, 35, p. 1-12.

(8) Olsen, K. H., Baldridge, W. S., and Callender, J. F. (1985) Rio Grande rift: an overview. Tectonophysics (submitted).

LOW-ANGLE NORMAL FAULTING AND ISOSTATIC RESPONSE IN THE GULF OF SUEZ: EVIDENCE FROM SEISMIC INTERPRETATION AND GEOMETRIC RECONSTRUCTION: S. K. Perry and S. Schamel, Earth Sciences and Resources Institute, University of South Carolina, Columbia, SC 29208

Tectonic extension within continental crust creates a variety of major features best classed as extensional orogens. These features have come under increasing attention in recent years, with the welding of field observation and theoretical concepts providing new insights. Most recent advances have come from the Basin and Range Province of the southwestern United States and from the North Sea (1, 2). Application of these geometric and isostatic concepts, in combination with seismic interpretation, to the southern Gulf of Suez, an active extensional orogen, allows generation of detailed structural maps and geometrically balanced sections which suggest a regional structural model. This paper concentrates on geometric models which should prove to be a valuable adjunct to numerical and thermal models for the rifting process.

Regional Geology

The Gulf of Suez, Red Sea and Gulf of Aqaba rifts form the northernmost extensions of the East African rift system (Fig. 1). The African and Arabian plates are moving apart, creating new oceanic crust in the southern Red Sea and the Gulf of Aden. The Suez rift is separated from the Red Sea by the Gulf of Aqaba transtensional system. The Suez rift itself lies between the African continent and the Sinai Peninsula. Elevated and eroded rift shoulders form extensive crystalline basement outcrops and bound a deep trough floored by a complex tilt-block mosaic and filled with synrift sediments. Total estimates of extension usually range around 25% (3).

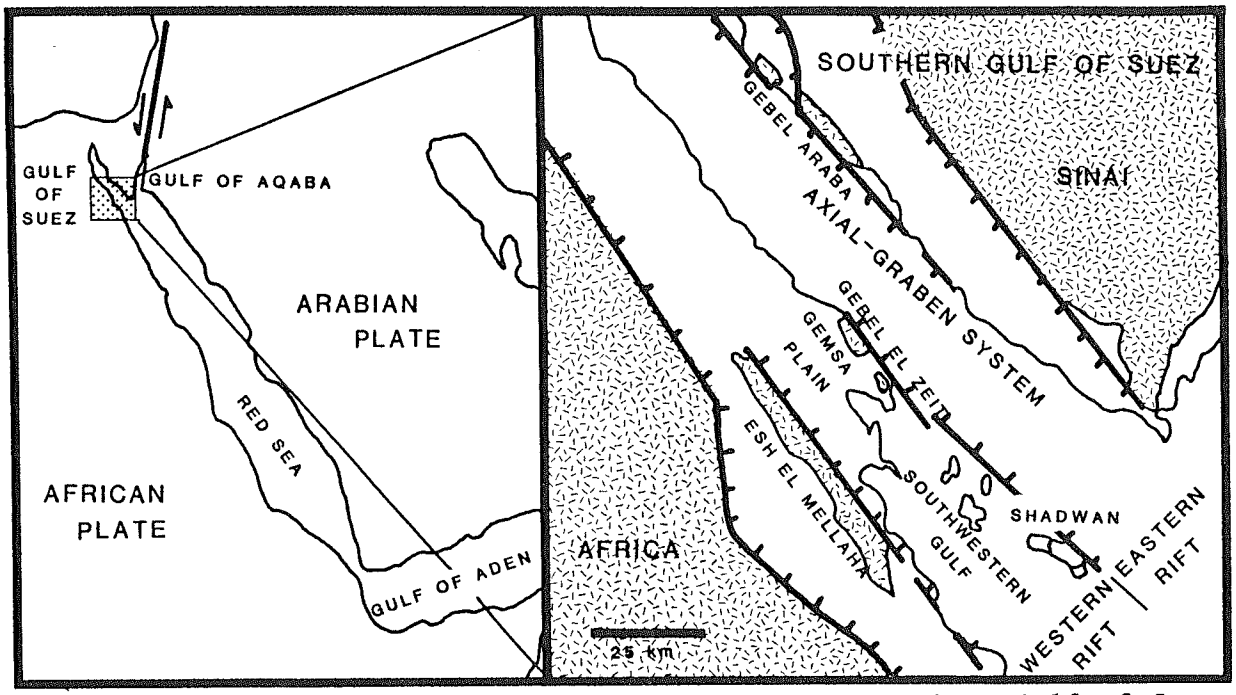

Figure 1: Regional geography of NE Africa and the southern Gulf of Suez.

Three rock groups are present: (1) an extremely complex Precambrian basement terrane; (2) widespread, relatively continuous prerift, Cambrian-Eocene platform sedimentary rocks; and (3) widely varying synrift fill of predominantly Neogene age. The basement and overlying platform succession were broken into numerous rift-parallel tilted fault blocks beginning in the Oligocene. Erosion stripped the top of the highest blocks and the rift shoulders, shedding clastics around the tilt block perimeters. Flooding of the rift in the early Miocene led to mixed carbonate and clastic deposition. During the middle Miocene, restricted conditions led to a build up of thick cyclic evaporites. Terrestrial and shallow marine depositional environments still dominate the gulf. Structural movements have continued through the present, with fresh fault scarps clearly visible and occasional earthquakes occurring.

Structural Geometries and Timing

Cross-strike variations in structural geometries and fault timing divide the southern Gulf of Suez into two major structural domains. The western portion of the rift preserves an early tilt-block mosaic, while the eastern half of the rift shows the superimposed development of a axial system of grabens probably bordered by relatively young steep faults.

Western rift. The western portion of the southern Gulf of Suez contains three discrete structural domains, each comprising a broad SW-dipping half-graben sub-basin floored by smaller tilt blocks having similar orientations (Fig. 1). The westernmost half-graben lies between the western border fault of the rift and the major bordering fault defining the eastern edge of the Esh el Mellaha tilt block. The other two half-grabens are along strike from one another immediately to the east and are delineated by the Esh el Mellaha border fault and the Gebel el Zeit-Shadwan Island structural high. These are the Gemsa Plain half-graben in the northwest and the southwestern Gulf of Suez immediately to the southeast. The two regions are separated by a zone of anomalous structures around Ras el Bahar.

Both the Gemsa Plain and southwestern Gulf of Suez half-grabens were analyzed in detail. Surface studies in the Gebel el Zeit and Esh el Mellaha ranges in combination with interpretation of seismic reflection data and well logs provided constraints for the construction of serialized, geometrically restorable cross sections. Subsurface information for the structurally simple Esh el Mellaha domain is not available. These sections, in combination with seismic structure maps, allowed construction of internally consistent, geometrically constrained structural maps. This has not previously been feasible in the Gulf of Suez because of ambiguities inherent in the seismic reflection data.

Differences in structural style and extensional quantity show that extension within the the rift is partitioned into discrete units on several scales. On the largest scale, the major structural domains are bounded by master listric faults and exhibit roughly uniform internal extension. In contrast, the amount of internal extension may differ substantially between these domains. It can be assumed that the total extension across the rift is equal, or decreasing gradually to the north. Similarly, the large tilt domains may be broken into suites of en echelon blocks along both listric and planar faults, themselves representing smaller scale partitioning of the extension within the domain.

Within this context, the southwestern Gulf of Suez half graben forms a discrete structural domain with roughly 15% internal extension. This is partitioned into numerous smaller, fault-bounded structural highs that rise and fall along strike, always maintaining approximately the same extension across the domain. In contrast, the Gemsa Plain was initially narrower than the southwestern Gulf and appears to represent roughly 50% extension. In this case, the domain is dominated by a single major tilt block, the Zeit block (Fig. 1). The western edge of this block lies deeply buried under the Gemsa Plain, abutting the Esh el Mellaha's eastern border fault, and the eastern, or leading, edge forms the complexly deformed Gebel el Zeit ranges. Between the two domains lies a transitional region of confused geology and limited data. Geometrically balanced sections show that both half grabens result from movement over an initially east-dipping and now subhorizontal detachment lying at roughly 30,000 feet. Furthermore, both domains are bordered on the east by through-going high-angle faults which break the original detachment. Some other portions of the region are also broken by these faults. These faults clearly post-date major tilt-block movement over the detachment.

The sedimentary fill of the sub-basins within the two half grabens shows the structural timing within the western gulf. Initial movements on the primary listric border faults of the half grabens occurred prior to the deposition of basal redbeds during the uppermost Oligocene. Very gentle tilting continued through the deposition of marine clastics, carbonates and evaporites of the Nukhul Formation which is probably of Aquitanian age. Rapid environmental differentiation and strongly tilted strata show that the half grabens developed rapidly during the early Burdigalian, with the southwestern Gulf half graben fragmenting into a suite of smaller tilt blocks. Erosion cut into the tilt-block crests and both capping and fringing reefs formed. These are preserved *in situ* along the Esh el Mellaha range and show no structural tilting, indicating that the Esh el Mellaha half graben stopped developing during the Burdigalian, when a major pause in structural activity is reported. The remainder of the western rift continued to develop rapidly with block tilts increasing steadily. Major tilting in the southwestern Gulf slowly decreased during deposition of middle and upper Miocene evaporites, with uniform gradual subsidence continuing. The Gemsa Plain sub-basin shows greater subsidence and tilting with less environmental differentiation. A major angular unconformity and both Pliocene and Pleistocene raised and tilted carbonates and beach terraces show continuing block tilting, while relatively thick Plio-Pleistocene clastics conformably overlie Miocene evaporites in the deeper portions of the sub-basin. Through-going faults greatly deform the Miocene section along the eastern margins of both half grabens indicating predominantly Pliocene and later movements.

Eastern Rift. Published descriptions and new studies of oil fields and surface outcrops in the eastern rift show that it differs from the western rift in both structural style and timing, with much more pronounced late development. During the Aquitanian and lower Burdigalian the eastern rift shows a structural development similar to that in the west, but with less well-defined half grabens, less throw on faults and thinner synrift deposits than in the west. During the upper Burdigalian and continuing into the middle Miocene the Sinai rift shoulder became eleveated, a broad tilt-block bench remained near sea level around Gebel Araba, and an *en echelon* series of grabens broke the region between the Sinai rift shoulder and the Gebel el

Zeit-Shadwan Island high, forming an axial-graben system. This movement waned during the upper Miocene, as do most structural movements in the Gulf, but accelerated rapidly during the Plio-Pleistocene. Subsidence in the axial-graben system during this time allowed local deposition of greater thicknesses of clastics and carbonates in the last 5 my than had been deposited in the Miocene. The formation of the axial-graben system also marks a great change in structural style, with subsidence between relatively steeply dipping and oppositely facing normal faults substituting for earlier rapid tilting.

Tectonic Model for the Southern Suez Rift

The three aspects of the Suez rift described above bear directly on its structural evolution: (1) the early Miocene development of a tilt-block mosaic forming and array of broad half grabens and focused in the west; (2) eastward propogation of deformation to the eastern rift during the early Miocene; and (3) the predominantly middle Miocene-through-Recent formation and growth of a depressed axial-graben system bordered by relatively high-angle faults.

We suggest that this pattern is a result of tilt-block movement over a low-angle detachment whose subsequent isostatic upwarping localized deep-seated deformation and forming the axial-graben system (4). Initial NNE-SSW extension during the Oligocene and earliest Miocene was accompanied by minor rotation on wide listric tilt blocks over a regional east-dipping low-angle detachment which formed half-graben sub-basins filled with thin redbed and Nukhul Formation sediments (Fig. 2-A). With increasing extension during the Burdigalian tilt-block rotation continued, extensionally thinning the upper crust over a passive lower crust. In response, isostatic uplift of the passive lower crust warped the detachment and overlying terrane into a broad arch, limiting gravity-driven tilt-block movement in the west (5) and creating a rift-parallel high in the Moho. This uplift stalled movement on the Esh el Mellaha

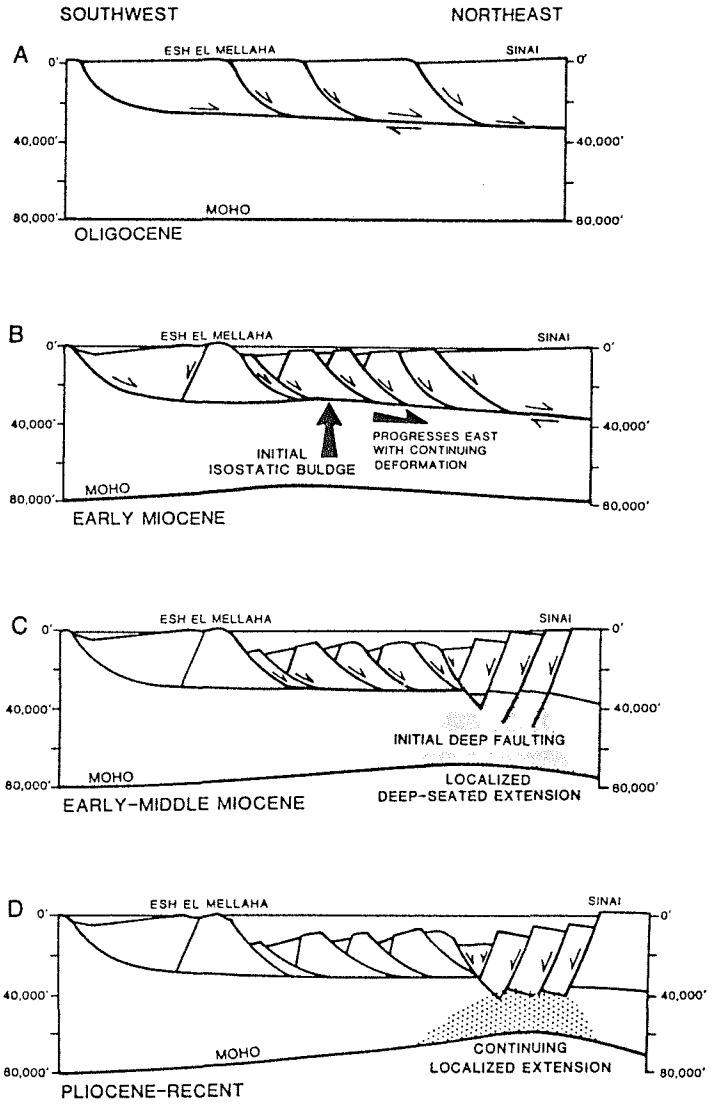

Figure 2: Evolutionary model.

tilt block by decreasing the dip of the detachment but allowed extension to concentrate within the southwestern Gulf by increasing detachment dip (Fig. 2-B). Deposition of the thick lower Miocene shales and marls resulted. With further extension during the upper Burdigalian, continuing isostatic uplift progressively uplifted and flattened the detachment beneath the southwestern Gulf and shifted the axis of the isostatic arch to the eastern rift (Fig. 2-C). At this point the majority of tectonic development in the west was complete. In conjunction with the uplift of the Sinai rift shoulder, probably a thermal response, a new set of relatively high-angle normal faults cut through the old detachment forming the axial-graben system. This faulting was greatly reactivated during the Plio-Pleistocene, a time of increased spreading in the Red Sea (6). These younger faults may root into a deeper detachment within more thermally mature crust, may merge directly into a zone of ductile flow under the rift, or may splay up from a zone of active intrusion within the lower crust. We favor this last possibility since mantle-derived oceanic crust must eventually form with continuing extension, as is shown in the southern Red Sea. This model is consistent with the observed early breakup of the rift into a series of broad half grabens and explains the eastward shift of deformation through time, the early cessation of rapid tilt-block movement in the west, and the late formation of a a depressed axial-graben system in the east.

This research suggests that early movement over low-angle detachments plays an important role in localizing deformation within rifts, and is undoubtedly a critical element in the formation of passive margins.

References Cited

(1) Anderson, R. E., Zoback, M. L., and Thompson, G. A., 1983, Implications of selected subsurface data on the structural form and evolution of some basins in the northern Basin and Range Province, Nevada and Utah: Geological Society of America Bulletin, v. 94, p. 1055-1072.

(2) Gibbs, A. D., 1983, Balanced cross section construction from seismic sections in areas of extensional tectonics: Journal of Structural Geology, v. 5, no. 2, p. 153-160.

(3) Garfunkel, Z., and Bartov, Y., 1977, The tectonics of the Suez Rift: Geological Survey of Israel Bulletin, v. 71, p. 1-44.

(4) Perry, S., and Schamel, S., 1984, Low-angle detachment and isostatic compensation in the Gulf of Suez, Egypt: Geological Society of America Abstracts with Programs, v. 16, no. 6, p. 622.

(5) Spencer, J. E., 1984, Role of tectonic denudation in warping and uplift of low-angle normal faults: Geology, v. 12, p. 95-98.

(6) Cochran, J. R., 1983, A model for development of the Red Sea: American Association of Petroleum Geologists Bulletin, v. 671, p. 41-69.

THE RELATIONSHIP OF EXTENSIONAL AND COMPRESSIONAL TECTONICS TO A PRECAMBRIAN FRACTURE SYSTEM IN THE EASTERN OVERTHRUST BELT, USA

Howard A. Pohn, United States Geological Survey, Reston, Va.

The central and southern Appalachians have a long history of interrelated extensional and compressional tectonics. It is proposed that each episode was controlled by a reactivation of a fracture system in the Precambrian basement.

Proprietary seismic-reflection profiles show a system of down-to-the-east Precambrian extensional faults. When under renewed extension, these faults produce features such as the western border faults of Mesozoic basins, and when under compression probably produce tectonic ramps in the overlying sedimentary cover rocks as well as the spatially and genetically related Alleghenian folds.

This system, which parallels the the Appalachian trend, is cut by a system of cross-strike hinge or scissors faults that have probable strike-slip movements. Reactivation of this cross-strike system appears to have produced lateral ramps that connect decollements at different stratigraphic levels and caused abrupt changes in fold wavelength along strike.

Continued reactivation of this cross-strike system is suggested by east-west border faults and Precambrian highs between Mesozoic basins. The present activity of this system is suggested by the fact that more than 35% of recent earthquakes are coincident with cross-strike faults and lateral ramps.

Many lateral ramps can be extrapolated seaward and are exactly coincident in strike and are nearly coincident in spacing with transform faults offshore. It is hypothesized that the cross-strike faults acted as zones of least resistance along which modern transform faults developed during periods of sea-floor spreading.

LOW-ANGLE NORMAL FAULTS - LOW DIFFERENTIAL STRESS AT MID CRUSTAL LEVELS? W.L. Power, Department of Geological Sciences, Brown University, Providence, Rhode Island 02912.

A simple model for frictional slip on pre-existing faults that considers the local stress state near the fault and the effect of non-hydrostatic fluid pressures predicts that low-angle normal faulting is restricted to areas of the crust characterized by low differential stress and nearly lithostatic fluid pressures. In part following (1), the model considers frictional slip on a cohesionless low-angle normal fault governed by the failure criterion $\tau = \mu_f \sigma_n^* = \mu_f(\sigma_n - P_f)$ where τ and σ_n are the shear and normal stresses across the fault plane, μ_f is the static coefficient of friction, and P_f is the pore fluid pressure (Fig. 1). As a first approximation, the model considers a vertical greatest principal compressive stress, σ_1. It is apparent that if slip on low-angle normal faults is governed by the above frictional failure criterion, slip on the low-angle normal fault occurs only if the least effective principal stress, $\sigma_3^* = \sigma_3 - P_f$, is tensile, whenever $\tan^{-1}(\mu_f) > d$, where d is the dip of the fault (Fig. 1). If detachment faulting occurs at any significant depth in the crust, $P_f > \sigma_3$ is required. In light of this conclusion I allow P_f to vary as necessary to allow slip on the low-angle normal fault.

An additional criterion for long term viability of the low-angle fault surface as a significant tectonic feature is that no failure occur in the wall rock. Following (2), the failure criterion for the intact wall rock can be approximated by the parabolic Griffith criterion in the tensile field (T = the tensile strength of the rock), and as a linear Coulomb envelope in the compressive field (C = 2T = the cohesive strength and μ_i is the coefficient of internal friction). The failure envelope for the intact rock limits the level of differential stress expected near active low-angle normal faults (Fig. 2). Most notably, low-angle normal faults which dip $< 15^0$ and have frictional sliding coefficients > 0.4, will only be viable tectonic elements in extending lithosphere if total differential stress near the faults is less than about four times the tensile strength of the rock.

The model has potentially important and interesting implications. Areas of the crust with active low-angle normal faults should have strengths comparable to the tensile strengths of the rocks involved. Active low-angle normal faults should be characterized by smaller earthquakes than any "Andersonian" fault at comparable depths, because the elastic strain energy of distortion stored in the wall rock of a fault is proportional to the square of the differential stress. Although evidence for seismic faulting on low-angle normal faults is rare (3,4), Jackson (4) has observed long period seismic signals radiated from nearly flat surfaces immediately following major earthquakes on nearby steep normal faults. Perhaps these long period signals are related to movement of fluids in sub-horizontal fault zones.

Because the model predicts that mid-crustal low-angle normal fault zones will have low strengths and low levels of seismicity, I suggest that the transition to macroscopic ductility in regions with active low-angle normal faults is controlled at least in part by fluid pressure enhanced cataclastic flow and fluid assisted stress corrosion cracking, rather than solely by thermally activated diffusion and dislocation creep. Interestingly, a recent description of chloritic breccia zones along low-angle fault surfaces in the Basin and Range province (5) preferred to describe the zones as "fluidized media" rather than as fault breccias.

Although the model assumes a pre-existing low-angle fault surface, and cannot explain the *initiation* of such surfaces, I speculate that many of the conditions which cause the initiation of low-angle normal fault surfaces are the same as the conditions needed to ensure their survival. I suggest a number of features that have been observed along low-angle faults in the southern Basin and Range province are consistent with the high fluid pressures and low differential stress levels predicted by the model; these include a) the common association of mineralization and low-angle faulting (6), b) the development of extensive cataclastic zones along low-angle fault surfaces, and c) the development of primary wavelike undulations of the fault surfaces (7).

REFERENCES - **(1)** Sibson, R.H. (1985) A note on fault reactivation. in press, Jour. Struct. Geol. **(2)** Brace, W.F. (1960) An extension of the Griffith theory of fracture to rocks. Jour.

Geophys. Res., **65** 3477-3480. **(3)** Smith, R.B. (1985) Kinematics and dynamics of an extending lithosphere: The Basin Range. in *Continental Extensional Tectonics - a special meeting of the Geological Society of London.* Durham, 1985. **(4)** Jackson, J. (1985) Active normal faulting and lithospheric extension. in *Continental Extensional Tectonics - a special meeting of the Geological Society of London.* Durham, 1985. **(5)** Rehrig, W.A. and Kerrich, R. (1985) Tectonic and economic significance of isotopic and geochemical data from mylonitic - detachment zones of metamorphic core complexes. in *Continental Extensional Tectonics - a special meeting of the Geological Society of London.* Durham, 1985. **(6)** Heidrick, T.L. and Wilkins, J. (1982) Base and precious metal mineralization related to low-angle tectonic features in the Whipple Mountains, California, and the Buckskin Mountains, Arizona. in Frost, E.G., and Martin, D.L., eds., *Mesozoic-Cenozoic Tectonic Evolution of the Colorado River Region* San Diego, CA, Cordilleran Publishers, 182-203. **(7)** John, B.E. (1984) Primary corrugations in Tertiary low-angle normal faults, SE California; porpoising mullion structures? Geol. Soc. Amer. Abstr. w. Programs, **16** 291.

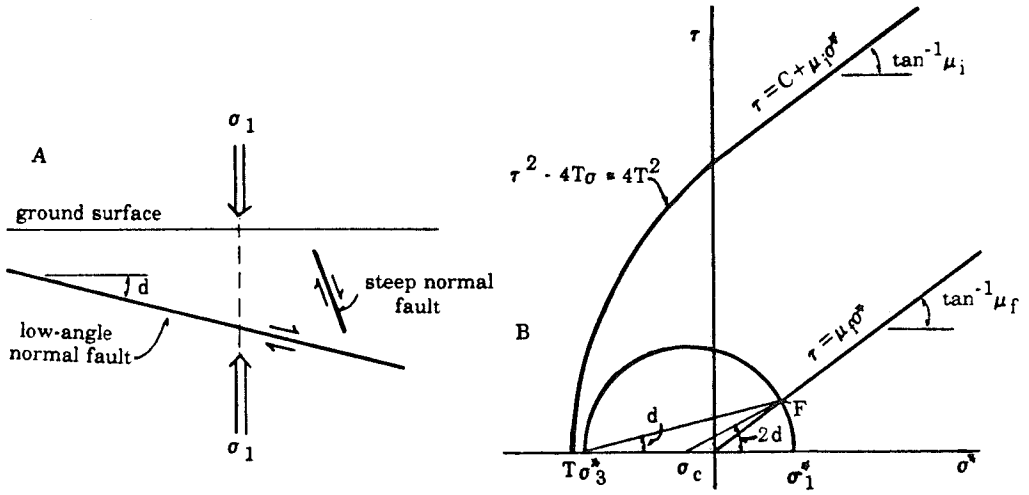

Figure 1. a) Angular relationships between σ_1, low-angle normal fault, and steep normal fault in the two-dimensional model. b) Mohr circle condition for slip on low-angle normal fault, in part after Sibson (1985). State of stress at fault surface represented by circle with center σ_c. Low-angle fault surface represented by point F.

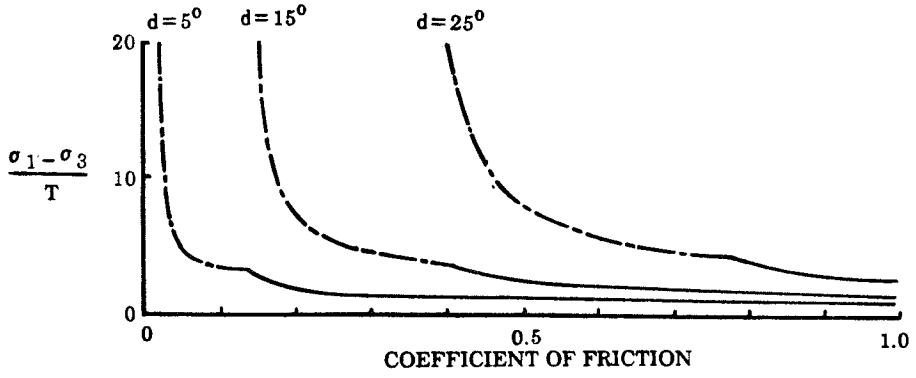

Figure 2. Normalized differential stresses for simultaneous failure of intact wall rock and slip on low-angle normal fault, as a function of μ_f. In the region below the curves slip on the low-angle normal fault alone is possible, while above the curves failure of the wall rock in either tension or shear occurs. Dashed lines represent condition for simultaneous shear failure and slip on the low-angle surface; solid lines the condition for simultaneous tension failure and slip on the low-angle surface.

LATE PRECAMBRIAN AULACOGENS OF THE NORTH CHINA CRATON.

Qian, Xianglin,Geology Department,Peking University,Beijing,the People's Republic of China.

According to tectonic styles the Precambrian evolution history of the North China craton may be subdivided into four stages: (1) Archean consolidation in 3.5-2.5 Ga, (2) Early Proterozoic rifting in 2.5-1.8 Ga, (3) Late Precambrian aulacogen in 1.8-0.8 Ga and (4) Platform regime after 0.8 Ga.

In the Late Precambrian aulacogen stage of the North China craton there were two main aulacogens,Yanliao and Zhongtiao (Y and Z),developed in Middle Proterozoic time with an age 1.8-1.0 Ga. Their NE trend made themselves to meet together in the central part of the craton and build up one great Y-Z aulacogen throughout the craton.

The Yanliao aulacogen which lies to the east of Beijing is filled up with 10 km thick shallow water sandstone,shale and carbonate sedimentary sequence,with a few thin layers of andesite in alkaline composition in its low part and with thick red conglomerate at its bottom. The synsedimentary active tectonic regime of the faulted boundaries of the aulacogen is indicated by the aboundant breccia of the physical weathering products with convincing paleogeomorphological elements at the bottom of each transgressive sequence. The subsidence of the Y-Z aulacogen was parallel to the compensation of the sedimentation there (Qian,1980). The Zhongtiao aulacogen which lies in the south of the craton is filled up with 10 km thick volcano-sedimentary formation in which the low part in 5 km thick comprises mostly andesite-rhyolite alkaline volcanic rocks with a few thin layers of basalt and the upper part consists of sandstone-shale and carbonate sedimentary rocks. This volcanic assemblage limited by NE trending sharply faulted boundaries links the coeval metamorphosed volcanic sequence in E-W trending Qinling belt to the south of the craton to form together a triangular outline in its thickness isopach map. The geochemistry of the volcanic rocks in the Zhongtiao aulacogen shows that they are shoshonite series or alkaline series of Coombs trend and straddle trend with Kennedy trend defined by Miyashiro. The increasing of K becomes much fast than the increasing of Na in the case of SiO_2 higher than 68 %,and the $^{87}Sr/^{86}Sr$ initial ratio is high enough in 0.7125 or more in the bottom of this volcanic rock series. So,these volcanic rocks not seem to be the products of differentiation with partial melting of the preexisting continental crust,and on the contrary the acid affinity of this series might be directly produced by the anatexis of the continental crust in the early evolution of the aulacogen stage. In dealing with the metamorphosed volcanic sequence,the coeval in the Qinling belt,it comprises bimodel non-alkalic basalt or tholeiitic basalt and and calc-alkalic rhyolite rocks,which show that in early time of Middle Proterozoe the Qinling mobile belt with the Zhongtiao aulacogen began to rifting and joined together to form a tripple junction. It might be asked how was the Late Precambrian history of the southern boundary of the craton. In fact

it was a new birth boundary in Early Proterozoic, because the Qinling mobile belt immediately cut the Early Proterozoic tectonic trend and structural elements of the craton which reseasonably extended far to the south of the present North China craton in Early Proterozoe (Qian,1982; Sun et al,1980;Tectonic map,1983).

The Guyuan buried aulacogen is the other NE trending one determined by geophysical exploration and drilling in an oil field in the southwest of the craton. The north Anhui aulacogen extends in WNW direction in the south of the craton in the age of 1.0-0.8 Ga and is unconformably overlain by Cambrian. It is filled up with about 5 km thick shallow water sandstone,shale and carbonate sedimentary sequence with a thin layer of andesite in a limited area.

In the northern hemisphere or Laurasia,the Late Precambrian aulacogens in comparative tectonics have many similarities in their evolution history. The Russian platform shows that there are the Late Precambrian Riphean aulacogens (1.8-1.0 Ga) in regular NE and NW trending throughout the platform,even the form or outline of the platform is of following these trends (Aksenov et al,1978). The Archean Superior province in the Canadian shield also has rectangular form,limited by the NE and NW lineaments bordering on the Proterozoic Churchill province and the Grenville, perhaps the Southern province as well (Burke,1980). In addition, the Late Precambrian Aravalli aulacogen of Gondwana in India also extends in the NE direction.(Fig)

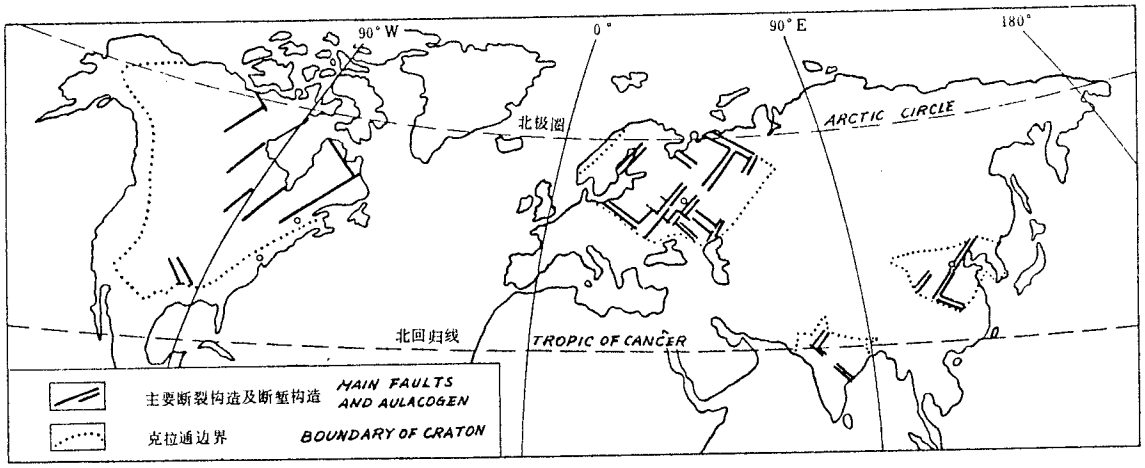

Discussion. Consequently,some quentions can be asked from the comparison of the evolution of the coeval Late Precambrian aulacogens:

1) What is the implication does the regularity of the tectonic trending of the Late Precambrian aulacogens. Are they Late Precambrian tectonic trends. If so,for what reason the unifying tectonic trends are maintained so far. Do they appear occasionally or in regularity.
2) Did the lithosphere on the earth be undergone a worldwide expansion in Late Precambrian in the process of cratonitization. Is it a background of the tectonic origin causing the Late Precambrian stage of aulacogen.

References

Aksenov Ye.M. et al., 1978. (in Russian,translated in"Intern. Geol. Rev" 1980, NO.4, 444-458.
Burke K., 1980. In"Continental Tectonics,Studies in Geophysics," 42-49.
Marine and continental tectonic map of China and environs, in scale I:5 000 000. 1983. Chinese Science Press.
Qian, Xianglin, 1980. Bull. of the Chinese Acad. of Geol. Sci. Series VI, 1, NO.1, 123-133. (in Chinese)
Qian, Xianglin, 1982. Coll. of Str. Geol, NO.2, 34-42.(in Chinese)
Sun, Shu et al., 1980. Scientia Geologica Sinica, NO.4, 314-322. (in Chinese)

RADIAL RIFT AND BLOCK TECTONICS AROUND THE THARSIS BULGE: INTRODUCTIONAL POSTULATION. J. Raitala, JPL, CALTECH, Pasadena, CA 91109 (on leave from Department of Astronomy, University of Oulu, Oulu, Finland).

The crest of the Tharsis bulge displays tensional tectonics especially within the Noctis Labyrinthus area (1). Other adjoining tensional tectonic structures associated with the bulge are the numerous radial fossae grabens, Vallis Marineris valley and other valleys and surface discontinuities. These structures are much more complex than the bulge crest although coupled together.

The origin of the radial structure system can evidently be traced back to the Tharsis bulge uplift. The classical concept of triple junctions could be involved although the radial pattern consists rather of several multiple junctions. The Vallis Marineris canyon could easily be interpreted as resembling a rift which forms an aulacogen. Other fossae graben zones clearly resemble linear rift zones extending outwards from the Tharsis bulge.

Although the Vallis Marineris canyon and radial fossae grabens have been extensively studied, their origin and formation mechanism is still the subject of numerous questions. Possible rift formation is only one point of view and does not explain the rifting mechanism and the radial pattern of these structures around the Tharsis bulge. Both active and passive rifting must be taken into account (2). An active mechanism can be easily accepted in the case of the Tharsis bulge itself, where doming is associated with the mantle plume impinging on the lithosphere and causing uplift and volcanic extrusions. The active volcanic doming and volcanic complex building is coupled with the mantle and lower lithosphere swelling, which in the case of the Tharsis bulge was regional around the deep source of magma generation.

The model of active doming and volcano constructing implies a mantle plume impinging on the base of the lithosphere, lithosphere thinning, the uplift of lithosphere and crust (3) and opening of the extrusion plumbing channels. Very large volumes of hot mantle material are required to thin the lithosphere by heat transfer, magma migration and pressure release melting (3). According to the active mechanism the building of a volcanic complex like the Tharsis bulge is caused by the rising huge mantle plume and adjoining extrusions which tap the generated magma.

The surrounding fossae and valley structures are caused by more passive crustal rifting due to tensional failure of the surface layers. The main rising mantle plume activated and regenerated a failure patterns radial to the centre of activity (4). These radial zones of weaknes are then most easily utilized by the rising mantle plume. Deep zones of weakness regulate the penetration and distribution of hot mantle rock into upper levels while, contrarily, the effective impingement of the hot mantle plume into the lithosphere opens up new weakness zones. Tensional

stresses from below the lithosphere make it fail. If the mantle uplift and doming is strong enough to break the lithosphere and crust but does not raise volcanic extrusions some kind of rift tectonics is acquired.

The branches of the main Tharsis mantle plume spread radially aroud the central volcanic area causing 1) radial fault opening, 2) adjoining minor doming and rifting along these fault zones and 3) minor block movements or stress transmissions through the blocks. The lithosphere is cold and dense in respect to the hot mantle rocks of the asthenosphere below and the decreased volcanic activity at the plume branches may instead occur in the form of intrusions than extrusions. The heated and intruded lithosphere is then slightly uplifted and domed which causes tensional opening of the initial crustal failure zone.

There are several main fossae/valley graben zones through the Tharsis bulge area. The SW-NE fossae graben zone evidently controlled the location of the major plumbing system and the formation of major Tharsis volcanoes: Arsia, Pavonis and Ascraeus Mons. There are also some smaller volcanoes at the northeastern Tharsis slope of this zone. Sirenum and Memnonia Fossae penetrate far into the terra highland southwest of the Tharsis bulge while the Tempe and Mariotis Fossae and Kasei Vallis valley system cut large terra highland islands which are surrounded by lava-flooded plains.

The large terra highland block southeast of the Tharsis bulge is bounded by Claritas/Thaumasia Fossae, Noctis Labyrinthus and Valles Marineris. Noctis Labyrinthus is situated at the highest crest of the Tharsis main bulge, the Syria Planum Swell, where the pattern of tensional fractures were created due to the major updoming (1). The Claritas and Thaumasia Fossae are associated with crustal doming as are also the extensional structures of Valles Marineris. The deep excavation of Valles Marineris is not caused solely by the doming although the erosion has evidently been strengthened by block margin tectonics.

There are several Thaumasia Fossae grabens which tend to cut the Solis-Sinai block concentrically to the Tharsis bulge. They do not extend as far as the Vallis Marineris border, however, but an interesting structural phenomenon is the abrupt steep fault-like extension of this zone nortward from the Vallis Marineris and perpendicular to it. Several major floods seem to have their origin within the intersection area of this north-south fault concentric to the Tharsis area north of Valles Marineris.

At the another northwestern side of the Tharsis bulge there is the Olympus Mons volcano and its large lava-plain aureole and adjoining grabens. The Olympus Mons area is beside the Tharsis bulge and can be considered to form a volcanic dome of its own, the Olympus Swell. This swell area has extruded a considerable amount of volcanic material and been active over a long period of time. It is possible to propose that the Syria Planum Swell, Pavonis Mons and Olympus Swell form a NW-SE structural zone which is perpendicular to the NE-SW zone of the main Tharsis volcanoes and adjoining NE-SW fossae grabens. This NW-SE zone is,

however, not so uniform and clear and the active crustal faulting associated with it branches into two fossae and valley zones cutting a southeastward stretching crustal block. The plumbing system, and of course the mantle plume connected with the Tharsis bulge has been effective and uniform leaving the Olympus Swell to be of minor importance.

The Alba Patera area has also slightly domed and faulted, as have the Sirenum/Memnonia and Claritas/Thaumasia Fossae. Alba and Olympus Swells have been "active" in a similar manner to the main Tharsis bulge itself. The Alba Swell was associated with old crustal doming and major volcanic extrusions. The fossae graben zones radial to the Tharsis bulge were relatively passive in rifting. There is no well defined relationship with major Tharsis-like volcano-building although the Alba Patera area has a slightly elevated topography. A strong case can be made for claiming that the Alba Patera fossae can be seen to have been caused by a branch plume associated with the early stage of the major Tharsis plume development.

The Sirenum and Memnonia fossae are relatively passive rift branches. Their rifting and faulting can be considered to have been caused by the Tharsis plume extension along a major previous fault zone direction also below the nearby highland areas. The horizontal extension was relatively small. There was no important volcanic activity along this southwestern branch of the Tharsis plume except within the Tharsis area itself near the Arsia Mons volcano (5). The southwestern part of the Tharsis area seems to have been exceptionally active and the Arsia Mons is considered to be the Mars' most remarkable volcano. This enormous activity may be partly explained by the existence of the proposed thick highland lithosphere which dammed off the main impinging plume to within near the centre of the Tharsis area.

The location and orientation (NE-SW direction) of Sirenum and Memnonia fossae indicate that they are closely associated with Tharsis development. It seems likely that the fossae graben formation was the result of stresses developed during the impinging of the plume into the lithosphere. Tectonics of these fossae are related to the crustal block formation as a consequence of the convecting Martian mantle.

The Kasei Vallis' erosional channel just north of Lunae Planum is an example of a valley system radial to the Tharsis bulge. It has been plowed open and wide by surface flows, which have destroyed most of the original radial structures. There are only some fragmental graben branches and patterns to be seen within the adjoining islands and highlands. Kasei Vallis lies along the northern boundary of the Lunae Planum block forming a broad zone between it and the Tempe Terra. The Kasei Vallis fossae has no such well-developed graben pattern as other fossae either because the surface flow erosion destroyed old grabens or the crustal doming was not so effective here and this tectonic zone has such a prominent appearance mainly due to the erosion which effectively opened the initially slight surface faults. The earliest deformation in the valley dates, however, from the

tectonic pre-flow era and especially the northern valley boundary is not shaped only by flow. The southern boundary was obviously a linear zone of weakness. There is a controversy as to wether the Kasei Vallis was tectonically active or passive. Some present tectonic structures could perhaps be expained as having been caused by mass removals, but this was surely an effect of minor importance and possibly only re-activated already existing faulf structures, thus giving raise to some well-developed graben patterns beside some most prominent erosional channels. The location of Kasei Vallis in the radial peripheral zone of the Tharsis area suggests quite a passive response of lithosphere movements and surface deformation to the impinging mantle plume is possible. The Kasei Vallis is, however, a well-defined crustal suture between the Lunae Planum ridged terra and Tempe Terra fossae graben highland and could be regarded as a boundary between these highland blocks.

The Tempe Terra is cut by two sets of fossae: Tempe Fossae which form a northeastern extension of the Sirenum Fossae - the main Tharsis volcanic zone, and Mareotis Fossae, which forms part of the northwestern boundary of the Tempe Terra area. Tempe Fossae extends into the cratered plains of Vastitas Borealis. The main doming and rifting of the northeastern periphereal Tharsis plume seems to have occurred within Tempe Terra where lithospheric thinning may be regarded as a cause of horizontal tensional stresses and graben formation. Tempe Terra fossae can be characterized by Tempe Swell formation due to the mantle plume penetration into the lithosphere.

The prominent occurrence of a NE-SW zone may, of course, depend on a pre-existing zone of weakness (6), but a rift may be also self-propagating, which is caused by tensional forces within a rift, extending the rift and causing its propagation outwards at both ends (3). This propagation is further forced by the swells caused by the mantle plume which is guided by the major zones of lithosphere weakness.

References

(1) Masson, Ph. (1980) Contribution to the structural interpretation of the Valles Marineris - Noctis Labyrinthus-Clarites Fossae region of Mars. Moon and Planets 22, p. 211-219.
(2) Sengör, A. M. C. and Burke, K. (1978) Relative timing of rifting and volcanism on Earth and its tectonic implications. Geophys. Res. Lett. 5, p. 419-421.
(3) Turcotte, D. L. (1982) Driving mechanisms of mountain building. In Mountain Building Processes edited by K. J. Hsü, Academic Press, London, p. 141-146.
(4) Muller, O. H. and Pollard, D. D. (1977) The stress state near Spanish Peaks, Colorado determined from a dike pattern. Pure and applied geoph. 115, p. 69-86.
(5) Mouginis-Mark, P.J., Zisk, S. H. and Downs, G. S. (1982) Ancient and modern slopes in the Tharsis region of Mars. Nature 297, p. 546-550.

(6) Mutch, T. A. and Saunders, R. S. (1976) The geologic development on Mars: A review. Space Sci. Rev. 19, p. 3-57.

The location of major volcanoes was controlled by tectonic zones but the volcanism then controlled the occurrence and opening of the radial, rift-like fossae and valley structures.

HEAT FLOW AND THERMAL PROCESSES IN THE JORNADA DEL MUERTO, NEW MEXICO

Marshall Reiter, New Mexico Bureau of Mines and Mineral Resources, Socorro, NM

Most heat-flow data in rifts are uncertain largely because of hydrologic disturbances in regions of extensive fracturing. Estimates of heat flow in deep petroleum tests within a large basin of the Rio Grande rift, which has suffered little syn-rift fracturing, may begin to provide clearer insight into the relationships between high heat flow and crustal thinning processes. The Jornada del Muerto is a large basin located in the Rio Grande rift of south-central New Mexico. The region of interest within the Jornada del Muerto is centered about 30 km east of the town of Truth or Consequences, and is approximately 60 km north-south by 30 km east-west (Figures 1a, 1b). High heat flows are estimated for the region (1; Figure 1b). Values increase from about 90 mWm^{-2} in the northern part of the study area to about 125 mWm^{-2} in the southern part. These high heat flows are rather enigmatic because in the immediate vicinities of the sites there is little evidence of Cenozoic volcanism or syn-rift extensional tectonics.

Young basaltic volcanics (~2-3 Ma; 2) are present at distances of 10-20 km east of the high-flow sites. Even though geothermal anomalies are quite unlikely to be caused by magma conduits at such distances, it is possible that information obtained from the volcanics can be related to the heat-flow data. Although most of the basalts along the Rio Grande rift appear to have risen quickly through the crust (3), some of the basalts at the western edge of the Jornada del Muerto show a modest amount of differentiation (4). This is consistent with, but not definitive of, lower crustal holding chambers. The geochemical data from the basalts implies a moho depth of about 31 km, a geothermal gradient of about 31°C/km, and a temperature of ~900°C at 30 km (4). From these data one may estimate a steady-state heat flow of ~96 mWm^{-2} (4; 5). This estimate assumes a crustal radiogenic layer having an exponentially decreasing radiogenic concentration with depth. The value of 96 mWm^{-2} is in close agreement with the average heat flow at the four northern sites in the study area and with the average heat flow estimated over much of the southern Rio Grande rift in New Mexico (~95 mWm^{-2}; 1; 5). Moho depths of ~31 km for the area (as estimated from the geochemical data) are in good agreement with estimates based upon seismic data (27-33 km; 6; 7; 8).

Figure 2 presents a geologic cross section through the Jornada del Muerto and adjoining areas. The location of the profile is shown by AA' in Figure 1b. The upper crustal section across the Jornada del Muerto is depicted as a synclinal structure, a remanent of pre-rift (probably Laramide) compression throughout the region (9). As such, there is little evidence of extensional tectonics which might be expected in a Cenozoic rift having a thin crust as discussed in the above paragraph. Consequently, the probable crustal thinning in the region is suggested to occur in the lower (non-elastic) crust.

Lachenbruch and Sass (10) examine in detail possible heat-flow increases resulting from the steady-state stretching, underplating, and intrusion of the lithosphere. Cook and co-workers (6) suggest several massive intrusions of the lower crust during rifting in the southern Rio Grande rift to explain the "regional" heat flow of ~95 mWm^{-2}. A somewhat different model relating to the high heat flow across the Jornada del Muerto will be discussed here. One may approximate the change in surface heat flow due to crustal thinning as,

$$\Delta Q_s = \Delta Q_m \quad , (1),$$

where ΔQ_s is the change in surface heat flow and ΔQ_m is the change in mantle heat flow. Although a specific mechanism for crustal thinning is not proposed, the fact that the radiogenic crustal layer is not included in equation (1) implies that crustal thinning is occurring only in the lower crust (below

the radiogenic layer). This is consistent with the suggestion that crustal thinning has likely occurred below the elastic layer as concluded above from geologic data. If moho temperatures remain constant during crustal thinning then it follows that,

$$\Delta Q_s = \Delta Q_m = [(Z_i - Z_p)/Z_p] \times Q_{mi} \quad , (2),$$

where Z_i is the initial crustal thickness, Z_p is the present crustal thickness, and Q_{mi} is the mantle heat flow before crustal thinning.

From equation (2) it may be noticed that estimates of crustal thicknesses both before crustal thinning, and at present, are required to calculate the resulting heat-flow increase. A pre-rift crustal thickness of 40-50 km may be a reasonable estimate based upon crustal thicknesses in nearby, less geologically disturbed areas; e.g. ~40 km in the Colorado Plateau and ~50 km in the Great Plains (11; 12). Present estimates of crustal thickness in the southern Rio Grande rift and in the Jornada del Muerto vary between 33 and 27 km, with the likelihood of a decrease in the depth of the moho going southward (6; 7; 8; 13). Therefore, one may estimate the regional crustal thinning across the Jornada del Muerto as ~33% ((45-30) km/45 km); although considerable uncertainty is present in this estimate.

Figure 3 shows the increase in heat flow with percent crustal thinning for the above model (using equation 2); 33% crustal thinning across the region would increase the heat flow ~24 mWm^{-2}. If a pre-rift heat flow of 67 mWm^{-2} is hypothesized then crustal thinning of ~36% would generate the mean heat flow for the 4 northern sites in the Jornada del Muerto (95 mWm^{-2}, Figure 1b). (Note that 67 mWm^{-2} is the approximate mean heat flow in the Colorado Plateau of New Mexico, a value that could be obtained by the thinning of a lithosphere initially similar to that in the Great Plains; 14; 15). The heat-flow anomaly resulting from a temperature increase maintained over time at 30 km is 84% realized after ~7 my. Therefore, if rifting started 32-27 Ma (16) one may anticipate that the heat-flow anomaly has been appreciably realized (even though the rifting is probably episodic). Recent volcanism in the western part of the Jornada del Muerto, at ~10-20 km distance from the heat-flow sites, is consistent with maintaining elevated mantle temperatures as required by the above model.

Consider now the pattern of heat flow in the Jornada del Muerto (Figure 1b). It would appear that in general the heat flow increases from north to south. This first order pattern is consistent with the suggestion that the moho becomes shallower going southward along the Rio Grande rift (13). The observed increase in heat flow could be generated by increased crustal thinning and/or by different levels of magma intrusion into the lower crust. We may separate the heat-flow data into 3 regions with values of ~90 mWm^{-2} in the north, 98 mWm^{-2} in the central area, and 125 mWm^{-2} in the south of the Jornada del Muerto (Figure 1b). The crustal thinning required to generate the respective non-radiogenic anomalies would be 32%, 39%, and ~55% (Figure 3). This would require present day crustal thickness of ~31, 28, and 20 km if the pre-rift crustal thickness was ~45 km. Values for crustal thicknesses of 33-27 km would be consistent with seismic interpretations as discussed above; however, a crustal thickness of 20 km is beyond present expectations. As such, the crustal thinning model as presented is consistent with heat-flow data in the northern and central regions of the Jornada del Muerto, but does not fully explain the values of ~125 mWm^{-2} in the southern region.

Morgan and co-workers (17) present a very interesting model in which southward ground-water flow along the Rio Grande rift is constrained between various basins to move upward, thereby elevating geothermal gradients. This model is likely to explain high heat flows at many areas along the Rio Grande rift; but in the southern part of the Jornada del Muerto it is suspected that

non-hydrologic phenomena are causing the elevated heat flows. Firstly, the deepest BHT data at the southernmost site is at great depth (3,556 m; 1) and is near or within Precambrian rocks; therefore, very little temperature effect from upward ground-water movement might be expected. Secondly, the elevation of the Precambrian surface deepens N to S along the Jornada del Muerto, and further deepens south of the heat-flow sites (18; 19). Therefore, boundaries in the southern part of the study area which could cause deep ground-water flow to be directed toward the surface, and thereby elevate near surface heat flows, are unexpected.

As mentioned above, models of regional crustal thinning and/or massive lower crustal intrusions generate thermal anomalies that could cause a "regional" heat flow of ~95 mWm^{-2} for the area; however, one must look further to attempt to understand the heat-flow values of ~125 mWm^{-2}. Consider the projection of the heat-flow estimates in the Jornada del Muerto on a N-S profile along 107° W long (Figures 1b, 4). The interpretation of the heat-flow change from ~90 to ~124 mWm^{-2} indicates a half width of ~6 km (determined from the 1/4 and 3/4 amplitude points of the anomaly). Alternative interpretations of the heat-flow increase (Figures 1b, 4) yield half widths of ~6 to ~11 km (although the distance between the sites having 98 and 127 mWm^{-2} implies a half width of < ~5-6 km; Figure 1b). If one assumes (only as an approximation) that a simple steady-state temperature step causes the increase in heat flow within the southern part of the study area, then a first-order estimate to the depth of the temperature step would be ~5-11 km. Temperature gradients at the heat-flow sites with higher values are ~40°C/km (1). These gradients are likely to become somewhat greater in the Precambrian upper crustal rocks because the high thermal conductivity of the largely limestone-dolomite sedimentary section would tend to create a lower gradient for a given heat flow. The mean gradient in the upper 10 km may be closer to ~45°C/km (this estimate considers the decrease in crustal radiogenic concentration with depth). Consequently, temperatures of ~245°C to ~515°C may be expected at depths of 5-11 km (including 20°C surface temperature). These temperatures are reasonable in terms of steady-state conduction or steady-state extensional models (e.g. 10; although the present estimates are slightly less, in part because of the upper ~3 km of high thermal conductivity material). The importance of the temperature estimates at 5-11 km is that they exceed, or are in the range of, temperatures suggested to demarcate elastic behavior in crustal rocks (i.e. beyond 250°C-450°C crustal materials no longer behave elastically; 20). It is therefore suggested that the geothermal anomaly in the southern Jornada del Muerto (~125-~95 mWm^{-2}) results from some type of mass movement-heat transfer mechanism operating in the crust just below the elastic layer. This conclusion is consistent with the geologic and geophysical data which describe a thin crust, apparently devoid of features indicative of extensional-tectonics in the upper part of the elastic crust.

REFERENCES

(1) Reiter, M., Eggleston, R. E., Broadwell, B. R., and Minier, J. (in prep.), Estimates of terrestrial heat flow from deep petroleum tests along the Rio Grande rift in central and southern New Mexico.

(2) Callender, J. F., Seager, W. R., and Swanberg, C. A. (1983) Late Tertiary and Quaternary tectonics and volcanism. Geothermal Resources of New Mexico: Scientific Map Series, New Mexico State University Energy Institute, Las Cruces.

(3) Renault, J. (1978) Overview of Rio Grande basalts with special reference to TiO_2 variation, in Guidebook to Rio Grande rift in New Mexico and

Colorado, New Mexico Bur. of Mines and Mineral Res. Cir. 163, p. 230-233.
(4) Warren, R. G. (1978) Characterization of the lower crust-upper mantle of the Engle Basin, Rio Grande rift, from a petrochemical and field geologic study of basalts and their inclusions. M.S. thesis, Univ. of New Mexico, 156 pp.
(5) Decker, E. R., and Smithson, S. B. (1975) Heat flow and gravity interpretations across the Rio Grande rift in southern New Mexico and west Texas. J. Geophys. Res., 80, p. 2542-2552.
(6) Cook, F. A., McCullar, D. B., Decker, E. R., and Smithson, S. B. (1979) Crustal structure and evolution of the southern Rio Grande rift, in Rio Grande rift: Tectonics and Magmatism, Am. Geophys. Union, p. 195-208.
(7) Keller, G. R., Braile, L. W., and Schlue, J. W. (1979) Regional crustal structure of the Rio Grande rift from surface wave dispersion measurements, in Rio Grande rift: Tectonics and Magmatism, Am. Geophys. Union, p. 115-126.
(8) Jaksha, L. H. (1982) Reconnaissance seismic refraction-reflection surveys in southwestern New Mexico. Geol. Soc. Am. Bull., 93, p. 1030-1037.
(9) Kelley, V. C. (1955) Regional tectonics of south-central New Mexico, in South-central New Mexico, New Mexico Geol. Soc., Socorro, p. 96-104.
(10) Lachenbruch, A. H., and Sass, J. H. (1978) Models of an extending lithosphere and heat flow in the Basin and Range Province, in Cenozoic Tectonics and Regional Geophysics of the western Cordillera. Geol. Soc. Am. Memoir 152, p. 209-250.
(11) Stewart, S. W., and Pakiser, L. C. (1962) Crustal structure in eastern New Mexico interpreted from the GNOME explosion. Bull. Seis. Soc. Am., 52, p. 1017-1030.
(12) Warren, D. H. (1969) A seismic refraction survey of crustal structure in central Arizona. Geol. Soc. Am. Bull., 80, p. 257-282.
(13) Toppozada, T. R., and Sanford, A. R. (1976) Crustal structure in central New Mexico interpreted from the Gas buggy explosion. Bull. Seis. Soc. Am., 66, p. 877-886.
(14) Reiter, M., Mansure, A. J., and Shearer, C. (1979) Geothermal characteristics of the Colorado Plateau. Tectonophysics, 61, p. 183-195.
(15) Bodell, J. M., and Chapman, D. S. (1982) Heat flow in the north-central Colorado Plateau, J. Geophys. Res., 87, p. 2869-2884.
(16) Chapin, C. E. (1979) Evolution of the Rio Grande rift--A summary, in Rio Grande rift: Tectonics and Magmatism, Am. Geophys. Union, p. 1-5.
(17) Morgan, P., Harder, V., Swanberg, C. A., and Daggett, P. H. (1982) A ground water convection model for Rio Grande rift geothermal resources. Geothermal Res. Council Trans., 5, p. 193-196.
(18) Foster, R. W. (1978) Selected data for deep drill holes along the Rio Grande rift in New Mexico, in Guidebook to Rio Grande rift in New Mexico and Colorado, New Mexico Bur. of Mines and Mineral Res. Cir. 163, p. 236-237.
(19) Seager, W. R. (pers. comm.).
(20) Chen, W. P., Molnar, P. (1983) Focal depths of intracontinental and intraplate earthquakes and their implications for the thermal and mechanical properties of the lithosphere. J. Geophys. Res., 88, p. 4183-4214.
(21) New Mexico Highway Geologic Map (1982) New Mexico Geological Society in cooperation with New Mexico Bur. of Mines and Mineral Res., Socorro.

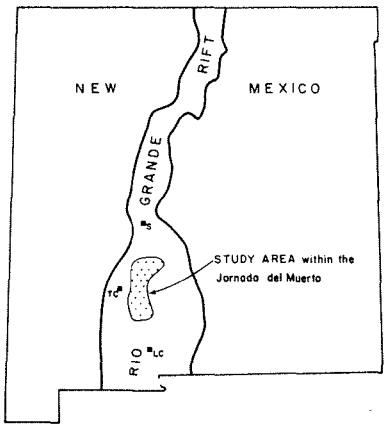

Figure 1a. Location map, S-Socorro, TC-Truth or Consequences, LC-Las Cruces.

Figure 1b (right). Study area, map after (2). Heat-flow estimates and measurements (large and small triangles respectively) in mWm^{-2} (1).

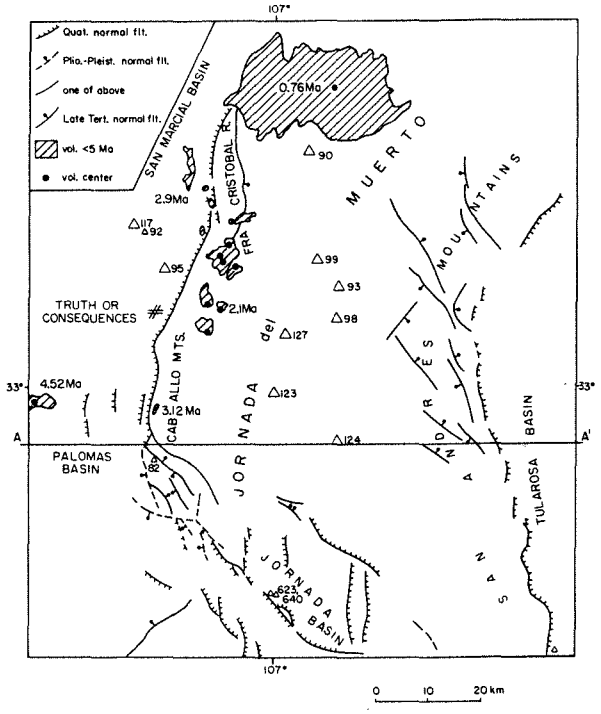

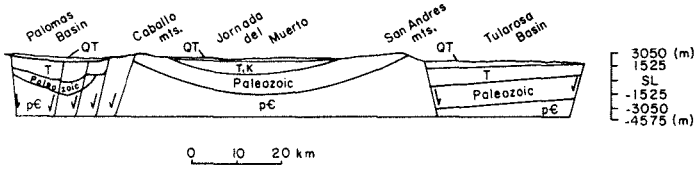

Figure 2 (left). Geologic cross section through the Jornada del Muerto, after (21).

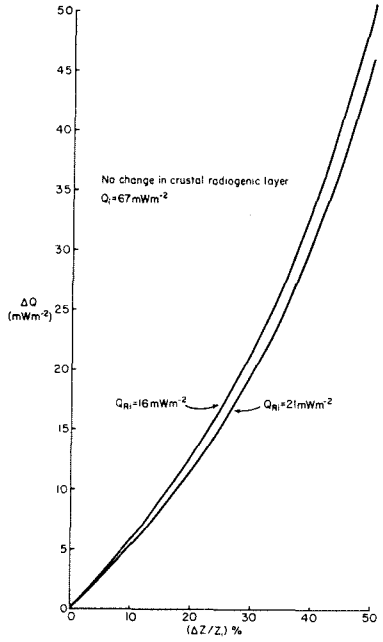

Figure 3. Heat-flow increase with % crustal thinning. Q_{Ri} is radiogenic.

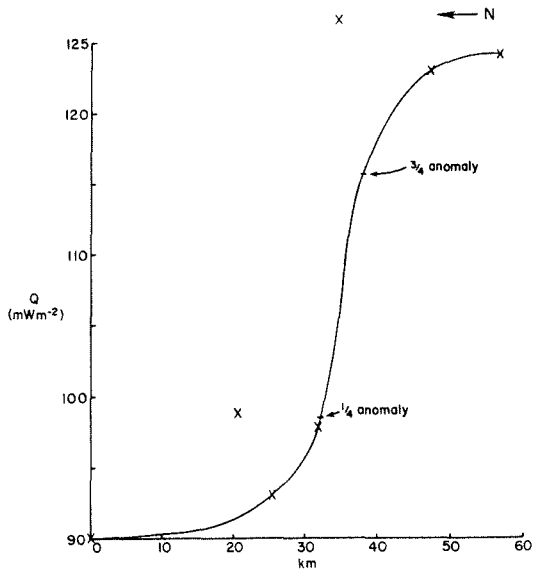

Figure 4. N-S heat-flow profile across area, x indicates data, solid line is interpretation.

CENOZOIC EXTENSION AND MAGMATISM IN ARIZONA; S. J. Reynolds and J. E. Spencer, Arizona Bureau of Geology and Mineral Technology, 845 N. Park, Tucson, AZ 85719

The Basin and Range Province of Arizona was the site of two episodes of Cenozoic extension that can be distinguished on the basis of timing, direction and style of extension, and associated magmatism (1,2). The first episode of extension occurred during Oligocene to mid-Miocene time and resulted in the formation of low-angle detachment faults, ductile shear zones (metamorphic core complexes), and regional domains of tilted fault blocks. Evidence for extreme middle Tertiary crustal extension in a NE-SW to ENE-WSW direction has been recognized in various parts of the Basin and Range of Arizona, especially in the Lake Mead area (3) and along the belt of metamorphic core complexes that crosses southern Arizona from Parker to Tucson (4). New geologic mapping and scrutiny of published geologic maps indicates that significant middle Tertiary extension is more widely distributed than previously thought. The state can be subdivided into regional tilt-block domains in which middle Tertiary rocks dip consistently in one direction (Fig. 1). The dip direction in any tilt-block domain is generally toward the breakaway of a low-angle detachment fault that underlies the tilt-block domain; we interpret this as indicating that normal faults in the upper plate of a detachment fault are generally synthetic, rather than antithetic, with respect to the detachment fault.

Detachment faults are subregional fault zones that originally formed with a low dip and that have accommodated normal slip of several kilometers to tens of kilometers (5,6). Large amounts of normal slip on some detachment faults have exhumed metamorphic core complexes that contain gently dipping mylonitic fabrics whose overall sense of shear is parallel to and in the same sense as transport on the associated detachment fault (7,8). These core-complex mylonites were formed by noncoaxial laminar flow along deeper segments of the detachment zone that were below the ductile-brittle transition. The principle causes of uplift and arching of the detachment zone are considered to be the following: 1) laterally variable isostatic uplift due to differential denudation; and 2) reverse drag above structurally deeper, listric normal faults (9) (Fig. 2). The relative importance of these two processes is generally unknown, and is probably quite variable between different detachment zones.

Middle Tertiary extension has exposed different levels of the pre-middle Tertiary crust. Rocks that were at mid-crustal levels prior to faulting are exposed in core complexes that contain thick (>1km) zones of penetrative mylonitic fabric, whereas shallower crustal levels are represented by thin (<100m) zones of less penetrative mylonitic fabrics that are confined to middle Tertiary plutons and their wall rocks. In these latter areas, the emplacement of synkinematic middle Tertiary plutons has caused local raising of geotherms and has permitted mylonitization to occur at levels that might otherwise have been above the brittle-ductile transition. Various levels of middle Tertiary crust are also exposed by wholesale rotation and subsequent erosion of large fault blocks. Some tilted fault blocks expose middle Tertiary plutons and dike swarms that represent the subsurface magma chambers and pathways, respectively, of middle Tertiary volcanics.

The main pulse of middle Tertiary felsic to mafic magmatism is time transgressive from east to west (10), but existing data are not sufficient to clearly demonstrate a state-wide, time-transgressive character for either the

initiation or termination of detachment faulting. Extension and detachment faulting began in some areas before significant magmatism, which suggests that magmatism and the associated elevation of geotherms are not necessary preconditions for the initiation of detachment faults. Numerical modeling requires that some of the proposed increases in geothermal gradients in middle Tertiary time are a consequence, not a cause, of detachment faulting.

Magnitudes of middle Tertiary extension of 50 to 100 percent are indicated by cross-sectional reconstructions of distended terrains and by evidence for total tectonic denudation of mid-crustal, core-complex tectonites during detachment faulting. This estimate is supported by comparisons of present crustal thickness (25km) of the Basin and Range Province with those that must have existed prior to extension in order to account for early Tertiary drainages that flowed onto the Colorado Plateau (present crustal thickness 40 km) from the presently topographically lower Basin and Range Province (11,12) (Fig. 3).

The middle Tertiary episode of extension and magmatism ended approximately 15 m.y. ago in all of Arizona except the Lake Mead area. It was replaced by the Basin and Range disturbance, which occurred in late Miocene and younger time and was characterized by dominantly basaltic volcanism and high-angle normal faulting that formed locally deep grabens filled with clastic sediments and nonmarine evaporites. The amount of extension during this event was relatively small (<15 percent) and occurred in an approximately east-west direction. The change to dominantly basaltic volcanism can be attributed to the initiation of through-going, high-angle faults that penetrated the cooling continental crust and permitted the easy ascent of mantle-derived magmas.

REFERENCES CITED

1. Shafiqullah, M., Damon, P. E., Lynch, D. J., Reynolds, S. J., Rehrig, W. A., and Raymond, R. H., 1980, K-Ar geochronology and geologic history of southwestern Arizona and adjacent areas, in Jenney, J. P., and Stone, C. (eds.), Studies in western Arizona: Arizona Geological Society Digest, v. 12, p. 201-260.
2. Zoback, M. L., Anderson, R. E., and Thompson, G. A., 1981, Cenozoic evolution of the state of stress and style of tectonism of the Basin and Range province of the western United States: Philosophical Transactions of the Royal Society of London, Series A, v. 300, p. 189-216.
3. Anderson, R. E., 1971, Thin-skinned distension of Tertiary rocks of southeastern Nevada: Geological Society of America Bulletin, v. 82, p. 43-58.
4. Crittenden, M. D., Coney, P. J., and Davis, G. H. (eds.), 1980, Cordilleran metamorphic core complexes: Geological Society of America Memoir 153, 490 p.
5. Wernicke, B., 1981, Low-angle normal faults in the Basin and Range Province: nappe tectonics in an extending orogen: Nature, v. 291, p. 645-648.
6. Reynolds, S. J., and Spencer, J. E., in press, Evidence for large-scale transport on the Bullard detachment fault, west-central Arizona: Geology, v. 13.
7. Davis, G. A., Lister, G. S., and Reynolds, S. J., 1983, Interpretation of Cordilleran core complexes as evolving crustal shear zones in an extending orogen: Geological Society of America Abstracts with Programs,

v. 15, p. 311.
8. Reynolds, S. J., 1985, Geology of the South Mountains, central Arizona: Arizona Bureau of Geology and Mineral Technology Bulletin 195, 61 p.
9. Spencer, J. E., 1984, Role of tectonic denudation in warping and uplift of low-angle normal faults: Geology, v. 12, p. 95-98.
10. Coney, P. J., and Reynolds, S. J., 1977, Cordilleran Benioff zones: Nature, v. 270, p. 403-406.
11. Peirce, H. W., Damon, P. E., and Shafiqullah, M., 1979, An Oligocene(?) Colorado Plateau edge in Arizona: Tectonophysics, v. 61, p. 1-24.
12. Wernicke, B., 1985, Uniform-sense normal simple shear of the continental lithosphere: Canadian Journal of Earth Sciences, v. 22, p. 108-125.

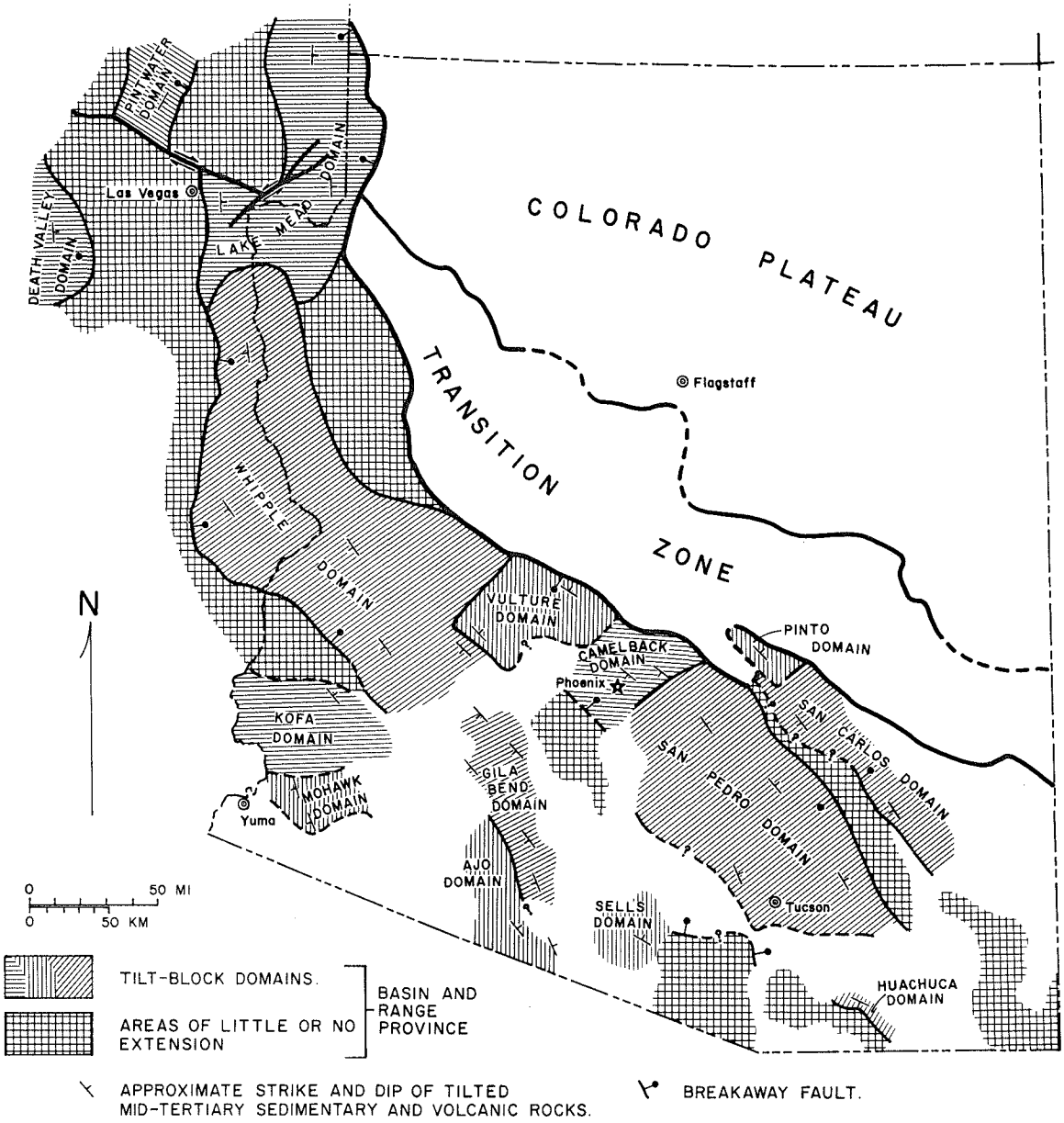

Figure 1. Map of tilt-block domains in the Basin and Range Province of Arizona and adjacent areas.

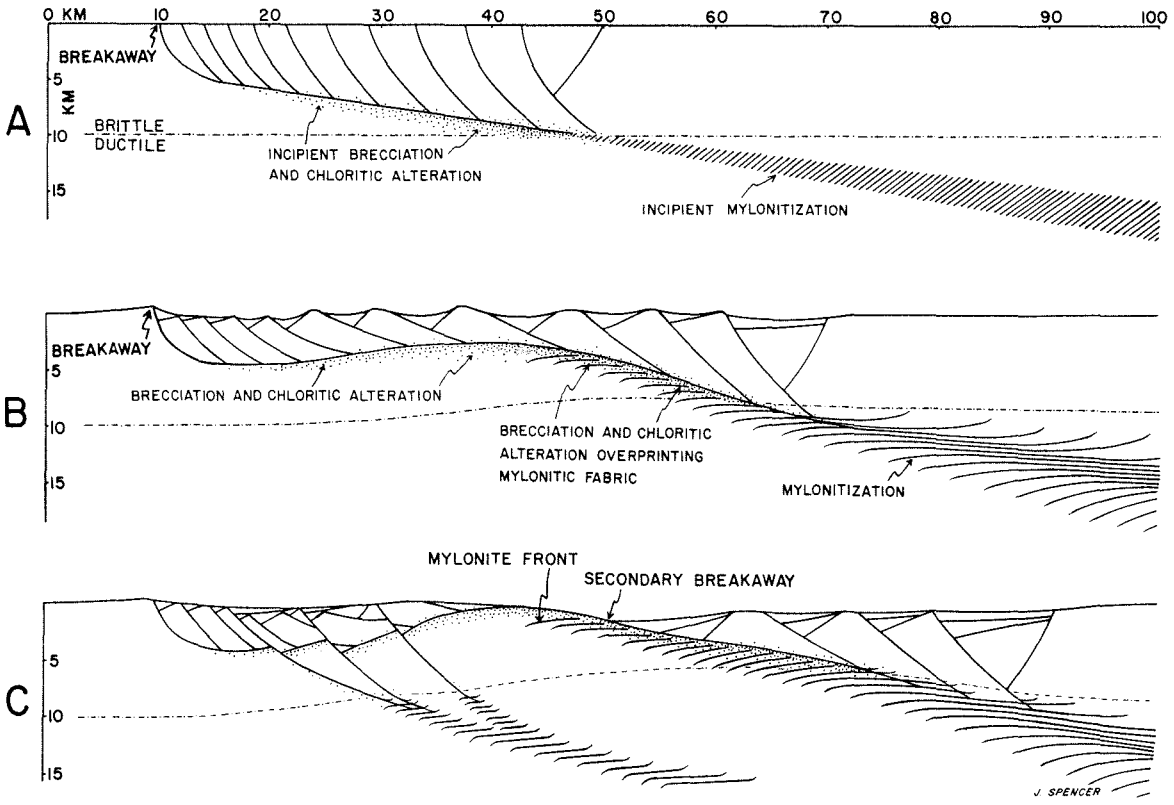

Figure 2. Schematic cross sections showing the evolution of detachment zones; (a) initiation of movement on the detachment zone; (b) isostatic uplift and arching due to variable amounts of upper-plate distension; and (c) one-sided denudation of original detachment zone, and arching caused by reverse drag above structurally deeper, listric normal faults.

Figure 3. Map of Arizona depicting crustal thicknesses and the location of metamorphic core complexes and early to middle Tertiary Rim gravels. The Rim gravels are located along the topographically high margin of the Colorado Plateau and were deposited by northeast-flowing drainages that drained the presently topographically lower Transition Zone and Basin and Range Provinces.

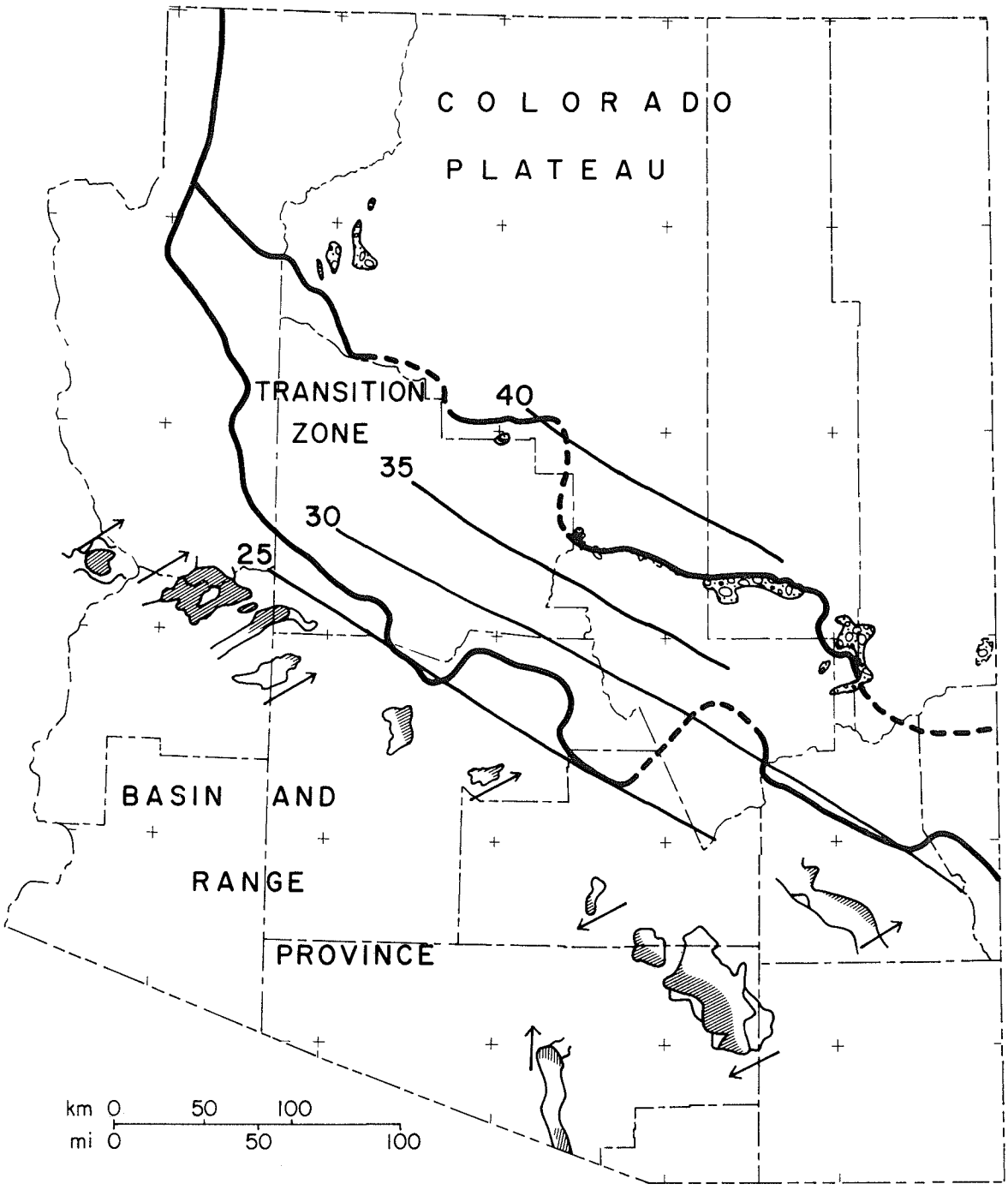

35 —— Crustal thickness contour (in km)

⟶ Sense of shear indicated by S and C surfaces in mylonitic rocks (relative movement direction of upper plate)

Lineated mylonitic rocks in metamorphic core complexes

Rim gravels (early to middle Tertiary)

Figure 3

A NUMERICAL STUDY OF FORCED LITHOSPHERIC THINNING; G. Schubert, UCLA, C. A. Anderson, Los Alamos National Laboratory, and E. Fishbein, UCLA.

Subsolidus lithospheric thinning by mantle plumes may be involved in the creation of swells, hotspots, and rifts. Among the major questions concerning this process are the timescale on which it occurs and the structure of the plumes. The lithosphere is known to have been substantially thinned in 10 Ma or less[1,2].

Previous studies[3-6] of the time required to thin the lithosphere by subsolidus convection are not in accord about the timescale of the process. Spohn and Schubert[5,6] concluded that sufficiently vigorous plumes could thin the lithosphere in 10 Ma, but the model only simulates the dynamics of the plume-lithosphere interaction in a way that does not specifically incorporate the material rheology or flow pattern. Emerman and Turcotte[4] found that the lithosphere cannot be thinned in 10 Ma, but their stagnation point solution cannot be matched to an external plume and boundary layer. Studies by Roberts[7] and Olson[8] indicate that within the corner region, at least for isoviscous vigorous convection, horizontal temperature variations are important. For fluids with strongly temperature dependent viscosity, the overlying rigid lid should enhance these effects that are not contained in the stagnation point solutions. We have sought to clarify this disagreement through a numerical finite element analysis of the subsolidus thinning mechanism.

Subsolidus lithospheric thinning is a process in which hot plume material warms the base of the lithosphere, entrains the heated lithospheric material in its flow, and carries the material away from the region of thinning. The phenomenon is basically one of forced convective heat transfer in a fluid with strongly temperature (and stress) dependent viscosity. Accordingly, we model the process as shown in Fig. 1. The parameters of the model are: T = temperature, u = horizontal velocity, w = vertical velocity, τ = shear stress, σ_x = normal stress, t = time, T_s = surface temperature, T_p = plume temperature, w_p = plume velocity, q = heat flux, and q_c = conductive heat flux. At time $t = 0$ we place hot plume material with temperature T_p at the base of a constant thickness lithospheric slab. The initial temperature in the lithosphere increases linearly with depth. Plume material is forced to enter the base of the computational box with conditions w_p, T_p. The MANTLE finite element code[9] is used to integrate the initial boundary value problem (heat, momentum, and continuity equations) with respect to time (and space) and to follow the thinning of the lithosphere (Fig. 1b). Plume plus lithospheric material is forced to leave the computational box along the right boundary as shown in Fig. 1b. The viscosity of the incompressible medium is taken to be proportional to the exponential of its inverse absolute temperature and to depend on the stress by a power law relation (some calculations were carried out with viscosity independent of stress). All other thermal, mechanical, and rheological properties are assumed to be constant. Lithospheric thinning times will be reported as functions of rheological parameters, w_p, and T_p.

Morris and Canright[10] have argued that in steady or quasi-steady convection of a strongly temperature dependent viscosity fluid the temperature difference across the plume is roughly a few times the temperature difference

needed to decrease the viscosity by a factor of e (provided the rigid lid remains intact). This provides an important constraint on subsolidus thinning rates by convective plumes. Current studies are focused on the lithospheric thinning by time-dependent plumes hypothesized by Morris to have large temperature differences across them.

References

1. Detrick R. S. and Crough S. T. (1978) Island subsidence, hot spots, and lithospheric thinning. J. Geophys Res., 83, p. 1236-1244.
2. Crough S. T. (1983) Hot spot swells. Ann. Rev. Earth & Planet. Sci., 11, p. 165-193.
3. Turcotte D. L. and Emerman S. H. (1983) Mechanisms of active and passive rifting. Tectonophys., 94, p. 39-50.
4. Emerman S. H. and Turcotte D. L. (1983) Stagnation flow with a temperature-dependent viscosity. J. Fluid Mech., 127, p. 507-517.
5. Spohn T. and Schubert G. (1982) Convective thinning of the lithosphere: a mechanism for the initiation of continental rifting. J. Geophys. Res., 87, p. 4669-4681.
6. Spohn T. and Schubert G. (1983) Convective thinning of the lithosphere: a mechanism for rifting and mid-plate vulcanism on Earth, Venus and Mars. Tectonophys., 95, p. 67-90.
7. Roberts, G. O. (1972) Fast viscous Benard convection. Geophys. Astrophys. Fluid Dyn., 12, p. 235-272.
8. Olson P. and Corcos G. N. (1980) A boundary layer model for mantle convection with surface plates. Geophys. J. R. Astron. Sci., 62, p. 195-219.
9. Thompson E. (1979) MANTLE: a finite element program for the thermomechanical analysis of mantle convection. NASA Tech. Rep. N79-24297.
10. Morris S. and Canright D. P. (1984) A boundary layer analysis of Benard convection in a fluid of strongly temperature-dependent viscosity. Phys. Earth Plan. Int., 36, p. 355-375.
11. Morris S. (1981) An asymptotic method for determining the transport of heat and matter by creeping flows with strongly variable viscosity. Ph.D. dissertation, John Hopkins Univ.

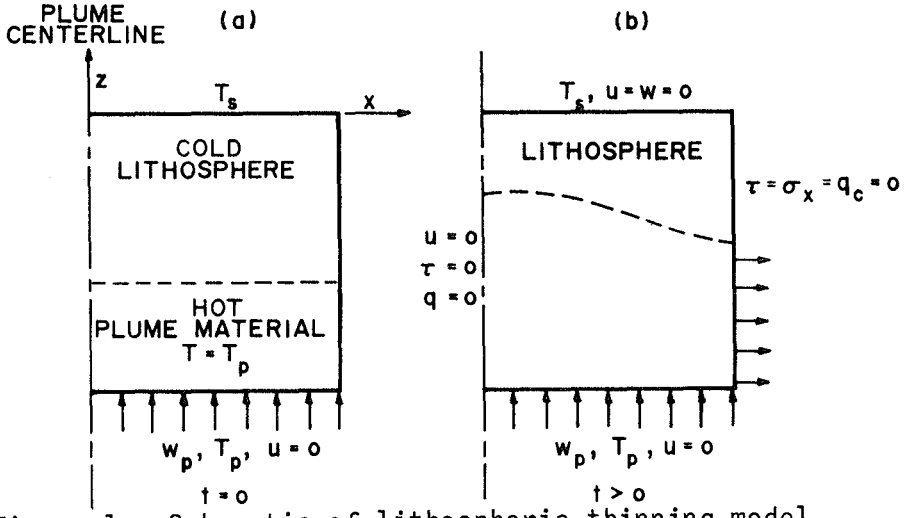

Figure 1. Schematic of lithospheric thinning model.

KINEMATICS OF A LARGE-SCALE INTRAPLATE EXTENDING LITHOSPHERE: THE BASIN-RANGE; Robert B. Smith, and Paul K. Eddington, Department of Geology and Geophysics, University of Utah, Salt Lake City, Utah 84112-1183.

Upper lithospheric structure of the Cordilleran Basin-Range (B-R) is characterised by an E-W symmetry of velocity layering. The crust is 25 km thick on its eastern active margin, thickening to 30 km within the central portion and thinning to ~25 km on the west. Pn velocities of 7.8-7.9 km/s characterize the upper mantle while an unusual upper-mantle low-velocity cushion, 7.4 km/s-7.5 km/s, occurs at a depth of ~25 km in the eastern B-R and underlies the area of active extension. An upper-crustal low-velocity zone in the eastern B-R shows a marked P-wave velocity inversion of 7% at depths of 7-10 km also in the area of greatest extension. The seismic velocity models for this region of intraplate extension suggests major differences from that of normal, thermally undeformed continental lithosphere.

Interpretations of seismic reflection data, demonstrate the presence of extensive low-angle reflections in the upper-crust of the eastern B-R at depths from near-surface to 7-10 km.(1) These reflections have been interpreted to represent low-angle normal fault detachments or reactivated thrusts. Seismic profiles across steeply-dipping normal faults in unconsolidated sediments show reflections from both planar to downward flatening (listric) faults that in most cases do not penetrate the low-angle detachments. These faults are interpreted as late Cenozoic and cataclastic-mylonitic zones of shear displacement. Areas of extreme crustal extension (up to 100% or more) in the Sevier Desert are underlain by pervasive very low-angle faults that apparently accommodated most of the extension.

Most of the interior of the B-R has evidence of late-Cenozoic faulting, but current seismicity occurs at or near its boundaries. Major seismicity (with magnitudes of 7+) in central Nevada is associated with normal faults and components of strike-slip. Whereas primarily dip-slip earthquakes occur along the Intermountain seismic belt that marks the eastern B-R. These seismic zones mark the areas of principal strain-release within the extending western North American plate. Important seismicity parameters that characterize this region of extension are: (1) maximum focal depths that seldom exceed 15 km and mark the maximum depth of brittle deformation, (2) the maximum magnitudes of ~7.7, and (3) dominant down-slip extension.

The recent Ms7.3, 1983 Borah Peak, Idaho earthquake has provided important insights into the mechanical processes accompanying brittle extension. Detailed aftershock data from this large earthquake: the 1959, M7.5 Hebgen Lake, Montana; and the 1954, M7.1 Dixie Valley, Nevada earthquakes show the following important characteristics: (1) mainshock nucleation at mid-crustal depths of ~15 km; (2) nucleation along moderate, 45^{0}-65^{0} dipping planar fault zones; (3) aftershock distributions that are clearly above the depths of the mainshock; (4) for the Borah Peak earthquake, equal vertical and horizontal components of ~1 m slip corresponding to 10^{-5} down-dip strain; and (5) mainshock/aftershock distributions that extend laterally beyond the surface faulting. The geometry and style of crustal faulting inferred from these large magnitude intraplate events is a paradox compared to fault-plane orientations

inferred from the observed seismic reflection data and modal planes of smaller regional earthquakes - the appearance of low-angle and listric faulting with Quaternary-Holocene displacement versus the through-going steeper-dip planar faults inferred from the large earthquakes.

Strain indicators (fault plane solutions, in situ stress, hydrofrac, etc.) indicate west to northwest extension along the western portion of the B-R but generally east-west extension along the eastern margin. Inversion of seismic moment tensors for the historical earthquake data suggest displacement rates of up to 7.5 mm/yr (10^{-17} s^{-1} to 10^{-16} s^{-1}) in central Nevada but decreasing to very low rates ($<10^{-17}$ s^{-1}) across the aseismic zones of the central Great Basin. Toward the eastern margin of the Basin-Range displacement rates increase to 1.3 mm/yr (10^{-16} - 10^{-17} s^{-1}). The principal deformation is produced by the magnitude 6+ earthquakes. The contemporary deformation associated with historical seismicity compared with displacement rates inferred from Quaternary-slip are of the same order (mm/yr) - implying a common driving mechanism since Late Cenozoic time. Vector solutions of intraplate motion[2] and cumulative displacements from our seismicity data argue for 9 to 11 mm/yr east-west opening of the northern B-R. This conclusion suggests that the principal deformation is related to brittle release with smaller amounts of aseismic creep. Satellite measurements across the region are not yet well enough established to infer long-range rates.

Vertical deformation of the Great Basin is difficult to assess, but interpretations of re-levelling (1920-1960), across the northern B-R, suggests a relative uplift, maximum innorthern Nevada, at rates as large as 3 mm/yr. Relative downwarp on the east and west margins of the B-R are also the sites of large Pleistocene Lakes (Lahonton and Bonneville) that were influenced by the compliance of the lithosphere.

Rheological models (principally thermal and compositionally controlled) of the B-R lithosphere suggest a complex structure. The upper lithosphere appears to be composed of a 7-10 km brittle upper-crust -- the seismogenic layer. The intermediate and lower crust is modeled as interbedded brittle and plastic layers followed by a thin, brittle upper-mantle. The large magnitude earthquakes appear to nucleate at the base of the upper-crustal brittle zone near the peak of the shear stress maximum. The low-angle listric and planar faults extend througout the upper and intermediate crust and only generally coincide with the theoretical brittle-ductile boundary.

These data and rheological properties provide input to a two-dimensional finite-element, visco-elastic modeling program (Lynch, 1984, personal comm.) that is used to interpret time and temperature dependent strain-rate models of lithospheric extension. Results of the computations will be discussed.

Lithospheric velocity models of the Yellowstone hotspot and its track the Snake River Plain (a youthful volcanic-tectonic area of active crustal extension within the northern Basin-Range) shows evidence of thermal perturbations of the lithosphere. At Yellowstone low-velocity upper-crust has been uplifted and extended by thermal expansion. Whereas subsidence associated with cooling produces significant topographic down-warp (~1 km) and rifting of the Snake River Plain. This model can be applied to an extending lithosphere if significant magmatic intrusion of the crust has accompanied extension.

BASIN AND RANGE DEFORMATION

Robert B. Smith and Paul K. Eddington

Mechanisms of B-R extension that have been suggested include: (1) lithospheric upwelling (mantle diapirism), (2) block tectonics, (3) a soft San Andreas transform fault, (4) ridge push from the Mid-Atlantic ridge, (5) bouyant uplift and concomitant extension, and (6) advection at the Basin-Range boundaries. None of the mechanisms can yet be clearly demonstrated. Although current data on velocity structure, strain rates, and rheological boundaries suggest a model of bouyant or vertically driven uplift with concomitant extension.

Important problems relative to intraplate lithospheric extension are: (1) The observation of low-angle listric and steep planar faulting in the same stress regime; (2) The role and importance of small earthquakes as indicators of sub-plate boundaries and their relationship to structure; (3) Thermal rheological factors controlling maximum focal depths and hence the thickness of the elastic lithosphere; (4) Can future large earthquakes nucleatre on low-angle or listric faults? Is there evidence of multiple shocks associated with large earthquakes suggesting shallow-dip nucleation merging into flat detachments? What percentage of extension is accommodated by earthquakes? and (6) What is the distribution of brittle and ductile deformation in contemporary deformation? Together these data, models, and questions point out the problems of understanding continental lithospheric extension that should be addressed and compared on a global scale.

References

(1) Smith, R.B. and Bruhn, R.L. (1984) Intraplate Extensional Tectonics of the Eastern Basin-Range: Influence on Structural Style from Seismic Reflection Data, Regional Tectonics, and Thermal-Mechanical Models of Brittle-Ductile Deformation. Jour. Geophys. Res., v.89, p.5733-5762.

(2) Minster, J.B. and Jordan, T.H. (1984) Vector Constraints on Quaternary Deformation of the Western United States East and West of the San Andreas Fault. In Tectonics and Sedimentation Along the California Margin, eds. Crouch, J.K. and Bachman, S.B., Pacific Section, Soc. Econ. Paleon. and Min., 15p.

RIFT SYSTEMS ON VENUS: AN ASSESSMENT OF MECHANICAL AND THERMAL MODELS. Sean C. Solomon, Dept. of Earth, Atmospheric, and Planetary Sciences, Massachusetts Institute of Technology, Cambridge, MA 02139; and James W. Head, Dept. of Geological Sciences, Brown University, Providence, RI 02912.

Introduction. The formation and distribution of major tectonic features on Venus are closely linked to the dominant mechanism of lithospheric heat loss [1]. Among the most spectacular and extensive of the major tectonic features on Venus are the chasmata, deep linear valleys generally interpreted to be the products of lithospheric extension and rifting [2-5]. Systems of chasmata and related features can be traced along several tectonic zones up to 20,000 km in linear extent [5]. In this paper we apply mechanical and thermal models for terrestrial continental rifting to the rift systems of Venus. The models are tested against known topographic and tectonic characteristics of Venus chasmata as well as independent information on the physical properties of the Venus crust and lithosphere.

Chasma Characteristics. Major systems of chasmata, readily identified from Pioneer Venus topographic data [2,3], are located in the Beta and Phoebe highland regions [4] and along the Aphrodite-Beta and Themis-Atla tectonic zones in the Venus equatorial highlands [5]. Smaller chasms have been identified elsewhere on the basis of radar imaging data [6]. Among the principal highland regions of Venus [7], Ishtar Terra may be distinguished as the only large highland area apparently lacking major rift structures.

Topographic profiles across major chasmata have similar characteristics from region to region [2-5]. The rift valleys are typically 75-100 km in width. The floors of the chasmata are up to 2.5 km deeper than ambient terrain levels, and the rims of the rifts are generally raised by 0.5 to 2.5 km. Because of the large footprint and spacing of the altimetry data [3], the rift widths may be slightly overestimated, and the maximum relief of rims and chasma floors may be somewhat greater than indicated here.

A major question is the relative contribution of volcanic construction and uplift to the observed rim heights. New high-resolution radar images of the rift system in central Beta Regio have allowed the tentative identification of a number of individual volcanic constructs along the boundaries of the rift [8] and an assessment of their relationship to local topography [4]. On the basis of these new data, the regions of maximum rim height appear to coincide with volcanic constructs. Rim heights are no more than 1-1.5 km in areas without discernible constructional contribution [8].

Graben Model. The first model proposed in the literature to explain the characteristics of Venus chasmata was the Vening-Meinesz graben model [5]. For this model [9] to predict the correct width of the rift valley or graben, however, the local thickness of the elastic lithosphere must be 45-70 km [5]. Such a great thickness for the elastic lithosphere of Venus is extremely unlikely; on the basis of laboratory data and the high surface temperature of Venus, the elastic lithosphere can be shown to be no more than a few kilometers in thickness [10].

Lithospheric Stretching Models. The failure of the graben model to explain the topographic characteristics of highland rifts on Venus led to the proposal of a lithospheric stretching model [11]. Such models have been applied successfully to explain the structures and subsidence histories of continental basins and rifted continental margins on Earth [12-14]. The

simplest of these models are locally one-dimensional and involve either uniform lithospheric stretching or different degrees of stretching for the crust and the thermal lithosphere. According to the two-layer stretching model of Turcotte [13], for instance, a crust of thickness C_o and density ρ_c and a lithosphere of thickness L_o (including the crust) is stretched under extension to new crustal and lithospheric thicknesses C and L. There is a resulting subsidence

$$s = \frac{(\rho_m - \rho_c)}{\rho_m} C_o (1 - \beta_c) - \frac{\alpha}{2} (T_m - T_o) L_o (1 - \beta_L) \quad (1)$$

where $\beta_c = C/C_o$ and $\beta_L = L/L_o$ are thinning factors for the crust and lithosphere, T_m and ρ_m are the temperature and density of the asthenosphere, T_o is the surface temperature, and α is the volumetric coefficient of thermal expansion for the lithosphere. The first term in (1) represents the isostatic result of crustal thinning; the second term represents the thermal result of lithospheric thinning.

One simple test of this model is to examine the implications of the topographic relief for the pre-rift thickness of the crust. If either the present rift significantly postdates the episode of extension [12,13] or the width of thinned lithosphere beneath a Venus rift is considerably greater than the width of the region of thinned crust [14], then the total rim-to-floor relief, excluding volcanic construction, across a rift on Venus is a measure of crustal thinning. Setting the first term in (1) equal to 3.5 to 4 km, and assuming $\rho_m = 3.4$ g/cm^3 and $\rho_m - \rho_c = 0.4$ g/cm^3, gives $C_o(1-\beta_c) = 30$-34 km. Since $\beta_c \geq 0$, a minimum thickness for the pre-rift highland crust on Venus is 30 km, a result at least consistent with available gravity and topographic data for Venus highlands, particularly highlands removed from the regions with the strongest signature of mantle dynamics in the long-wavelength gravity and topography fields [15,16]. A rift developed in a region of significantly thinner crust, perhaps including the Venus lowlands and midland plains [7], would be expected to display lesser relief than do the highland chasmata.

On the Origin of Raised Rims. A key issue for mechanisms of rift formation and evolution is the origin of the raised rims adjacent to Venus rift valleys. While localized topographic highs in Beta Regio may be identified from radar images as volcanic constructs [8], the constructional component of rim topography elsewhere along Venus chasmata is difficult to ascertain. A significant component of rim uplift appears to be generally present in terrestrial continental rift formation, an observation that has led to two-layer extensional models with the thermal lithosphere thinned over a zone of greater width than the region of crustal thinning [14]. Strictly kinematic models of this type do not conserve lithspheric mass; removal of the lower lithosphere by some mechanism (e.g., stoping) must be postulated. More complete thermal and dynamical models, however, yield rim uplift as a natural consequence of the lateral transport of heat following initial rifting, either by lithospheric conduction [17] or by the onset of convection in the heated lower lithosphere [18].

The simple two-layer stretching model of equation (1) may be tested against the implied thickness of the thermal lithosphere under the assumption that the raised rim of a Venus chasma is a response to lithospheric thinning and associated thermal uplift [19]. Setting the second term in (1) equal to 1 to 1.5 km, and adopting $\alpha = 3 \times 10^{-5}$°K^{-1} and $T_m - T_o = 10^3$°K, gives $L_o(1-\beta_L) = 70$ to 100 km. Since $\beta_L \geq 0$, the pre-rift thermal lithosphere is at least 70 km thick. Adding the thickness of the presumably unthinned highland crust

external to the rift valley would give a lower bound of 100 km to the pre-rift thermal lithosphere. It should be noted that the uplift attributed here to lithospheric thinning is in addition to any thermal contribution to the broad topographic rise of highland topography in areas of active rifting [20]; i.e., the average thickness of the thermal lithosphere would have to exceed 100 km, perhaps by a considerable amount, if a portion of the topographic rise of a rifted highland is attributed to a broad area of heating and thinning of the thermal lithosphere. If the physical properties governing convection in the Venus mantle are similar to those in the Earth's mantle, this requirement of a thick thermal lithosphere beneath the Venus highlands may be sufficient to rule out this simple stretching model, at least for models not including the effects of lateral heat transport.

It is also important to consider non-thermal explanations for uplift of Venus rift valley rims. In terrestrial rifts, early thermal uplift of rift margins may be sustained well after the heating event by the flexural rigidity of the thickening elastic lithosphere [21]. Such a process is not likely to be important for Venus, however, because of the small value of elastic lithosphere thickness expected even in the absence of extension [1,11]. Dynamic models of extension of a ductile lithosphere can also yield uplifted rims by material flow [22]; the relative contributions of thermal uplift and flow uplift remain to be explored for such models, however.

Conclusions. Lithospheric stretching models can account at least broadly for the topographic characteristics of Venus rift structures. With additional assumptions, such models provide bounds on the thicknesses of the crust and thermal lithosphere in the Venus highlands. Unresolved is the causative mechanism for rift formation, but the great length of ridge systems points to global-scale tectonic processes. We favor the view that the uplift of the margins of Venus rift systems involves a significant thermal component, which would indicate that these global processes are currently active. The lack of major rift structures in Ishtar Terra provides additional support for the hypothesis [11] that the most recent tectonic activity in that highland area has been dominantly compressional.

References.

[1] Solomon S.C. and Head J.W. (1982) Mechanisms for lithospheric heat transport on Venus: Implications for tectonic style and volcanism. J. Geophys. Res., 87, p. 9236-9246.
[2] Pettengill G.H., Ford P.G., Brown W.E., Kaula W.M., Masursky H., Eliason E. and McGill G.E. (1979) Venus: Preliminary topographic and surface imaging results from the Pioneer Orbiter. Science, 205, p. 90-93.
[3] Pettengill G.H., Eliason E., Ford P.G., Loriot G.B., Masursky H. and McGill G.E. (1980) Pioneer Venus radar results: Altimetry and surface properties. J. Geophys. Res., 85, p. 8261-8270.
[4] McGill G.E., Steenstrup S.J., Barton C. and Ford P.G. (1981) Continental rifting and the origin of Beta Regio, Venus. Geophys. Res. Lett., 8, p. 737-740.
[5] Schaber G.G. (1982) Venus: Limited extension and volcanism along zones of lithospheric weakness. Geophys. Res. Lett., 9, p. 499-502.
[6] Campbell D.B., Burns B.A. and Boriakoff V. (1979) Venus: Further evidence of impact cratering and tectonic activity from radar observations. Science, 204, p. 1424-1427.

[7] Masursky H., Eliason E., Ford P.G., McGill G.E., Pettengill G.H., Schaber G.G., and Schubert G. (1980) Pioneer Venus radar results: Geology from images and altimetry. J. Geophys. Res., 85, p. 8232-8260.
[8] Campbell D.B., Head J.W., Harmon J.K. and Hine A.A. (1984) Venus: Volcanism and rift formation in Beta Regio. Science, 226, p. 167-170.
[9] Vening Meinesz F.A. (1950) Les graben africains, resultat de compression ou de tension dans la croute terrestre? Bull. Inst. R. Colon. Belge, 21, p. 539-552.
[10] Solomon S.C. and Head J.W. (1984) Venus banded terrain: Tectonic models for band formation and their relationship to lithospheric thermal structure. J. Geophys. Res., 89, p. 6885-6897.
[11] Solomon S.C. and Head J.W. (1984) Rift structures on Venus: Implications of a lithospheric stretching model (abstract), Lunar Planet. Sci., 15, p. 806-807.
[12] McKenzie D. (1978) Some remarks on the development of sedimentary basins. Earth Planet Sci. Lett., 40, p. 25-32.
[13] Turcotte D.L. (1983) Mechanisms of crustal deformation. J. Geol. Soc. Lond., 140, pp. 702-724.
[14] Hellinger S.J. and Sclater J.G. (1983) Some comments on two-layer extensional models for the evolution of sedimentary basins. J. Geophys. Res., 88, p. 8251-8269.
[15] Sjogren W.L., Bills B.G., Birkeland P.W., Esposito P.B., Konopliv A.R., Mottinger N.A., Ritke S.J. and Phillips R.J. (1983) Venus gravity anomalies and their correlations with topography. J. Geophys. Res., 88, p. 1119-1128.
[16] Bowin C. (1983) Gravity, topography, and crustal evolution of Venus. Icarus, 56, p. 345-371.
[17] Jarvis G.T. (1984) An extensional model of graben subsidence--the first stage of basin evolution. Sed. Geol., 40, p. 13-31.
[18] Buck W.R. (1984) Small-scale convection and the evolution of the lithosphere. Ph.D. Thesis, M.I.T., Cambridge, MA, 256 pp.
[19] Spohn T. and Schubert G. (1983) Convective thinning of the lithosphere: A mechanism for rifting and mid-plate volcanism on Earth, Venus, and Mars. Tectonophysics, 94, p. 67-90.
[20] Morgan P. and Phillips R.J. (1983) Hot spot heat transfer: Its application to Venus and implications to Venus and Earth. J. Geophys. Res., 88, p. 8305-8317.
[21] Weissel J.K. and Karner G.D. (1984) Thermally-induced uplift of the southeast highlands of Australia (abstract). EOS Trans. AGU, 65, p. 1115.
[22] Zuber M.T., Parmentier E.M., and Head J.W. (1985) Ductile lithosphere extension: Implications for rifting of the Earth and Venus (abstract). Lunar Planet. Sci., 16, p. 948-949.

POSSIBLE ROLE OF CRUSTAL FLEXURE IN THE INITIAL DETACHMENT OF EXTENSIONAL ALLOCHTHONS; Jon E. Spencer, Arizona Bureau of Geology and Mineral Technology, 845 N. Park Ave., Tucson, AZ 85719

The existence of low-angle normal faults indicates that the ratio of shear stress (τ) to normal stress (σ_N) needed to cause slip on faults is substantially less than would be predicted based on experimental data. Because the tensional strength of rock at a large scale is exceedingly low, the upper plate of a low-angle normal fault cannot be pulled down the fault ramp, but must be driven down it by its own weight. The active or recently active Sevier Desert detachment fault in western Utah dips regionally at 12^{o} (1). The ratio of shear stress to normal stress due to the weight of the upper plate on a 12^{o}-dipping fault surface is 0.2. In contrast, laboratory experiments indicate that slip on fracture surfaces occurs with almost all rock types when (τ / σ_N) reaches values of 0.6 to 0.85 (2), corresponding to normal-fault dips of 30^{o} to 40^{o}. Seismological data indicate that low deviatoric stresses are associated with movement on faults of other geometries (3,4) and are not unique to low-angle normal faults. It thus appears that approximately planar fault zones with surface areas of hundreds to thousands of square kilometers have different mechanical properties than would be predicted based on laboratory studies of fractured rock.

Modeling of stresses associated with flexure of oceanic lithosphere at outer-arc rises indicates that deviatoric stresses greater than 5kb exist and are sustainable in oceanic lithosphere, and that failure occurs when τ / σ_N approaches 0.6 to 0.85 (5). Continental lithosphere differs from oceanic lithosphere in that a low-strength zone in the middle and lower crust is predicted to separate strong upper crust and strong upper mantle (6). This three-layer lithosphere rheology is consistent with seismicity data (7), and indicates that stresses of up to several kilobars should be sustainable in the upper crust. In situ stress measurements support the applicability of laboratory data to models of crustal rheology at near-surface levels away from fault zones (8).

I therefore conclude that fault initiation is a major tectonic event that results in formation of planar zones of weakness within which sustainable deviatoric stresses are only a small fraction of sustainable deviatoric stress levels in rocks that are fractured but do not contain throughgoing fault zones. The transition from fractured rock to a throughgoing, planar fault zone must result from many seismic events or from aseismic processes. If it occurred during a single seismic event, the stress drop would be very large and would be recognizable in seismological data; such events are not observed (3). The deviatoric stresses needed for formation of low-angle normal faults and initial mobilization of extensional allochthons are far greater than those produced by the weight of crustal rock on a gently dipping surface. This points to a fundamental mechanical problem: how are such high shear stresses achieved on gently dipping surfaces.

I propose that stresses associated with crustal flexure are essential for initial detachment of extensional allochthons, at least in cases where pre-existing faults are not utilized as detachment fault surfaces. Low-angle normal faults form as slip surfaces that release elastic energy associated with crustal flexure. Flexure in the western United States possibly resulted from at least two processes: [1] initial

moderate- to high-angle normal faulting caused unloading of the footwall block, resulting in slight to moderate isostatic uplift and concave-upward flexure of the footwall and associated development of flexure-generated stresses. Sequential initiation of progressively shallower faults resulted from continued extensional faulting and associated denudation, isostatic uplift, and flexure of the footwall. [2] Erosional denudation of the overthickened and topographically high, Mesozoic compressional orogenic belt caused isostatic uplift of the belt and flexure on its flanks. In this case, extensional faulting began in an upper crust that was already highly stressed due to flexure associated with erosional denudation and isostatic rebound. This second mechanism for flexure is consistent with some sedimentological data that suggest that subsidence over a broad area due to initial extension on gently dipping faults is followed by internal distension and high-angle faulting of the upper plate (9), rather than the reverse sequence in which initial high-angle faulting is followed by progressively lower angle faulting.

The sense of shear along the gently to moderately dipping neutral surface of a tapered lower plate undergoing concave-upward flexure would tend to drive rock above the surface down the regional dip of the surface. In an extensional environment of reduced lateral confining stress, the weight of the rock above the neutral surface would also tend to drive overlying rock down the surface. Stresses originating from both flexure and gravity interfere constructively, and the resultant state of stress may be essential for low-angle normal fault initiation (10).

References Cited

1. Allmendinger, R. W., Sharp, J. W., Von Tish, D., Serpa, L., Brown, L., Kaufman, S., Oliver, J., and Smith, R. B., 1983, Cenozoic and Mesozoic structure of the eastern Basin and Range Province, Utah, from COCORP seismic reflection data: Geology, v. 11, p. 532-536.
2. Byerlee, J., 1978, Friction of rocks: Pure and Applied Geophysics, v. 116, p. 615-626.
3. Raleigh, B., and Evernden, J., 1981, Case for low deviatoric stress in the lithosphere, in Mechanical behavior of crustal rocks: American Geophysical Union Geophysical Monograph no. 24, p. 173-186.
4. Lachenbruch, A. H., and Sass, J. H., 1980, Heat flow and energetics of the San Andreas fault zone: Journal of Geophysical Research, v. 85, p. 6185-6222.
5. Goetze, C., and Evans, B., 1979, Stress and temperature in the bending lithosphere as constrained by experimental rock mechanics: Geophysical Journal of the Royal Astronomical Society, v. 59, p. 463-478.
6. Brace, W. F., and Kohlstedt, D. L., 1980, Limits of lithospheric stress imposed by laboratory experiments: Journal of Geophysical Research, v. 85, p. 6248-6252.
7. Chen, W-. P., and Molnar, P., 1983, Focal depths of intracontinental earthquakes and their implications for thermal and mechanical properties of the lithosphere: Journal of Geophysical Research, v. 88, p. 4183-4214.
8. McGarr, A., and Gay, N.C., 1978, State of stress in the Earth's crust: Annual Review of Earth and Planetary Science, v. 6, p. 405-436.
9. Wernicke, Brian, 1985, Uniform-sense normal simple shear of the

continental lithosphere: Canadian Journal of Earth Science, v. 22, p. 108-125.

10. Spencer, J. E., 1982, Origin of folds of Tertiary low-angle fault surfaces, southeastern California and western Arizona, in Frost, E. G., and Martin, D. L., eds., Mesozoic-Cenozoic tectonic evolution of the Colorado River region, California, Arizona, and Nevada: San Diego, Cordilleran Publishers, p. 123-134.

THE EFFECTS OF STRAIN HEATING IN LITHOSPHERIC STRETCHING MODELS

Mike Stanton
Dennis Hodge (both at Department of Geological Sciences, SUNY at Buffalo, Amherst,N.Y. 14226)
Frank Cozzarelli (Department of Civil Engineering, SUNY at Buffalo, Amherst, N.Y., 14226)

Simple kinematic models of lithospheric stretching (1) require increased heat flow at the surface as the lithosphere is thinned. In these simple stretching models rock in the lower crust (material points in the mathematical models) will follow a particle path which curves upward towards the surface. A specific rock mass, thus, may actually decrease in temperature due to conductive heat loss even though the surface heat flow is increased. Widespread silicic igneous activity accompanying stretching suggests, however, that the lower crust is heated and we suggest that strain heating associated with stretching may be a source of the temperature increase in the lower crust. Numerical solutions to a simple stretching model show that the localization and magnitude of viscous strain heating is most significant in the uppermost mantle and lower crust as temperature increases above initial temperatures for these rocks can be as large as 70°C. It should be noted that in areas where extensive underplating of magmatic material occurs, the effect of strain heating in crustal rocks may be small compared to the heat from gabbroic intrusions (2).

The deformation by stretching of a continental type lithosphere has been formulated so that the problem can be solved by a continuum mechanical approach. The deformation, stress state, and temperature distribution are constrained to satisfy the physical laws of conservation of mass, energy, momentum, and an experimentally defined rheological response. The conservation of energy equation including a term for strain energy dissipation is expressed by:

$$2T_{xy}'\dot{\varepsilon}_{xy} = -k\frac{\partial^2\theta}{\partial z^2} + \rho c\frac{\dot{\varepsilon}_0}{a}(a-z)\frac{\partial\theta}{\partial z} + \rho c\frac{\partial\theta}{\partial t}$$

where $2T_{xy}'\dot{\varepsilon}_{xy}$ is the source term due to strain heating.

The continental lithosphere is assumed to have the rheology of an isotropic, incompressible, nonlinear viscous, two layered solid with the following constitutive law:

$$D_{ij} = A_1 \exp(-Q_1/R\theta)\, J_2'^{\,m} T_{ij}'$$

where A_1 and Q_1 are material constants for layer 1, the continental crust, which is assumed to be of a quartz rich composition and A_2 and Q_2 are material constants for the mantle which is assumed to consist of an olivine dominated material. The materials are further limited by upper yield stresses. The deformation field is prescribed in a manner to be consistent with simple stretching such that the model is two dimensional with an originally rectangular region (parallel to the axis) remaining rectangular (and parallel) after stretching.

Preliminary results (see figure 1) show that strain heating can provide significant temperature increases of up to 70°C for material points in a fairly wide zone in the crust and uppermost mantle. The initial model was assumed to have a high initial geologic strain rate of $10^{-14}s^{-1}$ and a normal continental crustal thickness of 35 km. Strain energy production is centered in a much narrower zone in the uppermost mantle where temperatures

in the mantle which controls the strength of the continental lithosphere (3) are lowest. Some of the heat produced from strain heating is conducted into the crust raising temperatures at material points inside the crust. The temperature increases in these zones may indicate that the previous estimates of the strength of the lithosphere undergoing stretching may have been overestimated. Results of temperature response in the lower crust due to strain heating suggests that large volumes of lower crust may be partially melted by strain heating during stretching without large scale heat influx from the invasion of mantle material into the crust.

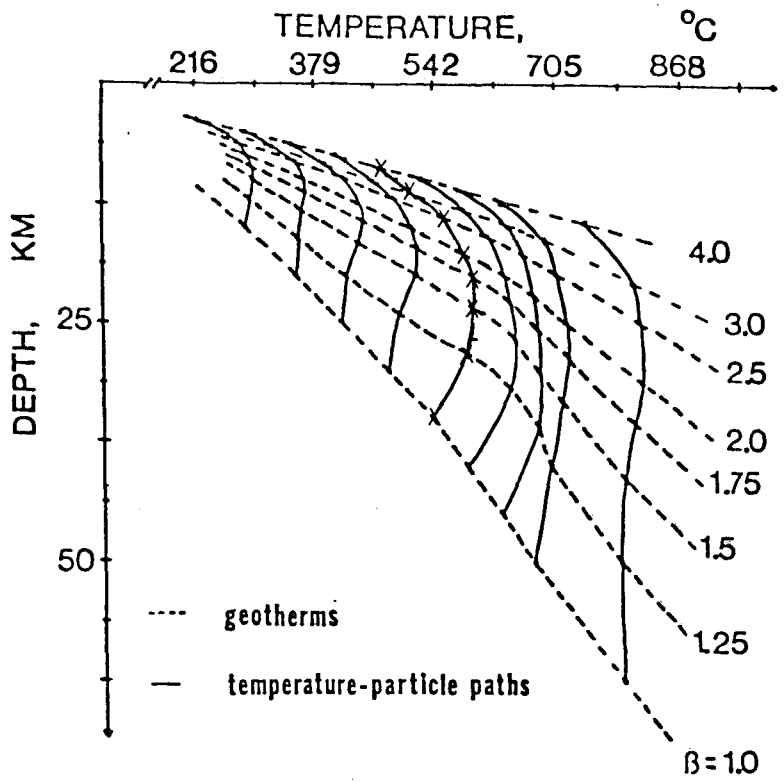

Figure 1 Geotherms for stretching with strain heating (in dashed lines) for different values of stretching, β. Temperature paths for particles which rise with stretching are shown in solid lines. The X mark the crust-mantle interface for different amounts of stretching. The strain rate is given by with $= 10^{-14} s^{-1}$.

References

(1) McKenzie, Dan, P., 1978, Some remarks on the development of sedimentary basins, Earth and Planetary Science Letters, 40, 25-32.

(2) Lachenbruch, A.H., and J.H. Sass, 1978, Models of an extending lithoshere and heat flow in the Basin and Range province, Geol. Soc. Am. Mem., 152, 209-250.

(3) England, Phillip, 1983, Constraints on the extension of continental lithosphere, Journal of Geophysical Research, 88, 1145-1152.

GEOMETRY OF MIOCENE EXTENSIONAL DEFORMATION, LOWER COLORADO RIVER REGION, SOUTHEASTERN CALIFORNIA AND SOUTHWESTERN ARIZONA: EVIDENCE FOR THE PRESENCE OF A REGIONAL LOW-ANGLE NORMAL FAULT; R.M. Tosdal and D.R. Sherrod, U.S. Geological Survey, 345 Middlefield Road, Menlo Park, CA 94025

The geometry of Miocene extensional deformation changes along a 120 km-long, northeast-trending transect from the southeastern Chocolate Mountains, southeastern California, to the Trigo and southern Dome Rock Mountains, southwestern Arizona (fig. 1). Based upon regional differences in the structural response to extension and estimated extensional strain, the transect can be divided into three northwesterly-trending structural domains. From southwest to northeast, These domains are: A) southeastern Chocolate-southernmost Trigo Mountains; B) central to northern Trigo Mountains; and C) Trigo Peaks-southern Dome Rock Mountains (Fig. 1). All structures formed during the deformation are brittle in style; fault rocks (1) are composed of gouge, cohesive gouge, and locally microbreccia. Younger high-angle dip-slip and strike-slip(?) faults are not discussed.

In each structural domain, exposed lithologic units are composed of Mesozoic crystalline rocks unconformably overlain by Oligocene to Early Miocene volcanic and minor interbedded sedimentary rocks (2-6). Breccia, conglomerate, and sandstone deposited synchronously with regional extension locally overlie the volcanic rocks. Extensional deformation largely postdated the main phase of volcanic activity, but rare rhyolitic tuff and flows interbedded with the syndeformational clastic rocks suggests that deformation began during the waning stages of volcanism. K-Ar isotopic ages indicate that deformation occurred in Miocene time, between about 22 and 13 m.y. ago (5,6).

In the southeastern Chocolate Mountains and southernmost Trigo Mountains domain (fig. 1), the Tertiary and Mesozoic rocks are broken into numerous blocks bounded by curviplanar normal faults. Movement along the faults has tilted the rocks gently to the west and southwest. Deformation and rotation of each block is typically independent of the adjacent block; for example, in one block the beds dip 10 to 20°, whereas in the adjacent block the identical rocks dip as much as 40°. The curviplanar normal faults consist of fault segments of contrasting attitudes and displacements. The more continuous fault segments are north to northwest-trending, moderately dipping (35-70°) normal faults. These normal faults abruptly terminate in north to northeast-trending, steeply dipping (60-80°) faults with inferred strike-slip to oblique-slip displacements. These steeply-dipping cross or transfer faults (7) commonly extend only short distances beyond the junction of the two fault segments. In three dimensions, the geometry of the curviplanar faults at the junctions is that of an elongate spoon or trough with its long axis parallel to the intersection of the two fault segments. This geometry suggests that the relative transport of the upper plate of the faults was parallel to the axis of the troughs, that is towards the northeast or east. Assuming a listric geometry for the faults, the angular relations between bedding in the Tertiary strata and the northwest-striking curviplanar faults (8) suggest approximately 10 to 20% extensional strain.

The trace of the curviplanar block-bounding faults as well as smaller faults within individual blocks are commonly controlled by pre-existing planar anisotropies such as lithologic and structural contacts. For example, the trace of the Gatuna fault (Fig. 1), which is the largest and most continuous of the curviplanar faults, closely follows the trace of the late Mesozoic Chocolate Mountains thrust (2) and the inferred trace of the Sortan fault (3). The curviplanar trace of the Gatuna fault may also be in part inherited from

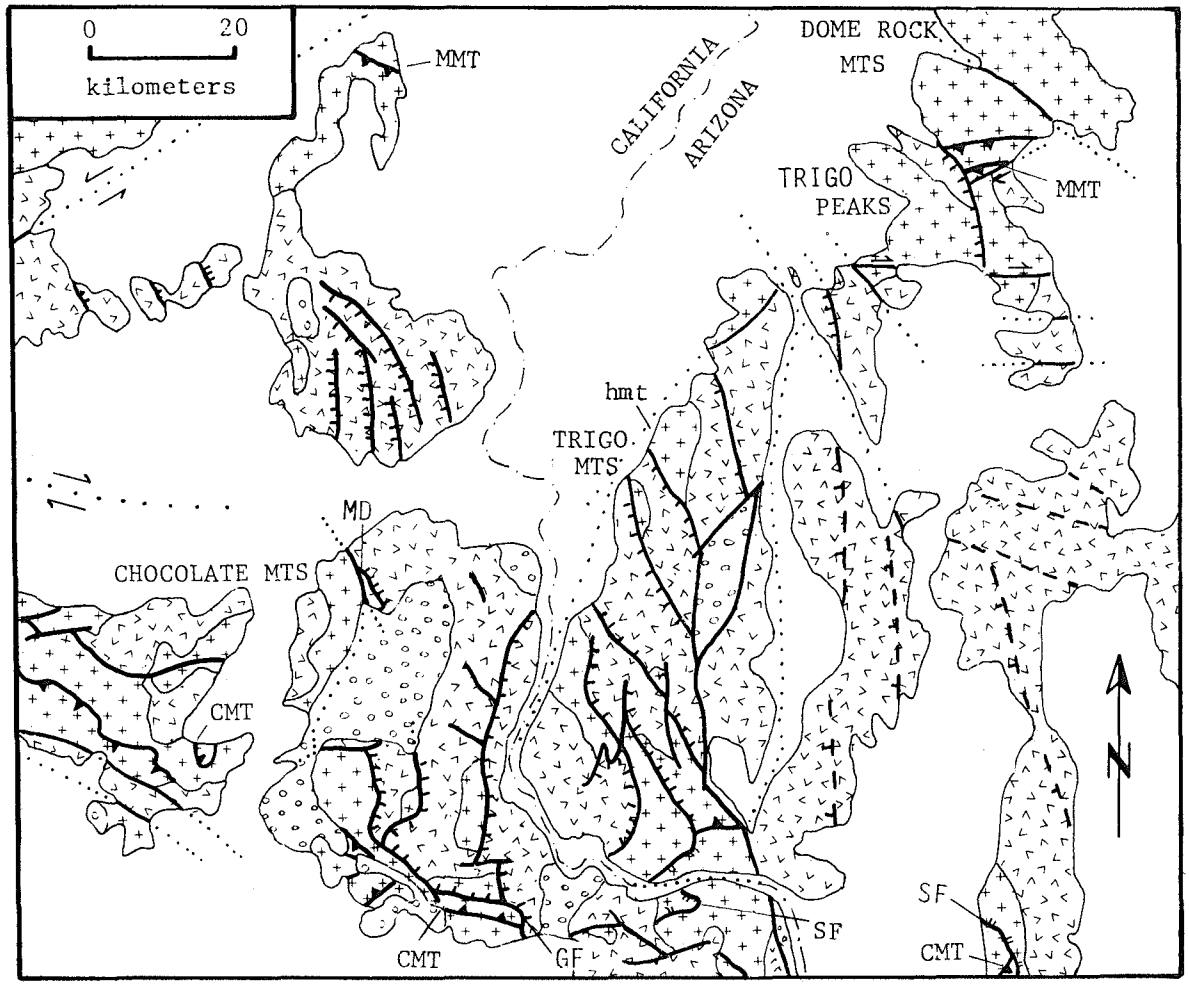

Figure 1. Generalized geologic map of the lower Colorado River region, southeastern California and southwestern Arizona. Geology shown in mountains range in the southeast part of the map is based on sir phots interpretation. CMT-Chocolate Mountains thrust, GF-Gatuna fault; MD-Midway detachment fault; MMT-Mule Mountains thrust; SF-Sortan fault; hmt-Hart Mountain mine.

open folds of the Chocolate Mountains thrust and planar fabrics of the thrust zone.

The Gatuna fault probably correlates with the Midway detachment fault (Fig. 1) (6), located some 20 km to the north. These faults together define the southwestern and western margins of the extended terranes.

The transition from the southeastern Chocolate-southern Trigo Mountains domain to the central to northern Trigo Mountains domain occurs over a zone of complex deformation about 10 km wide. Within the transition zone, faults characteristic of both domains are present. In addition, normal fault-bounded blocks, with little internal rotation and deformation of nearly flat-lying Tertiary rocks, are juxtaposed against blocks of moderately faulted and rotated rocks.

The Trigo Mountains domain (fig. 1) is composed of numerous northwest-trending structural panels ranging in width from ten's of meters to about a kikometer. The panels are bounded by shallowly-dipping normal faults that consistently dip 20 and 45^{o} to the southwestward. The Tertiary rocks and the unconformity with the underlying crystalline rocks dip 50 and 70^{o} northeastward. Listric geometry for the shallowly-dipping normal faults is suggested by the presence at higher structural levels of horsetail fault structures (7) that converge with depth to define a shallowly-dipping normal fault; this structure is best seen in the Hart Mountain mine area. Assuming a listric geometry for these faults (8), an extensional strain of approximately 30-40% is indicated.

Steeply dipping faults, which are antithetic to and bounded by the shallowly-dipping faults, break the larger panels into smaller blocks ; some of the antithetic faults cut shallowly-dipping faults. Many of the antithetic faults were initiated along oversteepened, northwest-dipping, lithologic contacts. Some of the antithetic faults have been previously interpreted as regional low-angle normal faults and cited as evidence for the presence of a very shallow, undulating regional low-angle normal or detachment fault now exposed in a series of antiformal culminations (10).

The simple pattern of northeast-tilted structural panels in the central to north Trigo Mountains domain extends northward into the Trigo Peaks-southern Dome Rock Mountains domain (fig. 1). In this domain, the northwest-trending structural panels are cut by several east striking high-angle tear faults with dextral strike-slip separation of as much as 5 km. These tear or transfer faults (7) formed in reponse to differential displacements between the apparently unrotated Dome Rock Mountains to the north and the imbricately-faulted Trigo Peaks to the south. (Because Mesozoic deformational fabrics in the Dome Rock Mountains are colinear with those in ranges to the west of the extended terrane, the range is apparently unrotated and is, therefore, a simple fault-bounded block). The transfer faults which separate the rotated from unrotated terranes closely follows and modifies segments of the Late Mesozoic Mule Mountains thrust (11). Temporal relations between the transfer faults and low-angle normal faults are obscure due to younger high-angle faults and alluvial cover; the tranfer and low-angle normal faults are inferred to be coeval and kinematically related. Estimated extensional strain is approximately 40%.

The observed variations in structural style and extensional strain from southeastern Chocolate Mountains to the Dome Rock Mountains suggest that the rocks exposed in this region constitutes the upper plate of a regional low-angle fault (fig 2a,b). This regional fault is inferred to be subparallel to other large low-angle normal or detachment faults located to the north and northeast (12) and thus probably dips gently to the northeast towards the

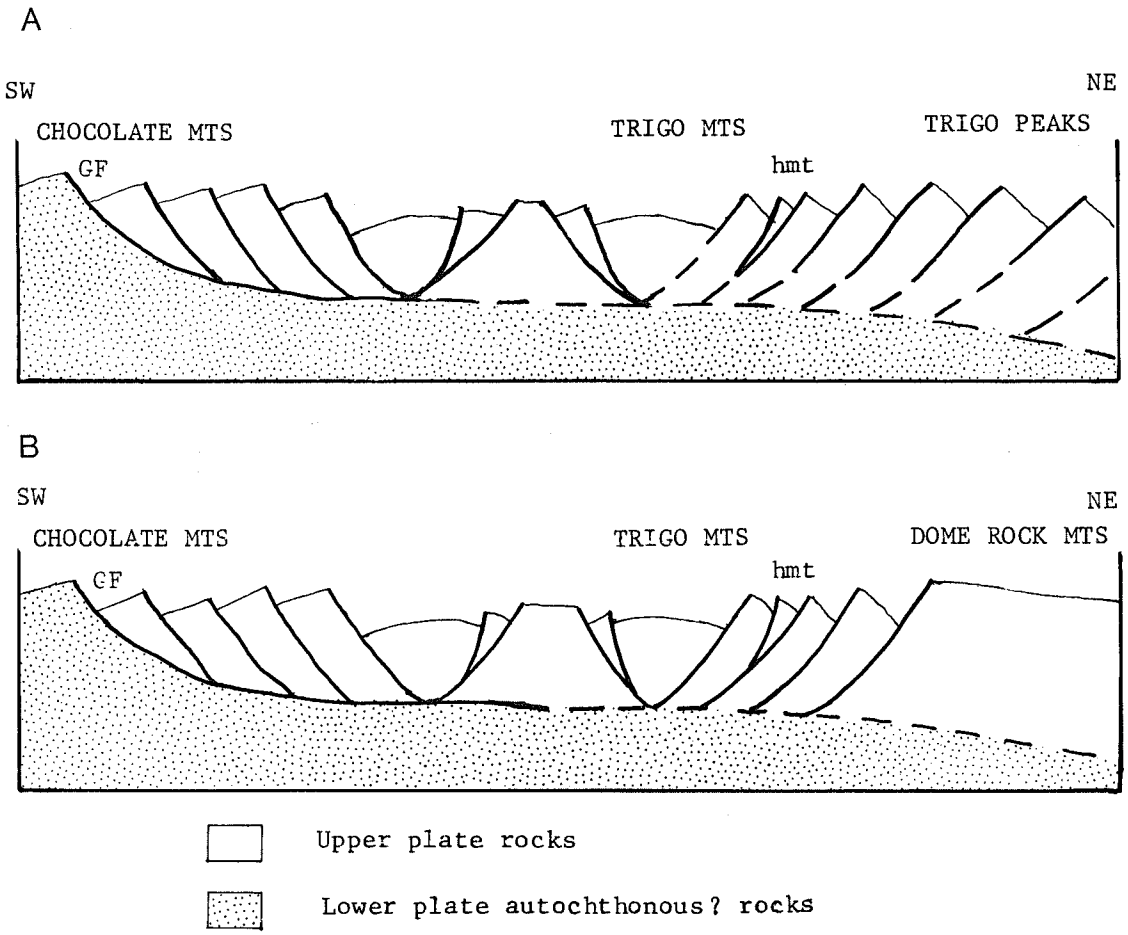

Figure 2. Schematic structural cross section along the transect between the southeastern Chocolate Mountains, California, and the Trigo Peaks and southern Dome Rock Mountains, southwestern Arizona. Syn- and post-extensional clastic rocks and younger faults are not shown on the cross section. Cross section are not drawn to scale and have a large vertical exageration. A) crossection between the southeastern Chocolate Mountains, to southwest, and the Trigo Peaks area, to the northeast; and B) cross section with the fault-bounded, unrotated Dome Rock Mountains projected into the line of the cross section. GF-Gatuna fault; hmt-Hart Mountain mine

Colorado Plateau. The headwall or breakway zone of the extensional allochthon is the Gatuna fault-Midway detachment of the southeasternmost Chocolate Mountains. In this model, the exposed southwest-dipping low-angle normal faults in the Trigo Mountains-Trigo Peaks-Dome Rock Mountains domains would be counter faults (7) and probably intersect the underlying regional sole fault at high angles. The lateral transition from the imbricately extended ranges of the Trigo Mountains-Trigo Peaks area to the apparently unrotated fault-bounded Dome Rock Mountains occurs across a complex zone of dextral transfer faults and low-angle normal faults. The Dome Rock Mountains block probably was also transported as part of the extensional allochthon.

This interpretation of the geometry of extensional deformation at depth in the lower Colorado River region differs significantly from a model which proposes a regional set of antiforms and synforms in a low-angle normal fault

that formed as a result of anastomozing brittle and ductile shear zones at depth (13). The planned CALCRUST seismic reflection profile crosses part of this transect and will provide an independent test of both models.

REFERENCES CITED

1. Sibson R.H. (1977) Fault rocks and fault mechanisms. J. Geol. Soc. London, 133, p.191-213.
2. Haxel G. and Dillon J.T. (1978) The Pelona-Orocopia Schist and Vincent-Chocolate Mountains thrust system, southern California, in Mesozoic Paleogeography of the western United States. Pacific section, Soc. Econ. Paleont. Mineral., Pacific Coast Paleogeography Symposium 2, p. 453-469.
3. Haxel G.B. Dillon, J.T., and Tosdal, R.M. (1985) Tectonic setting and lithology of the Winterhaven Formation, a new Mesozoic stratigraphic unit in southeasternmost California and southwestern Arizona. U.S. Geol. Survey Bull 1605 (in press).
4. Tosdal R.M. (1982) The Mule Mountains thrust in the Mule Mountains,California and its probable extension in the southern Dome Rock Mountains, Arizona, in Mesozoic-Cenozoic tectonic evolution of the Colorado River region, California, Nevada, and Nevada. p.55-60.
5. Crowe B.M. Crowell J.C. and Krumenacher Daniel (1979) Regional stratigraphy, K-Ar ages, and tectonic implications of Cenozoic volcanic rocks, southeastern California. Am. J. Sci., 279, p. 186-216.
6. Weaver B.F. (1982) Reconnaissance geology and K-Ar geochronology of the Trigo Mountains detachment terrane, Yuma County, Arizona. San Diego State University M.Sc. thesis, 119p.
7. Gibbs A.D. (1984) Structural evolution of extensional basin margins. J. Geol. Soc. London, 141, p. 609-620.
8. Wernike B. and Burchfiel B.C. (1982) Modes of extensional tectonics. J. Struct. Geol., 4, p. 104-15.
9. Berg L. Leveille G. and Geis P. (1982) Mid-Tertiary detachment faulting and manganese mineralization in the Midway Mountains, Imperial County, California, in Mesozoic-Cenozoic tectonic evolution of the Colorado River region, California, Arizona, and Nevada, p.298-312.
10. Frost E.G. and Martin D.L. (1982) Comparison of Mesozoic compressional tectonic with Mid-Tertiary detachment faulting in the Colorado River area, California, Arizona, and Nevada, in Geologic excursions in the California Desert. Geol. Soc. Am. Cord. Sect. Meeting Guidebook, p. 113-159.
11. Tosdal R.M. (1984) Tectonic significance of the Late Mesozoic Mule Mountains thrust, southeast California and southwest Arizona. Geol. Soc. Am. Abst. with Prog., 16, p. .
12. Spencer J.E. (1984) Geometry of low-angle faults in west-central Arizona. Fieldnotes, 14, p. 6-8.
13. Adams M.A. Hillemeyer F.L. and Frost E.G. (1982) Anastomosing shear zones-A geometric explanation for mid-Tertiary crustal extension in the detachment terrane of the Colorado River region, CA, AZ, and NV. Geol. Soc. Am. Abstr. with Prog., 15, p. 375.

SIMILARITIES AND CONTRASTS IN TECTONIC AND VOLCANIC STYLE AND HISTORY ALONG THE COLORADO PLATEAUS-TO-BASIN AND RANGE TRANSITION ZONE IN WESTERN ARIZONA: GEOLOGIC FRAMEWORK FOR TERTIARY EXTENSIONAL TECTONICS.

R. A. Young, Department of Geological Sciences, SUNY, Geneseo, NY 14454, E. H. McKee, U.S. Geological Survey, Menlo Park, CA 94025, J. H. Hartman, Department of Geology and Geophysics, University of Minnesota, Minneapolis, MN 55455, A. M. Simmons, Department of Geological Sciences, SUNY, Buffalo, NY 14226

Recent studies of the Colorado Plateaus-to-Basin and Range transition zone in the area from the Hualapai Plateau southeastward to the Mohon and Juniper Mountains (figure 1) permit a revised perspective on the early and middle Tertiary geology of this region in western Arizona (1-7). The tectonic events in this region are related to volcanic activity and hence can be isotopically dated. The period of middle to late Tertiary volcanism (25 to 15 m.y. ago) along the margin of the Colorado Plateaus corresponds with the ages of volcanism and detachment faulting in the adjacent Basin and Range province (12). This contemporaneity suggests a relationship between regional magmatic and tectonic events from the Basin and Range province across the transition zone and onto the Colorado Plateaus.

Middle Tertiary volcanism in the Aquarius Mountains began about 25 m.y. ago and can be divided into two episodes throughout the transition zone (3,4, 6,7,8). The older episode spanned the interval from 25 to 15 m.y. ago (late Oligocene to middle Miocene) and consists mainly of clinopyroxene-bearing, alkali-rich basalts and olivine tholeiites with lesser amounts of andesite, rhyodacite, and rhyolite (7,14). This was followed by an apparent gap in activity from about 15 to 10 m.y. ago. The younger period of volcanism spans the interval from 10 to 5 m.y. ago and is typified by the calc-alkaline basalt and low silica rhyolite suite exposed at the 8- to 9- m.y.-old Mt. Hope volcanic center (7,8).

The Oligocene and Miocene volcanic rocks rest unconformably on a regional, late Cretaceous and Paleocene (Laramide) erosion surface, recently confirmed by the identification of probable early Eocene fossils in the upper "rim gravel" section on the southern Coconino Plateau near Mt. Floyd (9,13). The disruption of the early Tertiary, north- to northeast-trending drainages across the present plateau margin by deformation along compressional Laramide structures permits a distinct separation of the major early and middle Tertiary structures (1,11). Further information concerning pre- and post-middle Miocene deformation is provided by the 17- to 18- m.y.-old Peach Springs Tuff, which in some places overlaps major structures and elsewhere is cut by major faults (5,6,10,15,16).

The late Cretaceous and early Tertiary monoclines and folds are inferred to have been active as late as early Eocene time in northwest Arizona, as deduced from their relations to the Paleocene and Eocene rim gravels (1). From the Hualapai Plateau to the Juniper Mountains region, Oligocene and middle Miocene (25 to 15 m.y.) volcanic centers and vents have close spatial relationships to the monoclines and folds. The younger Miocene (10- to 5- m.y.-old) volcanic rocks do not have any clear spatial association with the Laramide structures.

An outline of the Tertiary magmatic and tectonic history includes: 1) a late Eocene and Oligocene period of volcanic quiescence, possibly accompanied by sporadic normal faulting, 2) a late Oligocene to middle Miocene episode of extensional faulting and predominantly basaltic volcanism, possibly localized

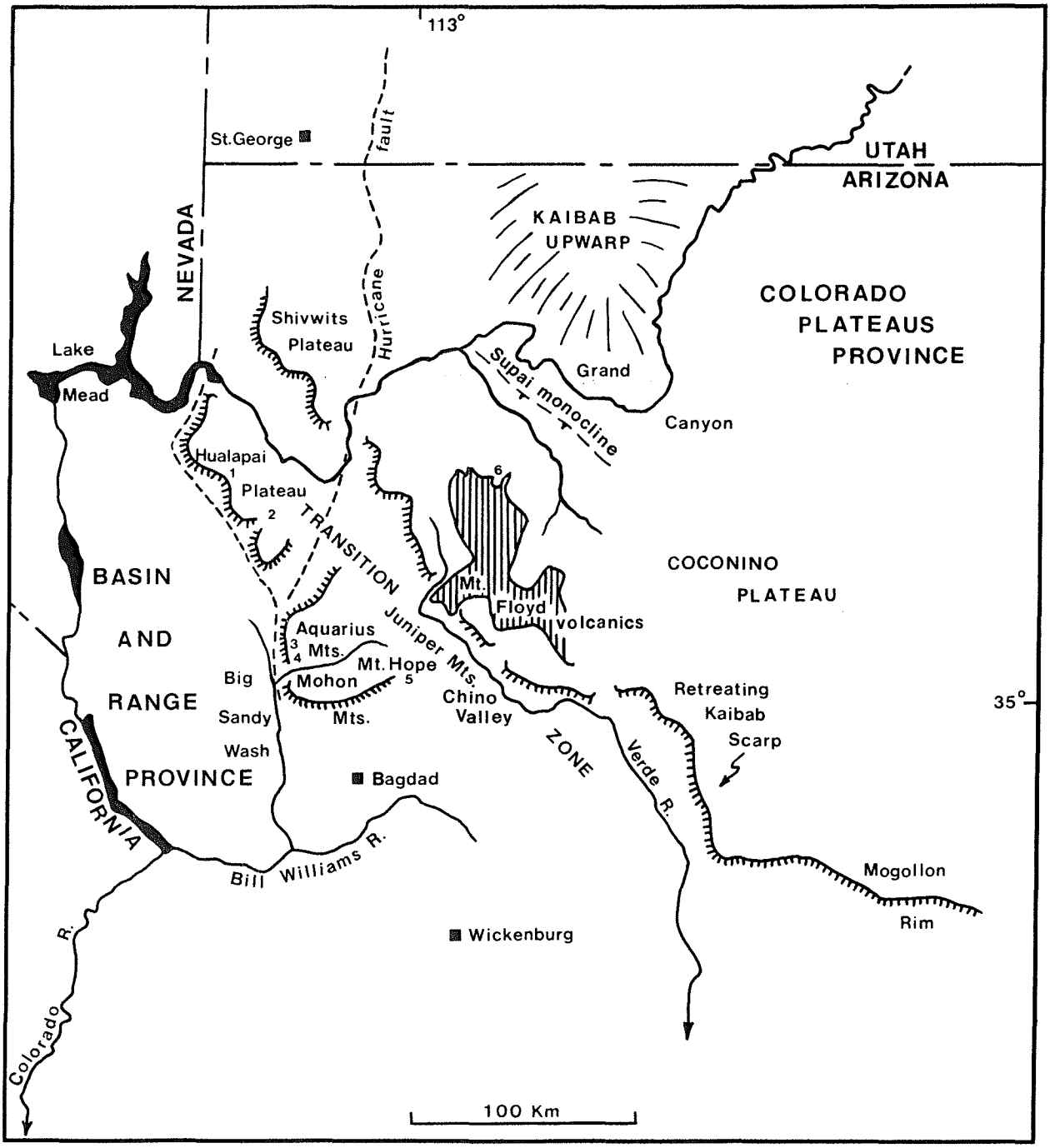

Figure 1. Features referred to in text and localities (numbers) where radiometric ages have been reported in publications by the authors. 1: 65.5 ± 3.5 m.y. granodiorite(?). 2: *18.3 ± 0.6 m.y. Peach Springs Tuff. 3: 18.2 ± 1.5 m.y. basalt. 4: 24.5 ± 3.5, 24.9 ± 0.9 m.y. basaltic andesites. 5: 8.0 ± 0.5 m.y. rhyolite, 8.5 ± 0.9 m.y. basalt (Mt. Hope). 6: *14.0 ± 0.6 m.y. basalt.

* Uncorrected for new ^{40}K constants.

along preexisting Laramide structures, 3) a middle Miocene interval (15 to 10 m.y. ago) of volcanic quiescence, and 4) a late Miocene and Pliocene period of predominantly basaltic volcanism.

The overall temporal and spatial relations between middle Tertiary volcanism and tectonism from the Basin and Range province onto the edge of the Colorado Plateaus province suggest that a single magmatic-tectonic episode affected the entire region more or less simultaneously during this period. The episode followed a post-Laramide (late Eocene through Oligocene) period of 25 million years of relative stability. Middle Tertiary volcanism did not migrate gradually eastward in a simple fashion onto the Colorado Plateaus. In fact, late Oligocene volcanism appears to be more voluminous near the Aquarius Mountains than throughout the adjacent Basin and Range province westward to the Colorado River. Any model proposed to explain the cause of extension and detachment faulting in the eastern part of the Basin and Range province must consider that the onset of volcanism appears to have been approximately synchronous from the Colorado River region of the Basin and Range across the transition zone and onto the edge of the Colorado Plateaus.

REFERENCES

(1) Young, R.A. (1985, in press) Geomorphic Evolution of the Colorado Plateau margin in west-central Arizona: A tectonic model to distinguish between the causes of rapid symmetrical scarp retreat and scarp dissection. 15th Annual Binghamton Geomorphology Symposium, Tectonic Geomorphology, Allen and Unwin.

(2) Young, R.A. (1982) Paleogeomorphologic evidence for the structural history of the Colorado Plateau margin in western Arizona. In: Frost, E.G. and Martin, D. (eds.) Mesozoic-Cenozoic Tectonic Evolution of the Colorado River Region, California, Arizona, and Nevada. Cordilleran Publishers, San Diego, p. 29-39.

(3) Young, R.A. (1979) Laramide deformation, erosion, and plutonism along the southwestern margin of the Colorado Plateau. Tectonophysics, 61, p. 25-47.

(4) Young, R.A. and McKee, E.H. (1978) early and Middle Cenozoic drainage and erosion in west-central Arizona. Geol. Soc. of Amer. Bull. 89, p. 1745-1750.

(5) Young, R.A. (1966) Cenozoic geology along the edge of the Colorado Plateau in NW Arizona (PhD Dissert.) St. Louis, Washington University, 167p, maps.

(6) Young, R.A. and Brennan, W.J. (1974) The Peach Springs Tuff--Its bearing on structural evolution of the Colorado Plateau and development of Cenozoic drainage in Mohave County, Arizona. Geol. Soc. Amer. Bull. 85, p. 83-90.

(7) Goff, F., Arney, B.H., and Eddy, A. (1982) Scapolite phenocrysts in a latite dome, northwest Arizona, U.S.A. Earth and Planetary Letters, 60, p. 86-90 (also map LA-9202, Los Alamos National Lab Informal Map).

(8) Simmons, A.M. (in progress) The geology of Mt. Hope, a silicic volcanic center in west-central Arizona (M.A. thesis) SUNY Buffalo, NY.

(9) Young, R.A. and Hartman, J.H. (1984) Early Eocene fluviolacustrine sediments near Grand Canyon, Arizona: Evidence for Laramide drainage across northern Arizona into southern Utah. Geol. Soc. Amer. Abstracts with Programs 16, No. 6, p. 703.

(10) Nielson-Pike, J.E. (1984) Peach Springs Tuff: Key to Tertiary Correlation, Colorado River, Arizona and California. Geol. Soc. Amer. Abstracts with Programs, 16, No. 6, p. 610.
(11) Drewes, H. (1978) The Cordilleran orogenic belt between Nevada and Chihuahua. Geol. Soc. Amer. Bull. 89, p. 641-657.
(12) Frost, E.G. and Martin, D. (eds.) (1982) Mesozoic-Cenozoic Tectonic Evolution of the Colorado River Region, California, Arizona, Nevada. Cordilleran Publishers, San Diego, 615 p.
(13) McKee, E.D. and McKee, E.H. (1972) Pliocene uplift of the Grand Canyon--time of drainage adjustment. Geol. Soc. Amer. Bull. 83, p. 1923-1932.
(14) Fuis, G.S. (1974) The geology and mechanics of formation of the Fort Rock Dome, Yavapai Co., Arizona (PhD Dissert.) Pasadena, Calif. Inst. of Tech., 279 p.
(15) West, N.W. and Glazner, A.F. (1985) Possible correlation of the Redfire and Peach Springs Tuffs: A 500 km^3 tuff in the Mohave Desert and western Arizona? Geol. Soc. Amer. Abstracts with Programs, 17, No. 6, p. 418.
(16) Brooks, W.E. and Marvin, R.F. (1985) Discordant isotopic ages and potassium metasomatism in volcanic rocks from Yavapai County, Arizona. Geol. Soc. Amer. Abstracts with programs, 17, No. 6, p. 344.

DUCTILE EXTENSION OF PLANETARY LITHOSPHERES. *M.T. Zuber* and *E.M. Parmentier*, Department of Geological Sciences, Brown University, Providence, R.I. 02912

To better understand the mechanics of large-scale extension, we consider the effects of ductile stretching of a strength and density stratified planetary lithosphere. On the earth, deformation occurs by brittle fracture in the near surface and by ductile flow at greater depths. In our simple rheological representation of the lithosphere, the brittle failure region is modeled as a strong plastic or power law viscous layer of uniform strength and the ductile flow regime as a power law substrate in which strength is either uniform or decreases exponentially with depth. Deformation occurs due to the growth of necking instabilities which initiate from small perturbations along the surface and layer/substrate interface. The horizontal length scale of deformation is controlled by the strong layer thickness h and by the growth rate spectrum q, which is a function of the strength and density stratification and the stress exponents in the layer and substrate. The wavenumber $k(=2\pi h/\lambda)$ that corresponds to the maximum growth rate defines the dominant wavelength of necking. An example of the growth rate spectrum for a strong plastic layer overlying a weaker viscous substrate is shown in Figure 1a.

If the position of an initial perturbation along the layer/substrate interface is prescribed, corresponding to, for example, either a localized thermal anomaly or a pre-existing structural weakness, deformation concentrates into a narrow zone surrounding the perturbation. The resultant topography consists of a depression and flanking uplifts, which is consistent with the morphology of terrestrial rift zones. Figure 2 shows the deformation of the strong layer for the growth rate spectrum in Figure 1a. In this example the only density contrast is at the surface and therefore none of the surface topography is isostatically supported by density contrasts at depth. The dynamically supported surface topography arises in response to the perturbing flow induced as the lithosphere extends and leads to regional compensation of the rift depression. For an initial perturbation that is narrower than the dominant wavelength, deformation concentrates into a zone comparable in width to the dominant wavelength. If the initial perturbation is wider than the dominant wavelength, the width of the deformed zone is controlled by the width of the initial perturbation. A surface layer with limiting plastic behavior produces a rift-like structure with a width consistent with the widths of continental rifts (1) if the strong layer thickness corresponds to the depth of brittle failure of quartz. This width is independent of the layer/substrate strength contrast. For a power law ($n=3$) surface layer, rift zone width varies with layer/substrate strength ratio to the one third power. If the strength of the layer is low compared to ρgh then the lithosphere is not unstable in extension. Over the range of conditions which result in unstable extension, rift zone width is about a factor of two greater than for the plastic layer case.

Many features with rift-like morphology consisting of linear depressions and flanking uplifts have been identified on Venus from Pioneer-Venus altimetry (2). Topographic profiles across one such rift zone in Beta Regio for which high resolution topography and radar images are available (3) are shown in Figure 3. The rift depression has a width greater than 100 km, and is bounded by topographic highs that may represent uplifted flanks. Solomon and Head (4) suggest that the thickness of the elastic lithosphere on Venus may be only 1-10 km thick on the basis of rock strength at high surface temperatures and on the spacing of features of presumed tectonic origin in the banded terrain. If the width of the rift is controlled by elastic flexure (5) this would require an elastic layer thickness in the range 45-60 km (2). If the rift zone formed in response to a necking instability, its width would imply a ductile lithosphere thickness of about 30 km if the near-surface region exhibits power law behavior.

If initial disturbances along layer interfaces are randomly distributed, necking of the layer develops with a spatial periodicity corresponding to the dominant wavelength, analogous to boudinage of layered crustal rocks. A model of large-scale continental deformation in which the lithosphere consists of a plastic surface layer of uniform strength over a weaker viscous substrate in which the strength decreases exponentially with depth has been applied to explain the periodic spacing of ranges in the Basin and Range Province (6). Recent experimental (7) and seismic (8) studies have shown the terrestrial continental lithosphere to consist of a strong upper crust and upper mantle separated by a weak lower crust. An extending lithosphere with this strength

stratification may produce a growth rate spectrum with two maxima and thus two dominant wavelengths of instability (9), as shown in Figure 1b. Shorter and longer wavelengths of deformation occur due to the presence of strong upper crustal and upper mantle regions, respectively. In the Basin and Range Province, the shorter wavelength of deformation correlates with the spacing of ranges while the longer wavelength disturbance correlates with regional topography and an associated Bouguer gravity anomaly as well as with alternating regions of consistent fault block tilt directions (tilt domains) as mapped by Stewart (10).

In the present small amplitude, linearized theory, total lithospheric deformation is determined from the superposition of the short and long wavelength disturbances. The short and long wavelength and the combined deformation fields are shown in Figure 4, which has been plotted with arbitrary amplitude to clearly illustrate the styles of deformation. In the short wavelength case, deformation is concentrated in the crust. The density and strength contrast at the crust-mantle boundary results in flat Moho, which is consistent with seismic reflection profiles of the Basin and Range (11, 12). In the long wavelength case, the most obvious deformational feature is upwarping at depth. In the combined case, the transition from brittle to ductile behavior at a depth approximately midway through the crust is apparent from the change in deformational style of initially square area elements. A region of enhanced extension occurs in the upper crust near the center of the diagram, where both short and long wavelength extension are maximum. The superposition of the deformation fields results in a localized zone of shearing near the base of the strong upper crust, which could be a mechanism for the formation of low-angle normal faults. In this model the brittle-ductile transition is not an actual surface of mechanical decoupling; instead shearing is vertically distributed in the upper part of the ductile lower crust. This model suggests that regions of maximum extension at depth need not correspond to regions of maximum extension at the surface.

We are currently examining models for finite amplitude extension of a strength and density stratified continental lithosphere. As suggested by the linearized, small amplitude theory, extension in the strong crustal and strong mantle layers may localize at different places along the layers. This will result in a horizontal distribution of extension in the mantle that is different from that in the upper crust and shearing on horizontal planes within the weak lower crust. This horizontal shearing may result in the formation of low-angle detatchments that root in areas which are horizontally removed from regions of near-surface extension (13,14).

References: (1)Ramberg, I.B., and Morgan, P. (1984) Physical characteristics and evolutionary trends of continental rifts. *Proc. 27th Int. Geol. Cong., 7,* 165-216. (2)Schaber, G.G. (1982) Venus: Limited extension and volcanism along zones of lithospheric weakness. *Geophys. Res. Lett., 9,* 499-502. (3)Campbell, D.B. et al. (1984) Venus: Volcanism and rift formation in Beta Regio. *Science, 226,* 167-170. (4)Solomon, S.C., and Head, J.W. (1984) Venus banded terrain: Tectonic models for band formation and their relationship to lithospheric thermal structure. *J. Geophys. Res., 89,* 6885-6897. (5)Vening Meinesz, F.A. (1950) Les 'graben' africains resultat de compression ou de tension dans la croute terrestre? *Koninkl. Belg. Kol. Inst. Bull., 21,* 539-552. (6)Fletcher, R.C., and Hallet, B. (1983) Unstable extension of the lithosphere: A mechanical model for basin-and-range structure. *J. Geophys. Res., 88,* 7457-7466. (7)Brace, W.F., and Kohlstedt, D.L. (1980) Limits on lithospheric stress imposed from laboratory experiments. *J. Geophys. Res., 85,* 6248-6252. (8)Chen, W.P., and Molnar, P. (1983) Focal depths of intracontinental and intraplate earthquakes and their implications for the thermal and mechanical properties of the lithosphere. *J. Geophys. Res., 88,* 4183-4214. (9)Zuber M.T., et al. (1984) Extension of continental lithosphere: A model for two scales of Basin and Range deformation. Submitted to *J. Geophys. Res.* (10)Stewart, J.H. (1971) Basin and Range structure: A system of horsts and grabens produced by deep-seated extension. *Geol. Soc. Am. Bull., 91,* 460-464. (11)Allmendinger, R.W., et al. (1984) Phanerozoic tectonics of the Basin and Range - Colorado Plateau transition from COCORP data and geologic data. *Proc. Int. Symp. Deep Struct. Cont. Crust, AGU Geodynamics Series,* in press. (12)Allmendinger, R.W., et al. (1983) Cenozoic and Mesozoic structure of the eastern Basin and Range Province, Utah, from COCORP seismic reflection data. *Geology, 10,* 532-536. (13)Anderson, R.E., et al. (1983) Implications of selected subsurface data on the

structural form and evolution of some basins in the northern Basin and Range Province, Nevada and Utah. *Geol. Soc. Am. Bull., 94,* 1055-1072. (14)Wernicke, B.P. (1981) Low-angle normal faults in the Basin and Range Province: Nappe tectonics in an extending orogen. *Nature, 291,* 645-648.

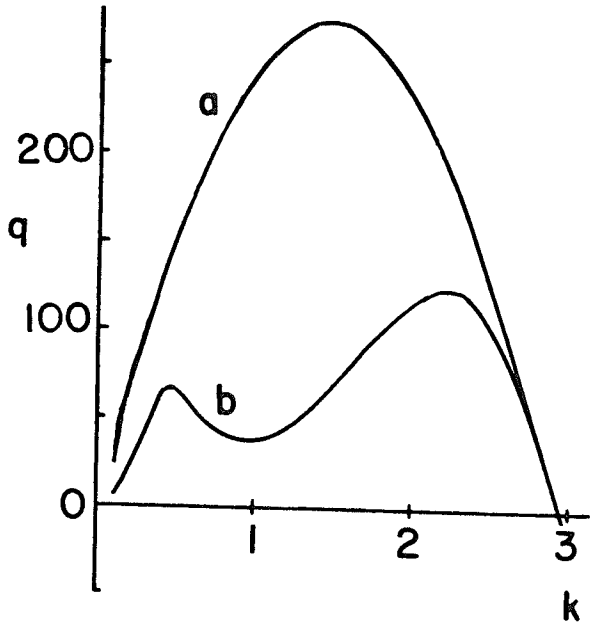

Figure 1. (a) Growth rate spectrum for an extending strong plastic layer over a viscous substrate. (b) Growth rate spectrum for an extending strong upper crust and upper mantle separated by a weak lower crust.

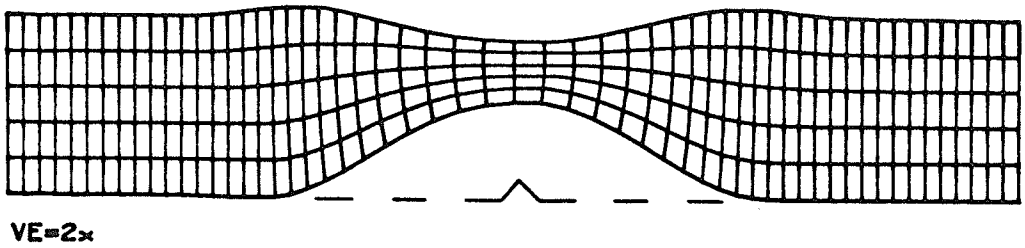

Figure 2. Strong layer deformation for the growth rate spectrum in Figure 1a. The surface topography consists of a central depression and flanking uplifts, which is consistent with the morphology of rift zones. The initial perturbation at the layer/substrate interface is shown by the dashed line.

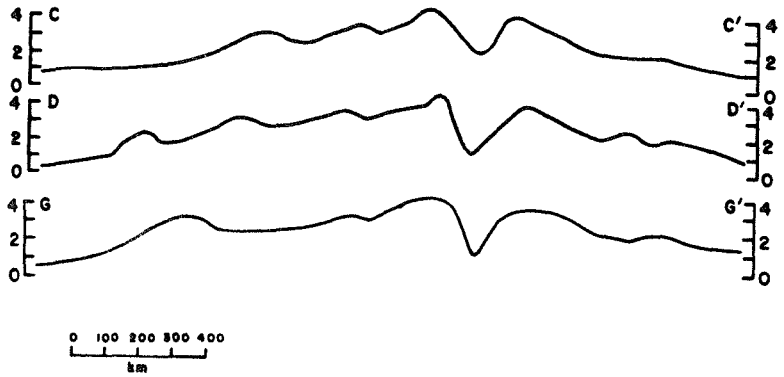

Figure 3. Topographic profiles across rift zone in Beta Regio, Venus. From Campbell et al. (1984).

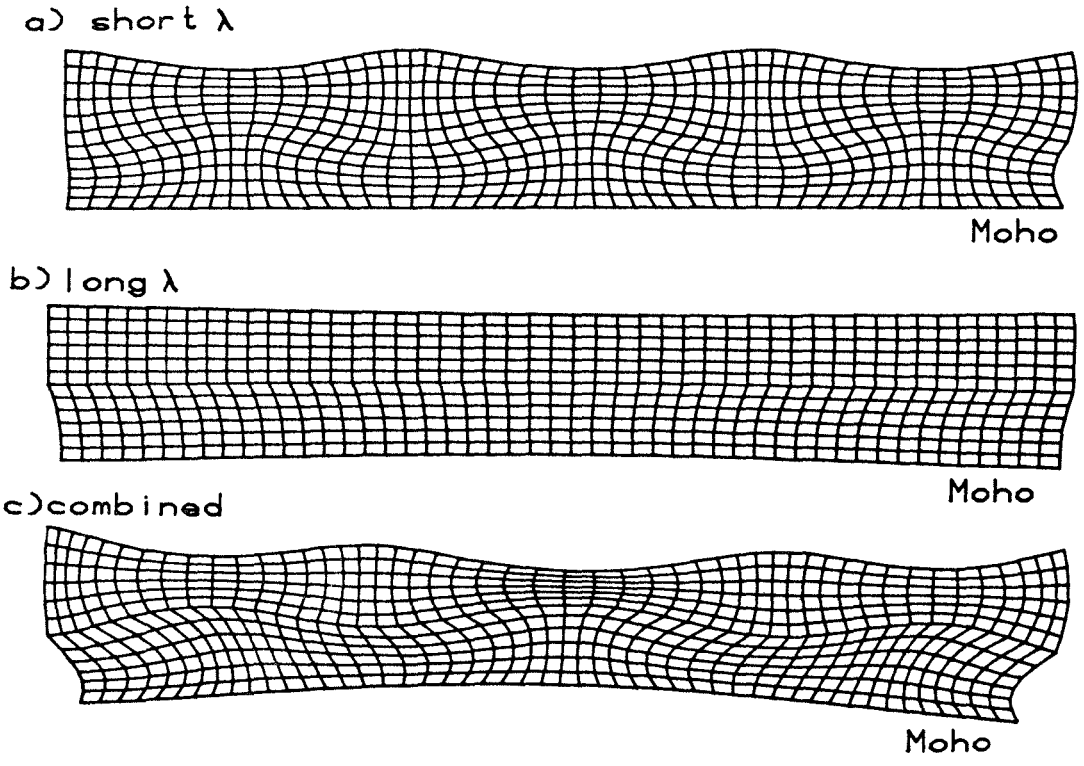

Figure 4. (a) Short wavelength, (b) long wavelength, and (c) combined deformation fields for the growth rate spectrum in Figure 1b. Note the presence of enhanced shearing at mid-crustal depths in (c).

U.S. GOVERNMENT PRINTING OFFICE: 1985—569-014/20792

AUTHOR INDEX

AUTHOR INDEX (continued)